CHAPTER 1

The Celestial Sphere

1.1 From Fig. 1.7, Earth makes $S/P_\oplus$ orbits about the Sun during the time required for another planet to make S/P orbits. If that other planet is a superior planet then Earth must make one extra trip around the Sun to overtake it, hence

$$\frac{S}{P_\oplus} = \frac{S}{P} + 1.$$

Similarly, for an inferior planet, that planet must make the extra trip, or

$$\frac{S}{P} = \frac{S}{P_\oplus} + 1.$$

Rearrangement gives Eq. (1.1).

1.2 For an inferior planet at greatest elongation, the positions of Earth (E), the planet (P), and the Sun (S) form a right triangle ($\angle EPS = 90°$). Thus $\cos(\angle PES) = \overline{EP}/\overline{ES}$.

From Fig. S1.1, the time required for a superior planet to go from opposition (point P_1) to quadrature (P_2) can be combined with its sidereal period (from Eq. 1.1) to find the angle $\angle P_1SP_2$. In the same time interval Earth will have moved through the angle $\angle E_1SE_2$. Since P_1, E_1, and S form a straight line, the angle $\angle P_2SE_2 = \angle E_1SE_2 - \angle P_1SP_2$. Now, using the right triangle at quadrature, $\overline{P_2S}/\overline{E_2S} = 1/\cos(\angle P_2SE_2)$.

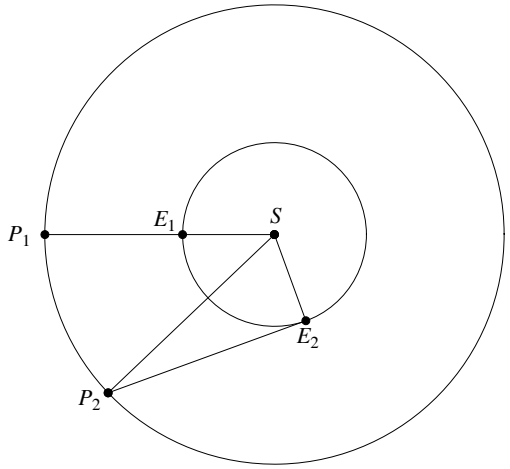

Figure S1.1: The relationship between synodic and sidereal periods for superior planets, as discussed in Problem 1.2.

1.3 (a) $P_{\rm Venus} = 224.7$ d, $P_{\rm Mars} = 687.0$ d

(b) Pluto. It travels the smallest fraction of its orbit before being "lapped" by Earth.

1.4 Vernal equinox: $\alpha = 0^{\rm h}$, $\delta = 0°$
Summer solstice: $\alpha = 6^{\rm h}$, $\delta = 23.5°$
Autumnal equinox: $\alpha = 12^{\rm h}$, $\delta = 0°$
Winter solstice: $\alpha = 18^{\rm h}$, $\delta = -23.5°$

1.5 (a) $(90^\circ - 42^\circ) + 23.5^\circ = 71.5^\circ$

(b) $(90^\circ - 42^\circ) - 23.5^\circ = 24.5^\circ$

1.6 (a) $90^\circ - L < \delta < 90^\circ$

(b) $L > 66.5^\circ$

(c) Strictly speaking, only at $L = \pm 90^\circ$. The Sun will move along the horizon at these latitudes.

1.7 (a) Both the year 2000 and the year 2004 were leap years, so each had 366 days. Therefore, the number of days between January 1, 2000 and January 1, 2006 is 2192 days. From January 1, 2006 to July 14, 2006 there are 194 days. Finally, from noon on July 14, 2006 to 16:15 UT is 4.25 hours, or 0.177 days. Thus, July 14, 2006 at 16:15 UT is JD 2453931.177.

(b) MJD 53930.677.

1.8 (a) $\Delta\alpha = 9^{\rm m}53.55^{\rm s} = 2.4731^\circ$, $\Delta\delta = 2^\circ 9' 16.2'' = 2.1545^\circ$. From Eq. (1.8), $\Delta\theta = 2.435^\circ$.

(b) $d = r\,\Delta\theta = 1.7 \times 10^{15}$ m $= 11{,}400$ AU.

1.9 (a) From Eqs. (1.2) and (1.3), $\Delta\alpha = 0.193628^\circ = 0.774512^{\rm m}$ and $\Delta\delta = -0.044211^\circ = -2.65266'$. This gives the 2010.0 precessed coordinates as $\alpha = 14^{\rm h}30^{\rm m}29.4^{\rm s}$, $\delta = -62^\circ 43' 25.26''$.

(b) From Eqs. (1.6) and (1.7), $\Delta\alpha = -5.46^{\rm s}$ and $\Delta\delta = 7.984''$.

(c) Precession makes the largest contribution.

1.10 In January the Sun is at a right ascension of approximately $19^{\rm h}$. This implies that a right ascension of roughly $7^{\rm h}$ is crossing the meridian at midnight. With about 14 hours of darkness this would imply observations of objects between right ascensions of 0 h and 14 h would be crossing the meridian during the course of the night (sunset to sunrise).

1.11 Using the identities, $\cos(90^\circ - t) = \sin t$ and $\sin(90^\circ - t) = \cos t$, together with the small-angle approximations $\cos\Delta\theta \approx 1$ and $\sin\Delta\theta \approx 1$, the expression immediately reduces to

$$\sin(\delta + \Delta\delta) = \sin\delta + \Delta\theta\cos\delta\cos\theta.$$

Using the identity $\sin(a + b) = \sin a\cos b + \cos a\sin b$, the expression now becomes

$$\sin\delta\cos\Delta\delta + \cos\delta\sin\Delta\delta = \sin\delta + \Delta\theta\cos\delta\cos\theta.$$

Assuming that $\cos\Delta\delta \approx 1$ and $\sin\Delta\delta \approx \Delta\delta$, Eq. (1.7) is obtained.

CHAPTER 2

Celestial Mechanics

2.1 From Fig. 2.4, note that

$$r^2 = (x - ae)^2 + y^2 \qquad \text{and} \qquad r'^2 = (x + ae)^2 + y^2.$$

Substituting Eq. (2.1) into the second expression gives

$$r = 2a - \sqrt{(x + ae)^2 + y^2}$$

which is now substituted into the first expression. After some rearrangement,

$$\frac{x^2}{a^2} + \frac{y^2}{a^2(1 - e^2)} = 1.$$

Finally, from Eq. (2.2),

$$\frac{x^2}{a^2} + \frac{y^2}{b^2} = 1.$$

2.2 The area integral in Cartesian coordinates is given by

$$A = \int_{-a}^{a} \int_{-b\sqrt{1-x^2/a^2}}^{b\sqrt{1-x^2/a^2}} dy\, dx = \frac{2b}{a} \int_{-a}^{a} \sqrt{a^2 - x^2}\, dx = \pi ab.$$

2.3 (a) From Eq. (2.3) the radial velocity is given by

$$v_r = \frac{dr}{dt} = \frac{a(1 - e^2)}{(1 + e\cos\theta)^2}\, e \sin\theta\, \frac{d\theta}{dt}. \tag{S2.1}$$

Using Eqs. (2.31) and (2.32)

$$\frac{d\theta}{dt} = \frac{2}{r^2}\frac{dA}{dt} = \frac{L}{\mu r^2}.$$

The angular momentum can be written in terms of the orbital period by integrating Kepler's second law. If we further substitute $A = \pi ab$ and $b = a(1 - e^2)^{1/2}$ then

$$L = 2\mu\pi a^2 (1 - e^2)^{1/2}/P.$$

Substituting L and r into the expression for $d\theta/dt$ gives

$$\frac{d\theta}{dt} = \frac{2\pi(1 + e\cos\theta)^2}{P(1 - e^2)^{3/2}}.$$

This can now be used in Eq. (S2.1), which simplifies to

$$v_r = \frac{2\pi ae \sin\theta}{P(1 - e^2)^{1/2}}.$$

Similarly, for the transverse velocity

$$v_\theta = r\,\frac{d\theta}{dt} = \frac{2\pi a(1 + e\cos\theta)}{(1 - e^2)^{1/2} P}.$$

(b) Equation (2.36) follows directly from $v^2 = v_r^2 + v_\theta^2$, Eq. (2.37) (Kepler's third law), and Eq. (2.3).

2.4 The total energy of the orbiting bodies is given by

$$E = \frac{1}{2}m_1 v_1^2 + \frac{1}{2}m_2 v_2^2 - G\frac{m_1 m_2}{r}$$

where $r = |\mathbf{r}_2 - \mathbf{r}_1|$. Now,

$$v_1 = \dot{r}_1 = -\frac{m_2}{m_1 + m_2}\dot{r} \qquad \text{and} \qquad v_2 = \dot{r}_2 = \frac{m_1}{m_1 + m_2}\dot{r}.$$

Finally, using $M = m_1 + m_2$, $\mu = m_1 m_2 / (m_1 + m_2)$, and $m_1 m_2 = \mu M$, we obtain Eq. (2.25).

2.5 Following a procedure similar to Problem 2.4,

$$\begin{aligned}\mathbf{L} &= m_1 \mathbf{r}_1 \times \mathbf{v}_1 + m_2 \mathbf{r}_2 \times \mathbf{v}_2 \\ &= m_1 \left[-\frac{m_2}{m_1 + m_2}\right]\mathbf{r} \times \left[-\frac{m_2}{m_1 + m_2}\right]\mathbf{v} \\ &\quad + m_2 \left[\frac{m_1}{m_1 + m_2}\right]\mathbf{r} \times \left[\frac{m_1}{m_1 + m_2}\right]\mathbf{v} \\ &= \mu \mathbf{r} \times \mathbf{v} = \mathbf{r} \times \mathbf{p}\end{aligned}$$

2.6 (a) The total orbital angular momentum of the Sun–Jupiter system is given by Eq. (2.30). Referring to the data in Appendicies A and C, $M_\odot = 1.989 \times 10^{30}$ kg, $M_J = 1.899 \times 10^{27}$ kg, $M = M_J + M_\odot = 1.991 \times 10^{30}$ kg, and $\mu = M_J M_\odot / (M_J + M_\odot) = 1.897 \times 10^{27}$ kg. Furthermore, $e = 0.0489$, $a = 5.2044$ AU $= 7.786 \times 10^{11}$ m. Substituting,

$$L_{\text{total orbit}} = \mu\sqrt{GMa\left(1 - e^2\right)} = 1.927 \times 10^{43} \text{ kg m}^2 \text{ s}^{-1}.$$

(b) The distance of the Sun from the center of mass is $a_\odot = \mu a / M_\odot = 7.426 \times 10^8$ m. The Sun's orbital speed is $v_\odot = 2\pi a_\odot / P_J = 12.46$ m s^{-1}, where $P_J = 3.743 \times 10^8$ s is the system's orbital period. Thus, for an assumed circular orbit,

$$L_{\text{Sun orbit}} = M_\odot a_\odot v_\odot = 1.840 \times 10^{40} \text{ kg m}^2 \text{ s}^{-1}.$$

(c) The distance of Jupiter from the center of mass is $a_J = \mu a / M_J = 7.778 \times 10^{11}$ m, and its orbital speed is $v_J = 2\pi a_J / P_J = 1.306 \times 10^4$ m s^{-1}. Again assuming a circular orbit,

$$L_{\text{Jupiter orbit}} = M_J a_J v_J = 1.929 \times 10^{43} \text{ kg m}^2 \text{ s}^{-1}.$$

This is in good agreement with

$$L_{\text{total orbit}} - L_{\text{Sun orbit}} = 1.925 \times 10^{43} \text{ kg m}^2 \text{ s}^{-1}.$$

(d) The moment of inertia of the Sun is approximately

$$I_\odot \sim \frac{2}{5} M_\odot R_\odot^2 \sim 3.85 \times 10^{47} \text{ kg m}^2$$

and the moment of inertia of Jupiter is approximately

$$I_J \sim \frac{2}{5} M_J R_J^2 \sim 3.62 \times 10^{42} \text{ kg m}^2.$$

(*Note:* Since the Sun and Jupiter are centrally condensed, these values are overestimates; see Section 23.2.) Using $\omega = 2\pi/P$,

$$L_{\text{Sun rotate}} = 1.078 \times 10^{42} \text{ kg m}^2 \text{ s}^{-1}$$

$$L_{\text{Jupiter rotate}} = 6.312 \times 10^{38} \text{ kg m}^2 \text{ s}^{-1}.$$

(e) Jupiter's orbital angular momentum.

2.7 (a) $v_{\text{esc}} = \sqrt{2GM_J/R_J} = 60.6 \text{ km s}^{-1}$

(b) $v_{\text{esc}} = \sqrt{2GM_\odot/1 \text{ AU}} = 42.1 \text{ km s}^{-1}$.

2.8 (a) From Kepler's third law (Eq. 2.37) with $a = R_\oplus + h = 6.99 \times 10^6$ m, $P = 5820$ s $= 96.9$ min.

(b) The orbital period of a geosynchronous satellite is the same as Earth's sidereal rotation period, or $P = 8.614 \times 10^4$ s. From Eq. (2.37), $a = 4.22 \times 10^7$ m, implying an altitude of $h = a - R_\oplus = 3.58 \times 10^7$ m $= 5.6 \text{ R}_\oplus$.

(c) A geosynchronous satellite must be "parked" over the equator and orbiting in the direction of Earth's rotation. This is because the center of the satellite's orbit is the center of mass of the Earth–satellite system (essentially Earth's center).

2.9 The integral average of the potential energy is given by

$$\langle U \rangle = \frac{1}{P} \int_0^P U(t)\, dt = -\frac{1}{P} \int_0^P \frac{GM\mu}{r(t)}\, dt.$$

Using Eqs. (2.31) and (2.32) to solve for dt in terms of $d\theta$, and making the appropriate changes in the limits of integration,

$$\langle U \rangle = -\frac{1}{P} \int_0^{2\pi} \frac{GM\mu^2 r}{L}\, d\theta.$$

Writing r in terms of θ via Eq. (2.3) leads to

$$\langle U \rangle = -\frac{GM\mu^2 a\left(1-e^2\right)}{PL} \int_0^{2\pi} \frac{d\theta}{1 + e\cos\theta}$$

$$= -\frac{2\pi GM\mu^2 a\left(1-e^2\right)^{1/2}}{PL}.$$

Using Eq. (2.30) to eliminate the total orbital angular momentum L, and Kepler's third law (Eq. 2.37) to replace the orbital period P, we arrive at

$$\langle U \rangle = -G\frac{M\mu}{a}.$$

2.10 Using the integral average from Problem 2.9

$$\langle r \rangle = \frac{1}{P} \int_0^P r(t)\, dt.$$

Using substitutions similar to the solution of Problem 2.9 we eventually arrive at

$$\langle r \rangle = \frac{a}{2\pi}\left(1-e^2\right)^{5/2} \int_0^{2\pi} \frac{d\theta}{(1 + e\cos\theta)^3}. \tag{S2.2}$$

It is evident that for $e = 0$, $\langle r \rangle = a$, as expected for perfectly circular motion. However, $\langle r \rangle$ deviates from a for other values of e. This function is most easily evaluted numerically. Employing a simple trapezoid method with 10^6 intervals, gives the results shown in Table S2.1.

Table S2.1: Results of the numerical evaluation of Eq. (S2.2) for Problem 2.10.

e	$\langle r \rangle / a$
0.00000	1.000000
0.10000	1.005000
0.20000	1.020000
0.30000	1.045000
0.40000	1.080000
0.50000	1.125000
0.60000	1.180000
0.70000	1.245000
0.80000	1.320000
0.90000	1.405000
0.95000	1.451250
0.99000	1.490050
0.99900	1.499001
0.99990	1.499900
0.99999	1.499990
1.00000	0.000000

2.11 Since planetary orbits are very nearly circular (except Mercury and Pluto), the assumption of perfectly circular motion was a good approximation. Furthermore, since a geocentric model maintains circular motion, it was very difficult to make any observational distinction between geocentric and heliocentric universes. (Parallax effects are far too small to be noticeable with the naked eye.)

2.12 (a) The graph of $\log_{10} P$ vs. $\log_{10} a$ for the Galilean moons is given in Fig. S2.1.

(b) Using the data for Io and Callisto, we find a slope of 1.5.

(c) Assuming that the mass of Jupiter is much greater than the masses of any of the Galilean moons, Kepler's third law can be written as

$$\log M + 2\log P = \log\left(\frac{4\pi^2}{G}\right) + 3\log a,$$

or

$$\log P = \frac{3}{2}\log a + \frac{1}{2}\log\left(\frac{4\pi^2}{G}\right) - \frac{1}{2}\log M.$$

$$= m\log a + b$$

where the y-intercept is

$$b = \frac{1}{2}\log\left(\frac{4\pi^2}{G}\right) - \frac{1}{2}\log M.$$

Solving for $\log M$ we have

$$\log M = \log\left(\frac{4\pi^2}{G}\right) - 2b.$$

Taking the slope as $m = 3/2$ and using the data for any of the Galilean moons we find $b = -7.753$ (in SI units). Solving gives $M = 1.900 \times 10^{27}$ kg, in good agreement with the value given in Appendix C and Problem 2.6.

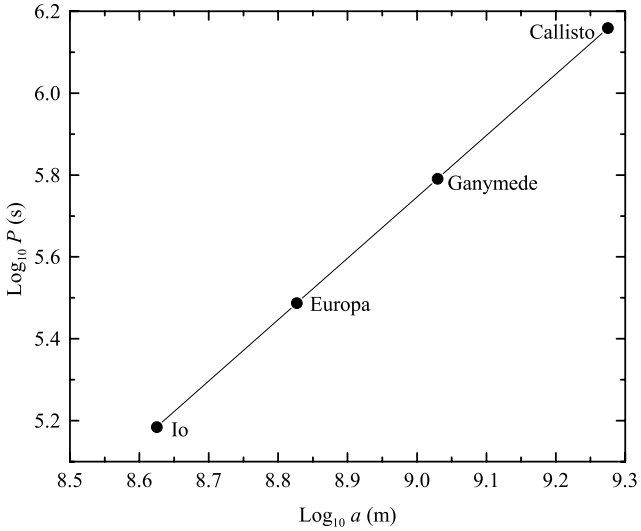

Figure S2.1: $\log_{10} P$ vs. $\log_{10} a$ for the Galilean moons.

2.13 (a) Since the velocity and position vectors are perpendicular at perihelion and aphelion, conservation of angular momentum leads to $r_p v_p = r_a v_a$. Thus

$$\frac{v_p}{v_a} = \frac{r_a}{r_p} = \frac{1+e}{1-e},$$

where the last relation is obtained from Eqs. (2.5) and (2.6).

(b) Conservation of energy at perihelion and aphelion gives

$$\frac{1}{2}\mu v_a^2 - G\frac{M\mu}{r_a} = \frac{1}{2}\mu v_p^2 - G\frac{M\mu}{r_p}.$$

Making use of Eqs. (2.5) and (2.6), and using the result of part (a) to replace v_p leads to

$$\frac{1}{2}v_a^2 - \frac{GM}{a(1+e)} = \frac{1}{2}v_a^2\left(\frac{1+e}{1-e}\right)^2 - \frac{GM}{1(1-e)}.$$

After some manipulation, we obtain Eq. (2.34); Eq. (2.33) follows immediately.

(c) The orbital angular momentum can now be obtained from

$$L = \mu r_p v_p = \mu a(1-e)\sqrt{\frac{GM}{a}\left(\frac{1+e}{1-e}\right)}.$$

Equation (2.30) follows directly.

2.14 (a) From Kepler's third law in the form $P^2 = a^3$ (P in years and a in AU), $a = 17.9$ AU.

(b) Since $m_{\text{comet}} \ll M_\odot$, Kepler's third law in the form of Eq. (2.37) gives

$$M_\odot \simeq \frac{4\pi^2 a^3}{GP^2} = 1.98 \times 10^{30} \text{ kg}.$$

(c) From Example 2.1.1, at perihelion $r_p = a(1-e) = 0.585$ AU and at aphelion $r_a = a(1+e) = 35.2$ AU.

(d) At perihelion, Eq. (2.33) gives $v_p = 55$ km s^{-1}, and at aphelion, Eq. (2.34) gives $v_a = 0.91$ km s^{-1}. When the comet is on the semiminor axis $r = a$, and Eq. (2.36) gives

$$v = \sqrt{\frac{GM_\odot}{a}} = 7.0 \text{ km s}^{-1}.$$

(e) $K_p/K_a = \left(v_p/v_a\right)^2 = 3650$.

2.15 Using 50,000 time steps, $r = \sqrt{x^2 + y^2} \simeq 1$ AU when $t \simeq 0.105$ yr. (*Note:* `Orbit` can be downloaded from the companion web site at `http://www.aw-bc.com/astrophysics`.)

2.16 The data are plotted in Fig. S2.2. (*Note:* `Orbit` can be downloaded from the companion web site at `http://www.aw-bc.com/astrophysics`.)

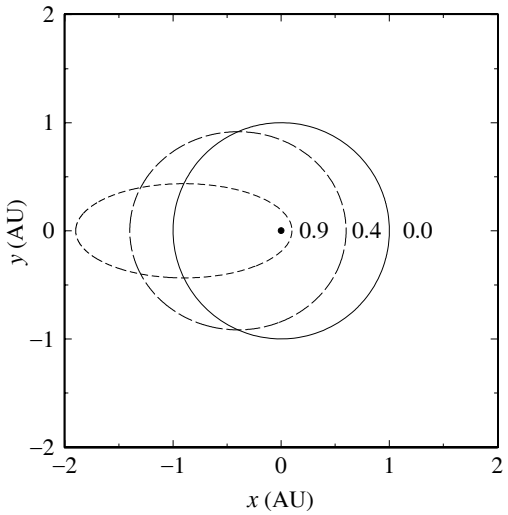

Figure S2.2: Results for Problem 2.16.

2.17 (*Note:* `Orbit` can be downloaded from the companion web site at `http://www.aw-bc.com/astrophysics`.)

(a) See Fig. S2.3.

(b) See Fig. S2.3.

(c) Figure S2.3 shows that the orbit of Mars is very close to a perfect circle, with the center of the circle slightly offset from the focal point of the ellipse. Kepler's early attempts at developing a model of the solar system based on perfect circles were not far off.

2.18 A modified Fortran 95 version of `Orbit` that works for this problem is given below.

(a) The orbits generated by the modified `Orbit` are shown in Fig. S2.4.

(b) The calculation indicates $S = 2.205$ yr.

(c) Eq. (1.1) yields a value of $S = 2.135$ yr. The results do not agree exactly because the derivation of Eq. (1.1) assumes constant speeds throughout the orbits.

(d) No, because the relative speeds during the partially-completed orbits are different.

(e) Since the orbits are not circular, Mars is at different distances from Earth during different oppositions. The closest opposition occurs when Earth is at aphelion and Mars is at perihelion, as in the start of this calculation.

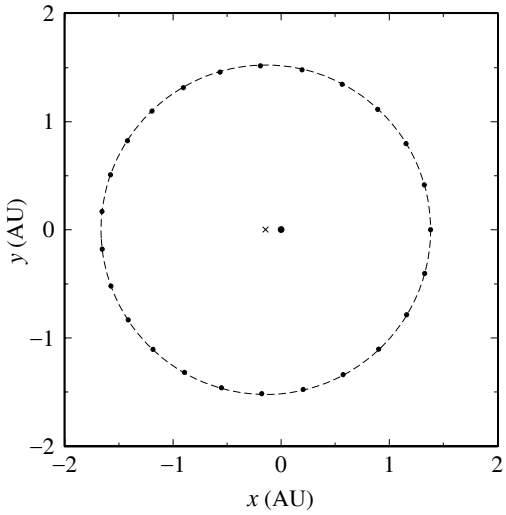

Figure S2.3: Results for Problem 2.17. The dots designate the elliptical orbit of Mars, and the principal focus of the ellipse is indicated by the circle at $(x, y) = (0, 0)$. The dashed line is for a perfect circle of radius $r = a = 1.5237$ AU centered at $x = -ae = -0.1423$ AU (marked by the $\times$).

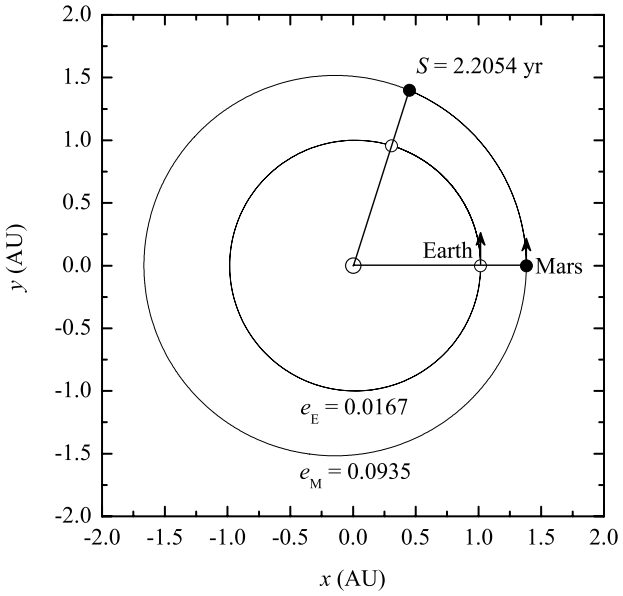

Figure S2.4: The orbits of Earth and Mars including correct eccentricities. The positions of two successive oppositions are shown. The first opposition occurs when Earth is at aphelion and Mars is at perihelion (the positions of closest approach).

```
PROGRAM Orbit
!
!   General Description:
!   ====================
!       Orbit computes the orbit of a small mass about a much larger mass,
!       or it can be considered as computing the motion of the reduced mass
!       about the center of mass.
!
!       "An Introduction to Modern Astrophysics", Appendix J
!       Bradley W. Carroll and Dale A. Ostlie
!       Second Edition, Addison Wesley, 2007
!
!       Weber State University
!       Ogden, UT
!       modastro@weber.edu
!-----------------------------------------------------------------------

!       **************This version has been modified for Problem 2.17******************

    USE Constants,  ONLY    :   i1, dp, G, AU, M_Sun, pi, two_pi, yr, &
                                radians_to_degrees, eps_dp

    IMPLICIT NONE
    REAL(dp)                ::  t, dt, LoM_E, LoM_M, P_E, P_M
    REAL(dp)                ::  Mstar, theta_E, dtheta_E, theta_M, dtheta_M, r_E, r_M
    INTEGER                 ::  n, k, kmax
    INTEGER(i1)             ::  ios         !I/O error flag
    REAL(dp)                ::  delta       !error range at end of period
    CHARACTER               ::  xpause

    REAL(dp), PARAMETER     ::  a_E = AU, a_M = 1.5236*AU, e_E = 0.0167, e_M = 0.0935

!   Open the output file
    OPEN (UNIT = 10, FILE = "Orbit.txt", STATUS = 'REPLACE', ACTION = 'WRITE', &
        IOSTAT = ios)
    IF (ios /= 0) THEN
        WRITE (*,'(" Unable to open Orbit.txt.  --- Terminating calculation")')
        STOP
    END IF


!   Convert entered values to conventional SI units
    Mstar = M_Sun

!   Calculate the orbital period of Earth in seconds using Kepler's Third Law (Eq. 2.37)
!   To be used to determine time steps
    P_E = SQRT(4*pi**2*a_E**3/(G*Mstar))

!   Enter the number of time steps and the time interval to be printed
    n = 100000
    n = n + 1   !increment to include t=0 (initial) point
    kmax = 100

!   Print header information for output file
    WRITE (10,'("t, theta_E, r_E, x_E, y_E, theta_M, r_M, x_M, y_M")')

!   Initialize print counter, angle, elapsed time, and time step.
    k = 1                   !printer counter
    theta_E = 0             !angle from direction to perihelion (radians)
    theta_M = 0

    t = 0                   !elapsed time (s)
    dt = P_E/(n-1)          !time step (s)
    delta = eps_dp          !allowable error at end of period

!   Start main time step loop
    DO
!       Calculate the distance from the principal focus using Eq. (2.3); Kepler's First Law.
        r_E = a_E*(1 - e_E**2)/(1 - e_E*COS(theta_E))       !Earth starts at aphelion
        r_M = a_M*(1 - e_M**2)/(1 + e_M*COS(theta_M))       !Mars starts at perihelion

!       If time to print, convert to cartesian coordinates.  Be sure to print last point also.
        IF (k == 1 .OR. (theta_E - theta_M)/two_pi > 1 + delta) &
            WRITE (10, '(9F10.4)') t/yr, theta_E*radians_to_degrees, r_E/AU, &
```

```
                                    r_E*COS(theta_E)/AU, r_E*SIN(theta_E)/AU, &
                                    theta_M*radians_to_degrees, r_M/AU, &
                                    r_M*COS(theta_M)/AU, r_M*SIN(theta_M)/AU

!       Exit the loop if Earth laps Mars.
        IF ((theta_E - theta_M)/two_pi > 1 + delta) EXIT

!       Prepare for the next time step:  Update the elapsed time.
        t = t + dt

!       Calculate the angular momentum per unit mass, L/m (Eq. 2.30).
        LoM_E = SQRT(G*Mstar*a_E*(1 - e_E**2))
        LoM_M = SQRT(G*Mstar*a_M*(1 - e_M**2))

!       Compute the next value for theta using the fixed time step by combining
!           Eq. (2.31) with Eq. (2.32), which is Kepler's Second Law.
        dtheta_E = LoM_E/r_E**2*dt
        theta_E = theta_E + dtheta_E

        dtheta_M = LOM_M/r_M**2*dt
        theta_M = theta_M + dtheta_M

!       Reset the print counter if necessary
        k = k + 1
        IF (k > kmax) k = 1

    END DO

    WRITE (*,'(/,"The calculation is finished and the data are in Orbit.txt")')

    WRITE (*,'(//,"Enter any character and press <enter> to exit:  ")', ADVANCE = 'NO')
    READ  (*,*) xpause
END PROGRAM Orbit
```

CHAPTER 3

The Continuous Spectrum of Light

3.1 (a) The parallax angle is $p = 33.6''/2 = 8.14 \times 10^{-5}$ rad. For a baseline $B = R_\oplus$ (Fig. 3.1),

$$d = \frac{B}{\tan p} = 7.83 \times 10^{10} \text{ m} = 0.523 \text{ AU}.$$

(b) Suppose that the clocks of the two observers are out of sync by an amount Δt, causing the baseline for their distance measurement to be $2B + v_{\text{rel}}\Delta t$ instead of $2B$. Here, v_{rel} is the relative velocity of Mars and the Earth at the time of opposition,

$$v_{\text{rel}} = 29.79 \text{ km s}^{-1} - 24.13 \text{ km s}^{-1} = 5.66 \text{ km s}^{-1}.$$

The calculated value (which is wrong) of the distance between Earth and Mars is

$$d_{\text{calc}} = \frac{R_\oplus}{\tan p},$$

while the actual value is

$$d_{\text{act}} = \frac{R_\oplus + 0.5 v_{\text{rel}}\Delta t}{\tan p}.$$

If the distance to Mars is to be measured to within 10 percent, then

$$\frac{d_{\text{act}} - d_{\text{calc}}}{d_{\text{act}}} = 0.1.$$

Inserting the expressions for d_{act} and d_{calc} and solving for Δt results in $\Delta t = 250$ s.

3.2 From Example 3.2.1, the solar constant is 1365 W m^{-2}. Using the inverse square law, Eq. (3.2), with $L = 100$ W gives $r = 0.0764$ m $= 7.64$ cm.

3.3 (a) From Eq. (3.1),

$$d = \frac{1}{p''} \text{ pc} = 2.64 \text{ pc} = 8.61 \text{ ly} = 5.44 \times 10^5 \text{ AU} = 8.14 \times 10^{16} \text{ m}.$$

(b) The distance modulus for Sirius is, from Eq. (3.6),

$$m - M = 5 \log_{10}(d/10 \text{ pc}) = -2.89.$$

3.4 From Example 3.6.1, the apparent bolometric magnitude of Sirius is $m = -1.53$. Then from the previous problem,

$$M = m + 2.89 = -1.53 + 2.89 = 1.36$$

is the absolute bolometric magnitude of Sirius. Using Eq. (3.7) with $M_{\text{Sun}} = 4.74$ leads to

$$L/L_\odot = 100^{(M_{\text{Sun}} - M)/5} = 22.5.$$

3.5 (a) Converting the subtended angle to radians gives $0.001'' = 4.85 \times 10^{-9}$ radians. Thus, the distance required is $d = 0.019\ \text{m}/4.85 \times 10^{-9} = 3.92 \times 10^6\ \text{m} = 3920\ \text{km}$.

(b) i. Assume that grows at a rate of approximately 5 cm/7 days $= 8 \times 10^{-8}\ \text{m s}^{-1}$. (I suspect it is an order of magnitude faster in the author's lawn!)

ii. $\theta = 0.000004''$ corresponds to roughly 2×10^{-11} radians. If SIM PlanetQuest is just able to resolve a change in the length of a blade of grass in one second, the spacecraft would need to be at a distance of

$$d = \frac{8 \times 10^{-8}\ \text{m s}^{-1}}{2 \times 10^{-11}\ \text{s}^{-1}} = 4\ \text{km}.$$

3.6 Equations (3.6) and (3.8) combine to give

$$m - 5\log_{10}\left(\frac{d}{10\ \text{pc}}\right) = M_{\text{Sun}} - 2.5\log_{10}\left(\frac{L}{L_\odot}\right).$$

Use the inverse square law, Eq. (3.2), to substitute $L = 4\pi d^2 F$ and $L_\odot = 4\pi(10\ \text{pc})^2 F_{10,\odot}$. The distance terms then cancel, resulting in Eq. (3.9).

3.7 (a) Use Eq. (3.13) for the force due to radiation pressure for an absorbing surface, and set $\theta = 0$. $\langle S \rangle$ is just the solar constant, $\langle S \rangle = 1365\ \text{W m}^{-2}$. From Newton's second law with $a = 9.8\ \text{m s}^{-1}$, the sail area is

$$A = \pi r^2 = \frac{cF_{\text{rad}}}{\langle S \rangle} = \frac{cma}{\langle S \rangle}.$$

Solving for the sail's radius gives $r = 91$ km. (The spacecraft is already orbiting the Sun, so the Sun's gravity is not included in this calculation.)

(b) The radiation pressure force for a reflecting surface, Eq. (3.14), is twice as great as for part (a), so the sail's radius is smaller by a factor of $\sqrt{2}$: $r = 64$ km.

3.8 (a) From the Stefan–Boltzmann equation, Eq. (3.16), $L = A\sigma T^4 = 696$ W.

(b) Wien's displacement law, Eq. (3.15), shows that $\lambda_{\text{max}} = 9477$ nm, in the infrared region of the electromagnetic spectrum.

(c) Again from Eq. (3.16), $L = 585$ W.

(d) The net energy per second lost is 696 W − 585 W = 111 W.

3.9 (a) The star's luminosity is (Eq. 3.17)

$$L = 4\pi R^2 \sigma T_e^4 = 1.17 \times 10^{31}\ \text{W} = 30{,}500\ \text{L}_\odot.$$

(b) From Eq. (3.7),

$$M = M_{\text{Sun}} - 2.5\log_{10}(L/L_\odot) = -6.47,$$

with $M_{\text{Sun}} = 4.74$ for the Sun's absolute bolometric magnitude.

(c) The star's apparent bolometric magnitude comes from Eq. (3.6):

$$m = M + 5\log_{10}(d/10\ \text{pc}) = -1.02.$$

(d) $m - M = 5.45$.

(e) Equation (3.18) gives the surface flux,

$$F = \sigma T_e^4 = 3.48 \times 10^{10}\ \text{W m}^{-2}.$$

(f) At the Earth, the inverse square law (Eq. 3.2) with $r = 123$ pc $= 3.8 \times 10^{18}$ m gives

$$F = \frac{L}{4\pi r^2} = 6.5 \times 10^{-8} \text{ W m}^{-2}.$$

This is 4.7×10^{-11} of the solar constant.

(g) Wien's law in the form of Eq. (3.19) shows that

$$\lambda_{\max} = \frac{(500 \text{ nm})(5800 \text{ K})}{28{,}000 \text{ K}} = 104 \text{ nm}.$$

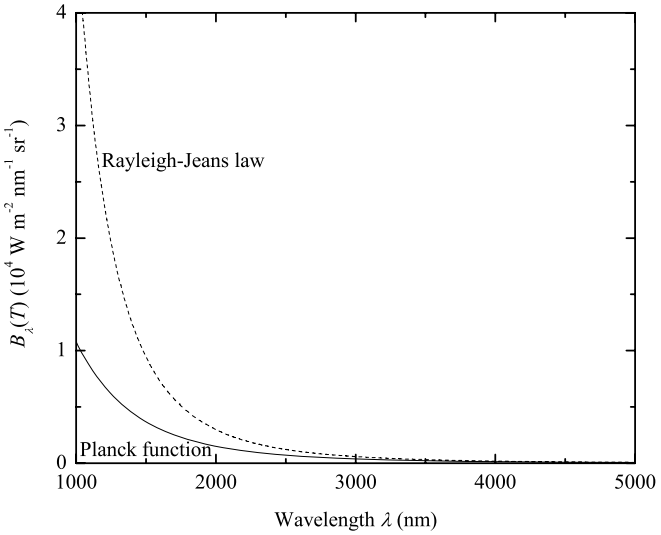

Figure S3.1: Results for Problem 3.10. The Planck function (solid line) and the Rayleigh–Jeans law (dashed line) are shown.

3.10 (a) When $\lambda \gg hc/kT$, we can approximate the denominator of the Planck function, Eq. (3.22), as

$$e^{hc/\lambda kT} - 1 \simeq 1 + \frac{hc}{\lambda kT} - 1 = \frac{hc}{\lambda kT}.$$

Inserting this into the Planck function results in the Rayleigh–Jeans law, $B_\lambda(T) \simeq 2ckT/\lambda^4$.

(b) As seen from Fig. S3.1, the Rayleigh–Jeans value is twice as large as the Planck function when $\lambda \simeq 2000$ nm.

3.11 At sufficiently short wavelengths, the exponential term in the denominator of Planck's function dominates, meaning that $e^{hc/\lambda kT} \gg 1$. Thus

$$B_\lambda \approx \left(2hc^2/\lambda^5\right) e^{-hc/\lambda kT},$$

which is just Eq. (3.21).

3.12 An extremum in the Planck function (Eq. 3.22),

$$B_\lambda = \frac{2hc^2/\lambda^5}{e^{hc/\lambda kT} - 1},$$

occurs when $dB_\lambda/d\lambda = 0$.

$$\frac{dB_\lambda}{d\lambda} = \frac{-10hc^2/\lambda^6}{e^{hc/\lambda kT}-1} - \frac{2hc^2/\lambda^5}{\left(e^{hc/\lambda kT}-1\right)^2}\left(-\frac{hc}{\lambda^2 kT}\right)e^{hc/\lambda kT} = 0,$$

which simplifies to

$$5\left(e^{hc/\lambda kT}-1\right) = \left(\frac{hc}{\lambda kT}\right)e^{hc/\lambda kT}.$$

Defining $x \equiv hc/\lambda kT$, this becomes

$$5(e^x - 1) = xe^x$$

which cannot be solved analytically. A numerical solution leads to $x = hc/\lambda_{\max}kT = 4.97$. Inserting values for h, c, and k results in $\lambda_{\max}T = 0.0029$ m K, which is Wien's law (Eq. 3.15).

3.13 (a) An extremum in the Planck function (Eq. 3.24),

$$B_\nu = \frac{2h\nu^3/c^2}{e^{h\nu/kT}-1},$$

occurs when $dB_\nu/d\nu = 0$.

$$\frac{dB_\nu}{d\nu} = \frac{6h\nu^2/c^2}{e^{h\nu/kT}-1} - \frac{2h\nu^3/c^2}{\left(e^{h\nu/kT}-1\right)^2}\left(\frac{h}{kT}\right)e^{h\nu/kT} = 0,$$

which simplifies to

$$3\left(e^{h\nu/kT}-1\right) = \left(\frac{h\nu}{kT}\right)e^{h\nu/kT}.$$

Defining $x \equiv h\nu/kT$, this becomes

$$3(e^x - 1) = xe^x$$

which cannot be solved analytically. A numerical solution leads to $x = h\nu_{\max}/kT = 2.82$. Inserting values for h and k results in $\nu_{\max}/T = 5.88 \times 10^{10}$ s^{-1} K^{-1}.

(b) Using $T_e = 5777$ K for the Sun, $\nu_{\max} = 3.40 \times 10^{14}$ Hz.

(c) $c/\nu_{\max} = 883$ nm, which is in the infrared region of the electromagnetic spectrum.

3.14 (a) Integrate Eq. (3.27) over all wavelengths,

$$L = \int_0^\infty L_\lambda\, d\lambda = \int_0^\infty \frac{8\pi^2 R^2 hc^2/\lambda^5}{e^{hc/\lambda kT}-1}\, d\lambda.$$

Defining $u = hc/\lambda kT$, the luminosity becomes

$$L = \frac{8\pi^2 R^2 k^4 T^4}{c^2 h^3}\int_0^\infty \frac{u^3\, du}{e^u - 1}.$$

The value of the integral is $\pi^4/15$, so

$$L = \frac{8\pi^6 R^2 k^4 T^4}{15c^2 h^3}.$$

(b) By comparing the result of part (a) with the Stefan–Boltzmann equation ($L = 4\pi R^2 \sigma T^4$, Eq. 3.17), we find that the Stefan–Boltzmann constant is given by

$$\sigma = \frac{2\pi^5 k^4}{15c^2 h^3}.$$

(c) Inserting values of k, c, and h results in

$$\sigma = 5.670400 \times 10^{-8} \text{ W m}^{-2} \text{ K}^{-4},$$

in perfect agreement with the value listed in Appendix A.

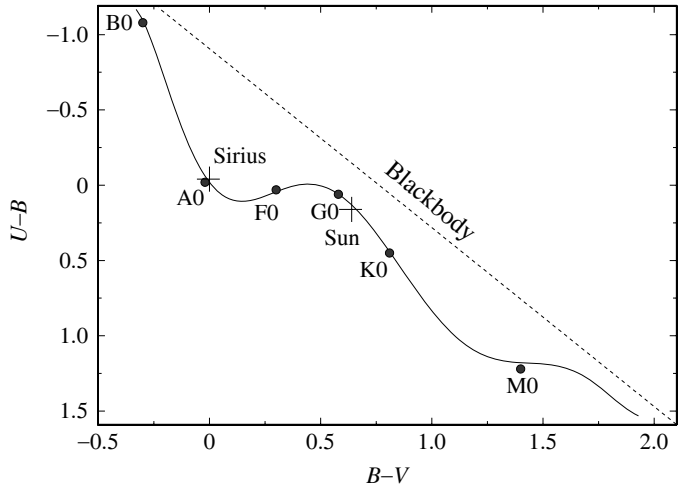

Figure S3.2: Results for Problem 3.15. This shows the locations of the Sun and Sirius on a color–color diagram.

3.15 (a) From Appendix G, the Sun's absolute visual magnitude is $M_V = 4.82$. From Example 3.2.2, the Sun's distance modulus is $m - M = -31.57$. Thus $V = M_V - 31.57 = -26.74$.

(b) From Appendix G, $B - V = 0.650$ and $U - B = 0.195$ for the Sun. So $B = V + 0.650 = -26.1$ and $M_B = B + 31.57 = 5.47$, while $U = B + 0.195 = -25.9$ and $M_U = U + 31.57 = 5.67$.

(c) See Fig. S3.2.

3.16 To find the filter through which Vega would appear brightest, we can take ratios of the radiant fluxes received through the filters. For the U and B filters, Eq. (3.31) shows that we are interested in

$$\frac{\int_0^\infty F_\lambda \mathcal{S}_U \, d\lambda}{\int_0^\infty F_\lambda \mathcal{S}_B \, d\lambda}.$$

The central wavelength of the U filter is $\lambda_U = 365$ nm, and $\Delta\lambda_U = 68$ nm is the bandwidth of the U filter. Similarly, for the B filter $\lambda_B = 440$ nm with $\Delta\lambda_B = 98$ nm, and for the V filter $\lambda_V = 550$ nm with $\Delta\lambda_V = 89$ nm. Assuming that $\mathcal{S} = 1$ inside the filter bandwidth and $\mathcal{S} = 0$ otherwise, and employing Eq. (3.29) for the monochromatic flux, the integrals can be approximated to obtain,

$$\frac{\int_0^\infty F_\lambda \mathcal{S}_U \, d\lambda}{\int_0^\infty F_\lambda \mathcal{S}_B \, d\lambda} \simeq \left(\frac{\lambda_B}{\lambda_U}\right)^5 \frac{e^{hc/\lambda_B kT} - 1}{e^{hc/\lambda_U kT} - 1} \left(\frac{\Delta\lambda_U}{\Delta\lambda_B}\right) = 0.862$$

for $T = 9600$ K. In the same manner,

$$\frac{\int_0^\infty F_\lambda \mathcal{S}_U \, d\lambda}{\int_0^\infty F_\lambda \mathcal{S}_V \, d\lambda} \simeq 1.42 \quad \text{and} \quad \frac{\int_0^\infty F_\lambda \mathcal{S}_B \, d\lambda}{\int_0^\infty F_\lambda \mathcal{S}_V \, d\lambda} \simeq 1.64.$$

So Vega would appear brightest when viewed through the B filter and faintest through the V filter.

3.17 From Eq. (3.32) and Eq. (3.29) for the monochromatic flux,

$$m_{\rm bol} = -2.5\log_{10}\left(\int_0^\infty F_\lambda\, d\lambda\right) + C_{\rm bol}$$

$$m_{\rm bol} = -2.5\log_{10}\left(\frac{\int_0^\infty L_\lambda\, d\lambda}{4\pi r^2}\right) + C_{\rm bol}$$

$$m_{\rm bol} = -2.5\log_{10}\left(\frac{L_\odot}{4\pi r^2}\right) + C_{\rm bol}.$$

At $r = 1$ AU, $L_\odot/4\pi r^2$ is just the solar constant. We have

$$-26.83 = -2.5\log_{10}(1365) + C_{\rm bol}$$

so $C_{\rm bol} = -18.99$.

3.18 According to Eq. (3.33) and Example 3.6.2,

$$U - B = -2.5\log_{10}\left(\frac{B_{365}\,\Delta\lambda_U}{B_{440}\,\Delta\lambda_B}\right) + C_{U-B}$$

and similarly for $B - V$. Here, B_{365} is the Planck function evaluated at the central wavelength of the U filter ($\lambda_U = 365$ nm) and $\Delta\lambda_U = 68$ nm is the bandwidth of the U filter. Similar expressions describe the B filter (centered at $\lambda_B = 440$ nm with $\Delta\lambda_B = 98$ nm) and the V filter (centered at $\lambda_V = 550$ nm with $\Delta\lambda_V = 89$ nm). From Example 3.6.2, the constants are $C_{U-B} = -0.87$ and $C_{B-V} = 0.65$. From Eq. (3.22) for the Planck function, we find for $T = 5777$ K

$$U - B = -2.5\log_{10}\left[\left(\frac{\lambda_B}{\lambda_U}\right)^5 \frac{e^{hc/\lambda_B kT} - 1}{e^{hc/\lambda_U kT} - 1}\left(\frac{\Delta\lambda_U}{\Delta\lambda_B}\right)\right] + C_{U-B} = -0.22,$$

which is quite different than the actual value of $U - B = +0.195$ for the Sun. In the same manner, the estimated value of $B - V$ is $+0.57$, which is in fair agreement with the actual value of $B - V = +0.65$ for the Sun.

3.19 (a) Following the procedure for Problem 3.18 with $T = 22{,}000$ K gives estimates of $U - B = -1.08$ (actual value is $U - B = -0.90$) and $B - V = -0.23$ (the value measured for Shaula).

(b) A parallax angle of $0.00464''$ implies a distance to Shaula of $d = 1/p = 216$ pc. From Eq. (3.6) and $V = 1.62$, $M_V = -5.05$.

CHAPTER 4

The Theory of Special Relativity

4.1 Inserting Eqs. (4.10)–(4.13) into Eq. (4.15) and simplifying results in

$$(a_{11}^2 - a_{41}^2c^2)x^2 - 2(a_{11}^2u + a_{41}a_{44}c^2)xt + y^2 + z^2 = (-a_{11}^2u^2 + a_{44}^2c^2)t^2.$$

For this to agree with Eq. (4.14), $x^2 + y^2 + z^2 = (ct)^2$, requires that

$$a_{11}^2 - a_{41}^2c^2 = 1$$

$$a_{11}^2u + a_{41}a_{44}c^2 = 0$$

$$-a_{11}^2u^2 + a_{44}^2c^2 = c^2$$

Solving these yields the values of a_{11}, a_{44}, and a_{41} given in the text.

4.2 Assume that events A and B occur on the x-axis. We can assume with no loss of generality that $x_B > x_A$ and that event A caused event B [so light has time to travel from A to B: $0 < x_B - x_A < c(t_B - t_A)$]. From Eq. (4.19), the time interval between events A and B as measured in frame S' is

$$t_B' - t_A' = \frac{(t_B - t_A) - u/c^2(x_B - x_A)}{\sqrt{1 - u^2/c^2}}.$$

As measured in frame S', event B will occur after event A ($t_B' - t_A' > 0$) if the numerator on the right-hand side is positive.

$$\text{numerator} = (t_B - t_A) - u/c^2(x_B - x_A)$$

$$= (t_B - t_A)\left\{1 - \left(\frac{u}{c}\right)\left[\frac{x_B - x_A}{c(t_B - t_A)}\right]\right\} > 0$$

because $u/c < 1$ and $0 < x_B - x_A < c(t_B - t_A)$. Thus $t_B' - t_A' > 0$, and cause precedes effect; event A occurs before event B, as measured in frame S'.

4.3 As measured in frame S, in time $\Delta t/2$ the mirror moves forward a distance $u\Delta t/2$ while the light ray travels a path of length $c\Delta t/2$. From the Pythagorean theorem,

$$\left(\frac{c\Delta t}{2}\right)^2 = \left(\frac{u\Delta t}{2}\right)^2 + d^2$$

while as measured in frame S', $d^2 = (c\Delta t'/2)^2$. Eliminating d gives

$$\left(\frac{c\Delta t}{2}\right)^2 = \left(\frac{u\Delta t}{2}\right)^2 + \left(\frac{c\Delta t'}{2}\right)^2.$$

Solving for Δt gives Eq. (4.26),

$$\Delta t = \frac{\Delta t'}{\sqrt{1 - u^2/c^2}}.$$

Identifying $\Delta t = \Delta t_{\text{moving}}$ and $\Delta t' = \Delta t_{\text{rest}}$ achieves the final result.

4.4 From Eq. (4.29), $L_{\text{moving}}/L_{\text{rest}} = \sqrt{1-u^2/c^2} = 1/2$, so $u/c = 1/\sqrt{2} = 0.866$.

4.5 For this problem, $\sqrt{1-u^2/c^2} = 0.6$.

(a) $\Delta t_P = (60\text{ m})/(0.8c) = 0.250\ \mu\text{s}$.

(b) The rider sees a train at rest of length

$$L_{\text{rest}} = \frac{L_{\text{moving}}}{\sqrt{1-u^2/c^2}} = \frac{60\text{ m}}{0.6} = 100\text{ m}.$$

(c) The rider sees a moving platform of length

$$L_{\text{moving}} = L_{\text{rest}}\sqrt{1-u^2/c^2} = (60\text{ m})(0.6) = 36\text{ m}.$$

(d) $\Delta t_T = (100\text{ m})/(0.8c) = 0.417\ \mu\text{s}$.

(e) According to T, the train is 100 m long and the moving platform is 36 m long. The time T measures for the platform to travel the extra 64 m is $(64\text{ m})/(0.8c) = 0.267\ \mu\text{s}$.

4.6 For this problem, $\sqrt{1-u^2/c^2} = 0.6$. When distances are given in light years, it is handy to express $c = 1\text{ ly yr}^{-1}$.

(a) The two events are the starship leaving Earth and arriving at α Centauri. According to an observer on Earth, these events occur at different locations, so the time measured by a clock on Earth is

$$(\Delta t)_{\text{moving}} = \frac{4\text{ ly}}{0.8c} = 5\text{ yr}.$$

(b) The starship pilot is at rest relative to the two events; they both occur just outside the door of the starship. According to the pilot, the trip takes

$$(\Delta t)_{\text{rest}} = (\Delta t)_{\text{moving}}\sqrt{1-u^2/c^2} = 3\text{ yr}.$$

(c) Using $L_{\text{rest}} = 4$ ly, the distance measured by the starship pilot may be found from

$$L_{\text{moving}} = L_{\text{rest}}\sqrt{1-u^2/c^2} = 2.4\text{ ly}.$$

(d) According to Eq. (4.31) with $\Delta t_{\text{rest}} = 6$ months and $\theta = 0$, the time interval between receiving the signals aboard the starship is

$$\Delta t_{\text{obs}} = \frac{\Delta t_{\text{rest}}(1+u/c)}{\sqrt{1-u^2/c^2}} = 18\text{ months}.$$

(e) The same as part (d).

(f) From the relativistic Doppler shift, Eq. (4.35),

$$\lambda_{\text{obs}} = \lambda_{\text{rest}}\sqrt{\frac{1+v_r/c}{1-v_r/c}} = (15\text{ cm})\sqrt{\frac{1+0.8}{1-0.8}} = 45\text{ cm}.$$

4.7 According to an observer on Earth, the signal sent from the starship just as it arrives at α Centauri reaches Earth 5 yr + 4 yr = 9 yr after the ship left Earth. The signals sent by the outbound starship arrive at 18 month intervals, when

$$t_E(\text{months}) = 0, 18, 36, 54, 72, 90, 108.$$

During the remaining year of the ten-year roundtrip journey (as measured on Earth), the signals reach Earth more frequently. According to Eq. (4.31) with $\Delta t_{\text{rest}} = 6$ months and $\theta = 180°$, the time interval between receiving the signals on Earth is

$$\Delta t_{\text{obs}} = \frac{\Delta t_{\text{rest}}(1 - u/c)}{\sqrt{1 - u^2/c^2}} = 2 \text{ months}.$$

The rest of the signals arrive on Earth at

$$t_E(\text{months}) = 110, 112, 114, 116, 118, 120.$$

The Earth observer has received 12 signals (not including $t_E = 0$), and so concludes that 6 years have passed onboard the starship during the round-trip journey to α Centauri, although ten years have passed on Earth.

According to the starship pilot, while outbound the starship receives a signal when

$$t_S(\text{months}) = 0, 18, 36.$$

At that point, the starship immediately reverses direction and travels back toward Earth. Again according to Eq. (4.31) with $\Delta t_{\text{rest}} = 6$ months and $\theta = 180°$, during the return trip the time interval between receiving the signals aboard the starship is 2 months. So the starship receives a signal from Earth when

$$t_S(\text{months}) = 38, 40, 42, 44, 46, 48, 50, 52, 54,$$
$$56, 58, 60, 62, 64, 66, 68, 70, 72.$$

At that point, the starship arrives at Earth. The starship has received 20 signals (not including $t_S = 0$), so the starship pilot deduces that 10 years have passed on Earth during the round-trip journey to α Centauri, although the pilot has aged only six years.

4.8 The redshift parameter for the quasar Q2203+29 is (Eq. 4.34)

$$z = \frac{\lambda_{\text{obs}} - \lambda_{\text{rest}}}{\lambda_{\text{rest}}} = \frac{656.8 \text{ nm} - 121.6 \text{ nm}}{121.6 \text{ nm}} = 4.40.$$

From Eq. (4.38), the speed of recession of the quasar is $v_r/c = 0.9337$.

4.9 The redshift parameter for the quasar 3C 446 is $z = 1.404$. From Eq. (4.37), if the quasar's luminosity is observed to vary over a time of $\Delta t_{\text{obs}} = 10$ days, then the time for the luminosity variation as measured in the quasar's rest frame is

$$\Delta t_{\text{rest}} = \frac{\Delta t_{\text{obs}}}{z + 1} = 4.16 \text{ days}.$$

4.10 Taking a differential of Eqs. (4.16) and (4.19) gives

$$dx' = \frac{dx - u\,dt}{\sqrt{1 - u^2/c^2}}$$

and

$$dt' = \frac{dt - u/c^2\,dx}{\sqrt{1 - u^2/c^2}}.$$

Dividing the first of these equations by the second, we find

$$\frac{dx'}{dt'} = \frac{dx - u\,dt}{dt - u/c^2\,dx} = \frac{dx/dt - u}{1 - (u/c^2)(dx/dt)}.$$

Substituting $v'_x = dx'/dt'$ and $v_x = dx/dt$ then produces Eq. (4.40).

In a similar manner, the differential version of Eq. (4.17) is $dy' = dy$. Dividing this by the dt' equation yields

$$\frac{dy'}{dt'} = \frac{dy\sqrt{1 - u^2/c^2}}{dt - u/c^2\,dx} = \frac{dy/dt\sqrt{1 - u^2/c^2}}{1 - (u/c^2)(dx/dt)}.$$

Substituting $v'_y = dy'/dt'$, $v_x = dx/dt$ and $v_y = dy/dt$ then produces Eq. (4.41). Equation (4.42) is obtained in the same way.

4.11 (a) As measured in frame S', the spacetime interval is

$$(\Delta s')^2 = (c\Delta t')^2 - (\Delta x')^2 - (\Delta y')^2 - (\Delta z')^2.$$

Using Eqs. (4.16)–(4.19), we have

$$(\Delta s')^2 = \left[\frac{c(\Delta t - u\Delta x/c^2)}{\sqrt{1 - u^2/c^2}}\right]^2 - \left(\frac{\Delta x - u\Delta t}{\sqrt{1 - u^2/c^2}}\right)^2 - (\Delta y)^2 - (\Delta z)^2.$$

After some algebra, this becomes

$$(\Delta s')^2 = \frac{(c^2 - u^2)(\Delta t)^2}{1 - u^2/c^2} + \frac{(u^2/c^2 - 1)(\Delta x)^2}{1 - u^2/c^2} - (\Delta y)^2 - (\Delta z)^2.$$

or

$$(\Delta s')^2 = (c\Delta t)^2 - (\Delta x)^2 - (\Delta y)^2 - (\Delta z)^2 = (\Delta s)^2.$$

(b) The time interval between two events that occur at the same location is the proper time interval, $\Delta\tau$. Setting $\Delta x = 0$, $\Delta y = 0$, and $\Delta z = 0$ and substituting $\Delta t = \Delta\tau$ in the expression for the interval, we find $\Delta s = c\Delta\tau$. The first event could have caused the second event because light had more than enough time to travel the zero distance between the two events.

(c) If $(\Delta s)^2 = 0$, then

$$c\Delta t = \sqrt{(\Delta x)^2 + (\Delta y)^2 + (\Delta z)^2}.$$

This says that light had exactly enough time to travel the distance between the two events. The first event could not have caused the second event unless light itself carried the causal information.

(d) The proper length (which we will call $\Delta\mathcal{L}$) of an object is obtained by measuring the difference in the positions of its ends at the same time. Setting $\Delta t = 0$ and substituting $(\Delta\mathcal{L})^2 = (\Delta x)^2 + (\Delta y)^2 + (\Delta z)^2$ in the expression for the interval, we find $\Delta\mathcal{L} = \sqrt{-(\Delta s)^2}$.

4.12 (a) This is a straightforward substitution.

(b) From the velocity transformations, Eqs. (4.40)–(4.42)

$$v_x{}' = \frac{c\sin\theta\cos\phi - u}{1 - u/c^2(c\sin\theta\cos\phi)}$$

$$v_y{}' = \frac{c\sin\theta\sin\phi\sqrt{1 - u^2/c^2}}{1 - u/c^2(c\sin\theta\cos\phi)}$$

$$v_z{}' = \frac{c\cos\theta\sqrt{1 - u^2/c^2}}{1 - u/c^2(c\sin\theta\cos\phi)}$$

Substituting this into $v' = \sqrt{{v_x}'^2 + {v_y}'^2 + {v_z}'^2}$ results in, after much manipulation,

$$v' = \frac{c}{1 - u/c(\sin\theta\cos\phi)} \times \left(1 - \frac{2u}{c}\sin\theta\cos\phi + \frac{u^2}{c^2}\sin^2\theta\cos^2\phi\right)^{1/2},$$

which is just $v' = c$.

4.13 Identify the frame S with Earth and frame S' with starship A, so $v_A = u = 0.8c$. The velocity of starship B as measured from Earth is $v_B = -0.6c$. Then the velocity of starship B as measured from starship A may be found using the velocity transformation (Eq. 4.40)

$${v_B}' = \frac{v_B - u}{1 - uv_B/c^2} = -0.946c.$$

The velocity of starship A as measured from starship B is then $+0.946c$.

4.14 According to Newton's second law, taking a time derivative of the relativistic momentum (Eq. 4.44) gives the force acting on a particle of mass m.

$$\frac{d\mathbf{p}}{dt} = \frac{d}{dt}\left(\frac{m\mathbf{v}}{\sqrt{1 - v^2/c^2}}\right).$$

Writing $v^2 = \mathbf{v}\cdot\mathbf{v}$ and using $\mathbf{F} = d\mathbf{p}/dt$, we find that

$$\mathbf{F} = \frac{m\,d\mathbf{v}/dt}{\sqrt{1 - v^2/c^2}} + \frac{m\mathbf{v}/c^2}{\left(1 - v^2/c^2\right)^{3/2}}\left(\mathbf{v}\cdot\frac{d\mathbf{v}}{dt}\right).$$

To simplify this, it is useful to take the vector dot product of this equation with the velocity vector.

$$\mathbf{F}\cdot\mathbf{v} = \frac{m\mathbf{v}\cdot d\mathbf{v}/dt}{\sqrt{1 - v^2/c^2}} + \frac{mv^2/c^2}{\left(1 - v^2/c^2\right)^{3/2}}\left(\mathbf{v}\cdot\frac{d\mathbf{v}}{dt}\right),$$

which reduces to

$$\mathbf{v}\cdot\frac{d\mathbf{v}}{dt} = \frac{\left(1 - v^2/c^2\right)^{3/2}}{m}\mathbf{F}\cdot\mathbf{v}.$$

Using this to replace $\mathbf{v}\cdot d\mathbf{v}/dt$ in the expression for $\mathbf{F}$ and solving for $\mathbf{a} = d\mathbf{v}/dt$ leads to the desired result,

$$\mathbf{a} = \frac{\mathbf{F}}{\gamma m} - \frac{\mathbf{v}}{\gamma mc^2}(\mathbf{F}\cdot\mathbf{v}).$$

4.15 (a) The particle starts at rest, so the velocity, force, and acceleration are in the same direction. In this case, the result of Problem 4.14 simplifies to

$$a = \frac{dv}{dt} = \frac{F}{\gamma m}\left(1 - \frac{v^2}{c^2}\right) = \frac{F}{m}\left(1 - \frac{v^2}{c^2}\right)^{3/2}.$$

Now integrate

$$\int_0^v \left(1 - \frac{v^2}{c^2}\right)^{-3/2} dv = \int_0^t \frac{F}{m}\,dt$$

to find

$$\frac{Ft}{m} = \frac{v}{\sqrt{1 - v^2/c^2}}.$$

Solving for v/c, we get

$$\frac{v}{c} = \frac{(F/m)t}{\sqrt{(F/m)^2 t^2 + c^2}}.$$

(b) Solving the above equation for the time t yields

$$t = \frac{1}{F/m} \frac{v}{\sqrt{1 - v^2/c^2}}.$$

If $F/m = g = 980$ cm s^{-2}, then the times to achieve the given speeds are

$$t(0.9c) = 6.32 \times 10^7 \text{ s (2.0 yr)}$$

$$t(0.99c) = 2.15 \times 10^8 \text{ s (6.8 yr)}$$

$$t(0.999c) = 6.84 \times 10^8 \text{ s (21.7 yr)}$$

$$t(0.9999c) = 2.16 \times 10^9 \text{ s (68.6 yr)}$$

$$t(1.0c) = \infty \text{ s (never!)}$$

4.16 From Eq. (4.45), setting the relativistic kinetic energy equal to the rest energy mc^2 gives $mc^2(\gamma - 1) = mc^2$, so $\gamma = 2$. Solving for velocity shows that $v/c = 1/\sqrt{2} = 0.866$.

4.17 From Eq. (4.45), the relativistic kinetic energy is

$$K = mc^2 \left(\frac{1}{\sqrt{1 - v^2/c^2}} - 1 \right).$$

At low speeds, $v/c \ll 1$, and we can use the first-order Taylor series $(1 - x^2)^{-1/2} \simeq 1 + x^2/2$. Thus, for low speeds,

$$K \simeq mc^2 \left[\left(1 + \frac{1}{2} \frac{v^2}{c^2} \right) - 1 \right] = \frac{1}{2} m v^2.$$

4.18 Begin with Eq. (4.46) for the total relativistic energy, $E = \gamma mc^2$. Squaring both sides and subtracting m^2c^4 from each side results in

$$E^2 - m^2c^4 = m^2c^4 \left(\gamma^2 - 1 \right) = mc^2(\gamma + 1)[mc^2(\gamma - 1)].$$

From Eq. (4.48), the left-hand side is equal to p^2c^2, while the term on the right-hand side in square brackets is the relativistic kinetic energy (Eq. 4.45). So

$$p^2c^2 = mc^2(\gamma + 1)K,$$

Solving for K gives

$$K = \frac{p^2}{(1 + \gamma)m}.$$

4.19 According to Eqs. (4.46) and (4.44), the total relativistic energy and relativistic momentum are $E = \gamma mc^2$ and $p = \gamma mv$. Multiplying the momentum by c, then squaring both equations and subtracting produces

$$E^2 - p^2c^2 = \gamma^2 m^2 c^4 - \gamma^2 m^2 v^2 c^2 = \gamma^2 m^2 c^4 \left(1 - \frac{v^2}{c^2} \right).$$

Because $\gamma^2 = 1/(1 - v^2/c^2)$, this reduces to $E^2 = p^2c^2 + m^2c^4$, which is the desired result.

CHAPTER 5

The Interaction of Light and Matter

5.1 (a) The rest wavelength for the Hα spectral line is $\lambda_{\rm rest} = 656.281$ nm. From Eq. (5.1), the radial velocity of Barnard's star is

$$v_r = \frac{c\,(\lambda_{\rm obs} - \lambda_{\rm rest})}{\lambda_{\rm rest}} = -113 \text{ km s}^{-1}.$$

(b) From Eq. (3.1), $d = (1/p'')$ pc $= 1.82$ pc. The transverse velocity of Barnard's star is (Eq. 1.5) $v_\theta = d\,\mu = 89.4$ km s^{-1}.

(c) $v = \sqrt{v_r^2 + v_\theta^2} = 144$ km s^{-1}.

5.2 (a) The distance between the grating's lines is $d = 3.33 \times 10^{-6}$ m. Using $d \sin\theta = n\lambda$ with $n = 2$, the angles are 20.695° for $\lambda = 588.997$ nm, and 20.717° for $\lambda = 589.594$ nm. The angle between the second-order spectra of these two lines is therefore $\Delta\theta = 0.0219$ Å.

(b) From Eq. (5.2), the number of lines that must be illuminated is

$$N = \frac{\lambda}{n\Delta\lambda} = 494,$$

where the average wavelength $\lambda = 589.296$ nm was used.

5.3 Using the values provided in Appendix A, it is found that $hc = 1239.8$ eV nm $\simeq 1240$ eV nm.

5.4 From Eq. (5.4),

$$\phi = \frac{hc}{\lambda} - K_{\rm max} = \frac{1240 \text{ eV nm}}{100 \text{ nm}} - 5 \text{ eV} = 7.4 \text{ eV}.$$

5.5 Referring to Figure 5.3, conservation of momentum gives

$$p_i = p_f \cos\theta + p_e \cos\phi$$

$$0 = p_f \sin\theta - p_e \sin\phi,$$

where p_i and p_f are the initial and final photon momenta, respectively, and p_e is the momentum of the recoiling electron. Rewriting these equations so that only terms involving the angle ϕ are on the right-hand side, and then squaring both equations and adding produces

$$p_i^2 - 2p_i p_f \cos\theta + p_f^2 = p_e^2.$$

Now multiply each side by c^2 and add $m_e^2 c^4$ to both sides. Using $E_i = p_i c$ and $E_f = p_f c$ (Eq. 5.5) for the initial and final photon energies, we find

$$m_e^2 c^4 + E_i^2 - 2E_i E_f \cos\theta + E_f^2 = p_e^2 c^2 + m_e^2 c^4 = E_e^2,$$

where the last term on the right comes from Eq. (4.48) for the total relativistic energy of the electron. However, the expression for the conservation of the total relativistic energy,

$$E_i + m_e c^2 = E_f + E_e$$

can be used to replace E_e in the preceding equation,

$$m_e^2c^4 + E_i^2 - 2E_iE_f\cos\theta + E_f^2 = (E_i - E_f + m_ec^2)^2.$$

This simplifies to

$$\frac{1}{E_f} - \frac{1}{E_i} = \frac{1}{m_ec^2}(1 - \cos\theta).$$

Using Eq. (5.5) for the photon energy, $E = hc/\lambda$, results in

$$\Delta\lambda = \lambda_f - \lambda_i = \frac{h}{m_ec}(1 - \cos\theta).$$

5.6 The change of wavelength is given by the Compton scattering formula, Eq. (5.6), but with the electron mass replaced by the proton mass,

$$\Delta\lambda = \lambda_f - \lambda_i = \frac{h}{m_pc}(1 - \cos\theta).$$

The characteristic change in wavelength is $h/m_pc = 1.32 \times 10^{-6}$ nm. This is smaller than the value of the Compton wavelength, $\lambda_C = h/m_ec = 0.00243$ nm, by a factor of $m_e/m_p = 5.4 \times 10^{-4}$.

5.7 Planck's constant has units of

$$\text{J s} = [\text{kg m}^2\ \text{s}^{-2}]\ \text{s} = \text{kg}\ [\text{m s}^{-1}]\ \text{m},$$

which are the units of angular momentum (mvr).

5.8 (a) For an atom with Z protons in the nucleus (charge Ze) and one electron (charge $-e$), Coulomb's law (Eq. 5.9) becomes

$$\mathbf{F} = -\frac{1}{4\pi\epsilon_0}\frac{Ze^2}{r^2}\hat{\mathbf{r}},$$

and the electrical potential energy becomes

$$U = -\frac{1}{4\pi\epsilon_0}\frac{Ze^2}{r}.$$

This means that the quantity "e^2" should be replaced by "Ze^2" wherever it appears in an expression for the hydrogen atom. Similarly, "e^4" should be replaced by "Z^2e^4." The result will be the corresponding expression for a one-electron atom with Z protons. From Eq. (5.13), the orbital radii are therefore

$$r_n = \frac{4\pi\epsilon_0\hbar^2}{\mu Ze^2}n^2 = \frac{a_0}{Z}n^2,$$

where $a_0 = 0.0529$ nm. The energies are

$$E_n = -\frac{\mu Z^2e^4}{32\pi^2\epsilon_0^2\hbar^2}\frac{1}{n^2} = -13.6\text{ eV}\frac{Z^2}{n^2}$$

from Eq. (5.14).

(b) $Z = 2$ for singly ionized helium (He II), and so for the ground state ($n = 1$),

$$r_1 = \frac{a_0}{2}(1^2) = 0.0265\text{ nm}$$

and

$$E_1 = -13.6\text{ eV}\frac{2^2}{1^2} = -54.4\text{ eV}.$$

The ionization energy is 54.4 eV.

(c) $Z = 3$ for doubly ionized lithium (Li III), and so for the ground state,

$$r_1 = \frac{a_0}{3}(1^2) = 0.0176 \text{ nm}$$

and

$$E_1 = -13.6 \text{ eV} \frac{3^2}{1^2} = -122 \text{ eV}.$$

The ionization energy is 122 eV.

5.9 (a) If the hydrogen atom were held together *solely* by the force of gravity, the force between the proton and electron would be supplied by Newton's law of universal gravitation (Eq. 2.11),

$$\mathbf{F} = -G\frac{m_p m_e}{r^2}\hat{\mathbf{r}},$$

and the potential energy is given by Eq. (2.14),

$$U = -G\frac{m_p m_e}{r}.$$

This means that the quantity "$e^2/4\pi\epsilon_0$" should be replaced by "$Gm_p m_e$" wherever it appears in an expression for the hydrogen atom. Similarly, "$e^4/16\pi^2\epsilon_0^2$" should be replaced by "$G^2 m_p^2 m_e^2$." The result will be the corresponding expression for the gravitational atom. From Eq. (5.13), the ground-state orbital radius ($n = 1$) is therefore

$$r_1 = \frac{\hbar^2}{\mu G m_p m_e} = 1.20 \times 10^{38} \text{ nm} = 8.03 \times 10^{17} \text{ AU}.$$

The ground-state energy is

$$E_1 = -\frac{\mu G^2 m_p^2 m_e^2}{2\hbar^2} = -2.64 \times 10^{-78} \text{ eV}.$$

from Eq. (5.14).

5.10 Use $1/\lambda = R_H(1/n_{\text{low}}^2 - 1/n_{\text{high}}^2)$ (Eq. 5.8 with $m = n_{\text{low}}$ and $n = n_{\text{high}}$) for the hydrogen wavelengths, and $E_{\text{photon}} = hc/\lambda$ (Eq. 5.5) for the photon energy. The possible transitions are $n_{\text{high}} = 3 \to n_{\text{low}} = 1$, $n_{\text{high}} = 3 \to n_{\text{low}} = 2$, and $n_{\text{high}} = 2 \to n_{\text{low}} = 1$. This results in

$$\lambda = 102.6 \text{ nm} \quad \text{and} \quad E_{\text{photon}} = 12.09 \text{ eV} \qquad (\text{for } 3 \to 1),$$

$$\lambda = 656.5 \text{ nm} \quad \text{and} \quad E_{\text{photon}} = \ 1.89 \text{ eV} \qquad (\text{for } 3 \to 2),$$

$$\lambda = 121.6 \text{ nm} \quad \text{and} \quad E_{\text{photon}} = 10.20 \text{ eV} \qquad (\text{for } 2 \to 1).$$

5.11 Use $1/\lambda = R_H(1/n_{\text{low}}^2 - 1/n_{\text{high}}^2)$ (Eq. 5.8 with $m = n_{\text{low}}$ and $n = n_{\text{high}}$) for the hydrogen wavelengths. The shortest wavelengths emitted for the Lyman series ($n_{\text{low}} = 1$), Balmer series ($n_{\text{low}} = 2$), and Paschen series ($n_{\text{low}} = 3$) occur for $n_{\text{high}} = \infty$. The series limits are therefore given by

$$\lambda_\infty = \frac{1}{R_H} n_{\text{low}}^2 = (91.18 \text{ nm}) n_{\text{low}}^2.$$

So

$$\lambda_\infty = 91.18 \text{ nm} \quad (\text{ultraviolet})$$

for the Lyman series limit,

$$\lambda_\infty = 364.7 \text{ nm} \quad \text{(near ultraviolet)}$$

for the Balmer series limit, and

$$\lambda_\infty = 820.6 \text{ nm} \quad \text{(infrared)}$$

for the Paschen series limit.

5.12 The wavelength of the electron is given by Eq. (5.17),

$$\lambda = \frac{h}{p} = \frac{h}{m_e v} = 1.45 \times 10^{-11} \text{ m} = 0.0145 \text{ nm}.$$

5.13 If the circumference of the electron's orbit is an integral number, n, of de Broglie wavelengths as shown in Fig. 5.15, then from Eq. (5.17)

$$n\lambda = \frac{nh}{p} = 2\pi r.$$

The momentum is $p = \mu v$ (using the reduced mass), so this may be expressed as $\mu v r = nh/2\pi$ or $L = n\hbar$, Bohr's condition for the quantization of angular momentum.

5.14 As shown in Example 5.4.2, the minimum speed of a particle (in this case, an electron) can be estimated using Heisenberg's uncertainty relation, Eq. (5.19), as

$$v_{\text{min}} = \frac{p_{\text{min}}}{m_e} \approx \frac{\Delta p}{m_e} \approx \frac{\hbar}{m_e \Delta x}.$$

With $\Delta x \approx 1.5 \times 10^{-12}$ m, the minimum speed of the electron is $v_{\text{min}} \approx 7.7 \times 10^7$ m s^{-1}, about 26% of the speed of light. Relativistic effects are important for white dwarf stars.

5.15 (a) From Eq. (5.20) with $\Delta t \approx 10^{-8}$ s, for the first excited state ($n = 2$) of hydrogen

$$\Delta E_2 \approx \frac{\hbar}{\Delta t} = 1.1 \times 10^{-26} \text{ J} = 6.9 \times 10^{-8} \text{ eV}.$$

(b) The wavelength of a photon involved in a transition between the ground state ($n = 1$) and the first excited state ($n = 2$) is given by $E_{\text{photon}} = E_2 - E_1$. From Eq. (5.3),

$$\frac{hc}{\lambda} = E_2 - E_1.$$

The uncertainty in λ caused by an uncertainty in E_2 is found by taking a derivative with respect to E_2 (holding E_1 constant):

$$-\frac{hc}{\lambda^2}\frac{d\lambda}{dE_2} = 1.$$

Writing $\Delta\lambda$ instead of $d\lambda$, ΔE_2 instead of dE_2, and ignoring the minus sign gives

$$\Delta\lambda = \frac{\lambda^2}{hc}\Delta E_2.$$

Similarly, the uncertainty in λ due to an uncertainty in E_1 is

$$\Delta\lambda = \frac{\lambda^2}{hc}\Delta E_1.$$

However, an electron can spend an arbitrarily long time in the ground state. For that reason, Δt is infinite and so $\Delta E_1 \approx \hbar/\Delta t = 0$. Thus

$$\Delta\lambda \approx \frac{\lambda^2}{hc}\,\Delta E_2.$$

From Eq. (5.8) with $m = 1$ and $n = 2$, the wavelength of the photon involved in this transition is 121.6 nm, so

$$\Delta\lambda \approx \frac{(121.6\text{ nm})^2}{1240\text{ eV·nm}}\,(6.9\times10^{-8}\text{ eV}) = 8.2\times10^{-7}\text{ nm}.$$

5.16 (a) The answers for $n = 1$ and $n = 2$ are in Table 8.2. For $n = 3$, the quantum numbers are

$$\begin{array}{llll}
n=3 & \ell=0 & m_\ell=0 & m_s=\pm1/2\\
n=3 & \ell=1 & m_\ell=1 & m_s=\pm1/2\\
n=3 & \ell=1 & m_\ell=0 & m_s=\pm1/2\\
n=3 & \ell=1 & m_\ell=-1 & m_s=\pm1/2\\
n=3 & \ell=2 & m_\ell=2 & m_s=\pm1/2\\
n=3 & \ell=2 & m_\ell=1 & m_s=\pm1/2\\
n=3 & \ell=2 & m_\ell=0 & m_s=\pm1/2\\
n=3 & \ell=2 & m_\ell=-1 & m_s=\pm1/2\\
n=3 & \ell=2 & m_\ell=-2 & m_s=\pm1/2
\end{array}$$

(b) In Table 8.2, for $n = 1$ there are $2n^2 = 2$ entries, and for $n = 2$ there are $2n^2 = 8$ entries. In the list above for $n = 3$, there are $2n^2 = 18$ entries. These are in agreement with the idea that the degeneracy of energy level n (denoted g_n) is $g_n = 2n^2$. In general, if the degeneracy of energy level n is $g_n = 2n^2$, then the degeneracy of energy level $n + 1$ is greater by an additional $2(2n + 1)$: the "$2n + 1$" is for the $2\ell+1$ values of m_ℓ when $\ell = n$, and the leading "2" is for the two values of m_s. That is, the degeneracy of energy level $n + 1$ is

$$g_{n+1} = g_n + 2(2n + 1) = 2n^2 + 2(2n + 1) = 2(n^2 + 2n + 1) = 2(n + 1)^2.$$

Because we know that $g_n = 2n^2$ for $n = 1$, this proof-by-induction shows that it holds for all values of n.

5.17 From Eq. (5.22), the normal Zeeman effect produces a frequency splitting given by

$$\Delta\nu = \frac{eB}{4\pi\mu} = 4.76\times10^{10}\text{ Hz}.$$

Using $\nu_0 = c/\lambda_0$ with $\lambda_0 = 656.281$ nm shows that the frequencies are

$$\begin{aligned}
\nu_0 + \Delta\nu &= 4.56853\times10^{14}\text{ Hz}\\
\nu_0 &= 4.56806\times10^{14}\text{ Hz}\\
\nu_0 - \Delta\nu &= 4.56758\times10^{14}\text{ Hz}.
\end{aligned}$$

The corresponding wavelengths are

$$\begin{aligned}
\frac{c}{\nu_0 + \Delta\nu} &= 656.212\text{ nm}\\
\frac{c}{\nu_0} &= 656.281\text{ nm}\\
\frac{c}{\nu_0 - \Delta\nu} &= 656.349\text{ nm}.
\end{aligned}$$

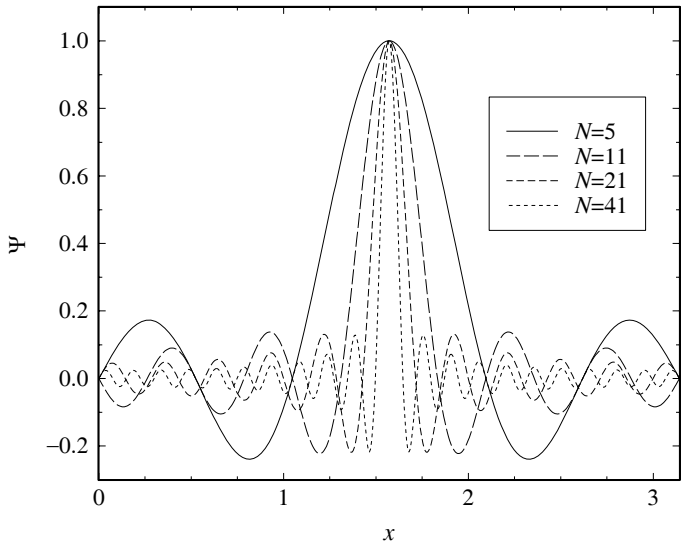

Figure S5.1: Results for Problem 5.18. Four wave pulses, Ψ, are constructed from a Fourier sine series.

5.18 See Fig. S5.1 for the graphs of $\Psi(x)$. If we take Δx to be the width of the graph where $\Psi = 0.5$, then

(a) $\Delta x \simeq 0.64$ when $N = 5$.

(b) $\Delta x \simeq 0.31$ when $N = 11$.

(c) $\Delta x \simeq 0.18$ when $N = 21$.

(d) $\Delta x \simeq 0.09$ when $N = 41$.

(e) The position of the particle is known with the least uncertainty for $N = 41$, when the graph of Ψ is most sharply peaked. The momentum of the particle is known with the least uncertainty for $N = 5$, when the graph of Ψ involves only three wavelengths (and hence only three momenta, $p = h/\lambda$).

CHAPTER 6

Telescopes

6.1 $\Omega_{\text{tot}} = \oint d\Omega = \int_{\phi=0}^{2\pi} \int_{\theta=0}^{\pi} \sin\theta \, d\theta \, d\phi = 4\pi.$

6.2 (a) Referring to Fig. S6.1, from similar triangles

$$\frac{h_o}{p} = \frac{h_i}{q} \qquad \text{and} \qquad \frac{h_o}{f} = \frac{h_i}{q - f}.$$

This implies that

$$\frac{h_o}{h_i} = \frac{p}{q} = \frac{f}{q - f}.$$

Rearranging,

$$\frac{1}{f} = \frac{1}{p} + \frac{1}{q}.$$

(b) If $p \gg f$, then

$$\frac{1}{f} - \frac{1}{q} \simeq 0,$$

which leads to $f \simeq q$.

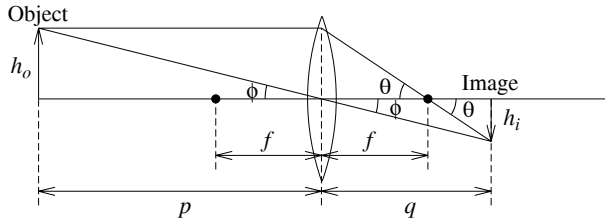

Figure S6.1: The ray diagram for the converging lens discussed in Problem 6.2.

6.3 For the first lens encountered by the incoming light

$$\frac{1}{q_1} = \frac{1}{f_1} - \frac{1}{p_1}.$$

The image of the first lens becomes the object (virtual) for the second lens, so $p_2 = -q_1$. Substituting into the previous expression,

$$\frac{1}{p_2} = \frac{1}{p_1} - \frac{1}{f_1}.$$

Using the relation for the second lens

$$\frac{1}{p_2} + \frac{1}{q_2} = \frac{1}{f_2} \qquad \text{leads to} \qquad \frac{1}{p_1} + \frac{1}{q_2} = \frac{1}{f_1} + \frac{1}{f_2}.$$

Assuming that the two lenses are close together, we can make the approximations that the object and image distances are essentially $p \simeq p_1$ and $q \simeq q_2$. Thus

$$\frac{1}{p} + \frac{1}{q} = \frac{1}{f_{\text{eff}}} \simeq \frac{1}{f_1} + \frac{1}{f_2}.$$

6.4 (a) From the lensmaker's formula (Eq. 6.2) for two lenses having different indexes of refraction but the same radii of curvature,

$$\frac{1}{f_1(\lambda)} = (n_{1,\lambda} - 1)\left(\frac{1}{R_1} + \frac{1}{R_2}\right)$$

$$\frac{1}{f_2(\lambda)} = (n_{2,\lambda} - 1)\left(\frac{1}{R_1} + \frac{1}{R_2}\right).$$

The effective focal length at a particular wavelength is now found using the result of Problem 6.3,

$$\frac{1}{f_{\text{eff},\lambda}} = (n_{1,\lambda} + n_{2,\lambda})\left(\frac{1}{R_1} + \frac{1}{R_2}\right) - 2\left(\frac{1}{R_1} + \frac{1}{R_2}\right).$$

If $f_{\text{eff},\lambda_1} = f_{\text{eff},\lambda_2}$ for two specific wavelengths, then

$$n_{1,\lambda_1} + n_{2,\lambda_1} = n_{1,\lambda_2} + n_{2,\lambda_2},$$

or

$$(n_{1,\lambda_1} - n_{1,\lambda_2}) = -(n_{2,\lambda_1} - n_{2,\lambda_2}).$$

(b) The focal lengths could remain equal for all wavelengths only if $n_{1,\lambda} = n_{2,\lambda} + \text{constant}$.

6.5 Referring to Fig. 6.15, let the height of the intermediate image (between the eyepiece and the objective) be h. Then

$$\tan\theta = \frac{h}{f_{\text{obj}}} \qquad \text{and} \qquad \tan\phi = \frac{h}{f_{\text{eye}}}.$$

For small angles, $\theta \simeq h/f_{\text{obj}}$ and $\phi \simeq h/f_{\text{eye}}$. Thus, the angular magnification is $m = \phi/\theta = f_{\text{obj}}/f_{\text{eye}}$.

6.6 (a) Since $\sin^2(\beta/2)\Big|_{\theta=0} = 0$ and $(\beta/2)^2\Big|_{\theta=0} = 0$, l'Hôpital's rule must be used to evaluate $I(\theta)$ in the limit as $\theta \to 0$. Differentiating the numerator and evaluating at $\theta = 0$,

$$\left.\frac{d\sin^2(\beta/2)}{d\theta}\right|_0 = \left[\sin\left(\frac{\beta}{2}\right)\right]\left[\cos\left(\frac{\beta}{2}\right)\right]\left(\frac{2\pi D}{\lambda}\cos\theta\right)\Bigg|_0 = 0.$$

Similarly, differentiating the denominator and evaluating at $\theta = 0$,

$$\left.\frac{d(\beta/2)^2}{d\theta}\right|_0 = \frac{\beta}{2}\left(\frac{2\pi D}{\lambda}\cos\theta\right)\Bigg|_0 = 0.$$

Since the ratio of the first derivatives is still undefined, it is necessary to evaluate the second derivatives. This leads to

$$\left.\frac{d^2\sin^2(\beta/2)}{d\theta^2}\right|_0 = \frac{2\pi^2 D^2}{\lambda^2}$$

$$\left.\frac{d^2(\beta/2)^2}{d\theta^2}\right|_0 = \frac{2\pi^2 D^2}{\lambda^2}$$

Since their ratio is unity, $I(0) = I_0$.

(b) The first minimum occurs when $\sin^2(\beta/2) = 0$, or $\beta = 2\pi$. This implies that $\sin\theta = \lambda/D$, or $\theta = 30°$.

6.7 (a) From Eq. (6.6), $\theta_{\rm eye} = 1.34 \times 10^{-4}$ rad $= 28''$.

(b) $\theta_{\rm moon} = 2R/d = 9.0 \times 10^{-3}$ rad $= 1900''$, implying $\theta_{\rm moon}/\theta_{\rm eye} = 33.7$. When Jupiter is at opposition (closest approach to Earth), $\theta_{\rm Jupiter} = 2.3 \times 10^{-4}$ rad $= 47''$, implying $\theta_{\rm Jupiter}/\theta_{\rm eye} = 1.7$. The resolution is worse during all other relative positions of Jupiter and Earth.

(c) It is possible for the disk of the Moon to be resolved with the naked eye. However, the disk of Jupiter is comparable to the eye's resolution limit; to distinguish any features on the surface of Jupiter, they would need to be nearly the size of the planet's disk.

6.8 (a) From Eq. (6.6), $\theta_{\rm min} = 3.4 \times 10^{-6}$ rad $= 0.69''$.

(b) Given the Moon's mean distance of 3.84×10^5 km, the minimum size of a crater that can be resolved is $h = d\theta = 1.3$ km.

(c) Atmospheric turbulence limits the resolution.

6.9 (a) The NTT focal ratio is $f/2.2$ and the diameter of the primary mirror is 3.58 m. From Eq. (6.7), $F = 2.2 = f/3.8$ m, giving $f = 8.36$ m.

(b) From Eq. (6.4), $d\theta/dy = 1/f = 0.120$ rad m^{-1}.

(c) $\Delta\theta = 2.9'' = 1.4 \times 10^{-5}$ rad, implying $\Delta y = f\,\Delta\theta = 11.8\ \mu$m.

6.10 Each of HST's WF/PC 2 CCD's is 800 pixels wide. With a plate scale of $0.0455''$ pixel^{-1} in the planetary mode, the angular field of view of a CCD is $36.4''$.

6.11 (a) $\nu_m = 1.43$ GHz, $\nu_\ell = 1.405$ GHz, and $\nu_u = 1.455$ GHz.

(b) Using Eq. (6.10) with $S(\nu) = S_0 = 2.5$ mJy and $D = 100$ m,

$$P = \int_A \int_\nu S(\nu)\, f_\nu\, d\nu\, dA$$

$$= \pi S_0 \left(\frac{D}{2}\right)^2 \int_{\nu_\ell}^{\nu_u} f_\nu\, d\nu.$$

Substituting the functional form for the filter function and evaluating the integral gives

$$P = \pi S_0 \left(\frac{D}{2}\right)^2 \left[\frac{1}{2}(\nu_u - \nu_\ell)\right] = 4.91 \times 10^{-18}\ \text{W}.$$

(c) At a distance d from the source, the power at the telescope is given by

$$P_{\rm rec} = P_{\rm emit} \frac{\pi (D/2)^2}{4\pi d^2}.$$

Solving for the emitted power, $P_{\rm emit} = 7.5 \times 10^{42}$ W.

6.12 One dish has a diameter of 25 m. Thus, the total collecting area of the 27 dishes is $27 \times \pi(25\ \text{m}/2)^2 = 1.325 \times 10^4$ m^2. If a single dish is to have the same collecting area, it must have a diameter of $D = 130$ m.

6.13 From Eq. (6.11), with $\sin\theta \simeq \theta$, $L = \lambda = 0.21$ m, and $d = 2R_\oplus = 1.28 \times 10^6$ m, $\theta = 1.65 \times 10^{-8}$ rad $= 0.0034''$.

6.14 Consider numbering each dish from 1 to 50. For dish 1 there are 49 distinct baselines, one for each pair of dishes. For dish 2 there are 48 additional baselines (we don't want to recount the baseline between 1 and 2). For dish 3 there are 47 additional baselines, and so on. The total number becomes $49 + 48 + \cdots + 1 = 1125$.

6.15 The projected resolution of SIM PlanetQuest is 4 μarcsec $= 0.000004'' = 2 \times 10^{-11}$ radians.

(a) If grass grows at a rate of 2 cm per week, this is equivalent to 3.3×10^{-8} m s^{-1}. From a distance of 10 km, SIM PlanetQuest can resolve a width of $D = \theta d = 0.2$ μm. It would take the grass approximately 6 s to grow the necessary length to be measured!

(b) Assuming a resolution of 4 μas, and a baseline of 2 AU, the measureable distance is $d = 2$ AU$/4$ μas $=$ 500 kpc.

(c) From Eq. (3.6) and using $M_V = 4.82$, $V = 28.3$.

(d) Assuming a limit of $V = 20$, Eq. (3.6) implies that Betelgeuse would be detectable from a distance of $d = 1$ Mpc.

6.16 Given the number of telescopes the student is asked to research, it may be useful to have the class split into teams and have each team subdivide the research.

(a) See Table S6.1.

(b) See Fig. S6.2.

(c) See Fig. S6.3.

Table S6.1: The wavelength ranges and energies of some ground-based and space-based telescopes. Numbers in parentheses represent power of 10; e.g., 3(-7) $= 3 \times 10^{-7}$.

Telescope	Spectrum region	Wavelength range (m)	Energy range (eV)	URL
VLA	radio	4 to 7(-3)	3(-7) to 2(-4)	www.vla.nrao.edu
ALMA	radio	1(-2) to 3.5(-4)	1(-4) to 4(-3)	www.alma.info/
Spitzer (SIRTF)	IR	1.8(-4) to 3(-6)	0.007 to 0.4	www.spitzer.caltech.edu/spitzer
JWST	IR to visible	2.7(-5) to 6(-7)	0.05 to 2	www.jwst.nasa.gov
VLT/VLTI	mid-IR to near-UV	2.5(-5) to 3(-7)	0.05 to 4	www.eso.org/vlt
Keck	mid-IR to near-UV	2.5(-5) to 3(-7)	0.05 to 4	www.keckobservatory.org
HST (Hubble)	near-IR to near-UV	2.5(-5) to 1.15(-7)	0.05 to 11	www.stsci.edu
IUE	UV	3.2(-7) to 1.15(-7)	3.9 to 11	archive.stsci.edu/iue
EUVE	UV	7.6(-8) to 7(-9)	16 to 177	www.ssl.berkeley.edu/euve/sci/EUVE.html
Chandra	X-ray	6.2(-9) to 1(-10)	20 to 1(4)	chandra.harvard.edu
CGRO	gamma rays	4(-11) to 4(-17)	3(4) to 3(10)	heasarc.gsfc.nasa.gov/docs/cgro

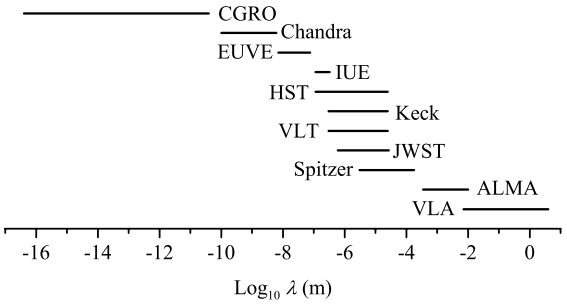

Figure S6.2: The photon wavelengths covered by some ground-based and space-based telescopes.

6.17 (a) See Fig. S6.4.

(b) See Fig. S6.4.

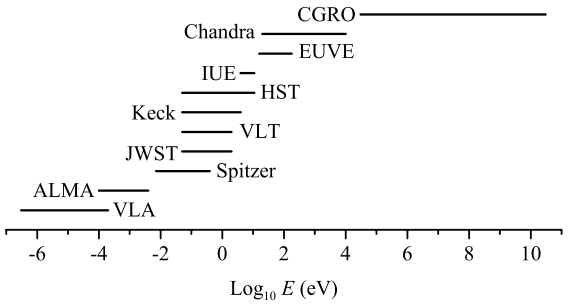

Figure S6.3: The photon energies covered by some ground-based and space-based telescopes.

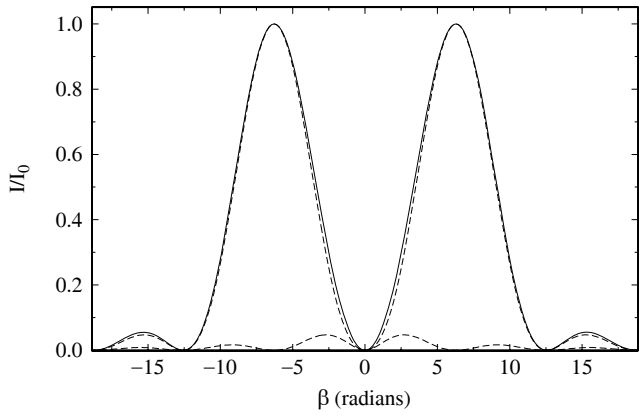

(a)

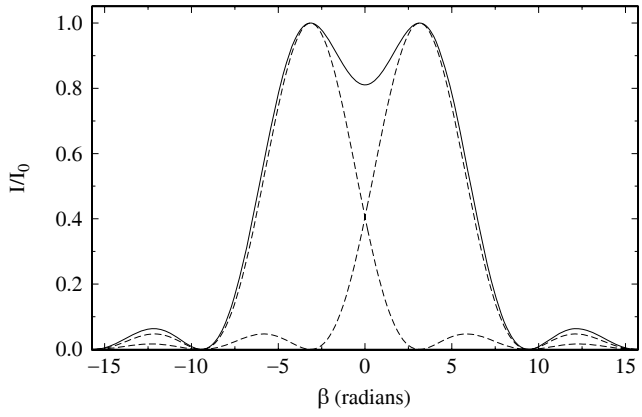

(b)

Figure S6.4: Solutions for Problem 6.18(a) and (b). The solid lines represent the sum of the intensity functions of each slit.

(c) As the sources get progressively closer together, a separation angle is reached where the sum of the two source intensities no longer yields a definable minimum, and it is no longer possible to resolve the sources.

CHAPTER 7

Binary Systems and Stellar Parameters

7.1 Referring to Figs. 2.11 and 2.12, $\mathbf{r} = \mathbf{r}_2 - \mathbf{r}_1$. Since $\mathbf{r}_1$ and $\mathbf{r}_2$ are oppositely directed relative to the center of mass, the separation between m_1 and m_2 is actually $r = r_1 + r_2$. From Eq. (7.1), $r_2/r_1 = a_2/a_1$, where a_1 and a_2 are the semimajor axes of the stars' elliptical orbits. Substituting,

$$r = r_2\left(\frac{a_1 + a_2}{a_2}\right).$$

Now, using Eq. (2.3) to represent r_2 in terms of θ,

$$r = (a_1 + a_2)\left(\frac{1 - e^2}{1 + e\cos\theta}\right).$$

From this result, $r_p = r(0°) = (a_1 + a_2)(1 - e)$ and $r_a = r(180°) = (a_1 + a_2)(1 + e)$, and the average of the two extremes is the semimajor axis of the reduced mass,

$$a = \frac{1}{2}\left(r_p + r_a\right) = a_1 + a_2.$$

7.2 (a) The probability of detecting the radial velocity variations is greatest when the $i = 90°$, while the probability goes to zero when $i = 0°$. This variation can be described by a sine function, or $w(i) = \sin i$. This weighting function is normalized as seen from evaluating

$$\int_0^{\pi/2} \sin i \, di = 1.$$

(b) The weighted average of $\sin^3 i$ is now

$$\begin{aligned}\langle \sin^3 i \rangle &= \int_0^{\pi/2} \sin^3 i \ \sin i \, di \\ &= \int_0^{\pi/2} \sin^4 i \, di \\ &= \left(\frac{3i}{8} - \frac{\sin 2i}{4} + \frac{\sin 4i}{32}\right)\Bigg|_0^{\pi/2} \\ &= \frac{3\pi}{16}.\end{aligned}$$

7.3 (a) For the smallest angle, $a\cos i = r_1 + r_2$, implying

$$i = \cos^{-1}\left(\frac{r_1 + r_2}{a}\right).$$

(b) $i = 88.5°$.

7.4 (a) For $p'' = 0.37921''$, the distance to Sirius is $d = 1/p'' = 2.63$ pc. This means that the linear size of the semimajor axis of the reduced mass is approximately $a = \alpha d = 3.00 \times 10^{12}$ m. Using Kepler's third law (Eq. 2.37),

$$m_A + m_B = \frac{4\pi^2}{GP^2} a^3 = 3.24\ \mathrm{M}_\odot.$$

Since $m_A a_A = m_B a_B$, we have that $m_A\,(1 + a_A/a_B) = 3.24\ \mathrm{M}_\odot$. Solving for the individual masses, $m_A = 2.21\ \mathrm{M}_\odot$ and $m_B = 1.03\ \mathrm{M}_\odot$.

(b) From Eq. (3.7), with the bolometric magnitude of the Sun taken to be 4.74, $L_A = 22.5\ \mathrm{L}_\odot$ and $L_B = 0.0240\ \mathrm{L}_\odot$.

(c) Using the Stefan–Boltzmann equation (3.17), $R = 5.85 \times 10^6$ m $= 0.0084\ \mathrm{R}_\odot = 0.917\ \mathrm{R}_\oplus$.

7.5 (a) From Eq. (7.6),

$$\left(m_b + m_f\right) \sin^3 i = \frac{P}{2\pi G} \left(v_{br} + v_{fr}\right)^3 = 8.65\ \mathrm{M}_\odot,$$

where the subscripts denote the bright (b) and faint (f) components, respectively.
From Eq. (7.5), $m_b = 2.03 m_f$, implying

$$m_f \sin^3 i = 2.85\ \mathrm{M}_\odot \qquad \text{and} \qquad m_b \sin^3 i = 5.80\ \mathrm{M}_\odot.$$

(b) Using $\langle \sin^3 i \rangle \sim 2/3$,

$$m_f \simeq 4.3\ \mathrm{M}_\odot \qquad \text{and} \qquad m_b \simeq 8.7\ \mathrm{M}_\odot.$$

7.6 (a) From Eq. (7.5), $m_B/m_A = 0.241$.

(b) From Eq. (7.6), $m_A + m_B = 5.13\ \mathrm{M}_\odot$.

(c) $m_A = 4.13\ \mathrm{M}_\odot$ and $m_B = 1.00\ \mathrm{M}_\odot$.

(d) According to Eqs. (7.8) and (7.9),

$$r_s = \frac{(v_A + v_B)}{2}\,(t_b - t_a) = 1.00\ \mathrm{R}_\odot,$$

and

$$r_\ell = r_s + \frac{(v_A + v_B)}{2}\,(t_c - t_b) = 2.11\ \mathrm{R}_\odot,$$

respectively.

(e) Brightness ratios can be determined from Eq. (3.3), giving (for the primary and secondary eclipses, respectively)

$$\frac{B_p}{B_0} = 0.0302 \qquad \text{and} \qquad \frac{B_s}{B_0} = 0.964.$$

Finally, using Eq. (7.11),

$$\frac{T_s}{T_\ell} = \left(\frac{1 - B_p/B_0}{1 - B_s/B_0}\right)^{1/4} = 2.28.$$

7.7 (a) The ratio of the durations of eclipses of minimum to maximum is approximately 0.9. (Lacy, *Astron. J.*, *105*, 637, 1993 finds the ratio of the radii to be 0.907 ± 0.015.) *Note:* In order to accurately obtain the ratio of the radii, the light curve must be carefully modeled, a process beyond the scope of this text. This part of the problem may be modified or omitted in a future revision.

(b) From the light curve $m_0 = 10.04$, $m_p = 10.76$, and $m_s = 10.68$. Using the procedure outlined in the solution to Problem 7.6,

$$\frac{B_p}{B_0} = 0.515 \qquad \text{and} \qquad \frac{B_s}{B_0} = 0.555.$$

This implies that $T_s / T_\ell = 1.090$.

7.8 (a) From upper left to lower right, the displayed images roughly correspond to the following phases: 0.00, 0.06, 0.13, 0.19, 0.25, 0.31, 0.38, 0.44, 0.50.

(b) In this binary system, the larger star is hotter. At the primary minimum (phase = 0.0), the maximum amount of the larger star is covered, implying the least total integrated flux (or luminosity). The primary minimum is not flat because the proximity of the secondary star leads to tidal distortion of the shapes of the stars, thus removing spherical symmetry. The brightness of the system increases until, at phase 0.25, the two stars are seen in profile. As the secondary passes behind the primary, the brightness decreases, reaching a flat minimum at phase 0.5. The secondary minimum is flat because the secondary (and the distortion effects) are occulted for a finite period of time.

7.9 See Fig. S7.1.

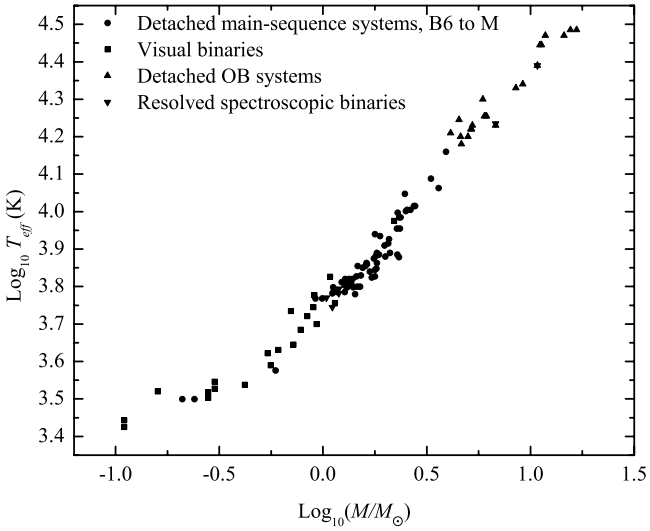

Figure S7.1: The relationship between effective temperature and mass for main sequence stars.

7.10 Massive planets with short orbital periods exert a greater force on the parent star, thus producing higher radial velocities of the stars themselves. In addition, shorter periods imply that a greater number of orbital periods can be measured over a given length of time.

7.11 From Eq. (7.7), it is evident that only $m \sin i$ can be determined, unless the angle of inclination can be determined independently (meaning that the system must be eclipsing).

7.12 (a) For the planet orbiting 51 Peg, $P = 4.23077$ d, and $a = 0.051$ AU. From Kepler's third law, the total mass of the system is $M = 0.99\ \mathrm{M}_\odot$. Since $m \sin i = 0.45\ \mathrm{M}_\mathrm{J} \ll M$, the mass of 51 Peg is approximately $0.99\ \mathrm{M}_\odot$.

(b) For the planet orbiting HD 168443c, $P = 1770$ d, and $a = 2.87$ AU. Again, from Kepler's third law, $M = 1.01\ \mathrm{M}_\odot$. We can again neglect the mass of the planet.

7.13 Considering the integrated flux over the projected solar disk, we have $\pi R_\odot^2 \sigma T_e^4$. The amount of light blocked by the transiting Jupiter is $\pi R_J^2 \sigma T_e^4$. Thus the relative change becomes

$$\frac{\Delta F}{F} = \frac{R_J^2}{R_\odot^2} = 0.0106$$

or just over 1%.

7.14 The fractional decrease in the flux appears to be approximately $1 - 0.983 = 0.017$. Using an approach similar to the solution of Problem 7.13, the ratio of the radius of the planet to the radius of the star is approximately $R_p/R_s = \sqrt{0.017} = 0.13$. The radius of the star is estimated to be $R_s = 1.1\ \mathrm{R}_\odot$, implying that the radius of the planet is approximately $R_p = 0.13 R_s = 1.27\ \mathrm{R_J}$, in agreement with the value found in the text.

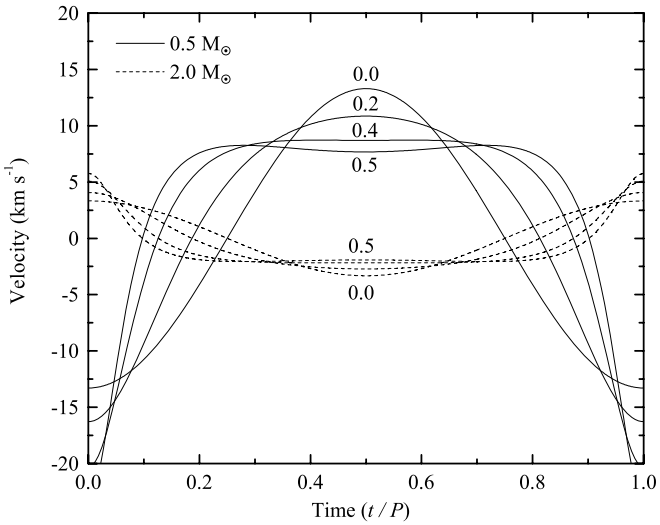

Figure S7.2: The variation of orbital velocity with eccentricity is plotted for one orbital period (Problem 7.15). The eccentricities are labeled on the diagram. $M_1 = 0.5\ \mathrm{M}_\odot$, $M_2 = 2.0\ \mathrm{M}_\odot$, $P = 1.8\ \mathrm{yr} = 657.46\ \mathrm{d}$, $i = 30°$, $\phi = 90°$.

7.15 (a) See Fig. S7.2. [*Note:* The effective temperatures and radii of the stars are irrelevant for this problem; any reasonable (and many unreasonable) values can be entered.]

(b) From Kepler's third law (Eq. 2.37), with $P = 1.8$ yr, $M_1 = 0.5\ \mathrm{M}_\odot$ and $M_2 = 2.0\ \mathrm{M}_\odot$, $a = 2.0$ AU. Also, since $m_1/m_2 = a_2/a_1$ (Eq. 7.1) and $a = a_1 + a_2 = 2.0$ AU, we have $a_1 = 1.6$ AU and $a_2 = 0.4$ AU. Now, the orbital velocities of the two stars are $v_1 = 2\pi a_1/P = 26.5\ \mathrm{km\ s^{-1}}$ and $v_2 = 2\pi a_2/P = 6.6\ \mathrm{km\ s^{-1}}$. Finally, taking into consideration the orbital inclination of 30°, the maximum observable radial velocities are $v_{1r,\,\mathrm{max}} = v_1 \sin i = 13.2\ \mathrm{km\ s^{-1}}$ and $v_{2r,\,\mathrm{max}} = v_2 \sin i = 3.351\ \mathrm{km\ s^{-1}}$.

(c) The eccentricity can be determined by considering the asymmetries in the velocity and/or light curves. In particular, the velocity curves deviate from being perfectly sinusoidal (the amount of deviation increasing with increasing e). Also, for an eclipsing system, the primary and secondary minima are not 180° out of phase if $e \neq 0$ (see e.g. Fig. 7.2).

7.16 See Fig. S7.3.

7.17 (a) See Fig. S7.4. Note that the relative phasing of minima are essentially correct, but that the relative depths of the minima differ somewhat from Fig. 7.2.

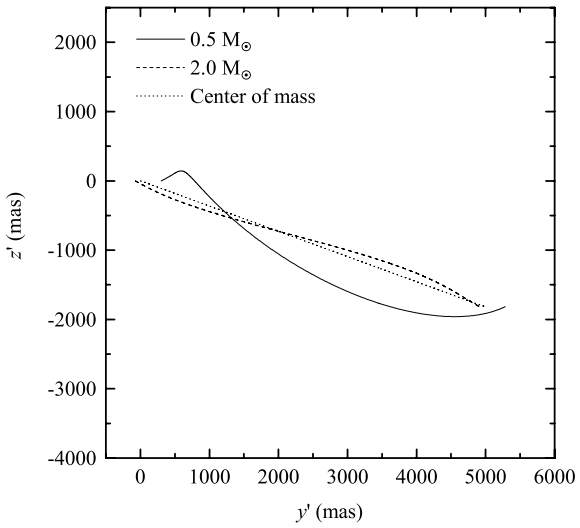

Figure S7.3: The motion of the binary system described in Problem 7.16.

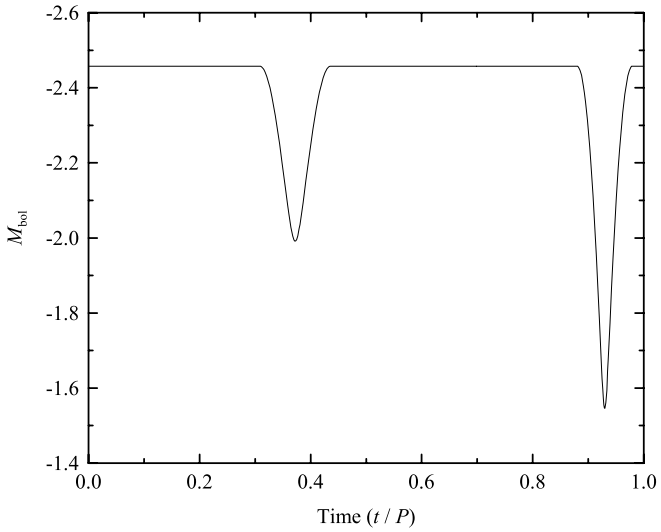

Figure S7.4: The synthetic light curve of YY Sgr produced by `TwoStars`; Problem 7.17(a).

(b) See Fig. S7.5.

7.18 Using the data in the text and the problem, the mass of the star can be determined from Kepler's third law to be approximately 1.1 $M_\odot$. Take the radius of the star to be roughly 1.1 $R_\odot$ for a main-sequence star. The mass of the planet is estimated to by 0.00086 $M_\odot$. From the data, `TwoStars` generates a bolometric light curve shown in Fig. S7.6. Note that the drop is just over 0.01 mag, in agreement with the value specified in the text.

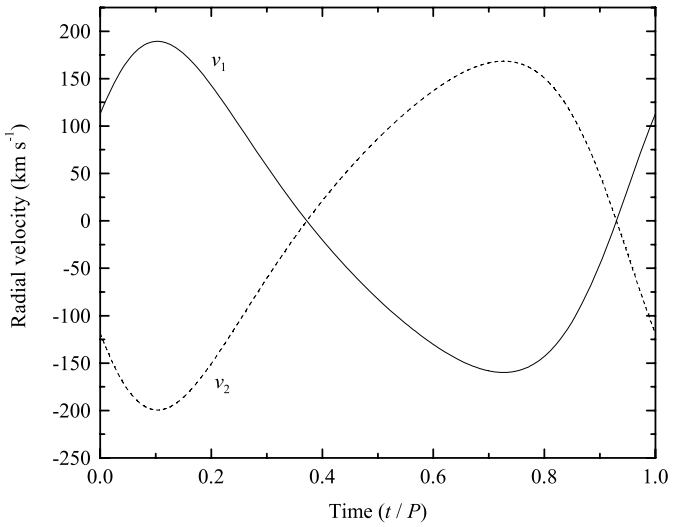

Figure S7.5: The radial velocities for both members of YY Sgr produced by `TwoStars`; Problem 7.17(b).

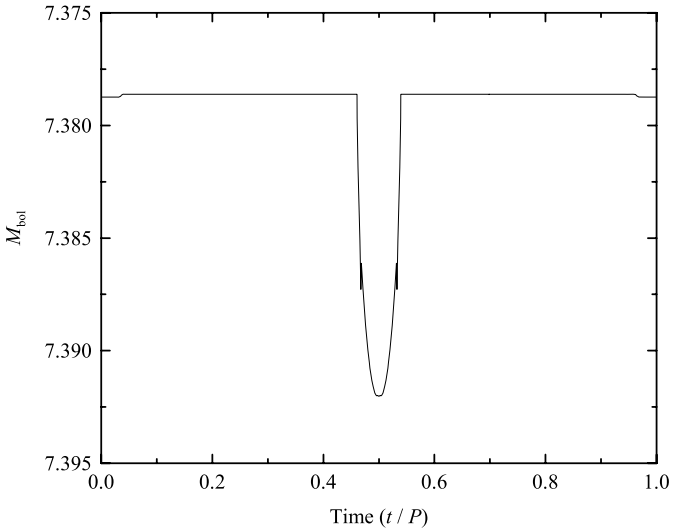

Figure S7.6: The synthetic light curve of OGLE-TR-56b for Prob. 7.18.

CHAPTER 8

The Classification of Stellar Spectra

8.1 In the following, it is easiest to express Boltzmann's constant as $k = 8.6174 \times 10^{-5}$ eV K^{-1}. At a room temperature of 300 K,

$$kT = 0.0259 \text{ eV} \approx \frac{1}{40} \text{ eV}.$$

If $kT = 1$ eV, then $T = 1.16 \times 10^4$ K. If $kT = 13.6$ eV, then $T = 1.58 \times 10^5$ K.

8.2 A straightforward conversion of units shows that

$$k = 8.6173423 \times 10^{-5} \text{ eV K}^{-1}.$$

8.3 The peak of the Maxwell–Boltzmann distribution, Fig. 8.6, shows that $n_v/n \simeq 6.5 \times 10^{-5}$ s m^{-1} where $v = v_{\rm mp}$. For a range of speeds $\Delta v = 2$ km s^{-1}, the fraction of hydrogen atoms within 1 km s^{-1} of the most probable speed is $(n_v/n)\Delta v \simeq 0.13$.

8.4 The most probable speed, $v_{\rm mp}$, occurs at the peak of the Maxwell–Boltzmann distribution, Eq. (8.1). Setting $dn_v/dv = 0$, we find

$$\frac{dn_v}{dv} = 4\pi n \left(\frac{m}{2\pi kT}\right)^{3/2} \frac{d}{dv}\left(e^{-mv^2/2kT}\, v^2\right) = 0.$$

This leads to

$$\left(-\frac{mv^3}{kT} + 2v\right) e^{-mv^2/2kT} = 0,$$

so that $v_{\rm mp} = \sqrt{2kT/m}$, which is Eq. (8.2).

8.5 Solving the Boltzmann equation, Eq. (8.6), for T gives

$$T = \frac{E_2 - E_1}{k \ln[(g_2/g_1) \,/\, (N_2/N_1)]}.$$

To find T when the number of atoms in the first excited state ($n = 2$) is only 1% of the number of atoms in the ground state ($n = 1$), use $g_1 = 2(1)^2 = 2$, $g_2 = 2(2)^2 = 8$, $E_1 = -13.6$ eV, and $E_2 = -3.40$ eV. Then, with $N_2/N_1 = 0.01$, $T = 1.97 \times 10^4$ K. If the number of atoms in the first excited state is only 10% of the number of atoms in the ground state, then $T = 3.21 \times 10^4$ K.

8.6 (a) We solve the Boltzmann equation, Eq. (8.6), for T:

$$T = \frac{E_3 - E_1}{k \ln[(g_3/g_1) \,/\, (N_3/N_1)]}.$$

Using the values in Problem 8.5 together with $g_3 = 2(3)^3 = 18$ and $E_3 = -1.51$ eV, we find that if $N_3/N_1 = 1$, then $T = 6.38 \times 10^4$ K.

(b) From the Boltzmann equation using $T = 85{,}400$ K, $N_3/N_1 = N_3/N = 1.74$.

(c) As $T \to \infty$, the exponential in the Boltzmann equation goes to unity and $N_b/N_a \to g_b/g_a$. The relative numbers of electrons in the $n = 1, 2, 3, \ldots$ orbitals will be $g_n = 2n^2 = 2, 8, 18, \ldots$. Although this will be the distribution that actually occurs for the neutral hydrogen atoms, at such high temperatures essentially all of the hydrogen atoms will have been ionized.

8.7 From Eq. (8.7), use $g_n = 2n^2$ and $E_1 = -13.6$ eV, $E_2 = -3.40$ eV, and $E_3 = -1.51$ eV with $T = 10{,}000$ K to get

$$\begin{aligned} Z_{\rm I} &= g_1 + g_2 e^{-(E_2 - E_1)/kT} + g_3 e^{-(E_3 - E_1)/kT} \\ &= 2 + 5.79 \times 10^{-5} + 1.45 \times 10^{-5}. \end{aligned}$$

Thus $Z_I \simeq 2$.

8.8 As $n \to \infty$, the expression for the partition function, Eq. (8.7), actually diverges. However, in reality the large-n terms can be ignored because as $n \to \infty$, the atomic orbitals overlap with those of neighboring atoms, and the electrons are no longer associated with a single nucleus.

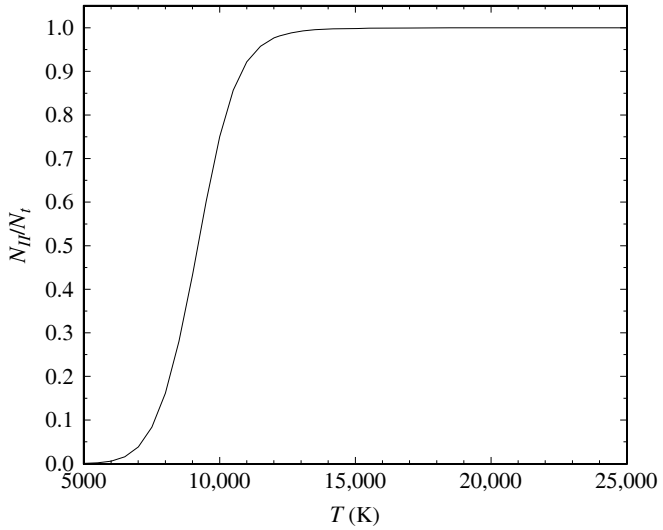

Figure S8.1: Results for Problem 8.9. $N_{\rm II}/N_t$ is shown for a box of hydrogen gas.

8.9 (a) Start by writing

$$\frac{N_{\rm II}}{N_t} = \frac{N_{\rm II}}{N_{\rm I} + N_{\rm II}} = \frac{N_{\rm II}/N_{\rm I}}{1 + N_{\rm II}/N_{\rm I}},$$

or

$$\frac{N_{\rm II}}{N_t}\left(1 + \frac{N_{\rm II}}{N_{\rm I}}\right) = \frac{N_{\rm II}}{N_{\rm I}}.$$

$N_{\rm II}/N_{\rm I}$ is given by the Saha equation, Eq. (8.8),

$$\frac{N_{\rm II}}{N_{\rm I}} = \frac{2Z_{\rm II}}{n_e Z_{\rm I}}\left(\frac{2\pi m_e kT}{h^2}\right)^{3/2} e^{-\chi_{\rm I}/kT}.$$

From Example 8.1.4, $Z_{\rm I} = 2$ and $Z_{\rm II} = 1$. The electron number density, n_e, is given by $n_e = N_{\rm II}/V$ because each ionized hydrogen atom contributes one free electron. The total number of hydrogen atoms and ions is $N_t = \rho V/(m_p + m_e) \simeq \rho V/m_p$. Here, $\rho = 10^{-6}$ kg m^{-3} is the density. The mass of the

electron is much less than the mass of the proton, and may be safely ignored in the expression for N_t. Combining these expressions produces

$$n_e = \frac{N_{\rm II}\rho}{N_t m_p}$$

for use in the Saha equation. With these substitutions, the Saha equation becomes

$$\frac{N_{\rm II}}{N_{\rm I}} = \frac{N_t}{N_{\rm II}}\frac{m_p}{\rho}\left(\frac{2\pi m_e kT}{h^2}\right)^{3/2} e^{-\chi_{\rm I}/kT}.$$

Substituting this into the above equation produces

$$\frac{N_{\rm II}}{N_t}\left[1 + \frac{N_t}{N_{\rm II}}\frac{m_p}{\rho}\left(\frac{2\pi m_e kT}{h^2}\right)^{3/2} e^{-\chi_{\rm I}/kT}\right] \frac{N_t}{N_{\rm II}}\frac{m_p}{\rho}\left(\frac{2\pi m_e kT}{h^2}\right)^{3/2} e^{-\chi_{\rm I}/kT}.$$

Multiplying each side by $N_{\rm II}/N_t$ and rearranging terms gives

$$\left(\frac{N_{\rm II}}{N_t}\right)^2 + \left(\frac{N_{\rm II}}{N_t}\right)\frac{m_p}{\rho}\left(\frac{2\pi m_e kT}{h^2}\right)^{3/2} e^{-\chi_{\rm I}/kT} - \frac{m_p}{\rho}\left(\frac{2\pi m_e kT}{h^2}\right)^{3/2} e^{-\chi_{\rm I}/kT} = 0.$$

(b) This is a quadratic equation of the form $ax^2 + bx + c = 0$, where

$$a = 1$$

$$b = \frac{m_p}{\rho}\left(\frac{2\pi m_e kT}{h^2}\right)^{3/2} e^{-\chi_{\rm I}/kT}$$

$$c = -b.$$

It therefore has the solution

$$\frac{N_{\rm II}}{N_t} = \frac{1}{2a}\left(-b + \sqrt{b^2 - 4ac}\right) = \frac{b}{2}\left(\sqrt{1 + 4/b} - 1\right).$$

Evaluating b for a range of temperatures between 5000 K and 25,000 K produces the graph shown in Fig. S8.1.

8.10 (a) Using the values given in the problem with Eq. (8.9), a form of the Saha equation that contains the electron pressure, results in

T (K)	$N_{\rm II}/N_{\rm I}$	$N_{\rm III}/N_{\rm II}$
5000	1.89×10^{-18}	4.33×10^{-49}
15,000	9.98×10^{-1}	2.42×10^{-11}
25,000	7.24×10^{3}	1.78×10^{-3}

In all cases, $N_{\rm II}/N_{\rm I} \gg N_{\rm III}/N_{\rm II}$, although the disparity decreases markedly with increasing temperature.

(b) Write

$$\frac{N_{\rm II}}{N_t} = \frac{N_{\rm II}}{N_{\rm I} + N_{\rm II} + N_{\rm III}}$$

$$= \frac{N_{\rm II}/N_{\rm I}}{1 + N_{\rm II}/N_{\rm I} + (N_{\rm III}/N_{\rm II})(N_{\rm II}/N_{\rm I})}.$$

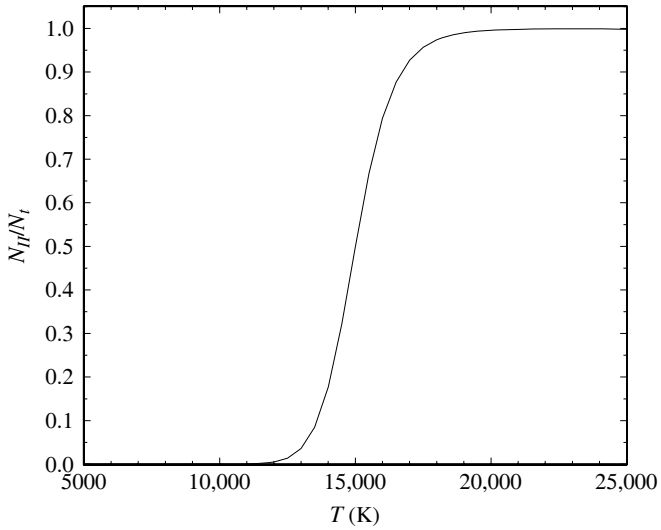

Figure S8.2: Results for Problem 8.10. $N_{\rm II}/N_t$ is shown for helium.

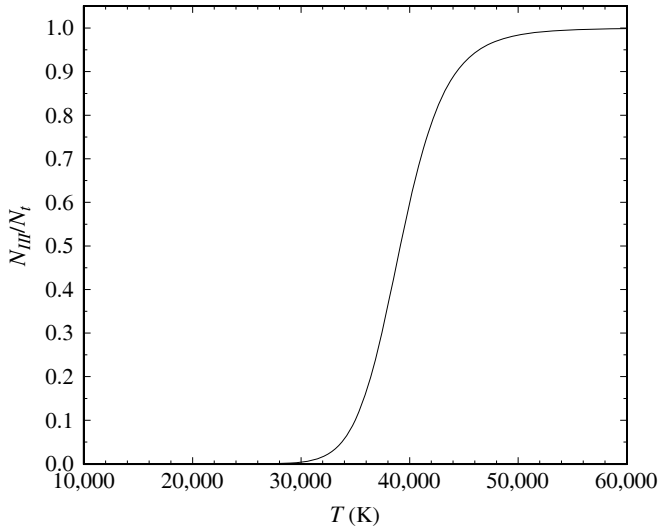

Figure S8.3: Results for Problem 8.11. $N_{\rm III}/N_t$ is shown for helium.

(c) First, note from the results of part (a) that the last term in the denominator $[(N_{\rm III}/N_{\rm II})(N_{\rm II}/N_{\rm I})]$ of $N_{\rm II}/N_t$ can be neglected for T between 5000 K and 25, 000 K. Use Eq. (8.9) with $Z_{\rm I} = 1$, $Z_{\rm II} = 2$, $\chi_{\rm I} = 24.6$ eV, and $P_e = 20$ N m^{-2} to evaluate $N_{\rm II}/N_{\rm I}$ for a range of values of T. As shown in Fig. S8.2, one-half of the He I atoms have been ionized when $T \simeq 1.5 \times 10^4$ K.

8.11 Follow the procedure of Problem 8.10 and write

$$\frac{N_{\rm III}}{N_t} = \frac{N_{\rm III}}{N_{\rm I} + N_{\rm II} + N_{\rm III}} = \frac{N_{\rm III}/N_{\rm II}}{1/(N_{\rm II}/N_{\rm I}) + 1 + (N_{\rm III}/N_{\rm II})}.$$

Use the values given in the Problem 8.10 (with $P_e = 1000$ N m^{-2}) with Eq. (8.9) to evaluate $N_{\rm III}/N_{\rm II}$ and $N_{\rm II}/N_{\rm I}$. This results in the graph shown in Fig. S8.3. One-half of the helium atoms have been twice-ionized when $T \simeq 4 \times 10^4$ K.

8.12 From Example 8.1.4 and the information given in the problem, use $Z_{\rm I} = 2$, $Z_{\rm II} = 1$, $\chi_{\rm I} = 13.6$ eV, $n_e = 6.1 \times 10^{31}$ m^{-3}, and $T = 1.57 \times 10^7$ K in the Saha equation, Eq. (8.8), to find that

$$\frac{N_{\rm II}}{N_t} = \frac{N_{\rm II}}{N_{\rm I} + N_{\rm II}} = \frac{N_{\rm II}/N_{\rm I}}{1 + N_{\rm II}/N_{\rm I}} = 0.709$$

at the center of the Sun. However, at the center of the Sun, the density of the gas is sufficiently great to perturb the hydrogen orbital energies and increase the amount of ionization (pressure ionization). As a result, practically all of the Sun's hydrogen is ionized at the Sun's center .

8.13 From the statement of the problem and Example 8.1.5, we have $Z_{\rm II} = 2.30$, $Z_{\rm III} = 1$, $P_e = 1.5$ N m^{-2}, $\chi_{\rm II} = 11.9$ eV, and $T = 5777$ K. Inserting these values into the alternative form of the Saha equation, Eq. (8.9), we find that $[N_{\rm III}/N_{\rm II}]_{\rm Ca} = 2.08 \times 10^{-3}$. Comparing this with $[N_{\rm II}/N_{\rm I}]_{\rm Ca} = 918$ from Example 8.1.5 shows that nearly all of the calcium atoms are in the form of Ca II, available for forming the H and K lines.

8.14 The Saha equation, Eq. (8.8), is

$$\frac{N_{i+1}}{N_i} = \frac{2Z_{i+1}}{n_e Z_i} \left(\frac{2\pi m_e k T}{h^2} \right)^{3/2} e^{-\chi_i / kT}.$$

Stars of the same spectral type have the atoms in their atmospheres in the same states of ionization and excitation. The left-hand side of the Saha equation will therefore have the same value for atoms of the same element. The right-hand side increases monotonically as T increases, and decreases monotonically as n_e increases. Because a giant star has a *lower* atmospheric density than a main-sequence star of the same spectral type, it must have a *lower* surface temperature to produce the same state of ionization of the atoms in its atmosphere.

8.15 The average density of a 1 $M_\odot$ white dwarf with a radius of $R = 0.01$ $R_\odot$ is

$$\overline{\rho} = \frac{M}{\frac{4}{3}\pi R^3} = 1.41 \times 10^9 \text{ kg m}^{-3}.$$

8.16 From the H–R diagram in Fig. 8.16, the star Formalhaut has an absolute visual magnitude of about $M_v \simeq 2.0$. The star has an apparent visual magnitude of $V = 1.19$. So, using Eq. (3.5), the distance to Formalhaut is about

$$d \simeq 10^{(m-M+5)/5} = 10^{(1.19-2.0+5)/5} \text{ pc} = 6.89 \text{ pc}.$$

CHAPTER 9

Stellar Atmospheres

9.1 Using Eq. (9.7) for the energy density of blackbody radiation, the energy of blackbody photons inside a spherical eyeball of radius $r_{\rm eye} = 1.5$ cm at a temperature of 310 K (37°C) is

$$E_{\rm bb} = \frac{4}{3}\pi r_{\rm eye}^3 a T^4 = 9.88 \times 10^{-11} \text{ J}.$$

The flux from a point-source light bulb ($L = 100$ W) at a distance $r = 1$ m is $F = L/4\pi r^2$ (Eq. 3.2), so the energy per second entering the pupil of area A is FA. The time for the light to cross the eyeball is $2r_{\rm eye}/c$ (neglecting the fluid within the eye). The energy from the light bulb within the eyeball is therefore

$$E_{\rm bulb} = 2FAr_{\rm eye}/c = \frac{2LAr_{\rm eye}}{4\pi r^2 c} = 7.96 \times 10^{-15} \text{ J},$$

more than four orders of magnitude smaller than $E_{\rm bb}$.

It is dark when you close your eyes because, according to Wien's law (Eq. 3.15), at 310 K the blackbody radiation peaks at $\lambda_{\rm max} = 9354.8$ nm in the infrared, and the eye's retina is not sensitive to such long wavelength photons.

9.2 (a) Dividing the specific blackbody energy density, Eq. (9.5), by the energy per photon hc/λ gives the specific number density,

$$n_\lambda \, d\lambda = \frac{8\pi/\lambda^4}{e^{hc/\lambda kT} - 1} \, d\lambda.$$

(b) Integrating the expression for n_λ over all wavelengths leads to an integral for the number density, n, that has the form

$$n = \int_0^\infty n_\lambda \, d\lambda = \frac{8\pi k^3 T^3}{h^3 c^3} \int_0^\infty \frac{x^2}{e^x - 1} \, dx,$$

where $x = hc/\lambda kT$. The value of the integral is 2.404114, so the number density is

$$n = (2.404)\frac{8\pi k^3 T^3}{h^3 c^3}. \tag{S9.1}$$

The number of photons inside an oven of volume $V = 0.5$ m^3 at a temperature of $T = 400$°F $= 477$ K is $N = nV = 1.1 \times 10^{15}$.

9.3 (a) The total energy density is given by Eq. (9.7)

$$u = \frac{4\sigma T^4}{c} = \frac{4T^4}{c}\left(\frac{2\pi^5 k^4}{15c^2 h^3}\right),$$

where we have used the expression found in Problem 3.14 for the Stefan–Boltzmann constant, σ. Furthermore, the total number density of blackbody photons was found in Problem 9.2 to be given by Eq. (S9.1). Thus, the average energy per photon is

$$\frac{u}{n} = \frac{\pi^4 kT}{15(2.404)} = 2.70kT.$$

(b) For $T = 1.57 \times 10^7$ K, $u/n = 3650$ eV. For $T = 5777$ K, $u/n = 1.34$ eV.

9.4 For blackbody radiation, $I_\lambda = B_\lambda$, and so Eq. (9.10) gives

$$P_{\text{rad}} = \frac{4\pi}{3c}\int_0^\infty B_\lambda(T)\,d\lambda = \frac{4\pi}{3c}\int_0^\infty \frac{2hc^2/\lambda^5}{e^{hc/\lambda kT}-1}\,d\lambda.$$

Defining $x = hc/\lambda kT$ leads to

$$P_{\text{rad}} = \frac{8\pi k^4 T^4}{3h^3c^3}\int_0^\infty \frac{x^3}{e^x-1}\,dx.$$

The integral is equal to $\pi^4/15$. Using this along with the expression found in Problem 3.14 for the Stefan–Boltzmann constant, $\sigma = 2\pi^5 k^4/15c^2h^3$, produces the desired result,

$$P_{\text{rad}} = \frac{4\sigma T^4}{3c} = \frac{1}{3}aT^4 = \frac{1}{3}u,$$

via the definition of the radiation constant, $a = 4\sigma/c$, and Eq. (9.7) for the blackbody energy density.

9.5 We start by integrating Eq. (9.8) with $I_\lambda = B_\lambda$ over all outward directions ($0 \le \theta \le \pi/2$).

$$F_\lambda\,d\lambda = B_\lambda\,d\lambda\int_{\phi=0}^{2\pi}\int_{\theta=0}^{\pi/2}\cos\theta\,\sin\theta\,d\theta\,d\phi = \pi B_\lambda\,d\lambda.$$

We now integrate over all wavelengths to find the total flux,

$$F = \int_0^\infty F_\lambda\,d\lambda = \pi\int_0^\infty B_\lambda\,d\lambda = \pi\frac{\sigma T^4}{\pi} = \sigma T^4.$$

where Eq. (3.28) was used for the integral of B_λ. Finally, integrating the flux over the surface area of a sphere of radius R gives

$$L = \int_{\phi=0}^{2\pi}\int_{\theta=0}^{\pi} FR^2\sin\theta\,d\theta\,d\phi = 4\pi R^2\sigma T^4,$$

which is Eq. (3.17).

9.6 According to Eq. (8.3), root-mean-square speed of the nitrogen molecules is

$$v_{\text{rms}} = \sqrt{\frac{3kT}{28m_p}} = 515\text{ m s}^{-1}.$$

Using the collision cross section $\sigma = \pi(2r)^2$ with Eq. (9.12), the mean free path is

$$\ell = \frac{1}{n\sigma} = \frac{1}{n\pi(2r)^2}.$$

The number density n of nitrogen molecules is

$$n = \frac{\rho}{28m_p} = 2.57 \times 10^{25}\text{ m}^{-3}.$$

The mean free path is therefore $\ell = 3.10 \times 10^{-7}$ m, and the average time between collisions is about $t \simeq \ell/v_{\text{rms}} = 6 \times 10^{-10}$ s = 0.6 ns.

9.7 Using values of $\kappa_{500} = 0.03\ \mathrm{m^2\ kg^{-1}}$ from Example 9.2.2 and $\rho = 1.2\ \mathrm{kg\ m^{-3}}$, the mean free path is

$$\ell = \frac{1}{\kappa_{500}\rho} = 21.8\ \mathrm{m}.$$

You always look back to an optical depth of about $\tau_\lambda = 2/3$; that is, about $2/3$ of a mean free path. Thus you could see to a distance of only $2\ell/3 = 18.5$ m.

9.8 Using Eq. (9.19) with a measurement of the specific intensity $I_\lambda = I_1$ at angle θ_1 gives

$$I_1 = I_{\lambda,0} e^{-\tau_{\lambda,0} \sec\theta_1},$$

or

$$\ln\left(\frac{I_1}{I_{\lambda,0}}\right) = -\tau_{\lambda,0} \sec\theta_1. \tag{S9.2}$$

Similarly, $I_\lambda = I_2$ at angle θ_2 gives

$$\ln\left(\frac{I_2}{I_{\lambda,0}}\right) = -\tau_{\lambda,0} \sec\theta_2. \tag{S9.3}$$

Subtracting these results in

$$\ln\left(\frac{I_1}{I_2}\right) = -\tau_{\lambda,0}(\sec\theta_1 - \sec\theta_2),$$

or

$$\tau_{\lambda,0} = \frac{\ln(I_1/I_2)}{\sec\theta_2 - \sec\theta_1}.$$

Solving Eqs. (S9.2) and (S9.3) for $\tau_{\lambda,0}$ and equating them produces

$$\frac{1}{\sec\theta_1}\ln\left(\frac{I_1}{I_{\lambda,0}}\right) = \frac{1}{\sec\theta_2}\ln\left(\frac{I_2}{I_{\lambda,0}}\right).$$

Solving for $I_{\lambda,0}$ yields

$$I_{\lambda,0} = \left(\frac{I_2^{\sec\theta_1}}{I_1^{\sec\theta_2}}\right)^{1/(\sec\theta_1 - \sec\theta_2)}.$$

9.9 Consider the problems from the reference frame in which the electron is initially at rest. Conservation of momentum gives $p_{\mathrm{photon}} = p_e$, which is

$$\frac{E_{\mathrm{photon}}}{c} = \gamma m_e v,$$

(Eqs. 4.44 and 5.5), where v is the final velocity of the electron. Conservation of total relativistic energy (Eq. 4.46) gives

$$E_{\mathrm{photon}} + m_e c^2 = \gamma m_e c^2.$$

Equating these expressions for E_{photon} leads to $v/c = (\gamma - 1)/\gamma$, which implies $v = 0$, $\gamma = 1$, and $E_{\mathrm{photon}} = 0$; a contradiction, since there is no photon to absorb! Thus an isolated electron cannot absorb a photon.

9.10 For constant density, a Kramers opacity law says that $\overline{\kappa} = CT^{-3.5}$, where C is a constant. Then at two temperatures T_1 and T_2,

$$\ln\overline{\kappa}_2 = \ln C - 3.5\ln T_2$$

$$\ln\overline{\kappa}_1 = \ln C - 3.5\ln T_1.$$

Subtracting these,

$$\frac{\ln \overline{\kappa}_2 - \ln \overline{\kappa}_1}{\ln T_2 - \ln T_1} = -3.5.$$

Because $\ln x = (\ln 10) \log_{10} x$, this expression is valid both for natural logs and logs to the base 10. Using Fig. 9.10, we choose $\log_{10} \rho = 0$ kg m^{-3} and draw the best-fitting straight line to the curve. Two well-separated points on this line are $\log_{10} \overline{\kappa}_1 = 1.19$ at $\log_{10} T_1 = 5.55$, and $\log_{10} \overline{\kappa}_2 = -0.867$ at $\log_{10} T_2 = 6.15$. For these two points,

$$\frac{\log_{10} \overline{\kappa}_2 - \log_{10} \overline{\kappa}_1}{\log_{10} T_2 - \log_{10} T_1} = -3.43 \simeq -3.5,$$

as expected for a Kramers opacity law.

9.11 (a) The average photon mean free path is

$$\ell = \frac{1}{\overline{\kappa}\rho} = \frac{1}{(0.217 \text{ m}^2 \text{ kg}^{-1})(1.5 \times 10^5 \text{ kg m}^{-3})} = 3 \times 10^{-5} \text{ m}.$$

(b) From Eq. (9.29), the number of random-walk steps of this size from the center to the surface of the Sun is

$$N = \left(\frac{d}{\ell}\right)^2 = \left(\frac{R_\odot}{\ell}\right)^2 = 5 \times 10^{26}.$$

The time for a photon to cover this many steps of size ℓ is

$$t = \frac{N\ell}{c} = 5 \times 10^{13} \text{ s},$$

almost two million years!

9.12 Because you always look back to an optical depth of about $\tau_\lambda = 2/3$, Eq. (9.17) implies that you see down to a depth s into the star given by

$$\int_0^s \kappa_\lambda \rho \, ds = \frac{2}{3}.$$

At wavelengths where the opacity is greatest, the value of s is smallest. If the temperature of the star's atmosphere increases outward, then a smaller value of s corresponds to looking at a higher temperature and brighter gas. At wavelengths where the opacity is greatest, you would therefore see *emission lines*.

9.13 A large hollow spherical shell of hot gas will look like a ring if you can see straight through the middle of the shell. That is, the shell must be *optically thin*, and an optically thin hot gas produces emission lines. Near the edge of the shell, where your line of sight passes through more gas, the shell appears brighter and you see a ring.

9.14 From Eq. (9.32), $j_\lambda = dI_\lambda / \rho \, ds$, so the emission coefficient has units of

$$\frac{\text{W m}^{-3} \text{ sr}^{-1}}{\left(\text{kg m}^{-3}\right)(\text{m})} = \frac{\left(\text{kg m}^2 \text{ s}^{-3}\right)\left(\text{m}^{-3} \text{ sr}^{-1}\right)}{\left(\text{kg m}^{-3}\right)(\text{m})} = \text{m s}^{-3} \text{ sr}^{-1}.$$

9.15 Equation (9.34),

$$-\frac{1}{\kappa_\lambda \rho} \frac{dI_\lambda}{ds} = I_\lambda - S_\lambda,$$

with κ_λ, ρ, and S_λ independent of position, can be integrated as

$$\int_{I_{\lambda,0}}^{I_\lambda} \frac{dI'_\lambda}{I'_\lambda - S_\lambda} = -\kappa_\lambda \rho \int_0^s ds',$$

where $I_{\lambda,0}$ is the value of the specific intensity at $s = 0$. This results in

$$\ln\left(\frac{I_\lambda - S_\lambda}{I_{\lambda,0} - S_\lambda}\right) = -\kappa_\lambda \rho s,$$

which simplifies to Eq. (9.35).

9.16 (a) Begin with the transfer equation, Eq. (9.34),

$$-\frac{1}{\kappa_\lambda \rho}\frac{dI_\lambda}{ds} = I_\lambda - S_\lambda.$$

Here, s is a distance measured along the light ray's direction of travel. In terms of the angle θ',

$$ds = \frac{dr}{\cos\theta'}.$$

Using this to replace ds in the transfer equation produces the desired result.

(b) Multiply each side of this form of the transfer equation by $\cos\theta'$, and integrate over all directions of the ray:

$$-\frac{1}{\kappa_\lambda \rho}\frac{d}{dr}\left(\int I_\lambda \cos^2\theta'\, d\Omega'\right) = \int I_\lambda \cos\theta'\, d\Omega' - S_\lambda \int \cos\theta'\, d\Omega',$$

where we have used the fact that the source function is isotropic to remove it from the integral. The integral on the left-hand side is $c P_{\mathrm{rad},\lambda}$, the radiation pressure (Eq. 9.9) multiplied by c, while the first integral on the right-hand side is F_λ, the radiative flux (Eq. 9.8). The second integral on the right-hand side is zero, so we have

$$-\frac{c}{\kappa_\lambda \rho}\frac{dP_{\mathrm{rad},\lambda}}{dr} = F_\lambda.$$

Finally, integrating over all wavelengths gives the final result,

$$\frac{dP_{\mathrm{rad}}}{dr} = -\frac{\overline{\kappa}\rho}{c} F_{\mathrm{rad}}.$$

9.17 The Eddington approximation assumes that the intensity of the radiation field is a constant I_{out} in the $+z$-direction (outward, $0 \le \theta \le \pi/2$), and a constant I_{in} in the $-z$-direction (inward, $\pi/2 < \theta \le \pi$). From Eq. (9.3),

$$\begin{aligned}
\langle I \rangle &= \frac{1}{4\pi}\left(\int_{\phi=0}^{2\pi}\int_{\theta=0}^{\pi/2} I_{\mathrm{out}} \sin\theta\, d\theta\, d\phi + \int_{\phi=0}^{2\pi}\int_{\theta=\pi/2}^{\pi} I_{\mathrm{in}} \sin\theta\, d\theta\, d\phi\right) \\
&= \frac{2\pi}{4\pi}\left(I_{\mathrm{out}}\int_{\theta=0}^{\pi/2} \sin\theta\, d\theta + I_{\mathrm{in}}\int_{\theta=\pi/2}^{\pi} \sin\theta\, d\theta\right) \\
&= \frac{1}{2}(I_{\mathrm{out}} + I_{\mathrm{in}}).
\end{aligned}$$

From Eq. (9.8),

$$\begin{aligned} F_{\text{rad}} &= \int_{\phi=0}^{2\pi}\int_{\theta=0}^{\pi/2} I_{\text{out}}\cos\theta\sin\theta\,d\theta\,d\phi + \int_{\phi=0}^{2\pi}\int_{\theta=\pi/2}^{\pi} I_{\text{in}}\cos\theta\sin\theta\,d\theta\,d\phi \\ &= 2\pi\left(I_{\text{out}}\int_{\theta=0}^{\pi/2}\cos\theta\sin\theta\,d\theta + I_{\text{in}}\int_{\theta=\pi/2}^{\pi}\cos\theta\sin\theta\,d\theta\right) \\ &= \pi(I_{\text{out}} - I_{\text{in}}). \end{aligned}$$

From Eq. (9.9),

$$\begin{aligned} P_{\text{rad}} &= \frac{1}{c}\left(\int_{\phi=0}^{2\pi}\int_{\theta=0}^{\pi/2} I_{\text{out}}\cos^2\theta\sin\theta\,d\theta\,d\phi + \int_{\phi=0}^{2\pi}\int_{\theta=\pi/2}^{\pi} I_{\text{in}}\cos^2\theta\sin\theta\,d\theta\,d\phi\right) \\ &= \frac{2\pi}{c}\left(I_{\text{out}}\int_{\theta=0}^{\pi/2}\cos^2\theta\sin\theta\,d\theta + I_{\text{in}}\int_{\theta=\pi/2}^{\pi}\cos^2\theta\sin\theta\,d\theta\right) \\ &= \frac{2\pi}{3c}(I_{\text{out}} + I_{\text{in}}) \\ &= \frac{4\pi}{3c}\langle I\rangle. \end{aligned}$$

9.18 Inserting Eq.(9.46) into Eq. (9.51) gives

$$I_{\text{out}} + I_{\text{in}} = \frac{3\sigma}{2\pi}T_e^4\left(\tau_v + \frac{2}{3}\right). \tag{S9.4}$$

Inserting Eq.(9.47) into Eq. (9.43) gives

$$I_{\text{out}} - I_{\text{in}} = \frac{\sigma}{\pi}T_e^4. \tag{S9.5}$$

Adding these, we find that

$$I_{\text{out}} = \frac{\sigma}{\pi}T_e^4\left(\frac{3}{4}\tau_v + 1\right).$$

Subtracting Eq. (S9.5) from Eq. (S9.4) results in

$$I_{\text{in}} = \frac{3\sigma}{4\pi}T_e^4\,\tau_v.$$

The radiation field will be isotropic to within 1% when

$$\frac{I_{\text{out}} - I_{\text{in}}}{\frac{1}{2}(I_{\text{out}} + I_{\text{in}})} = 0.01.$$

Using the above expressions, we have

$$\frac{\sigma T_e^4/\pi}{\frac{1}{2}\left[\left(\frac{3\sigma T_e^4}{2\pi}\right)\left(\tau_v + \frac{2}{3}\right)\right]} = 0.01,$$

or

$$\frac{4}{3\tau_v + 2} = 0.01,$$

so $\tau_v = 133$.

9.19 From Eq. (9.53), at the top of a star's atmosphere where $\tau_v = 0$, $T^4 = T_e^4/2$. Thus $T/T_e = (1/2)^{1/4} = 0.841$. If $T_e = 5777$ K, then at the top of the atmosphere $T = 4858$ K.

9.20 For a plane-parallel gray atmosphere in LTE, Eq. (9.44) states that $\langle I \rangle = S$. Using Eq. (9.50), we have

$$S = \langle I \rangle = \frac{3}{4\pi} F_{\rm rad} \left(\tau_v + \frac{2}{3} \right).$$

Evaluating this at $\tau_v = 2/3$ results in the Eddington–Barbier relation,

$$F_{\rm rad} = \pi S(\tau_v = 2/3).$$

9.21 If the source function does not vary with position, then Eq. (9.54) may be integrated to obtain

$$I_\lambda(0) = I_{\lambda,0} e^{-\tau_{\lambda,0}} + S_\lambda \left(1 - e^{-\tau_{\lambda,0}}\right).$$

If no radiation enters the gas from outside, then $I_{\lambda,0} = 0$. We consider two cases.

$\tau_{\lambda,0} \gg 1$: In this case, the source function is equal to the Planck function: $S_\lambda = B_\lambda$ (assuming thermodynamic equilibrium). The exponential is essentially zero, so we have

$$I_\lambda(0) = S_\lambda = B_\lambda,$$

and you will see blackbody radiation.

$\tau_{\lambda,0} \ll 1$: We can use $e^{-x} \simeq 1 - x$ to write

$$I_\lambda(0) \simeq S_\lambda[1 - (1 - \tau_{\lambda,0})] = S_\lambda \tau_{\lambda,0}.$$

For our slab of thickness L, $\tau_{\lambda,0} = \kappa_\lambda \rho L$ (Eq. 9.17). Recalling the definition of the source function, $S_\lambda \equiv j_\lambda/\kappa_\lambda$, we have

$$I_\lambda(0) \simeq \frac{j_\lambda}{\kappa_\lambda} (\kappa_\lambda \rho L) = j_\lambda \rho L.$$

Thus you will see emission lines at wavelengths where j_λ is large.

9.22 If the source function does not vary with position, then Eq. (9.54) may be integrated to obtain

$$I_\lambda(0) = I_{\lambda,0} e^{-\tau_{\lambda,0}} + S_\lambda \left(1 - e^{-\tau_{\lambda,0}}\right).$$

We consider two cases.

$\tau_{\lambda,0} \gg 1$: In this case, the source function is equal to the Planck function: $S_\lambda = B_\lambda$ (assuming thermodynamic equilibrium). The exponentials are essentially zero, so we have

$$I_\lambda(0) = S_\lambda = B_\lambda,$$

and you will see blackbody radiation.

$\tau_{\lambda,0} \ll 1$: We can use $e^{-x} \simeq 1 - x$ to write

$$I_\lambda(0) \simeq I_{\lambda,0}(1 - \tau_{\lambda,0}) + S_\lambda[1 - (1 - \tau_{\lambda,0})] = I_{\lambda,0} - \tau_{\lambda,0}(I_{\lambda,\circ} - S_\lambda).$$

For our slab of thickness L, $\tau_{\lambda,0} = \kappa_\lambda \rho L$ (Eq. 9.17). So we have

$$I_\lambda(0) \simeq I_{\lambda,0} - \kappa_\lambda \rho L (I_{\lambda,0} - S_\lambda).$$

If $I_{\lambda,0} > S_\lambda$, then you will see absorption lines superimposed on the incident spectrum ($I_{\lambda,0}$). If $I_{\lambda,0} < S_\lambda$, then you will see emission lines superimposed on the incident spectrum. The strength of the lines depends on the competition between the processes of absorption and emission. From the definition of the source function, $S_\lambda \equiv j_\lambda/\kappa_\lambda$,

$$I_\lambda(0) \simeq I_{\lambda,0} - \rho L(\kappa_\lambda I_{\lambda,0} - j_\lambda)$$

(c.f., Eq. 9.33).

9.23 Inserting $S_\lambda = a_\lambda + b_\lambda \tau_{\lambda,v}$ into Eq. (9.55), we have (omitting the λ subscripts for convenience)

$$\begin{aligned} I(0) &= \int_0^\infty (a + b\tau_v)\, \sec\theta\, e^{-\tau_v \sec\theta}\, d\tau_v \\ &= a \sec\theta \int_0^\infty e^{-\tau_v \sec\theta}\, d\tau_v + b \sec\theta \int_0^\infty \tau_v\, e^{-\tau_v \sec\theta}\, d\tau_v. \end{aligned}$$

The first integral on the right-hand side is $1/\sec\theta$, while the second can be integrated by parts, resulting in

$$\begin{aligned} I(0) &= a + b \sec\theta \left(\int_0^\infty \frac{e^{-\tau_v \sec\theta}}{\sec\theta}\, d\tau_v - \frac{\tau_v}{\sec\theta}\, e^{-\tau_v \sec\theta} \Bigg|_0^\infty \right) \\ &= a + b \sec\theta \left(\cos^2\theta - 0 \right). \end{aligned}$$

Restoring the λ subscripts, this is

$$I_\lambda(0) = a_\lambda + b_\lambda \cos\theta.$$

9.24 Assuming that there is zero flux received from the center of the line (as in the Schuster–Schwarzschild model), the equivalent width is equal to the area of the half-ellipse divided by the semimajor axis. From Eq. (2.4),

$$W = \frac{\pi ab/2}{a} = \frac{\pi b}{2}.$$

9.25 Heisenberg's uncertainty principle, Eq. (5.20), relates ΔE, the uncertainty in the energy of an atomic orbital, to Δt, the time an electron occupies the orbital before making a downward transition:

$$\Delta E \approx \frac{\hbar}{\Delta t} = \frac{h}{2\pi \Delta t}.$$

When an electron makes a downward transition from an initial to a final orbital, the energy of the emitted photon is (Eq. 5.3)

$$E_{\text{photon}} = \frac{hc}{\lambda} = E_i - E_f.$$

The uncertainty in λ caused by an uncertainty in E_i is found by taking a derivative with respect to E_i (holding E_f constant):

$$-\frac{hc}{\lambda^2} \frac{d\lambda}{dE_i} = 1.$$

Writing $\Delta\lambda$ instead of $d\lambda$, ΔE_i instead of dE_i, and ignoring the minus sign yields the magnitude of the uncertainty,

$$\Delta\lambda = \frac{\lambda^2}{hc}\, \Delta E_i.$$

Similarly, the magnitude of the uncertainty in λ due to an uncertainty in E_f is

$$\Delta\lambda = \frac{\lambda^2}{hc}\,\Delta E_f.$$

Adding these uncertainties and using the uncertainty principle to substitute for the ΔEs gives our result,

$$\Delta\lambda = \frac{\lambda^2}{hc}\left(\Delta E_i + \Delta E_f\right) \approx \frac{\lambda^2}{2\pi c}\left(\frac{1}{\Delta t_i} + \frac{1}{\Delta t_f}\right).$$

9.26 (a) For each of the wavelengths listed in Table 9.3, calculate the value of $\log_{10}(W/\lambda)$.

$$\log_{10}(W/\lambda) = -4.69 \quad \text{for the 330.298 nm line}$$
$$= -4.02 \quad \text{for the 589.594 nm line.}$$

These values can then be used with the general curve of growth for the Sun, Fig. 9.22, to obtain a value of $\log_{10}[fN_a(\lambda/500\text{ nm})]$ for each wavelength. The results are

$$\log_{10}\left(\frac{fN_a\lambda}{500\text{ nm}}\right) = 16.63 \quad \text{for the 330.298 nm line}$$
$$= 18.55 \quad \text{for the 589.594 nm line.}$$

Now calculate $\log_{10}[f(\lambda/500\text{ nm})]$ for each wavelength,

$$\log_{10}\left(\frac{f\lambda}{500\text{ nm}}\right) = -2.4899 \quad \text{for the 330.298 nm line}$$
$$= -0.4165 \quad \text{for the 589.594 nm line,}$$

and use

$$\log_{10} N_a = \log_{10}\left(\frac{fN_a\lambda}{500\text{ nm}}\right) - \log_{10}\left(\frac{f\lambda}{500\text{ nm}}\right)$$

to find

$$\log_{10} N_a = 19.12 \quad \text{for the 330.298 nm line}$$
$$= 18.96 \quad \text{for the 589.594 nm line.}$$

The average value of $\log_{10} N_a$ for this problem is 19.04, so $N_a = 1.10 \times 10^{19}\ \text{m}^{-2}$.

(b) Averaging the values of $\log_{10} N_a$ from this problem and Example 9.5.5 gives $\langle \log_{10} N_a \rangle = 19.02$. This average can be used to plot the positions of the four sodium absorption lines on Fig 9.22. With the values shown in Table S9.1, all of the points lie on the curve of growth.

9.27 (a) For each of the wavelengths listed in Table 9.4, calculate the value of $\log_{10}(W/\lambda)$.

$$\log_{10}(W/\lambda) = -3.697 \quad \text{for the 1093.8 nm line}$$
$$= -3.798 \quad \text{for the 1004.9 nm line.}$$

Use these with the general curve of growth for the Sun, Fig. 9.22, to obtain a value of $\log_{10}[fN_a(\lambda/500\text{ nm})]$ for each wavelength. The results are

$$\log_{10}\left(\frac{fN_a\lambda}{500\text{ nm}}\right) = 19.21 \quad \text{for the 1093.8 nm line}$$
$$= 18.96 \quad \text{for the 1004.9 nm line.}$$

Table S9.1: Results for Problem 9.26.

λ (nm)	$\log_{10}[f\langle N_a\rangle(\lambda/500\text{ nm})]$	$\log_{10}(W/\lambda)$
330.238	13.17	−4.58
330.298	12.53	−4.69
588.997	14.90	−3.90
589.594	14.60	−4.02

Now calculate $\log_{10}[f(\lambda/500\text{ nm})]$ for each wavelength,

$$\log_{10}\left(\frac{f\lambda}{500\text{ nm}}\right) = -0.9165 \quad \text{for the 1093.8 nm line}$$
$$= -1.2671 \quad \text{for the 1004.9 nm line,}$$

and use

$$\log_{10} N_a = \log_{10}\left(\frac{fN_a\lambda}{500\text{ nm}}\right) - \log_{10}\left(\frac{f\lambda}{500\text{ nm}}\right)$$

to find

$$\log_{10} N_a = 20.13 \quad \text{for the 1093.8 nm line}$$
$$= 20.23 \quad \text{for the 1004.9 nm line.}$$

The average value of $\log_{10} N_a$ for this problem is $\langle N_a\rangle = 20.18$, so $\langle N_a\rangle = 1.51\times10^{20}$ m^{-2}. This is the value of the number of neutral hydrogen atoms per unit area with an electron in the $n = 3$ orbit.

(b) The Boltzmann equation (Eq. 8.6) allows us to find the relative numbers of neutral hydrogen atoms in the $n = 3$, $n = 2$, and $n = 1$ states. From Eq. (5.14), $E_1 = -13.6$ eV, $E_2 = -3.40$ eV, and $E_3 = -1.51$ eV, and $g_n = 2n^2$ for hydrogen. For $T = 5800$ K from Example 9.5.5, we find $N_3/N_2 = 5.14\times10^{-2}$ and $N_3/N_1 = 2.82\times10^{-10}$. That is, for every neutral hydrogen atom in the $n = 3$ state, there are 19 in the $n = 2$ state and 3.55×10^9 in the $n = 1$ state. The number of neutral hydrogen atoms per unit area is then

$$\frac{N_1}{N_3}\langle N_a\rangle = 5.35\times10^{29}\text{ m}^{-2}.$$

The ratio of the number of ionized to neutral atoms is obtained from the Saha equation, Eq. (8.9), with $P_e = 1$ N m^{-2} (from Example 9.5.5), and $Z_{\rm I} = 2$, $Z_{\rm II} = 1$, and $\chi_{\rm I} = 13.6$ eV (from Example 8.1.4). The result shows that $N_{\rm II}/N_{\rm I} = 1.33\times10^{-4}$, so nearly all of the hydrogen atoms are neutral. Thus the above result gives the total number of hydrogen atoms per unit area, $N = 5.35\times10^{29}$ m^{-2}.

9.28 (a) See Table S9.2.

(b) See Fig. S9.1.

(c) See Table S9.2 and Fig. S9.1.

(d) The surface value of the temperature obtained from Eq. (9.53) is certainly more valid (on physical grounds) than the surface boundary condition of $T = 0$ employed by `StatStar`. However, given the numerous other approximations involved, `StatStar`'s surface value of $T = 0$ is adequate for our computational purposes.

9.29 (a) See Fig. S9.2.

(b) See Fig. S9.2.

Table S9.2: Results for Problem 9.28. $T_e = 5504$ K.

i	τ	`StatStar` T (K)	Eq. (9.53) T (K)
0	0	0	4628.29387
1	0.202	3379.636	4944.54379
2	0.249	3573.309	5010.27511
3	0.323	3826.212	5109.25693
4	0.435	4133.144	5247.76298
5	0.601	4488.02	5434.68901
6	0.837	4887.027	5672.40675
7	1.18	5329.075	5971.56257
8	1.67	5815.187	6331.32593
9	2.36	6347.784	6758.27250
10	3.35	6930.293	7251.69484
11	4.76	7566.856	7817.22609
12	6.76	8262.201	8456.53505
13	9.6	9021.603	9167.93293
14	13.6	9850.881	9961.57689
15	19.4	10756.42	10835.93954
16	27.5	11745.2	11802.05637
17	39.1	12824.86	12859.13228
18	55.5	14003.75	14023.06436
19	78.9	15290.96	15297.04393
20	112	16696.43	16685.66151
21	159	18231.02	18209.78084
22	226	19906.56	19873.14791
23	321	21735.99	21688.97654
24	455	23733.41	23670.55978
25	647	25914.21	25839.07014
26	918	28295.19	28199.43679
27	1300	30894.68	30778.36382
28	1850	33732.66	33593.27783
29	2620	36830.96	36662.39802
30	3720	40213.37	40008.77661
31	5280	43905.83	43659.68737
32	7480	47936.66	47642.36440
33	10600	52336.7	51988.38249
34	15000	57139.61	56721.79737
35	21300	62382.05	61894.51265
36	30200	68104.01	67520.02502
37	42700	74349.04	73640.96139
38	60500	81164.61	80321.39363
39	85600	88602.39	87603.73858
40	121000	96718.69	95532.96119
41	171000	105574.8	104163.8651

(c) The difference is greatest at mid angles (approximately 50°) and near 90°.

(d) Van Hamme's formula best mimics the observational data for the Sun.

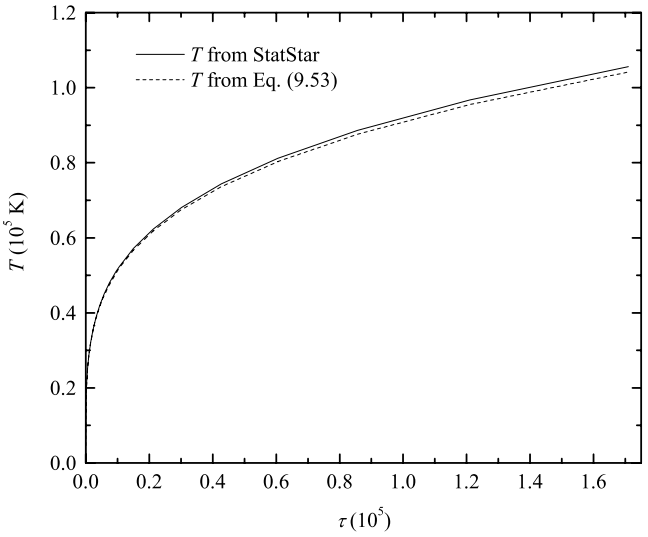

Figure S9.1: Results for Problem 9.28.

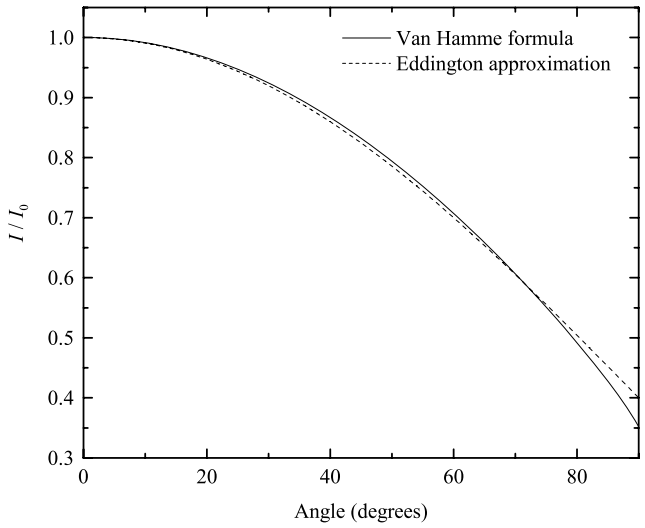

Figure S9.2: A comparison between the limb darkening formulae of Van Hamme and the Eddington approximation (Eq. 9.58).

CHAPTER 10

The Interiors of Stars

10.1 From Eq. (9.15), $dr = -d\tau/\overline{\kappa}\rho$. Substitution into Eq. (10.6) leads immediately to the final result.

10.2 The procedure is identical to the one that was used in Example 2.2.1 (see also Fig. 2.8). In this case however, $r < r_1$ and $r_1 < R < r_2$. After changing variables from θ to u, the limits of integration become $u = (R-r)^2$ to $u = (R+r)^2$. This leads to an integral of the form

$$F = \frac{\pi G m \rho}{2} \int_{r_1}^{r_2} \int_{(R-r)^2}^{(R+r)^2} \left[R\left(1 - \frac{R^2}{r^2}\right) u^{-3/2} + \frac{R}{r^2} u^{-1/2} \right] du\, dR.$$

After integrating over u, exact cancellation occurs, giving $F = 0$.

10.3 Assuming that the Sun is composed entirely of hydrogen atoms, the number of atoms in the Sun is approximately

$$N \simeq \frac{1\ \mathrm{M}_\odot}{m_H} = 1.2 \times 10^{57}.$$

If each atom releases 10 eV of energy during a chemical reaction, the time scale for chemical reactions would be

$$t_{\mathrm{chem}} = \frac{E_{\mathrm{chem}}}{L_\odot} = \frac{1.2 \times 10^{58}\ \mathrm{eV}}{3.84 \times 10^{26}\ \mathrm{W}} \simeq 5 \times 10^{12}\ \mathrm{s} = 1.6 \times 10^5\ \mathrm{yr}.$$

This is much shorter than the age of the solar system, and so the Sun's energy cannot be chemical.

10.4 (a) Using the reduced mass for a proton–proton collision, and equating kinetic energy to thermal energy,

$$\frac{3}{2} kT = \frac{1}{2} \mu_p v_{\mathrm{rms}}^2.$$

If particles with ten times the rms velocity can overcome the Coulomb barrier, then

$$v = 10 v_{\mathrm{rms}} = 10 \left(3kT/\mu_p\right)^{1/2}$$

and

$$\frac{e^2}{4\pi\epsilon_0 r} = \frac{1}{2}\mu_p v^2 = \frac{1}{2}(100)\left(\frac{3}{2}kT\right).$$

Taking the separation between charges to be $r \simeq 2$ fm,

$$T = \frac{4}{300k}\,\frac{e^2}{4\pi\epsilon_0 r} = 1.1 \times 10^8\ \mathrm{K}.$$

This value is approximately 7 times greater than the Sun's central temperature.

(b) From Eq. (8.1), and assuming identical velocity intervals, the ratio of atoms having velocities equal to 10 times the rms value to those having the rms value is given by

$$\frac{n_v}{n_{\mathrm{rms}}} = \frac{e^{-m(10v_{\mathrm{rms}})^2/2kT}\ (10v_{\mathrm{rms}})^2}{e^{-mv_{\mathrm{rms}}^2/2kT}\ v_{\mathrm{rms}}^2}$$

$$= 100\, e^{-99(mv_{\mathrm{rms}}^2/2kT)} = 100\, e^{-99(m/2kT)\,(3kT/2m)}$$

$$= 100\, e^{-74.3} = 5.7 \times 10^{-31}.$$

(c) Assuming pure hydrogen, the number of atomic nuclei in the Sun is approximately 1.2×10^{57} (see the solution to Problem 10.3). *If* $T \sim 1.1 \times 10^8$ K throughout the star, and *if* all nuclei with $v = 10 v_{\rm rms}$ can react, then the number of nuclei that will be involved in nuclear reactions is roughly

$$N_{\rm react} \simeq N \left(\frac{n_v}{n_{\rm rms}} \right) = 7 \times 10^{26}.$$

Given that in the proton–proton chain, 0.7% of the mass is converted into energy, the timescale for this process would be

$$t \simeq \frac{E}{L_\odot} = \frac{0.007 N_{\rm react} m_p c^2}{L_\odot} = \frac{7.2 \times 10^{14} \text{ J}}{3.84 \times 10^{26} \text{ W}} = 2 \times 10^{-12} \text{ s}.$$

Quantum mechanical tunneling is definitely required!

10.5 Beginning with Eq. (10.9) and substituting Eq. (8.1),

$$\begin{aligned} P &= \frac{1}{3} \int_0^\infty m n_v v^2 \, dv \\ &= \frac{1}{3} \int_0^\infty mn \left(\frac{m}{2\pi k T} \right)^{3/2} e^{-mv^2/2kT} \, 4\pi v^4 \, dv. \end{aligned}$$

Using the definite integral,

$$\int_0^\infty x^{2n} e^{-ax^2} \, dx = \frac{1 \cdot 3 \cdot 5 \ldots (2n-1)}{2^{n+1} a^n} \sqrt{\frac{\pi}{a}},$$

with $n = 2$ and $a = m/2kT$,

$$P = \frac{4\pi mn}{3} \left(\frac{m}{2\pi k T} \right)^{3/2} \frac{3\sqrt{\pi}}{2^3 \, (m/2kT)^{5/2}} = nkT.$$

10.6 From the non-relativistic expression for kinetic energy (E),

$$v = \sqrt{\frac{2E}{m}} \qquad \text{and} \qquad dv = \frac{1}{2} \sqrt{\frac{2}{mE}} \, dE.$$

Using the relation $n_v \, dv = n_E \, dE$ and making the appropriate substitutions in Eq. (8.1) leads directly to Eq. (10.28).

10.7 From Eq. (10.22), the gravitational potential energy of the Sun is approximately $U_g = -2.3 \times 10^{41}$ J. Using the virial theorem (Eq. 2.46), the thermal kinetic energy of the Sun is roughly $3NkT/2 = 1.2 \times 10^{41}$ J, where N is the number of particles in the Sun. Assuming that all of the hydrogen is ionized, then $N = 2.4 \times 10^{57}$ (see the solution to Problem 10.3 and assume that every hydrogen atom contributes a nucleus and a free electron). Solving for the temperature, $T = 2.4 \times 10^6$ K.

This value is roughly an order of magnitude less than than the estimate of the Sun's central temperature, but it is reasonable for an average temperature of the Sun.

10.8 According to the discussion between Eqs. (10.30) and (10.31),

$$\frac{U_c}{E} = \frac{Z_1 Z_2 e^2}{2\pi \epsilon_0 h v}.$$

Furthermore, using the non-relativistic expression, $v = \sqrt{2E/\mu_m}$,

$$\frac{U_c}{E} = \frac{Z_1 Z_2 e^2 \mu_m^{1/2}}{2^{1/2} 2\pi\epsilon_0 E^{1/2} h}.$$

After substituting into Eq. (10.30) and simplifying, we arrive at Eq. (10.31).

10.9 The energy at which the Gamow peak is a maximum occurs when

$$\frac{d}{dE}\left[e^{-(E/kT + bE^{-1/2})}\right] = 0,$$

or

$$-\left(\frac{1}{kT} - \frac{1}{2}bE^{-3/2}\right) e^{-(E/kT + bE^{-1/2})} = 0.$$

Solving for E gives Eq. (10.34).

10.10 From Eq. (10.47), $\epsilon_{pp} = 1.16 \times 10^{-3}$ W kg^{-1}, and from Eq. (10.59), $\epsilon_{\rm CNO} = 3.90 \times 10^{-4}$ W kg^{-1}. These results give $\epsilon_{pp}/\epsilon_{\rm CNO} = 2.97$.

10.11 Equation (10.62) is of the form

$$\epsilon_{3\alpha} = c\rho^2 Y^3 T_8^{-3} f_{3\alpha} e^{-\beta T_8^{-1}},$$

where $c \equiv 50.9$ W m^6 kg^{-3}, $\beta \equiv 44.027$, and $T_8 \equiv T/10^8$ K. Thus,

$$\ln \epsilon_{3\alpha} = \ln c + 2\ln\rho + 3\ln Y - 3\ln T_8 + \ln f_{3\alpha} - \beta T_8^{-1}.$$

Differentiating with respect to $\ln T_8$,

$$\frac{\partial \ln \epsilon_{3\alpha}}{\partial \ln T_8} = -3 - \frac{\partial\left(\beta T_8^{-1}\right)}{\partial \ln T_8} = -3 - T_8 \frac{\beta T_8^{-1}}{\partial T_8} = -3 + \frac{\beta}{T_8}.$$

Next, assuming a power law of the form

$$\epsilon_{3\alpha} = \epsilon'' T_8^{\alpha},$$

and again differentiating with respect to $\ln T_8$ gives

$$\frac{\partial \ln e_{3\alpha}}{\partial \ln T_8} = \alpha.$$

Comparing results,

$$\alpha = -3 + \frac{\beta}{T_8} = 41.027$$

when $T_8 = 1$ and $\epsilon'' = c\rho^2 Y^3 f_{3\alpha}$.

10.12 The Q-values for the three reaction steps are

$$Q_1 = \left(2m_{^1_1\mathrm{H}} - m_{^2_1\mathrm{H}} - m_{e^+}\right)c^2 = 0.933\ \mathrm{MeV} > 0$$

$$Q_2 = \left(m_{^2_1\mathrm{H}} + m_{^1_1\mathrm{H}} - m_{^3_2\mathrm{He}}\right)c^2 = 5.519\ \mathrm{MeV} > 0$$

$$Q_3 = \left(2m_{^3_2\mathrm{He}} - m_{^4_2\mathrm{He}} - 2m_{^1_1\mathrm{H}}\right)c^2 = 12.806\ \mathrm{MeV} > 0.$$

10.13 Using the approach suggested in Problem 10.12:

(a) 13.94 MeV (exothermic)

(b) −0.108 MeV (endothermic)

(c) 8.11 MeV (exothermic)

10.14 (a) ${}^{27}_{14}\mathrm{Si} \rightarrow {}^{27}_{13}\mathrm{Al} + e^+ + \nu$

(b) ${}^{27}_{13}\mathrm{Al} + {}^{1}_{1}\mathrm{H} \rightarrow {}^{24}_{12}\mathrm{Mg} + {}^{4}_{2}\mathrm{He}$

(c) ${}^{35}_{17}\mathrm{Cl} + {}^{1}_{1}\mathrm{H} \rightarrow {}^{36}_{18}\mathrm{Ar} + \gamma$

10.15 Beginning with the ideal gas law (Eq. 10.77), solving for V and substituting into Eq. (10.82) gives

$$P\left(\frac{nRT}{P}\right)^{\gamma} = K.$$

Solving for P results in Eq. (10.83), with $K' \equiv K/(nR)^{\gamma/(1-\gamma)}$.

10.16 We begin by using the equation of hydrostatic equilibrium (Eq. 10.6),

$$\frac{dP}{dr} = -G\frac{M_r\rho}{r^2},$$

to find

$$\frac{1}{\rho}\frac{dP}{dr} = -\frac{GM_r}{r^2}.$$

We also note that the potential energy of a point mass m brought in from infinity to a distance r *inside* the star is given by

$$U_g = -\int_{\infty}^{r} F_g\,dr = -\int_{\infty}^{r} -\frac{GM_r m}{r^2}dr.$$

This implies that,

$$\frac{dU_g}{dr} = \frac{GM_r m}{r^2},$$

or

$$\frac{d\Phi_g}{dr} = \frac{d(U_g/m)}{dr} = \frac{GM_r}{r^2}.$$

Thus

$$\frac{1}{\rho}\frac{dP}{dr} = -\frac{d\Phi_g}{dr}.$$

Substitution into Eq. (10.108) immediately leads to Eq. (10.109).

10.17 Beginning with Eq. (10.110) and setting $n = 0$ we have

$$\frac{d}{d\xi}\left[\xi^2\frac{dD_0}{d\xi}\right] = -\xi^2.$$

Integrating we have

$$\frac{dD_0}{d\xi} = -\frac{\xi}{3} + \frac{C'}{\xi^2}.$$

Applying the central boundary condition, $dD_0/d\xi = 0$ at $\xi = 0$, implies that $C' = 0$. Integrating a second time gives

$$D_0 = -\frac{\xi^2}{6} + C''.$$

Applying the normalizing condition $D_0(0) = 1$ implies that $C'' = 1$. Finally, if ξ_1 represents the surface of the polytrope, then $D_0(\xi_1) = 0$. This immediately gives $\xi_1 = \sqrt{6}$.

10.18 The density is parameterized in the Lane–Emden equation as $\rho(r) \equiv \rho_c[D_n(r)]^n$. Thus, for the case of $n = 0$, $\rho(r) = \rho_c$; the density is a constant throughout the star.

10.19 Using the derivative form for the total mass of the polytrope

$$M = -4\pi\lambda_n^3\rho_c\xi_1^2 \left.\frac{dD_n}{d\xi}\right|_{\xi_1},$$

and substituting the expression for

$$D_5(\xi) = [1 + \xi^2/3]^{-1/2}, \qquad \text{with } \xi_1 \to \infty$$

gives

$$M = \frac{4\pi}{3}\lambda_n^3\rho_c \left.\frac{\xi_1^3}{\left(1+\xi_1^2/3\right)^{3/2}}\right|_{\xi_1\to\infty} = \frac{4\pi}{3}\lambda_n^3\rho_c \left.\frac{1}{\left(1/\xi_1^2+1/3\right)^{3/2}}\right|_{\xi_1\to\infty} = 3^{3/2}\left(\frac{4\pi}{3}\lambda_n^3\rho_c\right).$$

Thus, the total mass is finite even though the surface boundary goes to infinity.

10.20 (a) See Fig. S10.1.

(b) The density concentration increases toward the center with increasing polytropic index.

(c) The $n = 1.5$ model represents adiabatic convection and the $n = 3$ model represents a radiative model. The adiabatic convection model will have a shallower density gradient.

(d) The shallower density gradient for the adiabatic model is consistent with an adiabatic gradient that tends to smooth out the structure. The steeper density gradient for the radiative model is consistent with gradients required to drive radiative flux.

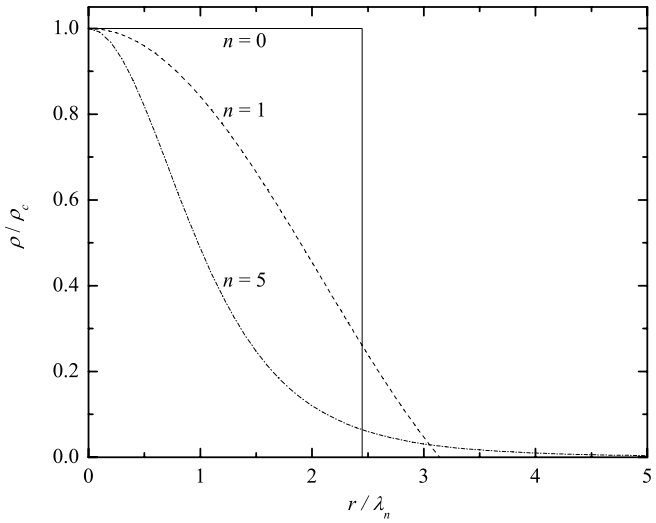

Figure S10.1: The density structures of $n = 0$, 1, and 5 polytropes.

10.21 For a 0.072 $M_\odot$ star, the luminosity is

$$L_{0.072} = 10^{-4.3}L_\odot = 1.92 \times 10^{22}\ \text{W}.$$

Assuming a pure hydrogen composition for simplicity, and if the entire star participates in the energy generation, the amount of energy released in the conversion of hydrogen to helium in a $0.072\ M_\odot$ star is

$$E_{0.072} = (\Delta m)c^2 = 0.007\,(0.072\ M_\odot)\,c^2 = 9.0 \times 10^{43}\ \text{J}.$$

Thus, the hydrogen-burning lifetime is

$$t_{0.072} \simeq \frac{E_{0.072}}{L_{0.072}} \simeq 5 \times 10^{21}\ \text{s} = 1.5 \times 10^{14}\ \text{yr}.$$

Similarly, for an $85\ M_\odot$ star with only the inner 10% of the star participating in nuclear reactions,

$$L_{85} = 10^{6.006} L_\odot = 3.9 \times 10^{32}\ \text{W}$$

$$E_{85} = (0.007)(0.1)(85\ M_\odot)c^2 = 1.1 \times 10^{46}\ \text{J}$$

$$t_{85} = \frac{E_{85}}{L_{85}} = 3 \times 10^{13}\ \text{s} = 9 \times 10^5\ \text{yr}.$$

10.22 From the Stefan–Boltzmann equation (Eq. 3.17), the radius of a star is given by

$$R = \left(\frac{L}{4\pi\sigma T^4}\right)^{1/2}.$$

Using the data from Problem 10.21, $R_{0.072} = 5.9 \times 10^7\ \text{m} = 0.082\ R_\odot$ and $R_{85} = 9.1 \times 10^9\ \text{m} = 13.1\ R_\odot$. Thus $R_{0.072}/R_{85} = 0.0063$.

10.23 The Eddington luminosity is given by Eq. (10.114).

(a) For $M = 0.072\ M_\odot$, $L_{\text{Ed}} = 3.6 \times 10^{31}\ \text{W} = 9.4 \times 10^4\ L_\odot$, implying that $L/L_{\text{Ed}} = 5 \times 10^{-10}$. Radiation pressure does not play a significant role in the stability of a low-mass star.

(b) For $M = 120\ M_\odot$, we may consider electron scattering as an appropriate opacity (the surface is ionized at that temperature). In this case $\kappa = 0.02(1 + X) = 0.034$, and $L_{\text{Ed}} = 4.6 \times 10^6\ L_\odot$. The actual luminosity of the $120\ M_\odot$ star is about $1.8 \times 10^6\ L_\odot$, and so the Eddington luminosity is only about 2.5 times greater than the actual luminosity. Clearly radiation pressure plays a significant role in this case.

10.24 (a) The Lane–Emden equation is a second-order differential equation. One very powerful tool in numerical analysis is to write second-order equations as two first-order equations, one of which is the derivative of the function that you are trying to solve. Beginning with Eq. (10.110) and taking the derivatives leads to

$$\frac{d^2 D_n}{d\xi^2} + \frac{2}{\xi}\frac{dD_n}{d\xi} + D_n^n = 0.$$

Letting

$$f_n(\xi) \equiv \frac{dD_n}{d\xi}$$

gives

$$\frac{df_n}{d\xi} = -D_n^n - \frac{2}{\xi} f_n.$$

These last two coupled equations can now be integrated to produce $D_n(\xi)$. Using a simple Euler method,

$$D_n(\xi_{i+1}) = D_n(\xi_i) + h f_n(\xi_i)$$

and

$$f_n(\xi_{i+1}) = f_n(\xi_i) + h\left[-D_n^n(\xi_i) - \frac{2}{\xi_i} f_n(\xi_i)\right]$$

where h is the step size and $\xi_{i+1} = \xi_i + h$ are the values of ξ for steps $i + 1$ and i, respectively. Finally, $\rho/\rho_c = D_n^n$ gives the density of the polytrope.
A simple Fortran 95 code that implements these ideas is given:

```
PROGRAM LaneEmden

IMPLICIT NONE
REAL(8)     h, f_i, f_ip1, D_i, D_ip1, n, xi

    OPEN(UNIT = 10, FILE = "LaneEmden.txt")

    WRITE (*,'(A)',ADVANCE = 'NO')  "Enter the value of the polytropic index:  "
    READ (*,*) n

    xi = 0                  !Starting value of xi
    h = 0.0001              !step size

    D_i = 1                 !Boundary condition of function
    f_i = 0                 !Boundary condition of first derivative

    WRITE (10,'(3F13.6)')    xi, D_i, f_i

    DO
        xi = h + xi
        D_ip1 = D_i + f_i*h
        f_ip1 = f_i + (-D_i**n - 2/xi*f_i)*h

        IF (D_ip1 < 0 .OR. xi > 10) EXIT

        D_i = D_ip1
        f_i = F_ip1

        !The density relative to the central density is rho/rho_c = D_i**n
        WRITE (10,'(3F13.6)')    xi, D_i**n, f_i
    END DO
END PROGRAM LaneEmden
```

(b) See Fig. S10.2.

10.25 Download the data set for Appendix L for this problem from `www.aw-bc.com/astrophysics`. The model is contained in the file `M1p0ModelX0p7Z0p008.dat`. In order to use the data for the two adjacent zones from Appendix L, we must calculate averages and differences; the results are given in Table S10.1. The two zones that are used in this calculation are $i = 397$ and $i = 398$.

For Eq. (10.6):

$$\frac{dP}{dr} \simeq \frac{P_{i+1} - P_i}{r_{i+1} - r_i} = -9.30 \times 10^6 \text{ N m}^{-3}$$

$$-G\frac{\overline{M_r}\,\overline{\rho}}{\overline{r}^2} \simeq -8.83 \times 10^6 \text{ N m}^{-3}$$

$$\text{rel. error} = -0.0527.$$

For Eq. (10.7):

$$\frac{dM_r}{dr} \simeq 5.135 \times 10^{21} \text{ kg m}^{-1}$$

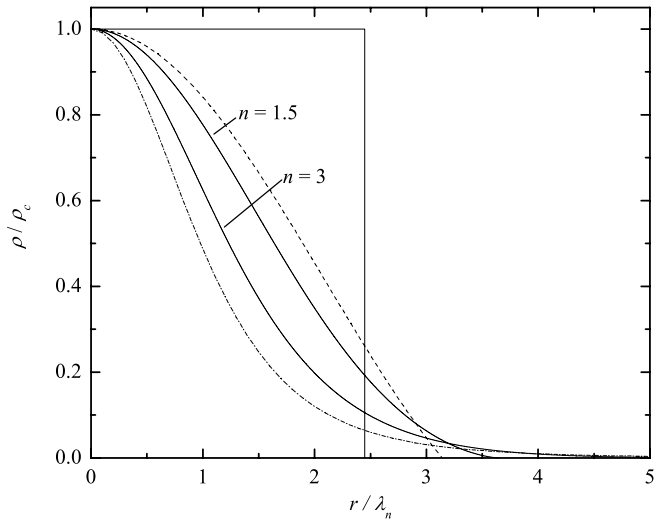

Figure S10.2: The density structures of $n = 1.5$ and $n = 3$ polytropes. The density structures of $n = 0$, 1, and 5 polytropes from Problem 10.20 are included for reference; see Fig. S10.1.

Table S10.1: `StatStar` data from the downloaded 1 $M_\odot$ model for Problem 10.25.

shell	r	1 - M_r/Ms	M_r	L_r	
397	2.728E+08	2.049E−01	1.581E+30	3.297E+26	
398	2.654E+08	2.244E−01	1.543E+30	3.297E+26	
ave	2.691E+08	2.147E−01	1.562E+30	3.297E+26	
diff	−0.074E+08	0.195E−01	−0.038E+30	0.000E+26	

shell	T	P	rho	kap	eps
397	4.941E+06	3.804E+14	5.748E+03	4.512E−01	5.963E−07
398	5.140E+06	4.492E+14	6.524E+03	4.395E−01	8.557E−07
ave	5.040E+06	4.148E+14	6.136E+03	4.454E−01	7.260E−07
diff	0.199E+06	0.688E+14	0.776E+03	−0.117E−01	2.594E−07

$$4\pi\overline{r^2}\,\overline{\rho} \simeq 5.584 \times 10^{21} \text{ kg m}^{-1}$$

$$\text{rel. error} = 0.0804.$$

For Eq. (10.36):

$$\frac{dL_r}{dr} \simeq 0 \text{ W m}^{-1}$$

$$4\pi\overline{r^2}\,\overline{\rho\epsilon} \simeq 2.487 \times 10^{19} \text{ W m}^{-1}$$

$$\text{rel. error} = 1.000.$$

Note that in this case the output did not display enough significant figures in the luminosity to make a reason-

able determination of ΔL_r. Round-off errors (even internal errors before displaying results) can be critical issues to deal with in numerical modeling.

For Eq. (10.68):

$$\frac{dT}{dr} \simeq -2.689 \times 10^{-2} \text{ K m}^{-1}$$

$$-\frac{3}{4ac}\frac{\overline{\kappa\rho}}{\overline{T}^3}\frac{\overline{L}_r}{4\pi\overline{r}^2} \simeq -2.558 \times 10^{-2} \text{ K m}^{-1}$$

$$\text{rel. error} = 0.0512.$$

Table S10.2: Results for Problem 10.26. T_c, P_c, ρ_c, and ϵ_c are all in SI units. The values are obtained from the last zone above the central core.

Mass ($M_\odot$)	T_c	P_c	ρ_c	ϵ_c
0.75	1.182×10^7	1.031×10^{16}	6.146×10^4	5.620×10^{-4}
1.00	1.494×10^7	1.514×10^{16}	7.202×10^4	2.451×10^{-2}

10.26 The (near) central conditions for the 0.75 $M_\odot$ and 1.0 $M_\odot$ models are given in Table S10.2. For the simple Runge–Kutta shooting method that is used in `StatStar`, the extrapolated central conditions are very sensitive to the surface boundary conditions. Using the values of the last zone above the central core are more smoothly-varying and reliable for comparisons between models.

In order to support the extra mass of the 1.0 $M_\odot$ model, the central pressure and temperature are increased over the values for the 0.75 $M_\odot$ model. Because the central pressure increases rapidly with stellar mass, the central density is also greater for the 1 $M_\odot$ star. Since the central nuclear energy generation rate is a function of both the temperature and density in that region, ϵ is greater for the 1 $M_\odot$ star as well.

10.27 The input data for the zero-age main-sequence models are given in Table S10.3. Note that a region of convergence exists in the effective temperature–luminosity plane. The models given here are only representative of the possible solutions at each mass. It is also important to note that `Statstar` was written to be relatively transparent to the student for pedagogical reasons. Consequently, special automated, iterative convergence techniques have not been included in the code. Furthermore, since it is necessary to have fairly tight convergence criteria at the center of the star in order to produce a physically reasonable main sequence, and since the numerical procedure amounts to a shooting method from the surface to the center, the code is quite sensitive to initial starting conditions. This may lead to some initial frustration for some students attempting to find a converged model.

(a) See Figure S10.3. Note that the coarseness of the core is evident in L_r and T. This arises because the core solution is simply extrapolated from the last good zone computed by the Runge–Kutta method. A more sophisticated iterative procedure guaranteeing that the central boundary conditions are strictly enforced is not used in the pedogogical `StatStar` code.

(b) For a 1 $M_\odot$ star, L_r reaches 99% of its surface value at a temperature of about 7.3×10^6 K. It reaches 50% at a temperature of about 1.2×10^7 K. The 50% level is roughly consistent with the "back-of-the-envelope" calculation. Quantum mechanical tunneling is important in stellar nuclear reaction rates.

(c) For a 1 $M_\odot$ star, when L_r reaches 99% of its surface value, $M_r/M_\star \simeq 0.537$, and when it reaches 50%, $M_r/M_\star \simeq 0.0768$.

Table S10.3: Input data for Problem 10.27. All models have $X = 0.7$ and $Z = 0.008$.

M ($M_\odot$)	T_e (K)	L ($L_\odot$)	M ($M_\odot$)	T_e (K)	L ($L_\odot$)
0.50	2287.7	0.0215	4.50	18906.2	516.0
0.60	2862.3	0.0570	4.75	19498.7	624.2
0.70	3465.5	0.1300	5.00	20069.0	745.7
0.75	3788.5	0.1890	5.25	20601.5	880.5
0.80	4109.3	0.2650	5.50	21072.5	1029.0
0.90	4755.5	0.4940	5.75	21585.8	1192.0
1.00	5402.0	0.8590	6.00	22089.0	1372.0
1.10	6117.0	1.4170	6.50	22982.7	1778.9
1.20	6802.3	2.2200	7.00	23810.0	2253.0
1.30	7458.6	3.2900	7.50	24613.0	2794.0
1.40	8062.9	4.6800	8.00	25366.5	3409.0
1.50	8644.6	6.4080	8.50	26052.5	4097.0
1.60	9146.0	8.5000	9.00	26722.0	4857.0
1.70	9596.3	11.0000	9.50	27330.0	5696.0
1.75	9852.6	12.5000	10.00	27933.0	6607.0
1.80	10074.2	14.1000	10.50	28523.0	7601.0
1.90	10546.0	17.8000	11.00	29109.5	8675.0
2.00	10952.6	22.0500	11.50	29648.0	9824.0
2.25	11950.9	35.8000	12.00	30149.0	11050.0
2.50	12903.1	55.1000	12.50	30627.0	12354.0
2.75	13811.0	80.7000	13.00	31096.0	13727.0
3.00	14671.0	113.5000	13.50	31532.1	15170.0
3.25	15479.5	155.2000	13.75	31768.3	15925.0
3.50	16236.5	205.8000	14.00	32009.5	16695.0
3.75	16957.0	266.5000	14.50	32449.7	18254.0
4.00	17639.0	338.1000	15.00	32873.3	19920.0
4.25	18289.4	420.6000			

(d) See Figure S10.4 for parts (i)–(iii). Note that the onset of the strongly temperature-dependent CNO cycle results in a very rapid rise in the core value of ϵ (the graph displays $\log_{10} \epsilon_c$ rather than ϵ_c directly) and a *decrease* in the core value of the density.

Figure S10.5 shows the increase in the size of the central convection zone with increasing stellar mass. Note that the size of the convection zone mirrors the increase in ϵ, indicated in Figure S10.4. Figure S10.6 shows the results for parts (v) and (vi).

(e) See Figures S10.7 and S10.8. For the `StatStar` main sequence, $\alpha \simeq 5.3$ for $M < 1.5\ M_\odot$, $\alpha \simeq 3.9$ for $1.5\ M_\odot < M < 4.5\ M_\odot$, and $\alpha \simeq 3.0$ for $M > 4.5\ M_\odot$.

10.28 *Note:* You may wish to review the discussion at the beginning of the solution to Problem 10.27.

Main-sequence models for $X = 0.7$, $Z = 0.01$ are given in Table S10.4. Figure S10.9 also compares the higher-Z main sequence with the one for $Z = 0.008$, calculated in Problem 10.27. Notice that the higher-Z main sequence is shifted to cooler temperatures and lower luminosities. This is consistent with the discussion of Example 9.5.4 regarding the fact that the low-Z subdwarfs are shifted to the left of the main sequence.

(a) The $Z = 0.008$ model has the largest central temperature and central density.

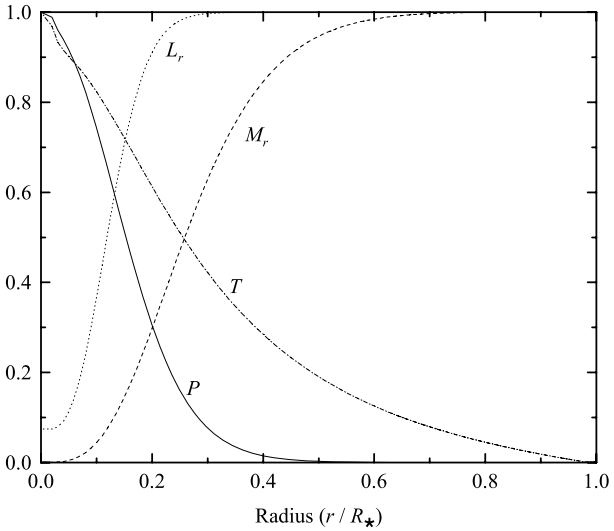

Figure S10.3: The results of Problem 10.27(a) for a 1 $M_\odot$ model with $L = 0.859\ L_\odot$ and $T_e = 5402$ K.

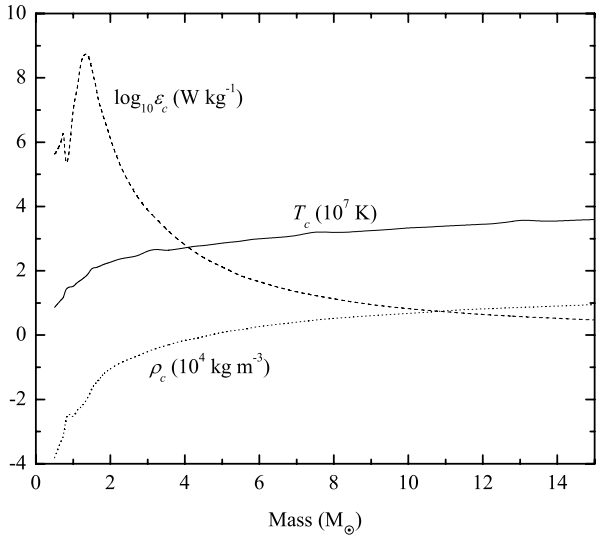

Figure S10.4: The results of Problem 10.27(d), parts (i)–(iii), with $X = 0.7$ and $Z = 0.008$. Note that the values plotted are actually the last zone above the central core. This was done because the core extrapolation procedure is rather coarse.

(b) The $Z = 0.010$ model has the largest value for the opacity at the center, and throughout the star. This is due primarily to the bound–free opacity equation (Eq. 9.22), which is proportional to Z (more electronic transitions are available). A larger opacity results in a slightly inflated star, having a lower density and temperature near the surface. As a consequence, the temperature gradient (Eq. 10.68) is shallower there. Integrating inward, the lower density and temperature means that the energy generation rate is diminished (e.g., Eq. 10.47), resulting in a lower luminosity for the star (Eq. 10.36).

(c) The $Z = 0.008$ model has the largest energy generation rate because of the larger values for the temperature and density.

(d) The $Z = 0.010$ model has a lower effective temperature and a lower luminosity. This is because the

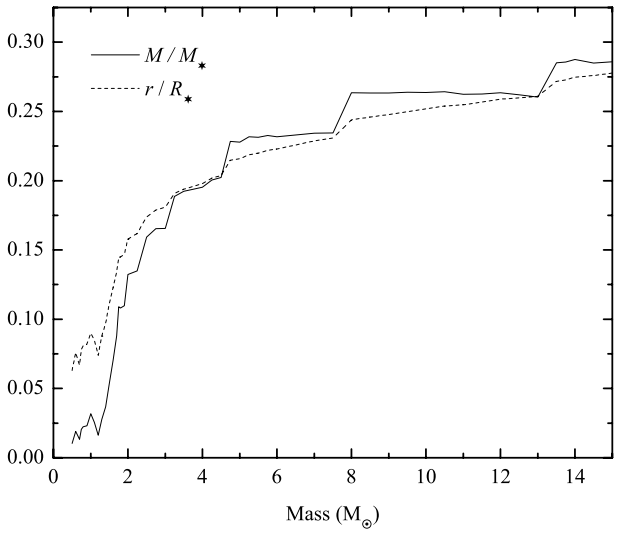

Figure S10.5: The results of Problem 10.27(d), part (iv), with $X = 0.7$ and $Z = 0.008$.

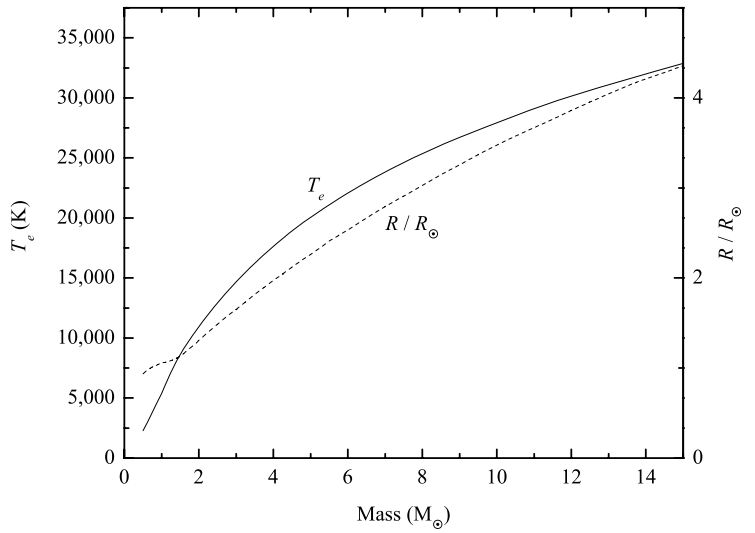

Figure S10.6: The results of Problem 10.27(d), parts (v)–(vi), with $X = 0.7$ and $Z = 0.008$.

opacity has inflated the model, decreasing ϵ and consequently decreasing L.

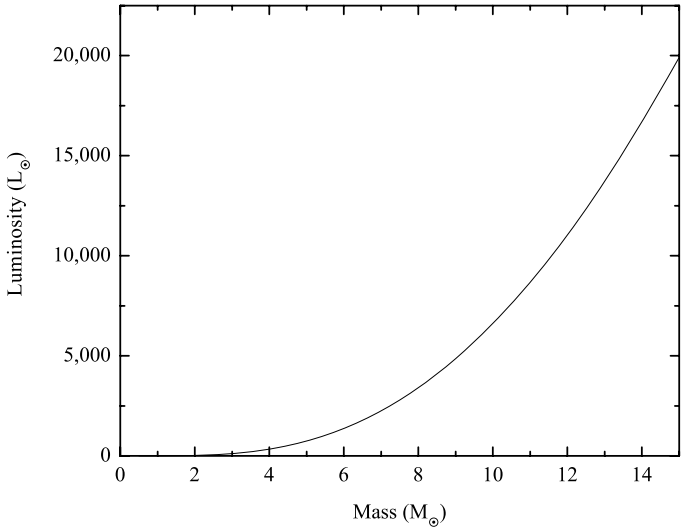

Figure S10.7: The results of Problem 10.27(e), part (i), with $X = 0.7$ and $Z = 0.008$.

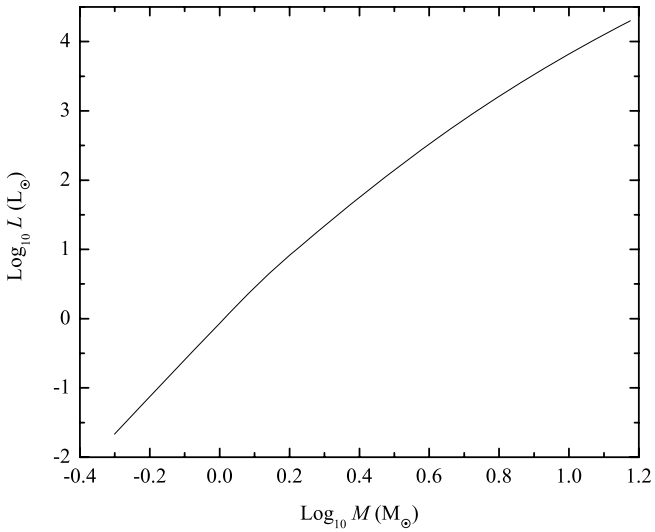

Figure S10.8: The results of Problem 10.27(e), part (ii), with $X = 0.7$ and $Z = 0.008$.

Table S10.4: Input data for Problem 10.27. All models have $X = 0.7$ and $Z = 0.01$.

M ($M_\odot$)	T_e (K)	L ($L_\odot$)	M ($M_\odot$)	T_e (K)	L ($L_\odot$)
0.70	3274.00	0.1100	4.50	18409.20	489.3
0.75	3583.50	0.1610	4.75	18989.50	593.5
0.80	3901.80	0.2290	5.00	19556.80	710.0
0.90	4550.85	0.4365	5.25	20092.30	840.3
1.00	5196.30	0.7600	5.50	20610.30	985.0
1.10	5842.30	1.2500	5.75	21058.70	1143.8
1.20	6486.30	1.9350	6.00	21546.10	1319.0
1.30	7119.90	2.8980	6.50	22444.00	1715.0
1.40	7717.70	4.1300	7.00	23267.50	2178.0
1.50	8219.00	5.6200	7.50	24062.50	2711.0
1.60	8714.00	7.5000	8.00	24819.50	3317.0
1.70	9200.50	9.8000	8.50	25539.00	3996.0
1.75	9426.30	11.1200	9.00	26213.70	4741.0
1.80	9647.10	12.5600	9.50	26847.00	5570.0
1.90	10066.10	15.8300	10.00	27439.00	6475.0
2.00	10514.80	19.8000	10.50	28037.50	7460.0
2.25	11515.00	32.5800	11.00	28631.00	8525.0
2.50	12445.50	50.2000	11.50	29141.00	9656.0
2.75	13313.20	73.9000	12.00	29640.50	10870.0
3.00	14146.50	104.7000	12.50	30149.50	12164.0
3.25	14947.10	143.9000	13.00	30663.50	13538.0
3.50	15718.50	192.0000	13.50	31104.00	14972.0
3.75	16458.50	249.5000	14.00	31578.50	16493.0
4.00	17164.60	318.0000	14.50	32014.50	18036.0
4.25	17824.00	398.0000	15.00	32423.00	19699.0

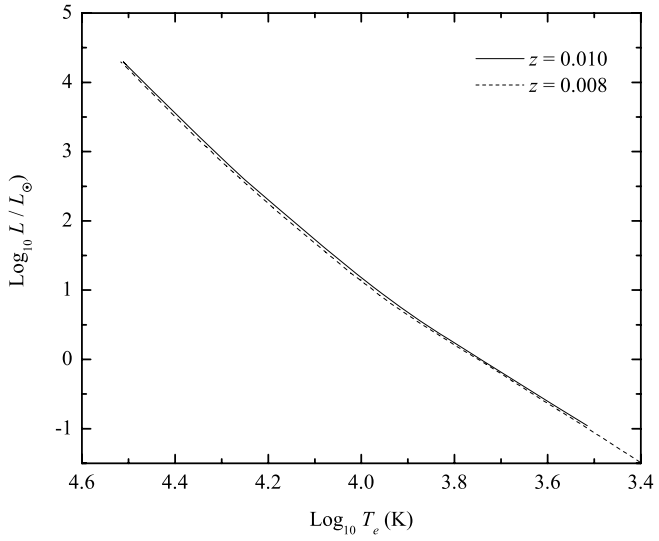

Figure S10.9: The results of Problem 10.28. Two main sequences are shown, $X = 0.7$ and $Z = 0.01$, and $X = 0.7$ and $Z = 0.008$.

CHAPTER 11

The Sun

11.1 From Eq. (3.17), $L = 4\pi R^2 \sigma T_e^4$,

$$\frac{T_i}{T_\odot} = \left(\frac{L_i}{L_\odot}\right)^{1/4} \left(\frac{R_\odot}{R_i}\right)^{1/2} \simeq (0.677)^{1/4} \left(\frac{1}{0.869}\right)^{1/2} = 0.973.$$

Using $T_\odot = 5777$ K, we find $T_i = 5621$ K, as indicated in Figure 11.1.

11.2 (a) The rate at which the Sun is converting its mass into energy is

$$\frac{L_\odot}{c^2} = 4.27 \times 10^9 \text{ kg s}^{-1} = 6.77 \times 10^{-14} \text{ M}_\odot \text{ yr}^{-1}.$$

(b) In Example 11.2.1, the Sun's mass loss rate due to the solar wind was found to be $\dot{M}_\odot \simeq 3 \times 10^{-14}$ $\text{M}_\odot$ yr^{-1}, roughly one-half the value found in part (a).

(c) The Sun's lifetime on the main sequence is about 10^{10} yr. Thus, the combined mass-loss rates of nuclear fusion and the solar wind would imply a total mass loss of about 10^{-3} $\text{M}_\odot$ over that period, which is not a significant fraction of the Sun's total mass.

11.3 The ionization potential of the H^- ion is $\chi_i = 0.75$ eV $= 1.2 \times 10^{-19}$ J. Using $Z_{i+1} = Z_\text{H} = 2$, $Z_i = Z_{\text{H}^-} = 1$, $P_e = 1.5$ N m^{-2}, and $T = 5777$ K, the Saha equation (Eq. 8.9) gives

$$\frac{N_\text{H}}{N_{\text{H}^-}} = \frac{2kTZ_\text{H}}{P_e Z_{\text{H}^-}} \left(\frac{2\pi m_e kT}{h^2}\right)^{3/2} e^{-\chi_i/kT} = 5 \times 10^7.$$

11.4 From the Boltzmann equation (Eq. 8.6), the number of hydrogen atoms in the $n = 3$ relative to the number in the $n = 1$ state is given by

$$\frac{N_3}{N_1} = \frac{g_3}{g_1} e^{-(E_3 - E_1)/kT} = 2.5 \times 10^{-10},$$

where $g_3 = 2(3)^2 = 18$, $g_1 = 2(1)^2 = 2$, $E_3 = -13.6 \text{ eV}/3^2 = -1.511$ eV, $E_1 = -13.6$ eV, and $T = 5777$ K. Assuming that the vast majority of all hydrogen atoms are in the ground state, the ratio of H^- ions to atoms in the $n = 3$ state is

$$\frac{N_{\text{H}^-}}{N_3} \simeq \left(\frac{N_{\text{H}^-}}{N_\text{H}}\right)\left(\frac{N_1}{N_3}\right) = \left(\frac{1}{5 \times 10^7}\right)\left(\frac{1}{2.4 \times 10^{-10}}\right) \simeq 79.$$

11.5 The combined effects of turbulence and thermal motions results in Doppler broadening of the form (Eq. 9.63). For Hα absorption in the Sun's photosphere, $\lambda_\alpha = 656.280$ nm, $T = 5777$ K, and $m = m_H$.

(a) Assuming $v_\text{turb} = 0$, $(\Delta\lambda)_{1/2} = 0.0355879$ nm.

(b) From observational data, $v_\text{turb} \simeq 0.4$ km s^{-1}. If this term is included in Eq. (9.63), $(\Delta\lambda)_{1/2} = 0.0356177$ nm.

(c) $v_{\rm turb}^2/(2kT/m) = 0.00168 \ll 1$.

(d) $\delta(\Delta\lambda)_{1/2}/(\Delta\lambda)_{1/2} = 0.084\%$. Turbulence does not make a significant contribution in the solar photosphere.

11.6 From the data given in the text on page 366 and in the statement of the problem, Eq. (9.62) gives

$$\begin{aligned}(\Delta\lambda)_{1/2,\mathrm{L}\alpha} &= 0.0123 \text{ nm}\\ (\Delta\lambda)_{1/2,\mathrm{C\ III}} &= 0.0061 \text{ nm}\\ (\Delta\lambda)_{1/2,\mathrm{O\ VI}} &= 0.010 \text{ nm}\\ (\Delta\lambda)_{1/2,\mathrm{Mg\ X}} &= 0.011 \text{ nm}\end{aligned}$$

11.7 (a) The Planck function (Eq. 3.22) is given by

$$B_\lambda(T) = \frac{2hc^2/\lambda^5}{e^{hc/\lambda kT} - 1}.$$

Integrating over wavelength between two closely spaced wavelengths, λ_1 and λ_2, gives

$$\int_{\lambda_1}^{\lambda_2} B_\lambda(T)\, d\lambda \simeq B_\lambda(T)\, \Delta\lambda,$$

where $\Delta\lambda = \lambda_2 - \lambda_1$. Taking $\Delta\lambda$ to be 0.1 nm over each of two different wavelength regions centered on λ_a and λ_b, and taking the ratios of the intensities we find

$$\frac{B_a\,\Delta\lambda}{B_b\,\Delta\lambda} \simeq \left(\frac{\lambda_b}{\lambda_a}\right)^5 \frac{e^{hc/\lambda_b kT} - 1}{e^{hc/\lambda_a kT} - 1} \simeq \left(\frac{\lambda_b}{\lambda_a}\right)^5 e^{\frac{hc}{kT}\left(\frac{1}{\lambda_b} - \frac{1}{\lambda_a}\right)}.$$

(This last expression arises because $e^{hc/\lambda kT} \gg 1$.) Taking the natural logarithm of both sides gives

$$\ln\left(\frac{B_a}{B_b}\right) = 5\ln\left(\frac{\lambda_b}{\lambda_a}\right) + \frac{hc}{kT}\left(\frac{1}{\lambda_b} - \frac{1}{\lambda_a}\right).$$

Using $\lambda_a = 10$ nm and $\lambda_b = 100$ nm leads to the desired result.

(b) Substituting the appropriate wavelengths and using the Sun's effective temperature gives $\ln(B_a/B_b) = -213$.

(c) $e^y = 10^x$ implies $x = y/\ln 10$. Since $y = -213$, we find $x = -92.6$.

11.8 Assuming $\gamma = 5/3$, Eq. (10.84) gives an adiabatic sound speed of 10 km s^{-1}. From Example 10.4.2, an "average" sound speed for the Sun is about 400 km s^{-1}. From Example 11.2.2, the sound speed at the top of the photosphere is about 7 km s^{-1}. The sound speed clearly increases with depth.

11.9 Starting with Eq. (9.15), solving for ds, assuming that κ_λ and ρ are constants over the interval of interest, and integrating,

$$d = \int_0^d ds = -\int_0^{\tau_{0,\lambda}} \frac{1}{\kappa_\lambda \rho}\, d\tau_\lambda = -\frac{\tau_{0,\lambda}}{\kappa_\lambda \rho}.$$

Taking $\tau_{0,\lambda} = 2/3$, the depth observed at λ_1 is $d_1 = 117$ km and the depth observed at λ_2 is $d_2 = 101$ km. This means that it is possible to probe the atmosphere at a greater depth in λ_1, by an amount $\Delta d = 16$ km.

11.10 (a) The pressure scale height is given by Eq. (10.70). From Example 11.2.2, $P = 140$ N m^{-2} and $\rho = 4.9 \times 10^{-6}$ kg m^{-3}. Furthermore, $g = GM_\odot/R_\odot^2 = 274$ m s^{-2}. Thus $H_P = 104.0$ km.

(b) If $\alpha = \ell/H_P = 2.2$, then $\ell = 229$ km. Since the observed Doppler velocity of solar granulation is approximately $v_{\rm turb} = 0.4$ km s^{-1}, the time required for a convective bubble to travel one mixing length is about $t = \ell/v_{\rm turb} = 570$ s $= 9.6$ min. This compares well with observed granulation lifetimes of five to ten minutes.

11.11 Beginning with Eq. (11.5), assuming that the gas is isothermal, and integrating over radius, we have

$$\int_{n_0}^{n(r)} \frac{dn}{n} = -\frac{GM_\odot m_p}{2kT} \int_{r_0}^{r} \frac{1}{r^2}\, dr.$$

This immediately results in

$$\ln\left[\frac{n(r)}{n_0}\right] = \frac{GM_\odot m_p}{2kT}\left(\frac{1}{r} - \frac{1}{r_0}\right) = -\frac{GM_\odot m_p}{2kTr_0}\left(1 - \frac{r_0}{r}\right).$$

Solving for $n(r)$ gives Eq. (11.6).

11.12 From Eq. (11.10), $P_m = B^2/2\mu_0$. Using $B = 0.2$ T gives $P_m = 1.59 \times 10^4$ N m^{-2}. Thus, $P_m/P_g \sim 0.8$ according to this rough estimate.

11.13 (a) From Eq. (11.9), $u_m = B^2/2\mu_0 = 360$ J m^{-3}.

(b) Assuming that the magnetic energy density is constant throughout the volume in question, if $E = 10^{25}$ J are to be released, the required volume is $V = E/u_m = 2.8 \times 10^{22}$ m^3.

(c) Taking $V \sim \ell^3$, gives $\ell \sim 3 \times 10^4$ km. Given that large flares can reach lengths of $\ell_{\rm flare} = 100{,}000$ km, $\ell \sim 0.3\ell_{\rm flare}$.

(d) From Eq. (11.11), and assuming a density characteristic of the top of the solar photosphere ($\rho \simeq 4.9 \times 10^{-6}$ kg m^{-3}), the velocity of an Alfvén wave is

$$v_m = \frac{B}{\sqrt{\mu_0 \rho}} \simeq 12 \text{ km s}^{-1}.$$

Thus it would take an Alfvén wave $t = \ell/v_m \sim 2500$ s $= 0.7$ hr to travel the length of the flare.

(e) Based on the "back-of-the-envelope" nature of the calculation, magnetic energy seems to be a reasonable source of solar flares.

11.14 CMEs are responsible for roughly 4×10^{15} kg of mass loss per year. The solar wind mass loss rate is approximately 3×10^{-14} M$_\odot$ yr^{-1}, which is equivalent to about 6×10^{16} kg yr^{-1}. Thus, the mass loss from CMEs is 7% of the total mass loss of the solar wind.

11.15 (a) The kinetic energy is approximately $K = 8 \times 10^{23}$ J, which is roughly 10% of the energy of a large flare.

(b) The transit time is roughly $t = 1$ AU$/400$ km s$^{-1} = 4 \times 10^5$ s $= 4$ d.

(c) Given that astronomers are constantly monitoring the Sun, the appearance of a solar flare or CME directed toward Earth gives a warning that charged particles from the Sun are headed toward us.

11.16 (a) From Eq. (5.22), if $B = 0.3$ T,

$$\Delta\nu = \frac{eB}{4\pi\mu} = 4.2 \times 10^9 \text{ Hz},$$

where $\mu \simeq m_e$.

(b) Beginning with $\lambda\nu = c$, $d\lambda = -\left(c/\nu^2\right)\, d\nu$. This can be rewritten in the form

$$\frac{d\lambda}{\lambda} = -\frac{\lambda}{c}\, d\nu.$$

Using $\lambda = 630.25$ nm and $d\nu \simeq \Delta\nu = 4.2 \times 10^9$ Hz, we find $\Delta\lambda/\lambda = 8.8 \times 10^{-6}$.

11.17 The rotation frequency at the base of the tachocline is approximately $f = \Omega/2\pi = 430$ nHz. This corresponds to a rotation period of $P = 1/f = 2.3 \times 10^6$ s $= 27$ d.

11.18 From the thermodynamic work integral, $W = \int_{V_i}^{V_f} P\, dV$, we have $P = \partial W/\partial V$, which is an energy density.

CHAPTER 12

The Interstellar Medium and Star Formation

12.1 (a) According to Eq. (12.1), $m_V = M_V + 5\log_{10} d - 5 + a_V = -1.1 + 5\log_{10} 700 - 5 = 8.1$ mag. ($a_V = 0$.)

(b) Using $a_V = 1.1$ mag, $m_V = 9.2$ mag.

(c) If extinction is not considered, using $m_V = 9.2$ mag leads to a distance estimate of 1160 pc (see Eq. 3.5), which is in error by about 65.7%.

12.2 The luminosity of the star is given by $L_\star = 4\pi R_\star^2 \sigma T_\star^4$. Letting d be the distance to the star, r_g be the radius of the spherical dust grain, and assuming that the grain is a perfectly absorbing black body, the rate at which energy is absorbed by the grain is

$$\frac{dE_{\text{absorb}}}{dt} = L_\star \left(\frac{\pi r_g^2}{4\pi d^2} \right).$$

If the grain temperature is T_g, the rate at which the grain emits energy is

$$\frac{dE_{\text{emit}}}{dt} = 4\pi r_g^2 \sigma T_g^4.$$

In thermodynamic equilibrium the two rates must be equal. Equating and solving for the grain temperature gives

$$T_g = \left(\frac{R_\star}{2d} \right)^{1/2} T_\star.$$

For an F0 main-sequence star, $T_\star = 7300$ K and $R_\star = 1.4\ \mathrm{R}_\odot$. At a distance of $d = 100$ AU, $T_g = 41.7$ K.

12.3 The hydrogen atom's ground-state spin flip produces a photon of frequency $\nu = 1420$ MHz. This implies that the energy difference between the two energy levels is $\Delta E = h\nu = 9.41 \times 10^{-25}$ J $= 5.88\ \mu$eV. If thermal energy is sufficient, then $kT \sim \Delta E$, or $T \sim \Delta E/k = 0.068$ K. Yes, the temperatures of H I clouds are sufficient to produce this low-energy state.

12.4 Note that there is an error in the coefficient of Eq. 12.7 in the first printing of the text; the equation should read

$$\tau_H = 5.2 \times 10^{-23} \frac{N_H}{T\Delta v}.$$

Taking $\tau_H = 0.5$, $T = 100$ K, and $\Delta v = 10$ km s^{-1}, Eq. (12.7) gives $N_H = 9.6 \times 10^{24}$ m^{-2}. Since $N_H = n_H d$, $d = 31.2$ pc. (*Note:* Δv is expressed in units of km s^{-1} in Eq. 12.7.)

12.5 Typically $n_{\text{CO}} \simeq 10^{-4} n_{\text{H}_2}$, giving $n_{\text{CO}} \simeq 10^4$ m^{-3}. Also, the mean molecular weight of the two molecules is $\mu = m_{\text{H}_2} m_{\text{CO}} / \left(m_{\text{H}_2} m_{\text{CO}} \right)$. Using $m_{\text{H}_2} \simeq 2$ u and $m_{\text{CO}} \simeq 28$ u, $\mu \simeq 1.9$ u.

For a total kinetic energy of E in the center-of-mass frame, $v = \sqrt{2E/\mu}$. Taking the translational kinetic energy to be $E = 3kT/2$, we have

$$v_{\text{avg}} \simeq \sqrt{\frac{3kT}{\mu}} = 450 \text{ m s}^{-1}.$$

From Eq. (10.29), the number of collisions per second between two species with number densities n_x and n_i is

$$r_{ix} = \int_0^\infty n_x n_i \sigma(E)\, v(E)\, \frac{n_E}{n}\, dE.$$

Assuming for simplicity that $\sigma(E) \simeq \pi(2r)^2$ is roughly constant over the appropriate energies ($2r$ is the distance between molecule centers for a grazing collision),

$$r_{ix} \simeq 4\pi r^2 n_x n_i \int_0^\infty v(e)\, \frac{n_E}{n}\, dE \simeq 4\pi r^2 n_x n_i v_{\text{avg}}.$$

Using the number densities of the two species, together with $r_{ix} \sim 0.1$ nm, $r \simeq 6 \times 10^{-5}$ m^{-3} s^{-1}.

12.6 Because CO is much more common than ^{13}CO or C^{18}O, it is much more likely that the GMC will be optically thick to CO, thereby making it much more difficult to see deeply into the cloud.

12.7 (a) The distances of the two masses from the center of mass can be written in terms of the reduced mass and their separation from each other (r) as $r_1 = (\mu/m_1)\, r$ and $r_2 = (\mu/m_2)\, r$. Substituting into the expression for the moment of inertia,

$$I = m_1 \left(\frac{\mu^2}{m_1^2}\right) r^2 + m_2 \left(\frac{\mu^2}{m_2^2}\right) r^2 = \mu r^2.$$

(b) $\mu_{12} = 6.856$ u and $\mu_{13} = 7.172$ u, giving $I_{12} = 1.639 \times 10^{-46}$ kg m^2 and $I_{13} = 1.715 \times 10^{-46}$ kg m^2.

(c) $E_{\text{rot}} = \ell(\ell + 1)\hbar^2/2I$. Thus, $E_2 = 3\hbar^2/I$ and $E_3 = 6\hbar^2/I$, giving $\Delta E_{12} = 3\hbar^2/I_{12} = 2.034 \times 10^{-22}$ J $= 0.00127$ eV. This corresponds to a wavelength of $\lambda_{12} = hc/\Delta E_{12} = 0.976$ mm. This is in the deep infrared.

(d) $\Delta E_{13} = 1.947 \times 10^{-22}$ J, giving $\lambda_{13} = 1.02$ mm. Thus, $\Delta\lambda = \lambda_{13} - \lambda_{12} = 0.044$ mm. Isotopes are revealed by subtle wavelength shifts in molecular spectra.

12.8 (a) Oxygen is much less abundant than hydrogen, and therefore, any photons emitted by a downward transition of an oxygen atom are much more likely to escape the cloud, rather than being reabsorbed. The photons then carry away cloud energy, resulting in cooling of the cloud. Oxygen atoms are also likely to emit infrared photons, while hydrogen will likely emit visible and ultraviolet photons.

(b) Hot cores are quite optically thick ($A_V \sim 50$ to 1000) and have high number densities. It is very difficult for photons to escape from the interiors of hot cores. Hot cores are also the site of mass star formation, resulting in UV and X-ray photons, along with shocks that can heat the core.

12.9 As the density of a cloud increases, the likelihood of excitation collisions increases. As long as the cloud is not too optically thick, the resulting deexcitations liberate photons from the cloud, resulting in cooling.

12.10 Using $T = 10$ K, $\mu = 1$, and $\rho_0 = 3 \times 10^{-17}$ kg m^{-3}, Eq. (12.16) gives $R_J = 4 \times 10^{11}$ m $= 3$ AU for the dense core of the GMC.

12.11 Substitution of Eq. (12.18) into (Eq. 12.14) leads immediately to

$$M_J \simeq \left(\frac{5}{G}\right)^{3/2}\left(\frac{3}{4\pi\rho_0}\right)^{1/2} v_T^3.$$

Employing the ideal gas law, $P_0 = \rho_0 kT/\mu m_H$ along with Eq. (12.18) also leads to

$$\rho_0 = P_0/v_T^2.$$

Substitution gives the desired result.

12.12 Hydrostatic equilibrium is only possible through a pressure *gradient*, dP/dr. In order for a constant density cloud to remain static, magnetic fields must be present to trap ions. According to the ideal gas law, constant mass density in an isothermal gas of constant composition (constant μ) requires a constant pressure.

12.13 (a) From the data given in Example 12.2.1 and the ideal gas law, $P_c \sim \rho_0 kT/\mu m_H = 1.2\times10^{-12}$ N m^{-2}. Using $R_J = 4\times10^{11}$ m (see the solution to Problem 12.10) gives $|dP/dr| \sim P_c/R_J = 3\times10^{-24}$ N m^{-3}.

(b) For $M_r = 10\ \mathrm{M}_\odot$ and $r = R_J$, $GM_r\rho/r^2 = 2.5\times10^{-19}$ N m^{-3}. This implies that

$$\frac{|dP/dr|}{GM_r\rho/r^2} \sim 10^{-5}.$$

The pressure gradient is not sufficient to keep the dense core in hydrostatic equilibrium.

(c) Noting that $\rho \propto r^{-3}$ gives

$$\left|\frac{dP}{dr}\right| \sim \frac{\rho_0 kT/\mu m_H}{r} \propto r^{-4}.$$

Similarly

$$\frac{GM_r\rho}{r^2} \propto r^{-5}.$$

This r dependence yields

$$\frac{|dP/dr|}{GM_r\rho/r^2} \propto r.$$

As $r \to 0$, $GM_r\rho/r^2 \ll |dP/dr|$.

12.14 The gravitational acceleration at the surface of a cloud of mass M_J and radius R_J is $g = GM_J/R_J^2$. Assuming that g remains constant during the entire collapse, the time for the cloud to fall a distance R_J, starting from rest, is given by

$$R_J = \frac{1}{2}gt^2 = \left(\frac{GM_J}{2R_J^2}\right)t^2.$$

Solving for the time and using

$$M_J = \frac{4}{3}\pi R_J^3\rho_0$$

results in

$$t = \left(\frac{2R_J^3}{GM_J}\right)^{1/2} = \left[\frac{2R_J^3}{G\left(\frac{4}{3}\pi R_J^3\rho_0\right)}\right]^{1/2} = \left(\frac{3}{2\pi G\rho_0}\right)^{1/2},$$

which differs from Eq. (12.26) for the free-fall time by a factor of

$$\sqrt{\frac{3/2\pi}{3\pi/32}} = 1.27.$$

12.15 The sound speed is given by Eq. (10.84),

$$v_s = \sqrt{\gamma P/\rho}.$$

Assuming an ideal monatomic gas, $\gamma = 5/3$. Furthermore, referring to Example 12.2.1 and the calculation in Problem 12.13(a), $\rho_0 \simeq 3\times10^{-17}$ kg m^{-3} and $P_c \simeq 1.2\times10^{-12}$ N m^{-2}. These values give $v_s \simeq 260$ m s^{-1}. From Problem 12.10, $R_J \simeq R_J = 4\times10^{11}$ m, so that $t_s = 2R_J/v_s = 3\times10^9$ s $= 100$ yr. The adiabatic sound speed transit time should be less than the free-fall time, otherwise the free-fall will become supersonic and shocks will develop.

12.16 Beginning with the expression just prior to Eq. (12.28),

$$M_J^{5/2} = \frac{4\pi}{G^{3/2}} R_J^{9/2} e\sigma T^4,$$

and writing $R_J = (3M_J/4\pi\rho_0)^{1/3}$ gives

$$M_J^{5/2} = \frac{4\pi}{G^{3/2}} \left(\frac{3M_J}{4\pi\rho_0}\right)^{3/2} e\sigma T^4.$$

Solving for ρ_0 in Eq. (12.14) and substituting leads to

$$M_J = \frac{1}{(4\pi)^{1/2}} \frac{1}{G^{3/2}} \left(\frac{5k}{m_H}\right)^{9/4} \frac{1}{\sigma}^{1/2} \frac{T}{\mu^{9/4} e^{1/2}}.$$

Substituting the values of the constants gives Eq. (12.28).

12.17 Suppose that the cloud is spherically symmetric with constant density, then from Eq. (10.22),

$$u_g \equiv \frac{|U_g|}{V} = \frac{3GM^2/5R}{4\pi R^3/3} = \frac{9}{20\pi} \frac{GM^2}{R^4}.$$

Using $M_J = 10\ \mathrm{M}_\odot$ (Example 12.2.1) and $R_J = 4\times10^{11}$ m (solution to Problem 12.10) gives $u_g = 1.5\times10^5$ J m^{-3}. From Eq. (11.9), $u_m = B^2/2\mu_0 = 4\times10^{-13}$ J m^{-3}. In this case $u_m/u_g \sim 3\times10^{-18}$ and magnetic effects are not significant. However, magnetic fields can be important in other situations.

12.18 (a) Adding a centripetal acceleration term to Eq. (12.19) gives

$$\frac{d^2r}{dt^2} = v_r \frac{dv_r}{dr} = -\frac{GM_r}{r^2} + \omega^2 r.$$

From conservation of angular momentum (assuming rigid-body rotation), $I_0\omega_0 = I\omega$, where I is the moment of inertia of the cloud. Since $I \propto r^2$ (the proportionality factor being a function of the mass distribution), $\omega \simeq r_0^2\omega_0/r^2$. (Note that since the geometry will change from nearly spherical to having a planar component, the proportionality factor also changes, but only slightly; this effect is neglected in this calculation.) Substituting the expression for ω,

$$v_r \frac{dv_r}{dr} = -\frac{GM_r}{r^2} + \frac{{r_0}^4}{r^3}{\omega_0}^2.$$

Integrating from v_0 at r_0 to v_f at r_f gives

$$\frac{1}{2}\left(v_{r,f}^2 - v_{r,0}^2\right) = GM_r\left(\frac{1}{r_f} - \frac{1}{r_0}\right) - \frac{1}{2}\omega_0^2 r_0^4 \left(\frac{1}{r_f^2} - \frac{1}{r_0^2}\right).$$

Initially $v_{r,0} = 0$, and when the collapse is halted $v_{r,f} = 0$. Thus the left-hand side is zero. Furthermore, since we are assuming that the initial cloud is much larger than the final configuration, $r_0 \gg r_f$, implying $1/r_f - 1/r_0 \simeq 1/r_0$ and $1/r_f^2 - 1/r_0^2 \simeq 1/r_f^2$. Substituting, and solving for r_f gives

$$r_f = \frac{\omega_0^2 r_0^2}{2GM_r}.$$

(b) $\omega_0 = \sqrt{2GM_r r_f}/r_0^2 = 2.7 \times 10^{-16}$ rad s^{-1}.

(c) $v_{\theta,0} = \omega_0 r_0 = 4.10$ m s^{-1}.

(d) From conservation of angular momentum, $I_0\omega_0 = I_f\omega_f$. Using $I_0 = \frac{2}{5}Mr^2$ and $I_f = \frac{1}{2}Mr^2$, $\omega_f = \frac{4}{5}\left(\frac{r_0}{r_f}\right)^2 \omega_0 = 2.3 \times 10^{-10}$ rad s^{-1}. This gives $v_{\theta,f} = \omega_f r_f = 3.4$ km s^{-1}. (Note that this differs from the approximation made in part (a) by a factor of 0.8.)

(e) $P_\theta = 2\pi r_f/v_{\theta,f} = 2.8 \times 10^{10}$ s $= 880$ yr, while from Kepler's third law, $P^2 = 4\pi^2 r^3/GM$, $P = 3.2 \times 10^{10}$ s $= 1000$ yr. Rigid-body rotation is inconsistent with Keplerian motion.

12.19 From Example 11.2.1, $\dot{M} = 4\pi r^2 \rho v$. Solving for the density, $\rho = \dot{M}/4\pi r^2 v = 2.8 \times 10^{-17}$ kg m^{-3}. This is similar to the density of the dense core of the giant molecular cloud, and exceeds the density of a typical diffuse hydrogen cloud.

CHAPTER 13

Main Sequence and Post-Main-Sequence Stellar Evolution

13.1 (a) See Table S13.1

Table S13.1: The elapsed time between points in Fig. 13.1 for a 5 $M_\odot$ star.

Between Points	Elapsed Time (Myr)	Percentage of Main-Sequence Time
2 – 3	1.5234	1.64
3 – 4	0.1144	0.12
4 – 5	0.3483	0.37
5 – 6	0.2890	0.31
6 – 7	4.1727	4.49
7 – 8	1.5045	1.62
8 – 9	6.3200	6.80
9 – 10	1.246	1.34

(b) The Hertzsprung gap occurs between points 3 and 5. The total elapsed time is 0.4627 Myr, which is only 0.49% of the time spent on the main sequence between points 1 and 2.

(c) The blueward portion of the horizontal branch occurs between points 7 and 8, which amounts to 1.62% of the main-sequence lifetime.

(d) The redward portion of the horizontal branch occurs between points 8 and 9, amounting to 6.8% of the main-sequence lifetime.

13.2 The Kelvin–Helmholtz timescale is given by $t_{\rm KH} = \Delta E_g / L$, where L is the luminosity of the star and $\Delta E_g = 3GM^2/10R$ (Eq. 10.23). From Fig. 13.1, for a 5 $M_\odot$ star on the subgiant branch, $L \sim 10^3$ $L_\odot$ and $T_e \sim 10^{3.9}$ K, implying a radius of 17 $R_\odot$. This gives $E_g \simeq 1.7 \times 10^{41}$ J. Finally, $t_{\rm KH} \simeq 4.4 \times 10^{11}$ s = 14,000 yr.

From Table S13.1, the time spent between points 4 and 5 in Fig. 13.1 is roughly 350,000 yr. This is about 25 times longer than the "back-of-the-envelope" Kelvin–Helmholtz timescale.

13.3 (a) Beginning with Eq. (13.7), differentiate with respect to the mass of the isothermal core, M_{ic}, and set the result to zero. This gives

$$\frac{\partial P_{ic}}{\partial M_{ic}} = \frac{3}{4\pi R_{ic}^3}\left(\frac{kT_{ic}}{\mu_{ic} m_H} - \frac{2}{5}\frac{GM_{ic}}{R_{ic}}\right) = 0.$$

Solving for R_{ic} leads immediately to Eq. (13.8).

(b) Substituting the expression for R_{ic} (Eq. 13.8) into Eq. (13.7) and simplifying gives Eq. (13.9).

13.4 The ratio of X'_{13}/X_{12} should increase. This is because the X'_{13} composition "bump" will be mixed in together with a lower concentration of X_{12}.

13.5 The "back-of-the-envelope" estimate of the temperature required for nuclear burning (Eq. 10.27) is given by

$$T_{\rm quantum} = \frac{4}{3}\frac{\mu_m Z_1^2 Z_2^2 e^4}{kh^2}.$$

For the first step of the triple alpha process, two helium nuclei must interact. Setting $\mu_m = m_{\rm He}m_{\rm He}/(m_{\rm He} + m_{\rm He}) = m_{\rm He}/2 \simeq 2$ u and $Z_1 = Z_2 = 2$, gives $T_{\rm quantum} = 6 \times 10^8$ K.

13.6 (a) An increase in luminosity, L, leads to increased radiation pressure, enhancing mass loss. A decrease in the surface gravity, g, means that the surface material is less tightly bound, also enhancing mass loss. As the radius, R, of the star increases for given values of L and g, the surface flux decreases, decreasing the effect of radiation pressure.

(b) For $L = 7000\ {\rm L}_\odot$ and $T = 3000$ K, the Stefan-Boltzmann equation (Eq. 3.17) gives $R = 310\ {\rm R}_\odot$. This implies that $g/g_\odot = 1.04 \times 10^{-5}$. Assuming that $\eta = 1$, $\dot{M} = -8.7 \times 10^{-7}\ {\rm M}_\odot\ {\rm yr}^{-1}$.

13.7 (a) Since in solar units $g/g_\odot = M/R^2$, direct substitution leads immediately to the desired result.

(b) Multiplying the result of part (a) through by M gives

$$M\,\frac{dM}{dt} = -c\eta LR,$$

where $c \equiv 4 \times 10^{13}$. Integrating from M_0 at $t = 0$ to M at t gives

$$M = \left(M_0^2 - 2c\eta LRt\right)^{1/2}.$$

(c) See Fig. S13.1.

(d) Choosing $M_0 = 1\ {\rm M}_\odot$ and $M = 0.6\ {\rm M}_\odot$, gives $t = 369{,}000$ yr.

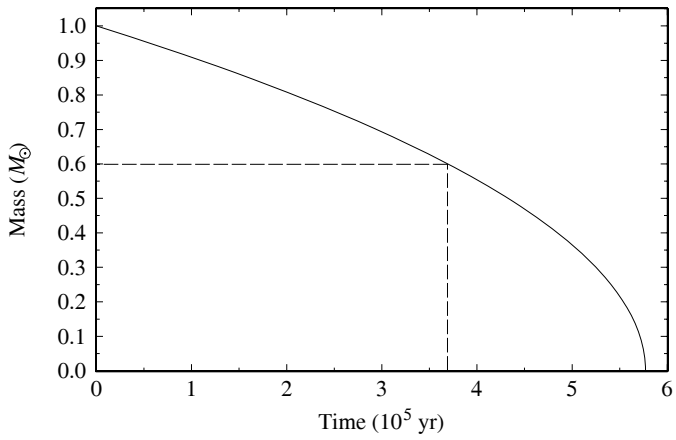

Figure S13.1: Mass as a function of time, assuming a Reimers mass loss rate, for constant $L = 7000\ {\rm L}_\odot$, $R = 310\ {\rm R}_\odot$, and $\eta = 1$. See Problem 13.7.

13.8 (a) Using $16' = 0.0047$ rad gives $d = (213\ {\rm pc})(0.0047\ {\rm rad}) = 0.99$ pc.

(b) The age of the nebula is approximately $t \simeq d/2v = 24{,}000$ yr.

13.9 Color-magnitude diagrams of young galactic clusters, such as h and χ Persei (Fig. 13.18), reveal an incomplete main sequence. The stars on the lower end of the main sequence are missing while cool stars of greater luminosity are lying above the main sequence instead. The presence of these stars is not explained by the old theory. Furthermore, color-magnitude diagrams of old globular clusters, such as M3 (Fig. 13.17) show that the upper main sequence is missing, replaced by the distinct presence of a red giant branch connecting the lower portion of the main sequence to the red giant stars. A horizontal branch is also present that does not lead to upper-main-sequence stars. These observations for old clusters would suggest that red giant stars cannot be producing upper-main-sequence stars.

13.10 (a) The contraction time to the main sequence for a 0.8 $M_\odot$ star is about 68 Myr while the main-sequence lifetime of a 15 $M_\odot$ star (between points 1 and 2 on Fig. 13.1) is about 11 Myr. It takes significantly longer for the 0.8 $M_\odot$ star to reach the main sequence than it does for the 15 $M_\odot$ star to evolve off the main sequence. This is consistent with the presence of red giants and massive stars leaving the main sequence before low-mass stars have arrived onto the main sequence in Fig. 13.18.

(b) According to Table 13.1, 68 Myr would be the main sequence lifetime of roughly a 6 $M_\odot$ star.

13.11 (a) From Table 13.1, the main-sequence lifetime of a 0.8 $M_\odot$ star is about 18.8 Gyr, which is much longer than the present age of the universe. This implies that 0.8 $M_\odot$ stars haven't had time to evolve off the main sequence yet. The Sun's main-sequence lifetime is about 10 Gyr, which is less than the age of the universe. For stars much below 1 $M_\odot$, the universe isn't old enough yet for those stars to have evolved off the main sequence, and so there is no observational data to compare with theoretical models.

(b) No, simply because there hasn't been enough time elapsed for those stars to leave the main sequence, even if the globular cluster formed very near the beginning of the universe.

13.12 (a) From Eq. (3.8),

$$M_B - M_{B,\odot} = -2.5 \log_{10} (L_B/L_{B,\odot})$$

$$M_V - M_{V,\odot} = -2.5 \log_{10} (L_V/L_{V,\odot}) .$$

Subtracting and using the identity $M_B - M_V = B - V$, we find that

$$B - V = 2.5 \log_{10} (L_V/L_B) - 2.5 \log_{10} (L_{V,\odot}/L_{B,\odot}) + (B_\odot - V_\odot) .$$

(b) When placed on the same color-magnitude diagram, the red giant branch of M15 is shifted noticably to the left (blueward) relative to 47 Tuc.

(c) Since M15 is less metal-rich than 47 Tuc, fewer electrons are available in the atmospheres of its stars relative to the stars in 47 Tuc. This means that more atoms are in higher states of ionization because fewer electrons are available for recombination (recall the Saha equation). As a consequence, the opacity is reduced in the atmospheres of M15 stars relative to 47 Tuc stars, and we can see down into deeper, hotter layers of stars in M15 relative to stars in 47 Tuc.

13.13 From Fig. 13.17, the turn-off point occurs at about $B - V = 0.4$, corresponding to a value of $V = 19.2$. According to the composite main sequence of Fig. 13.19, $B - V = 0.4$ corresponds to $M_V = 3.6$. Assuming no interstellar extinction between Earth and M3 ($a_\lambda = 0$), Eq. (12.1),

$$V = M_V + 5 \log_{10} d - 5 + a_\lambda,$$

implies $d = 13$ kpc. (*Note:* The actual distance is estimated to be 9.7 kpc.)

CHAPTER 14

Stellar Pulsation

14.1 From Fig. 14.1, Mira's visual apparent magnitude varies between $V \approx 2$ (although this varies significantly) and $V \approx 9.5$. From Eq. (3.3), the ratio of the radiant flux (which is also the luminosity ratio) received from Mira is

$$\frac{F_{\text{bright}}}{F_{\text{dim}}} = 100^{(9.5-2)/5} = 1000.$$

Although Mira's light curve is not sinusoidal, we will approximate it as

$$V = 5.75 + 3.75\cos\theta,$$

where $0 \leq \theta \leq 2\pi$ for one pulsation cycle. Mira will be visible to the naked eye roughly when $V \leq 6$, or when $\cos\theta \leq 0.07$. This occurs for $86° \leq \theta \leq 274°$, which is $188°/360° \approx 50\%$ of Mira's pulsation cycle.

14.2 For an uncertainty of $\Delta M \approx 0.5$, the uncertainty in the calculated distance obtained from Eq. (3.5) is about

$$\frac{\Delta d}{d} = \frac{10^{(m-M+\Delta M+5)/5} - 10^{(m-M+5)/5}}{10^{(m-M+5)/5}} = 0.26.$$

14.3 Referring to Fig. 14.22, the two M100 Cepheids nearest the best fit line have periods and apparent visual magnitudes of $\log_{10} P_1 \simeq 1.36$, $V_1 \simeq 26.3$, and $\log_{10} P_2 \simeq 1.62$, $V_2 \simeq 25.5$. According to the period–luminosity relation (Eq. 14.2), the absolute visual magnitudes of these stars are $M_{V,1} = -5.24$ and $M_{V,2} = -5.97$. The distances to these Cepheids obtained *neglecting extinction* from Eq. (3.5) are $d_1 = 20.3$ Mpc and $d_2 = 19.7$ Mpc. *Including extinction*, as in Eq. (12.1), we find $d_1 = 19.0$ Mpc and $d_2 = 18.4$ Mpc. One of these distances lies within the range of 17.1 ± 1.8 Mpc, and the other lies just outside the range.

14.4 W Virginis stars are about four times less luminous than classical Cepheids, so Eq. (3.7) shows that

$$M_{\text{W Vir}} - M_{\text{Ceph}} = -2.5\log_{10}\left(\frac{L_{\text{W Vir}}}{L_{\text{Ceph}}}\right) = 1.51.$$

From Eq. (14.2) then gives a period–luminosity relation for the W Virginis stars,

$$M_{\langle V\rangle} = -2.81\log_{10} P_{\text{d}} + 0.08.$$

This is plotted in Fig. S14.1.

14.5 Assuming that the oscillations of δ Cephei are sinusoidal, its radius varies about an equilibrium value R_0 as

$$R(t) = R_0 + A\sin\left(\frac{2\pi t}{\Pi}\right).$$

The surface velocity is

$$v(t) = \frac{dR(t)}{dt} = \frac{2\pi A}{\Pi}\cos\left(\frac{2\pi t}{\Pi}\right).$$

For a period of $\Pi = 5^{\text{d}}8^{\text{h}}48^{\text{m}} = 4.64 \times 10^5$ s and a surface velocity amplitude of 19 km s^{-1}, we find

$$A = \frac{v_{\max}\Pi}{2\pi} = 1.40 \times 10^9 \text{ m} \simeq 2.0\ \text{R}_\odot.$$

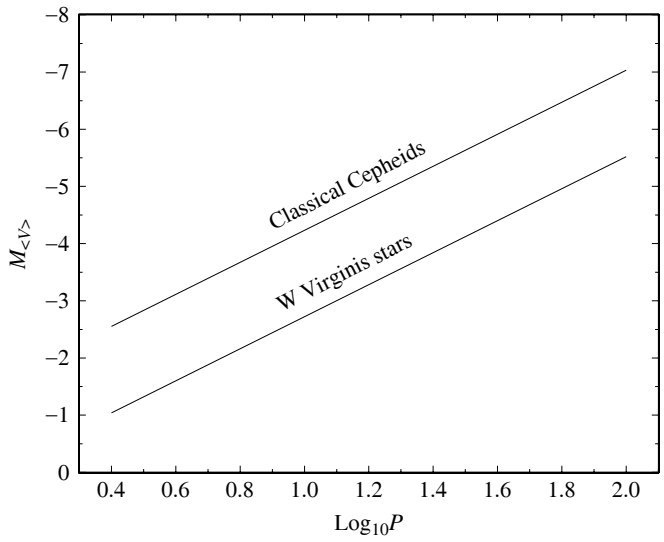

Figure S14.1: Results for Problem 14.4.

14.6 From Eq. (14.6) with $\gamma = 5/3$ and $\overline{\rho}_\odot = 1410\ \mathrm{kg\ m^{-3}}$, $\Pi \approx 5.48 \times 10^3$ s, or 91.4 minutes.

14.7 Setting $P = P_0 + \delta P$ and $R = R_0 + \delta R$, we have

$$\begin{aligned}
(P_0 + \delta P)(R_0 + \delta R)^{3\gamma} &= P_0 R_0^{3\gamma} \\
P_0 \left(1 + \frac{\delta P}{P_0}\right) R_0^{3\gamma} \left(1 + \frac{\delta R}{R_0}\right)^{3\gamma} &= P_0 R_0^{3\gamma} \\
\left(1 + \frac{\delta P}{P_0}\right) \left(1 + 3\gamma \frac{\delta R}{R_0} + \cdots\right) &= 1 \\
\frac{\delta P}{P_0} &= -3\gamma \frac{\delta R}{R_0}.
\end{aligned}$$

to first order in the deltas.

14.8 (a) Setting $L = L_0 + \delta L$, $R = R_0 + \delta R$, and $T = T_0 + \delta T$ in the Stefan–Boltzmann equation (Eq. 3.17), we have

$$\begin{aligned}
L_0 + \delta L &= 4\pi (R_0 + \delta R)^2 \sigma (T_0 + \delta T)^2 \\
L_0 \left(1 + \frac{\delta L}{L_0}\right) &= 4\pi R_0^2 \left(1 + \frac{\delta R}{R_0}\right)^2 \sigma T_0^4 \left(1 + \frac{\delta T}{T_0}\right)^4.
\end{aligned}$$

Cancelling the $L_0 = 4\pi R_0^2 \sigma T_0^4$, we have

$$\begin{aligned}
\left(1 + \frac{\delta L}{L_0}\right) &= \left(1 + 2\frac{\delta R}{R_0} + \cdots\right) \left(1 + 4\frac{\delta T}{T_0} + \cdots\right) \\
\frac{\delta L}{L_0} &= 2\frac{\delta R}{R_0} + 4\frac{\delta T}{T_0}
\end{aligned}$$

to first order in the deltas.

(b) The adiabatic relation $TV^{\gamma-1} = \text{constant}$ can be expressed as $TR^{3(\gamma-1)} = \text{constant}$. Setting $T = T_0 + \delta T$ and $R = R_0 + \delta R$, this becomes

$$\begin{aligned}(T_0 + \delta T)(R_0 + \delta R)^{3(\gamma-1)} &= T_0 R_0^{3(\gamma-1)} \\ T_0\left(1 + \frac{\delta T}{T_0}\right) R_0^{3(\gamma-1)} \left(1 + \frac{\delta R}{R_0}\right)^{3(\gamma-1)} &= T_0 R_0^{3(\gamma-1)} \\ \left(1 + \frac{\delta T}{T_0}\right)\left[1 + 3(\gamma-1)\frac{\delta R}{R_0} + \cdots\right] &= 1 \\ \frac{\delta T}{T_0} &= -3(\gamma-1)\frac{\delta R}{R_0}.\end{aligned}$$

to first order in the deltas. Substituting this into the result from part (a) gives

$$\frac{\delta L}{L_0} = 2\frac{\delta R}{R_0} + 4\left[-3(\gamma-1)\frac{\delta R}{R_0}\right] = 2(-6\gamma + 7)\frac{\delta R}{R_0}.$$

Using $\gamma = 5/3$ for an ideal monatomic gas, we find

$$\frac{\delta L}{L_0} = -6\frac{\delta R}{R_0}.$$

14.9 Expanding a general potential energy function, $U(r)$, in a Taylor series about the origin results in

$$U(r) = U(0) + \left.\frac{dU}{dr}\right|_0 r + \frac{1}{2}\left.\frac{d^2U}{dr^2}\right|_0 r^2 + \cdots,$$

where the higher-order terms may be neglected for small displacements from the origin. Because the origin is a stable equilibrium point, $dU/dr = 0$ at the origin and $d^2U/dr^2 > 0$ there. The force on the particle is therefore

$$\mathbf{F} = -\frac{dU(r)}{dr}\hat{\mathbf{r}} \simeq -\left.\frac{d^2U}{dr^2}\right|_0 r\,\hat{\mathbf{r}} = -\left.\frac{d^2U}{dr^2}\right|_0 \mathbf{r},$$

which is in the form of Hooke's law for a spring. The particle will therefore undergo simple harmonic motion for small displacements from the origin.

14.10 See Fig. S14.2.

14.11 The condition for convection to occur is that $A > 0$, where A is given by Eq. (14.17). That is,

$$\frac{1}{\rho}\frac{d\rho}{dr} > \frac{1}{\gamma P}\frac{dP}{dr}. \tag{S14.1}$$

Differentiating the ideal gas law, Eq. (10.11), with respect to r (assuming $\mu = \text{constant}$) and solving for $d\rho/dr$ gives

$$\frac{1}{\rho}\frac{d\rho}{dr} = \frac{1}{P}\frac{dP}{dr} - \frac{1}{T}\frac{dT}{dr}.$$

Using this to replace the left-hand side of Eq. (S14.1) gives

$$\frac{1}{P}\frac{dP}{dr} - \frac{1}{T}\frac{dT}{dr} > \frac{1}{\gamma P}\frac{dP}{dr}$$

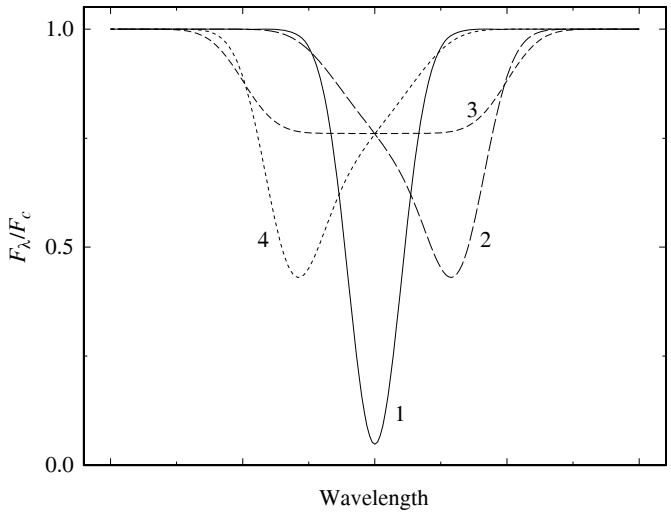

Figure S14.2: Results for Problem 14.10. Shown are the line profiles for points of view 1–4 of Fig. 14.23; the line profiles for points of view 5–8 are the same as those for 1–4. Note that the line profiles for points of view 1 and 5 are not Doppler shifted.

or

$$\left(1 - \frac{1}{\gamma}\right) \frac{T}{P} \frac{dP}{dr} > \frac{dT}{dr}.$$

The quantity on the left-hand side is the adiabatic temperature gradient (Eq. 10.88), while the right-hand side is the star's actual temperature gradient. Thus we have the condition for convection to occur,

$$\left.\frac{dT}{dr}\right|_{\text{ad}} > \left.\frac{dT}{dr}\right|_{\text{act}}.$$

Recognizing that both temperature gradients are negative, we recover Eq. (10.94).

14.12 Using the data in Table 14.2, we have the average pressure $\overline{P} = 9.1409 \times 10^3$ N m^{-2} and

$$\frac{dP}{dr} \simeq \frac{\Delta P}{\Delta r} = -0.0605 \text{ N m}^{-3}.$$

The average density is $\overline{\rho} = 2.2108 \times 10^{-4}$ kg m^{-3} and

$$\frac{d\rho}{dr} \simeq \frac{\Delta \rho}{\Delta r} = -7.63 \times 10^{-10} \text{ kg m}^{-4}.$$

So for $\gamma = 5/3$,

$$A = \frac{1}{\overline{\rho}} \frac{d\rho}{dr} - \frac{1}{\gamma \overline{P}} \frac{dP}{dr} = 5.21 \times 10^{-7} \text{ m}^{-1}.$$

Note that $A > 0$, as expected in a convection zone. Using a surface gravity of $g = GM_\odot / R_\odot^2 = 274$ m s^{-2}, the time scale for convection is $t_c \simeq 237$ s, nearly four minutes. This falls within the observed range of 3–8 minutes for the Sun's p-modes.

14.13 (a) Referring to Eq. (14.20),

$$m \frac{dv}{dt} = -\frac{GMm}{R^2} + 4\pi R^2 P,$$

this is just Newton's second law. The left-hand side is of course ma. The first term on the right is the inward force of gravity on the shell of mass m, while the second term on the right is the outward pressure force acting on the shell of surface area $4\pi R^2$.

(b) Substituting $V_i = 4\pi R_i^3/3$, and similarly for V_f, into $P_i V_i^\gamma = P_f V_f^\gamma$ gives, after cancelling the constants, $P_i R_i^{3\gamma} = P_f R_f^{3\gamma}$.

(c) Making the substitutions given in the problem, Eq. (14.20) becomes

$$m\,\frac{v_f - v_i}{t} = -\frac{GMm}{R_i^2} + 4\pi R_i^2 P_i,$$

or

$$v_f = v_i + \left(\frac{4\pi R_i^2 P_i}{m} - \frac{GM}{R_i^2}\right) t,$$

which is Eq. (14.24). Similarly, for $v = dR/dt$, we have

$$v_f = \frac{R_f - R_i}{t}$$

or

$$R_f = R_i + v_f t,$$

which is Eq. (14.25)

(d) See Figs. S14.3–S14.5. Note that the graphs are not perfectly sinusoidal, especially P vs. t. This is a nonlinear calculation.

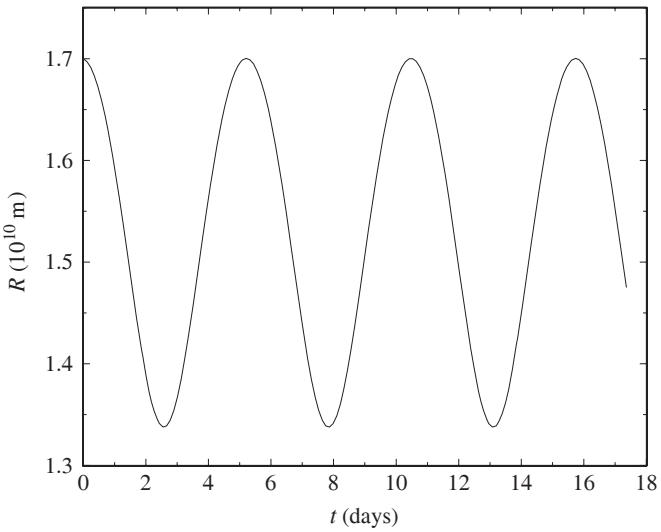

Figure S14.3: R vs. t for Problem 14.13.

(e) From the results of the calculations and the graphs, the period of the oscillation is $\Pi = 5.25\,\mathrm{d} = 4.53 \times 10^5$ s, and the equilibrium radius is $R_0 = 1.52 \times 10^{10}$ m. Equation (14.14) for the period of the *linearized* one-zone model (using $\rho_0 = 0.680$ kg m^{-3}) gives $\Pi_{\mathrm{lin}} = 4.56 \times 10^5$ s $= 5.28$ d, in good agreement with the nonlinear period. The parameters used in this problem were chosen to produce a result close to δ Cephei's measured period of $\Pi_{\mathrm{obs}} = 5^{\mathrm{d}}8^{\mathrm{h}}48^{\mathrm{m}} = 5.37$ d.

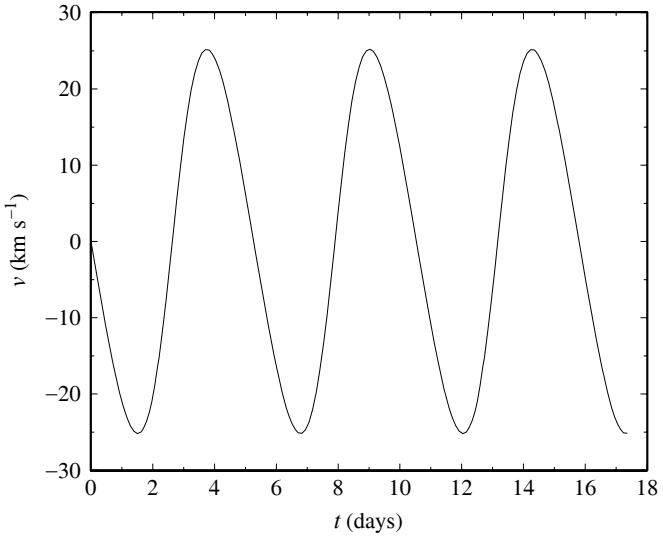

Figure S14.4: v vs. t for Problem 14.13.

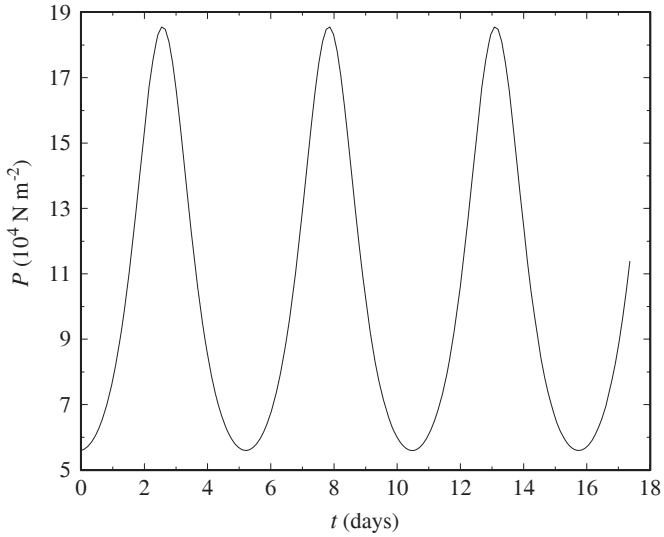

Figure S14.5: P vs. t for Problem 14.13.

CHAPTER 15

The Fate of Massive Stars

15.1 Using a mass estimate for η Carinae of roughly 120 $M_\odot$, the Eddington luminosity (Eq. 10.6) is $L_{\rm Ed} \simeq 4.6 \times 10^6$ $L_\odot$. This closely corresponds to star's present quiescent of 5×10^6 $M_\odot$; η Carinae is at the Eddington limit.

15.2 (a) The distance to η Car is estimated to be 2300 pc. Assuming that $A_V = 1.7$, Eq. (12.1) implies that $M_V \simeq M_{\rm bol} \simeq -13.5$. From Eq. (3.8), and using $M_{\rm Sun} = 4.74$, $L = 2 \times 10^7$ $L_\odot$.

(b) If the luminosity found in part (a) were maintained over 20 yr, the total energy output would have been 4.8×10^{42} J.

(c) $K = 1.2 \times 10^{42}$ J.

15.3 The linear extent of one of the lobes is $\ell = (8.5'')(2300\ {\rm pc}) = 0.095\ {\rm pc} = 20{,}000\ {\rm AU} = 3 \times 10^{15}$ m. Assuming a constant expansion rate of $v = 650\ {\rm km\ s^{-1}}$, $t = \ell/v = 4.5 \times 10^9$ s $= 140$ yr. If the velocity has been accelerating somewhat over time due to radiation pressure (as in the Crab supernova remnant), this value would be a slight underestimate.

15.4 (a) From Eq. (15.9),

$$\frac{dN}{N} = -\lambda t.$$

Integrating and solving for N gives Eq. (15.10).

(b) Since $N = N_0/2$ when $t = \tau_{1/2}$,

$$\frac{1}{2} = e^{-\lambda \tau_{1/2}}.$$

Solving for λ gives the desired result.

15.5 Using Eq. (10.23), and letting $f = 0.01$ be the fraction of the total energy that goes into neutrinos that eject the remaining mass, the kinetic energy deposited into the ejecta becomes

$$\Delta E_v = \frac{3}{10} f G M_\odot^2 \left(\frac{1}{r_f} - \frac{1}{r_i} \right),$$

where r_i is the radius of the core at the start of the collapse and r_f is the core's final radius.

The amount of energy needed to eject 9 $M_\odot$ of material out of the potential well created by the remaining 1 $M_\odot$ is

$$E_{\rm need} = \frac{9 G M_\odot^2}{\langle r_9 \rangle}$$

where $\langle r_9 \rangle$ is an average radius of the 9 $M_\odot$ before the core collapses.

Equating the two expressions leads to

$$r_f = \left(\frac{30}{f \langle r_9 \rangle} + \frac{1}{r_i} \right)^{-1}.$$

Assuming that the initial radius of the core is approximately the radius of Earth ($R_\oplus$) and that $\langle r_9 \rangle \sim 100\ \mathrm{R}_\odot$ (roughly the radius of a 10 $\mathrm{M}_\odot$ supergiant; see Appendix G), we find $r_f = 5000$ km $= 0.8\ \mathrm{R}_\oplus$. On the other hand, if we assume that all of the 9 $\mathrm{M}_\odot$ is located in a thin shell just above the collapsing core, then $\langle r_9 \rangle \sim R_\oplus$, and $r_f = 2$ km. Using an intermediate and crude "guestimate" of $\langle r_9 \rangle = 1\ \mathrm{R}_\odot$ for a centrally-condensed supergiant, we have $r_f = 220$ km.

There appears to be plenty of energy available in the graviational collapse of the core to eject the 9 $\mathrm{M}_\odot$ of overlying material (recall that the final core radius quoted in the text is roughly 50 km).

15.6 (a) Using $2' = 5.82 \times 10^{-4}$ rad and $4' = 1.16 \times 10^{-3}$ rad, $d_2 = (2000\ \mathrm{pc})(5.82 \times 10^{-4}\ \mathrm{rad}) = 1.2$ pc and $d_4 = (2000\ \mathrm{pc})(1.16 \times 10^{-3}\ \mathrm{rad}) = 2.3$ pc.

(b) The time required for the Crab supernova remnant to travel its longer dimension at an expansion speed of 1450 km s^{-1} (if assumed to be constant) is roughly $t \simeq d_4/2v = 780$ yr. This is a shorter time than the known age of about 940 yr, and indicates that the expansion is accelerating.

15.7 Using $M_{\mathrm{bol}} = -17$, Eq. (3.6) gives $m = M + 5\log_{10}(d/10\ \mathrm{pc}) = -5.5$, which is brighter than Venus.

15.8 Using a central core density of $\rho_0 \sim 10^{13}$ kg m^{-3} for a 15 $\mathrm{M}_\odot$ star, the time for the homologous collapse of the inner core is roughly given by

$$t_{\mathrm{ff}} = \left(\frac{3\pi}{32}\frac{1}{G\rho_0}\right)^{1/2} = 0.021\ \mathrm{s}.$$

15.9 (a) Letting ϵ be the amount of energy released by the decay of one nucleus, the total luminosity produced by the supernova remnant is

$$L = \epsilon\frac{dN}{dt} = -\epsilon\lambda N = -\epsilon\lambda N_0 e^{-\lambda t}.$$

Using the identity, $\log_{10} L = (\log_{10} e)(\ln L)$,

$$\frac{d\log_{10} L}{dt} = \frac{\log_{10} e}{L}\frac{dL}{dt}.$$

Substituting L and $dL/dt = \epsilon\lambda^2 N_0 e^{-\lambda t}$ gives

$$\frac{d\log_{10} L}{dt} = -(\log_{10} e)\,\lambda = -0.434\lambda.$$

(b) Beginning with Eq. (3.8),

$$M_{\mathrm{bol}} = M_{\mathrm{Sun}} - 2.5\log_{10}\left(\frac{L}{L_\odot}\right),$$

and solving for $\log_{10} L$ gives

$$\log_{10} L = \frac{M_{\mathrm{bol}} - M_{\mathrm{Sun}}}{2.5} + \log_{10} L_\odot.$$

Differentiating with respect to time,

$$\frac{d\log_{10} L}{dt} = -\frac{1}{2.5}\frac{dM_{\mathrm{bol}}}{dt}.$$

Substituting into the result of part (a) (Eq. 15.11) and rewriting gives Eq. (15.12),

$$\frac{dM_{\mathrm{bol}}}{dt} = 1.086\lambda.$$

15.10 For a half-life of $\tau_{1/2} = 77.7$ d, the decay constant is $\lambda = \ln 2/\tau_{1/2} = 0.0089$ d^{-1}. Using Eq. (15.12), $dM/dt = 0.0097$ mag d^{-1}.

15.11 The number of $^{56}_{27}$Co atoms in $0.075\ M_\odot$ of cobalt-56 is roughly

$$N_0 = \frac{0.075\ M_\odot}{56\ \text{u}} = 1.6 \times 10^{54}.$$

The half-life of $^{56}_{27}$Co is $\tau_{1/2} = 77.7$ d $= 6.71 \times 10^6$ s. This corresponds to a decay constant of

$$\lambda = \frac{\ln 2}{\tau_{1/2}} = 1.03 \times 10^{-7}\ \text{s}^{-1}.$$

The number of decays per second for N nuclei is just λN. Taking the energy released per decay to be $\epsilon = 3.72$ MeV $= 5.96 \times 10^{-13}$ J, the luminosity of the supernova remnant is $L = \epsilon\lambda N$.

(a) Just after the formation of the cobalt, the initial decay luminosity is $L_0 = \epsilon\lambda N_0 = 9.8 \times 10^{34}$ W $= 2.6 \times 10^8\ L_\odot$.

(b) After a time t, $N = N_0 e^{-\lambda t}$, implying $L = L_0 e^{-\lambda t}$. This gives $L = 3.79 \times 10^{33}$ W $= 9.9 \times 10^6\ L_\odot$.

(c) These results are in excellent agreement with Fig. 15.12.

15.12 The neutrino energy flux at Earth was

$$E/A = (4.2\ \text{MeV})(1.3 \times 10^{14}\ \text{m}^{-2}) = 87\ \text{J m}^{-2}.$$

Assuming an isotropic emission of neutrinos from SN 1987A, and given the distance of $d = 50$ kpc to the LMC, the total energy output was roughly $E = (4\pi d^2)(E/A) = 2.6 \times 10^{45}$ J.

15.13 From Eq. (10.22), $U_g = -3GM^2/5R = 3 \times 10^{46}$ J. This is approximately one order of magnitude greater than the neutrino energy estimate of the previous problem.

15.14 A gamma-ray burst is observed roughly once per day. If there are 100,000 neutron stars in our Galaxy, and *if* we were to assume that they are responsible for the bursts, each neutron star would need to undergo an event approximately once every $100{,}000/365 = 274$ yr.

15.15 The rest-mass energy of the electron and positron are converted into two gamma-ray photons, or $E_\gamma = m_e c^2 = 511$ keV.

15.16 If the number densities of sources with energies E_1 and E_2 are n_1 and n_2, respectively, then the number of sources with a fluence equal to or greater than S is

$$N(S) = \frac{4}{3}\pi n_1 r_1^3(S) + \frac{4}{3}\pi n_2 r_2^3(S).$$

but $r_1(s) = (E_1/4\pi S)^{3/2}$, and similarly for r_2. As a result,

$$N(S) = \frac{4\pi}{3}\left[n_1\left(\frac{E_1}{4\pi}\right)^{3/2} + n_2\left(\frac{E_2}{4\pi}\right)^{3/2}\right] S^{-3/2}.$$

15.17 (a) 48 J

(b) Assuming that the energy is entirely kinetic energy, $v = 25.9$ m s^{-1}.

(c) The speed in part (b) corresponds to 58 mph, more than half the speed of a top major-league fastball!

15.18 Assuming a typical magnetic field strength of 10^{-10} T throughout the Galaxy, $r = 3 \times 10^{20}$ m $= 10$ kpc. The value obtained by this order-of-magnitude estimate is characteristic of the size of the Milky Way. Lower-energy cosmic rays are likely bound to the Galaxy.

15.19 From the power law expression, $\log F = \log C - \alpha \log E$, implying that for values of F_1 and F_2 corresponding to E_1 and E_2, respectively,

$$\alpha = -\frac{\log(F_2/F_1)}{\log(E_2/E_1)}.$$

The flux at $E_1 = 10^{11}$ eV is approximately $F_1 = 10^{-1}$ m^{-2} sr^{-1} s^{-1} GeV^{-1} and the flux at $E_2 = 10^{16}$ eV is about $F_2 = 5 \times 10^{-14}$ with the appropriate units. This yeilds $\alpha = 2.5$.

At the "ankle", $E_3 = 5 \times 10^{18}$ eV with $F_3 = 5 \times 10^{-24}$ in the appropriate units. In the region between the "knee" and the "ankle", $\alpha = 3.7$.

15.20 The Lorentz factor for a 10^{20} eV proton is given by

$$\gamma = \frac{E}{m_p c^2} = 1 \times 10^{11}.$$

CHAPTER 16

The Degenerate Remnants of Stars

16.1 (a) From Eq. (7.2), the ratio of the masses of 40 Eri B and C is

$$\frac{m_C}{m_B} = \frac{a_B}{a_C} = 0.37.$$

To find a, the semimajor axis of the orbit, the distance to 40 Eri B and C must first be found from Eq. (3.1),

$$d = \frac{1}{p''} = \frac{1}{0.201''} = 4.98 \text{ pc} = 1.535 \times 10^{17} \text{ m}.$$

The angular extent of the semimajor axis is $\alpha = 6.89'' = 3.34 \times 10^{-5}$ rad, and so the semimajor axis is $a = \alpha d = 5.127 \times 10^{12}$ m. Using Kepler's third law, Eq. (2.37), with an orbital period of $P = 247.9 \text{ yr} = 7.823 \times 10^9$ s then gives the sum of the masses of 40 Eri B and C,

$$m_B + m_C = \frac{4\pi^2}{GP^2} a^3 = 1.303 \times 10^{30} \text{ kg} = 0.655 \text{ M}_\odot.$$

Solving for the individual masses, $m_B = 0.478 \text{ M}_\odot$ and $m_C = 0.177 \text{ M}_\odot$.

(b) Using Eq. (3.7),

$$L_B = 100^{(M_{\text{Sun}} - M_B)/5} \text{ L}_\odot = 100^{(4.76-9.6)/5} \text{ L}_\odot = 0.0116 \text{ L}_\odot.$$

(c) From the Stefan–Boltzmann equation, Eq. (3.17),

$$R_B = \frac{1}{T_B^2} \sqrt{\frac{L_B}{4\pi\sigma}} = 8.74 \times 10^6 \text{ m}.$$

This is slightly larger than the size of Earth

$$R_B = 0.0126 \text{ R}_\odot = 1.37 \text{ R}_\oplus = 1.59 \text{ R}_{\text{Sirius B}}.$$

(d) The average density of 40 Eri B is $\rho = 3.37 \times 10^8 \text{ kg m}^{-3}$. This is less than the average density of Sirius B ($\approx 3 \times 10^9 \text{ kg m}^{-3}$). Sirius B has a larger mass (1.05 $\text{M}_\odot$), and so its electrons must be more closely confined (greater n_e) to produce the greater electron degeneracy pressure required to support the star.

(e) For 40 Eri B,

$$\text{mass} \times \text{volume} = 2.69 \times 10^{51} \text{ kg m}^3,$$

and for Sirius B,

$$\text{mass} \times \text{volume} = 1.45 \times 10^{51} \text{ kg m}^3.$$

The lower value for Sirius B is an indication that it is smaller than might be anticipated from the mass-volume relation. It is sufficiently dense that its electrons are moving at relativistic speeds, providing less support than expected from the nonrelativistic expression for the electron degeneracy pressure.

16.2 As the temperature of a DB white dwarf drops below 12,000 K, there would be insufficient excitation of its He I atoms. No absorption lines would be formed without one of the electrons in the $n = 2$ orbital. Because DB white dwarfs do not have any hydrogen lines either, the cooling would presumably transform it from a DB into a DC white dwarf, with a spectrum devoid of lines.

16.3 If the entire luminosity of Sirius B were produced by hydrogen burning, then the nuclear energy generation rate would be about

$$\epsilon_B \approx \frac{L_B}{M_B} = \frac{0.03\ \mathrm{L}_\odot}{1.053\ \mathrm{M}_\odot} = 5.5 \times 10^{-6}\ \mathrm{W\ kg^{-1}}.$$

The density and interior temperature of Sirius B are taken to be $\rho_B = 3 \times 10^9$ kg m^{-3} and $T = 10^7$ K (the latter value suitable for an estimate of an upper limit for X). We can estimate the value of X for the pp chain from Eq. (10.47) with $\epsilon_{pp} = \epsilon_B$, $\psi_{pp} = 1$ and $f_{pp} = 1$. Then

$$X = \left(\frac{\epsilon_{pp}}{\epsilon'_{0,pp} \rho \psi_{pp} f_{pp} T_6^4} \right)^{1/2} \approx 4 \times 10^{-4}.$$

For the CNO cycle, Eq. (10.59) with $\epsilon_{\mathrm{CNO}} = \epsilon_B$ and $X_{\mathrm{CNO}} = 1$ gives

$$X = \frac{\epsilon_{\mathrm{CNO}}}{\epsilon'_{\circ,\mathrm{CNO}} \rho X_{\mathrm{CNO}} T_6^{19.9}} \approx 3 \times 10^{-5}.$$

The smaller of these values may be taken as a rough upper limit for X.

16.4 Using the average density of 3.0×10^9 kg m^{-3}, a central temperature of 3×10^7 K, and a mean molecular weight of $\mu = 12/7 = 1.71$ for a composition of pure carbon-12 (see Eq. 10.16), the ideal gas pressure at the center of Sirius B is (Eq. 10.11)

$$P_g = \frac{\rho k T}{\mu m_H} = 4.35 \times 10^{20}\ \mathrm{N\ m^{-2}}.$$

The radiation pressure at the center is (Eq. 10.19)

$$P_{\mathrm{rad}} = \frac{1}{3} a T^4 = 2.04 \times 10^{14}\ \mathrm{N\ m^{-2}}.$$

These are both much smaller than the estimated central pressure of 3.8×10^{22} N m^{-2} obtained from Eq. (16.1), so both the gas and radiation pressure are too feeble to support Sirius B.

16.5 Using Eq. (16.4) for the electron number density, the pressure of an ideal gas of electrons, Eq. (10.10), is

$$P = n_e k T = \left[\left(\frac{Z}{A} \right) \frac{\rho}{m_H} \right] k T.$$

If we set this equal to the pressure of a degenerate electron gas, then Eq. (16.12) gives

$$\frac{T}{\rho^{2/3}} = \frac{\hbar^2}{5 m_e k} \left[\frac{3\pi^2}{m_H} \left(\frac{Z}{A} \right) \right]^{2/3}.$$

This differs from Eq. (16.6) by a factor of 3/5.

16.6 Equation (16.7) for the pressure integral is

$$P \approx \frac{1}{3} n_e p v.$$

The electron number density is (Eq. 16.4)

$$n_e = \left(\frac{Z}{A}\right)\frac{\rho}{m_H},$$

the momentum is (Eq. 16.8) $p \approx \hbar n_e^{1/3}$, and $v = c$ in the extreme relativistic limit. Substituting these into the expression for P gives the desired result.

16.7 (a) The Lorentz factor is given by Eq. (4.20),

$$\gamma = \frac{1}{\sqrt{1 - u^2/c^2}}.$$

When $\gamma = 1.1$, $v/c = 0.417$.

(b) Solving Eq. (16.10) for the density and using the value for v/c from part (a) and $Z/A = 1/2$, we find that

$$\rho = \left(\frac{A}{Z}\right) m_H \left(\frac{m_e v}{\hbar}\right)^3 = 4.2 \times 10^9 \text{ kg m}^{-3}.$$

16.8 (a) The average density of a 0.6 $M_\odot$ white dwarf of radius 0.012 $R_\odot$ is $\rho = 4.89 \times 10^8$ kg m^{-3}. The average separation between neighboring nuclei is, with $A = 12$,

$$r = \left(\frac{3Am_H}{4\pi\rho}\right)^{1/3} = 2.14 \times 10^{-12} \text{ m}.$$

(b) For $Z = 6$,

$$T_c = \frac{Z^2 e^2}{4\pi\epsilon_0 r k \Gamma} = 1.76 \times 10^6 \text{ K}.$$

(c) From Eq. (16.19), $L_{\rm wd} = C T_c^{7/2}$, where

$$C = 6.65 \times 10^{-3} \left(\frac{M_{\rm wd}}{M_\odot}\right) \frac{\mu}{Z(1+X)} = 0.056 \text{ W K}^{-7/2}$$

using $X = 0$, $Z = 0.1$, and $\mu = 1.4$ from Example 16.5.1. The luminosity of the white dwarf is thus $L_{\rm wd} = 4.0 \times 10^{20}$ W, or about 1.1×10^{-6} $L_\odot$.

(d) The number of carbon nuclei is

$$N = \frac{M_{\rm wd}}{Am_H} = 5.9 \times 10^{55}.$$

If each nucleus releases a latent heat kT_c, then the white dwarf could sustain its luminosity for a time

$$t = \frac{NkT_c}{L_{\rm wd}} = 3.6 \times 10^{18} \text{ s} \simeq 1.1 \times 10^{11} \text{ yr}.$$

This is about twenty times longer than the period of slower cooling (5×10^9 yr) displayed in Fig. 16.9. The longer time scale is due to the lower core temperature of the white dwarf considered in this problem.

16.9 The density of the liquid-drop model of the nucleus is

$$\rho = \frac{Am_H}{\frac{4}{3}\pi r^3} = \frac{Am_H}{\frac{4}{3}\pi(r_0 A^{1/3})^3} = \frac{3m_H}{4\pi r_0^3} = 2.3 \times 10^{17} \text{ kg m}^{-3}.$$

16.10 Using $\rho_{\rm ns} = 6.65 \times 10^{17}$ kg m^{-3} for the density of the neutron star and $M_{\rm Moon} = 7.35 \times 10^{22}$ kg for the mass of the Moon (Appendix C), the radius of the Moon would be

$$r = \left(\frac{3M_{\rm Moon}}{4\pi\rho_{\rm ns}} \right)^{1/3} = 30 \text{ m}.$$

16.11 (a) If the lower mass is at R and the upper mass is at $R + dr$, then

$$\begin{aligned} \frac{F_{\rm lower}}{F_{\rm upper}} &= \frac{F(R)}{F(R+dr)} \\ &\simeq \frac{F(R)}{F(R) + [(dF/dr)|_R]\,dr)} \\ &= \left[1 + \frac{1}{F(R)} \left. \frac{dF}{dr} \right|_R dr \right]^{-1}. \end{aligned}$$

Using Eq. (2.11),

$$\frac{dF}{dr} = -2G\frac{Mm}{r^3},$$

and so

$$\begin{aligned} \frac{F_{\rm lower}}{F_{\rm upper}} &\simeq \left(1 - \frac{R^2}{GMm} \frac{2GMm}{R^3}\, dr \right)^{-1} \\ &= \left(1 - \frac{2dr}{R} \right)^{-1}. \end{aligned}$$

Using $R = 10^4$ m and $r = 0.01$ m, this is

$$\frac{F_{\rm lower}}{F_{\rm upper}} \simeq 1.0000002.$$

(b) The iron cube has a mass of 0.00786 kg and sides of length $dr = 0.01$ m. Imagine that half of the cube's mass, $m = 0.00393$ kg, is concentrated at its top and bottom surfaces. The stress on the cube may then be estimated as

$$\begin{aligned} \text{stress} &\simeq \frac{F_{\rm lower} - F_{\rm upper}}{(10^{-4}\ \text{m}^2)} \\ &\simeq \frac{F_{\rm lower}}{(10^{-4}\ \text{m}^2)} \left(1 - \frac{F_{\rm upper}}{F_{\rm lower}} \right) \\ &= G\frac{Mm}{R^2} \frac{1}{(10^{-4}\ \text{m}^2)} \left[1 - \left(1 - \frac{2\,dr}{R} \right) \right] \\ &= \frac{2GMm\,dr}{(10^{-4}\ \text{m}^2)R^3} \\ &= 1.46 \times 10^8 \text{ N m}^{-2}. \end{aligned}$$

An iron meteoroid falling toward the surface of a neutron star would be stretched (to the point of rupturing) into a thin ribbon.

16.12 First, estimate the speed of the neutrons using an analog of Eq. (16.10),

$$v = \frac{p}{m_n} = \frac{\hbar}{m_n} n_n^{1/3} = \frac{\hbar}{m_n} \left(\frac{\rho}{m_n}\right)^{1/3}.$$

For $\rho = 1.5 \times 10^{18}$ kg m^{-3}, $v = 6 \times 10^7$ m s^{-1}. Since $v = 0.2c$, we can use Eq. (16.12), replacing $m_e \to m_n$ and $Z/A \to 1$, to obtain an expression for the nonrelativistic neutron degeneracy pressure,

$$P = \frac{\left(3\pi^2\right)^{2/3}}{5} \frac{\hbar^2}{m_n} \left(\frac{\rho}{m_n}\right)^{5/3} = 1.1 \times 10^{34} \text{ N m}^{-2}.$$

This is about 6×10^{11} times the central pressure of 1.9×10^{22} N m^{-2} estimated for the center of Sirius B.

16.13 Use $\rho = 4 \times 10^{14}$ kg m^{-3} for the density at neutron drip.

(a) Equation (16.15) for the relativistic electron degeneracy pressure with $Z/A = 36/118$ gives

$$P = \frac{\left(3\pi^2\right)^{1/3}}{4} \hbar c \left[\left(\frac{Z}{A}\right) \frac{\rho}{m_H}\right]^{4/3} = 7.4 \times 10^{28} \text{ N m}^{-2}.$$

(b) From an analog of Eq. (16.10), the speed of the neutrons is

$$v = \frac{p}{m_n} = \frac{\hbar}{m_n} n_n^{1/3} = \frac{\hbar}{m_n} \left(\frac{\rho}{m_n}\right)^{1/3}.$$

For $\rho = 4 \times 10^{14}$ kg m^{-3}, $v = 4 \times 10^6$ m s^{-1}. From Eq. (16.12) with $m_e \to m_n$ and $Z/A \to 1$, the nonrelativistic neutron degeneracy pressure is

$$P = \frac{\left(3\pi^2\right)^{2/3}}{5} \frac{\hbar^2}{m_n} \left(\frac{\rho}{m_n}\right)^{5/3} = 1.2 \times 10^{28} \text{ N m}^{-2}.$$

This is comparable to the electron degeneracy pressure found in part (a).

16.14 (a) Using $P_\odot = 26$ d $= 2.25 \times 10^6$ s for the Sun's rotation period, Eq. (16.26) gives

$$P_{\text{ns}} = P_\odot \left(\frac{R_{\text{ns}}}{R_\odot}\right)^2 = 4.6 \times 10^{-4} \text{ s}.$$

Coincidentally, this is about the minimum rotation period for a typical neutron star.

(b) For "frozen-in" magnetic field lines,

$$B_\odot 4\pi R_\odot^2 = B_{\text{ns}} 4\pi R_{\text{ns}}^2.$$

Taking $B_\odot = 2 \times 10^{-4}$ T for a typical solar magnetic field near the surface, we find

$$B_{\text{ns}} = B_\odot \left(\frac{R_\odot}{R_{\text{ns}}}\right)^2 = 9.7 \times 10^5 \text{ T}.$$

16.15 The average density of Sirius B is $\rho_{\text{wd}} = 3.0 \times 10^9$ kg m^{-3}, and the average density of a 1.4 $M_\odot$ neutron star is $\rho_{\text{ns}} = 6.65 \times 10^{17}$ kg m^{-3}.

(a) Using $\gamma = 5/3$, Eq. (14.14) for the fundamental radial pulsation period may be written as

$$\Pi = 2\pi \sqrt{\frac{3}{4\pi G\rho}}.$$

results in

$$\Pi_{\rm wd} = 6.9 \text{ s}$$

$$\Pi_{\rm ns} = 4.6 \times 10^{-4} \text{ s}.$$

$P_{\rm wd}$ is above the period range of 0.25 s to 2 s observed for most pulsars, and $P_{\rm ns}$ is below it.

(b) Using Eq. (16.29) with the definition of the star's average density, ρ, we find that the minimum rotation period is equal to the fundamental radial pulsation period,

$$P_{\rm min} = 2\pi \sqrt{\frac{R^3}{GM}} = 2\pi \sqrt{\frac{3}{4\pi G\rho}} = \Pi.$$

So

$$P_{\rm min,wd} = \Pi_{\rm wd} = 6.9 \text{ s}$$

and

$$P_{\rm min,ns} = \Pi_{\rm ns} = 4.6 \times 10^{-4} \text{ s}.$$

(c) The mathematical equality of the model star's fundamental radial pulsation period and its minimum rotation period is established in parts (a) and (b). However, the physical basis for this result is found in the virial theorem. The fundamental radial pulsation period is basically the time for a sound wave to cross the star, and so is proportional to the star's radius R and inversely proportional to the speed of sound $v_s = \sqrt{\gamma kT/\mu m_H}$. Thus

$$\Pi \propto R/v_s \propto R/\sqrt{T/m} \propto R/\sqrt{K/m}$$

(Eq. 10.17), where T is the temperature, m is the average mass of a gas particle, and K is the average kinetic energy per particle. On the other hand, the minimum rotation period occurs when the star's surface is no longer gravitationally bound. That is, a gas particle of mass m at the star's surface is essentially orbiting the star. The orbital speed at the surface is $v_{\rm orbit} = \sqrt{GM/R} = \sqrt{-U/m}$, where U is the gravitational potential energy of the particle at the star's surface (Eq. 2.14). Then

$$2\pi R/P_{\rm min} = v_{\rm orbit} = \sqrt{-U/m},$$

Therefore

$$P_{\rm min} \propto R/\sqrt{-U/m}.$$

But according to the virial theorem (Eq. 2.46), $-2\langle K\rangle = \langle U\rangle$, and so $\Pi \propto P_{\rm min}$. The virial theorem relates the average kinetic energy of the gas particles (which determines the sound speed, and hence the pulsation period) to the average potential energy of the gas particles (which determines the minimum rotation period).

16.16 (a) The minimum rotation period for a 1.4 $M_\odot$ neutron star is, from part (b) of Problem 16.15, $P_{\rm min} = 4.6 \times 10^{-4}$ s.

(b) Solve

$$R = 0.5(E + P)$$

and

$$\frac{E - P}{R} = \frac{5\Omega^2 R^3}{4GM}$$

for E and P to get

$$E = R\left(1 + \frac{5\Omega^2 R^3}{8GM}\right)$$

and

$$P = R\left(1 - \frac{5\Omega^2 R^4}{8GM}\right).$$

For twice the minimum rotation period,

$$\frac{2\pi}{\Omega} = 2P_{\min} = 4\pi\sqrt{\frac{R^3}{GM}}$$

or

$$\Omega^2 = \frac{GM}{4R^3}.$$

The equatorial and polar radii then become, with $R = 10$ km,

$$E = R\left(1 + \frac{5}{32}\right) = 11.56 \text{ km}$$

and

$$P = R\left(1 - \frac{5}{32}\right) = 8.44 \text{ km}.$$

16.17 At some instant of time, the period of PSR 1937+214 was determined to be $P = 0.00155780644887275$ s. A change of the last "5" to a "6" is a change of $\Delta P = 10^{-17}$ s. With a period derivative of $\dot{P} = 1.051054 \times 10^{-19}$ s s^{-1}, the time for this change to occur is

$$\Delta t = \frac{\Delta P}{\dot{P}} = 95.14 \text{ s}.$$

16.18 (a) From $P\dot{P} = P\,dP/dt = P_0\dot{P}_0$, we have

$$\int_{P_0}^{P} P\,dP = P_0\dot{P}_0 \int_0^t dt',$$

which results in

$$P = \left(P_0^2 + 2P_0\dot{P}_0 t\right)^{1/2}.$$

(b) In time dt, the pulsar completes dt/P rotations, and the pulsar clock (which wrongly assumes that each pulse has a duration P_0) advances a time $dt_p = P_\circ\, dt/P$. When the perfect clock displays a time $t = P_0/\dot{P}_0$, the pulsar clock will display a time

$$\begin{aligned} t_P &= \int_0^{P_0/\dot{P}_0} \frac{P_0}{P}\,dt \\ &= P_0 \int_0^{P_0/\dot{P}_0} \left(P_0^2 + 2P_0\dot{P}_0 t\right)^{-1/2} dt \\ &= (\sqrt{3} - 1)\frac{P_0}{\dot{P}_0}. \end{aligned}$$

16.19 Assume that angular momentum, $L = I\omega$ with $I = \frac{2}{5}MR^2$, was conserved during the contraction of the Crab neutron star. Then

$$L = I\omega = \frac{2}{5}MR^2\left(\frac{2\pi}{P}\right) = \text{constant},$$

where P is the period of the Crab pulsar. Then

$$dL = \frac{4\pi}{5}M\left(\frac{2R\,dR}{P} - \frac{R^2\,dP}{P^2}\right) = 0.$$

Solving for the change in the neutron star's radius,

$$dR = \frac{R}{2}\frac{dP}{P}.$$

Using $dP/P = 10^{-8}$ and $R = 10^4$ m, we find $dR = 5 \times 10^{-5}$ m.

16.20 From Eq. (16.33), the magnetic field at the pole of the pulsar is

$$B = \frac{1}{2\pi R^3 \sin\theta}\sqrt{\frac{3\mu_0 c^3 I P \dot{P}}{2\pi}}.$$

The moment of inertia of a uniform sphere of radius $R = 10$ km and mass $M = 1.4\ \mathrm{M}_\odot$ is $I = 1.1 \times 10^{38}$ kg m^2. Using $P = 0.237$ s, $\dot{P} = 1.1 \times 10^{-14}$, and $\theta = 90°$, we estimate $B \simeq 3.4 \times 10^8$ T for the Geminga pulsar.

16.21 (a) The radius of the light cylinder around a rotating neutron star is $R_c = cP/2\pi$ (see Fig. 16.26), where P is the rotation period. Assume $R_{\rm ns} = 10$ km for a typical neutron star. The period of the Crab pulsar is $P_{\rm Crab} = 0.0333$ s, so

$$R_{c,\rm Crab} = 1.59 \times 10^6\ \text{m} = 159R_{\rm ns}.$$

The period of PSR 1841−0456 is $P_{1841} = 11.8$ s, so

$$R_{c,1841} = 5.6 \times 10^8\ \text{m} = 5.6 \times 10^4 R_{\rm ns}.$$

(b) Assuming that the two pulsars have comparable magnetic field strengths at their surfaces, the ratio of their magnetic fields at the light cylinder is

$$\frac{B_{\rm Crab}}{B_{1841}} \simeq \left(\frac{R_{c,1841}}{R_{\rm Crab}}\right)^3 = 4.4 \times 10^7.$$

16.22 (a) From Eq. (16.32),

$$P\dot{P} = P\,\frac{dP}{dt} = \frac{8\pi^3 B^2 R^6 \sin^2\theta}{3\mu_0 c^3 I}. \tag{S16.1}$$

Integrating from $t = 0$ when the pulsar's period was P_0 to t and period P gives

$$\int_{P_0}^{P} P\,dP = \frac{8\pi^3 B^2 R^6 \sin^2\theta}{3\mu_0 c^3 I}\int_0^t dt'.$$

This results in

$$P = \left(P_0^2 + \frac{16\pi^3 B^2 R^6 \sin^2\theta\, t}{3\mu_0 c^3 I}\right)^{1/2}. \tag{S16.2}$$

[Note that $P\dot{P}$ is constant. This relation was seen earlier in Problem 16.18(a).]

(b) If $P_0 \ll P$, then solving Eq. (S16.2) for t results in

$$t = \frac{3\mu_0 c^3 I P^2}{16\pi^3 B^2 R^6 \sin^2\theta}.$$

Combining this with Eq. (S16.1) gives

$$t = \frac{P}{2\dot{P}}.$$

(c) Using $P = 0.0333$ s and $\dot{P} = 4.21 \times 10^{-13}$ for the Crab pulsar results in

$$t = 3.95 \times 10^{10} \text{ s} = 1250 \text{ yr}$$

for the age of the Crab pulsar. The Crab supernova occurred in A.D. 1054, so its present age (A.D. 2006) is 952 yr. The value of t is high by about 33%.

16.23 The ratio of the magnetic force to the gravitational force is

$$\frac{F_m}{F_g} = \frac{evB}{mg}.$$

At the neutron star's equator, the velocity of the charged particle is $v = 2\pi R/P$, where P is the period of the pulsar. Then, for a proton at the surface of the Crab Pulsar, using $R = 10$ km, $B = 10^8$ T, $P = 0.0333$ s, and $g = 1.86 \times 10^{12}$ m s^{-2},

$$\frac{F_m}{F_g} = \frac{2\pi eBR}{Pm_p g} = 9.7 \times 10^9.$$

16.24 The minimum energy required to create an electron-positron pair is

$$E_{\min} = 2m_e c^2 = 1.64 \times 10^{-13} \text{ J} = 1.02 \text{ MeV}.$$

From Eq. (5.3), the wavelength of a photon with this energy is

$$\lambda = \frac{hc}{E_{\min}} = 1.21 \times 10^{-12} \text{ m} = 0.00121\text{nm}.$$

From Table 3.1, this is a gamma-ray photon.

16.25 For a 1° subpulse, $\theta = 0.5°$ in Eq. (4.43) for the headlight effect. Using this with the Lorentz factor γ (Eq. 4.20), we have

$$\sin\theta = \frac{1}{\gamma} = \sqrt{1 - u^2/c^2}.$$

Solving for u/c,

$$\frac{u}{c} = \sqrt{1 - \sin^2\theta} = 0.999962.$$

CHAPTER 17

Black Holes

17.1 This effect is analogous to the motion of two stars in a binary system as they orbit their common center of mass.

17.2 Suppose the photon in Fig. 17.11 travels at an angle θ measured from the vertical. Note that the frequency meter must be shifted along the lab's ceiling to the endpoint of the photon's path. According to the observer on the ground, if the photon travels a distance d from the floor to the ceiling of the lab, then the lab has fallen a vertical distance $h = d\cos\theta$ in a time $t = d/c$. The downward speed of the frequency meter is thus $v = gt = gd/c = gh/c\cos\theta$, and the component of the meter's velocity in the direction of the photon's point of origin is $v\cos\theta = gh/c$. The rest of the argument leading to Eq. (17.6) is unchanged.

17.3 With $\ell = 1000$ m, the distance fallen is

$$d = \frac{1}{2}gt^2 = \frac{1}{2}\left(\frac{\ell}{c}\right) = 5.45 \times 10^{-11}\ \text{m}.$$

17.4 Let $r_s = R_\oplus$ be the position of a person at sea level, let $r_L = r_s + 3.1$ km be the position of a person in Leadville, and let Δt_0 be the lifetime of that person. According to Eq. (17.13), an observer at a great distance would measure the person's lifetime at sea level and at Leadville as

$$\Delta t_{\infty,s} = \Delta t_0 \left(1 - \frac{2GM_\oplus}{r_s c^2}\right)^{-1/2}$$

and

$$\Delta t_{\infty,L} = \Delta t_0 \left(1 - \frac{2GM_\oplus}{r_L c^2}\right)^{-1/2},$$

respectively. Thus

$$\begin{aligned}
\Delta t_{\infty,s} - \Delta t_{\infty,L} &= \Delta t_{\infty,L}\left[\frac{\Delta t_{\infty,s}}{\Delta t_{\infty,L}} - 1\right] \\
&= \Delta t_{\infty,L}\left[\left(1 - \frac{2GM_\oplus}{r_s c^2}\right)^{-1/2}\left(1 - \frac{2GM_\oplus}{r_L c^2}\right)^{1/2} - 1\right] \\
&\simeq \Delta t_{\infty,L}\left[\left(1 + \frac{GM_\oplus}{r_s c^2}\right)\left(1 - \frac{GM_\oplus}{r_L c^2}\right) - 1\right] \\
&\simeq \Delta t_{\infty,L}\left[\frac{GM_\oplus}{r_L c^2}\left(\frac{r_L - r_s}{r_s r_L}\right)\right].
\end{aligned}$$

Taking $\Delta t_{\infty,L} \simeq 75$ yr $= 2.37 \times 10^9$ s, we have

$$\Delta t_{\infty,s} - \Delta t_{\infty,L} = 3.38 \times 10^{-13}\,\Delta t_{\infty,L} = 8.0 \times 10^{-4}\ \text{s}.$$

17.5 (a) From Eq. (17.5), the radius of curvature of the light beam is

$$r_c = \frac{c^2}{g} = \frac{c^2 R^2}{GM}.$$

At the surface of a 1.4 $M_\odot$ neutron star of radius $R = 10^4$ m, $r_c = 4.84 \times 10^4$ m. This is comparable with the 10 km radius of the neutron star, and shows that general relativity can not be neglected when studying neutron stars.

(b) If $\Delta t_0 = 1$ hr $= 3600$ s passes at the surface of the neutron star, then Eq. (17.13) shows that the time that passes at a great distance is

$$\Delta t_\infty = \Delta t_0 \left(1 - \frac{2GM}{Rc^2}\right)^{-1/2} = 4700 \text{ s},$$

greater than 1 hour by over 18 minutes! The approximate expression, Eq. (17.14), gives

$$\Delta t_\infty = \Delta t_0 \left(1 - \frac{GM}{Rc^2}\right)^{-1} = 4540 \text{ s}.$$

The difference between these two results shows that gravity cannot be considered "weak" at the surface of a neutron star.

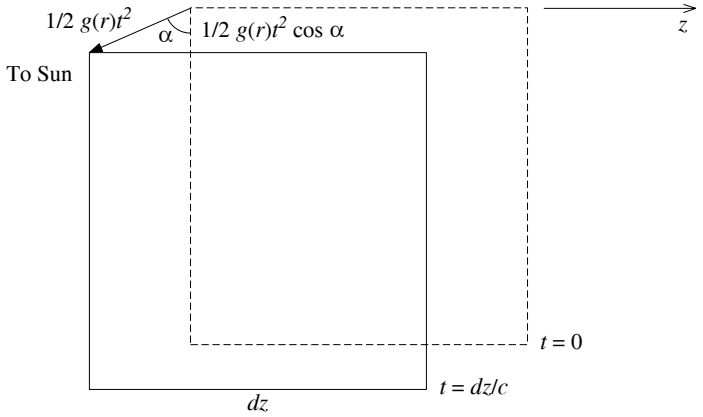

Figure S17.1: Falling local inertial reference frame for Problem 17.6.

17.6 (a) Figure S17.1 shows a rectangular local inertial reference frame of width dz at two times: when the photon (not shown) enters the left-hand side at time $t = 0$, and when the photon exits the right-hand side at time $t = dz/c$. (For clarity, the figure greatly exaggerates the distance the frame falls.) In this time, the frame has fallen a distance of

$$\frac{1}{2} g(r) t^2,$$

toward the Sun, where r is the distance between the frame and the Sun, and $g(r) = GM_\odot/r^2$ is the local gravitational acceleration. The perpendicular distance of the frame from the z-axis is then

$$\frac{1}{2} g(r) t^2 \cos\alpha.$$

Referring to Fig. 17.10 with ℓ replaced by dz, ϕ replaced by $d\phi$, and $\frac{1}{2}gt^2$ replaced by $\frac{1}{2}g(r)t^2\cos\alpha$, we have

$$\left[\frac{1}{2} g(r) t^2 \cos\alpha\right] \Big/ dz = \left[\frac{dz}{2\cos(d\phi/2)}\right] \Big/ \overline{OD}.$$

Because $d\phi$ is so small, we can set $\cos(d\phi/2) \simeq 1$ and $\overline{OD} \simeq r_c$, the radius of curvature of the photon's path. Thus, in radians,

$$d\phi = \frac{dz}{r_c} = \frac{g(r)t^2 \cos\alpha}{dz} = \frac{GM_\odot}{r^2}\left(\frac{dz}{c}\right)^2 \frac{\cos\alpha}{dz}.$$

Defining $g_0 \equiv GM_\odot/r_0^2$, where $r_0 = r\cos\alpha$ is the distance of closest approach, we obtain

$$d\phi = \frac{g_0 \cos^3\alpha}{c^2}\, dz.$$

(b) To find the total angular deflection, ϕ, we integrate $d\phi$ from $\alpha = -\pi/2$ to $+\pi/2$. Using $z = r_0 \tan\alpha$, we have $dz = r_0 \sec^2\alpha\, d\alpha$. Thus

$$\phi = \int_{-\infty}^{\infty} \frac{g_0 \cos^3\alpha}{c^2}\, dz = \frac{g_0 r_0}{c^2}\int_{-\pi/2}^{\pi/2} \cos\alpha\, d\alpha = \frac{2g_0 r_0}{c^2} = \frac{2GM_\odot}{r_0 c^2}.$$

Assuming the photon just grazes the Sun's surface, we set $r_0 = R_\odot$ and find

$$\phi = \frac{2GM_\odot}{R_\odot c^2} = 4.24 \times 10^{-6}\ \text{rad} = 0.875''.$$

(c) The answer to part (b) is half of the correct value of $1.75''$. In general, the correct result for the angular deflection of a photon that passes within a distance r_0 of a spherical mass M is

$$\phi = \frac{4GM}{r_0 c^2},$$

twice the previous result. Our derivation in parts (a) and (b) included only the effect of the curvature of space, and not the equal contribution of time running more slowly in the curved spacetime near the Sun. The photon spends more time near the Sun (as measured by a distant observer), and so suffers a larger angular deflection.

17.7 (a) Elsewhere: $(\Delta s)^2 = (c\Delta t)^2 - (\Delta\ell)^2 < 0$.

(b) Future lightcone: $(\Delta s)^2 > 0$ and $t > 0$.

(c) Future lightcone: $(\Delta s)^2 > 0$ and $t > 0$.

(d) Elsewhere: $(\Delta s)^2 < 0$.

(e) Past lightcone: $(\Delta s)^2 > 0$ and $t < 0$.

(f) Future lightcone: $(\Delta s)^2 > 0$ and $t > 0$.

(g) Elsewhere: $(\Delta s)^2 < 0$.

(h) Elsewhere: $(\Delta s)^2 < 0$.

17.8 For this problem, the Lorentz factor (Eq. 4.20) is $\gamma = 3.20$. It is convenient to express the speed of light as $c = 1\ \text{ly yr}^{-1}$.

(a) $\Delta t_B = 11.7\ \text{ly}/0.95c = 12.3\ \text{yr}$.

(b) From Eq. (4.27) with $\Delta t_B = \Delta t_{\text{moving}}$,

$$\Delta t_A = \frac{\Delta t_B}{\gamma} = 3.85\ \text{yr}.$$

(c) The elapsed time according to Alice's watch is $2\Delta t_A = 7.70$ yr.

(d) The elapsed time according to Bob's watch is $2\Delta t_B = 24.6$ yr. Thus Alice will be 16.9 yr younger than Bob.

In Fig. 17.14, we can take events A and B to be Alice's leaving and arriving back on Earth, and C to be her turn-around at τ Ceti. Then Bob's worldline is the straight segment, $A \rightarrow B$, and Alice's worldline is $A \rightarrow C \rightarrow B$. The straight worldline has the longer interval.

17.9 (a) Gravitational time dilation affects both the rate at which photons are emitted by a blackbody and the frequency of each photon. Both effects decrease the luminosity of the blackbody as measured by a distant observer. According to Eq. (17.13), if Δt is the time between photons as measured at the surface of the blackbody, then the time between photons as measured at infinity is

$$\Delta t_\infty = \Delta t \left(1 - \frac{2GM}{Rc^2}\right)^{-1/2}.$$

Similarly, if ν is the frequency of a photon measured at the surface of the blackbody, then the frequency of the photon measured at infinity is

$$\nu_\infty = \nu \left(1 - \frac{2GM}{Rc^2}\right)^{1/2}.$$

From Eq. (5.3), $E_{\text{photon}} = h\nu$; the energy of every photon is therefore decreased by a factor of

$$\left(1 - \frac{2GM}{Rc^2}\right)^{1/2}.$$

Thus if L is the luminosity measured at the surface of the blackbody, then an observer at infinity measures

$$L_\infty = L \left(1 - \frac{2GM}{Rc^2}\right).$$

(b) Both observers measure the same value for the speed of light, so $c = \lambda_\infty \nu_\infty = \lambda\nu$. Both observers use Wien's law, Eq. (3.15), to determine the blackbody's temperature, so $\lambda_{\text{max},\infty} T_\infty = \lambda_{\text{max}} T$. Equation (17.13) then shows that

$$T_\infty = T\left(\frac{\lambda_{\text{max}}}{\lambda_{\text{max},\infty}}\right) = T\left(\frac{\nu_\infty}{\nu}\right) = T\left(1 - \frac{2GM}{Rc^2}\right)^{1/2}.$$

(c) Both observers use the Stefan–Boltzmann law, Eq. (3.17). Their values of the radius (determined at infinity, R_∞, and at the surface of the spherical blackbody, R) are related to their values of the luminosity and the effective temperature by

$$\frac{L_\infty}{L} = \frac{R_\infty^2 T_\infty^4}{R^2 T^4}.$$

Using the results of parts (a) and (b), this is

$$R_\infty = R\left(\frac{T}{T_\infty}\right)^2 \left(\frac{L_\infty}{L}\right)^{1/2} = \frac{R}{\sqrt{1 - 2GM/Rc^2}}.$$

17.10 Start with Eq. (2.17) with $r = R$ for the escape velocity at the surface of a spherical object of mass M and radius R. This can be written in terms of the object's average density as

$$v_{\rm esc} = \sqrt{\frac{2GM}{R}} = \sqrt{\frac{8\pi GR^2\rho}{3}}.$$

Using $\rho = \rho_\oplus = 5515\ \text{kg m}^{-3}$ (Appendix C) and $R = 250R_\odot$, we find

$$v_{\rm esc} = \sqrt{\frac{8\pi G(250R_\odot)^2\rho_\oplus}{3}} = 3.06 \times 10^8\ \text{m s}^{-1} \simeq c.$$

17.11 If the Sun were suddenly to become a black hole, there would be no effect on the orbits of the planets. In either case, the same Schwarzschild metric (Eq. 17.22) describes the curved spacetime through which the planets move (for $r > R_\odot$).

17.12 (a) The Schwarzschild radius (Eq. 17.27), $R_S = 2GM/c^2$, evaluated for these black holes is

$$\begin{aligned} R_S &= 1.48 \times 10^{-15}\ \text{m} \quad \text{for } 10^{12}\ \text{kg} \\ &= 2.95 \times 10^{4}\ \ \text{m} \quad \text{for } 10\ \text{M}_\odot \\ &= 2.95 \times 10^{8}\ \ \text{m} \quad \text{for } 10^5\ \text{M}_\odot \\ &= 2.95 \times 10^{12}\ \text{m} \quad \text{for } 10^9\ \text{M}_\odot. \end{aligned}$$

(b) The average density of each of these black holes is

$$\begin{aligned} \rho &= \frac{M}{\frac{4}{3}\pi R_S^3} \\ &= 7.36 \times 10^{55}\ \text{kg m}^{-3} \quad \text{for } 10^{15}\ \text{g} \\ &= 1.85 \times 10^{17}\ \text{kg m}^{-3} \quad \text{for } 10\ \text{M}_\odot \\ &= 1.85 \times 10^{9}\ \ \text{kg m}^{-3} \quad \text{for } 10^5\ \text{M}_\odot \\ &= 1.85 \times 10^{1}\ \ \text{kg m}^{-3} \quad \text{for } 10^9\ \text{M}_\odot. \end{aligned}$$

17.13 (a) Begin by using Eq. (17.27) for the Schwarzschild radius to express Eq. (17.23) for the differential proper distance along a radial line in terms of R_S,

$$d\mathcal{L} = \frac{dr}{\sqrt{1 - R_S/r}}.$$

The proper distance, $\Delta\mathcal{L}$, from the event horizon ($r = R_S$) to a final radial coordinate r is then found by integrating $d\mathcal{L}$,

$$\begin{aligned} \Delta\mathcal{L} &= \int_{R_S}^{r} \frac{dr'}{\sqrt{1 - R_S/r'}} \\ &= \left[\sqrt{r'^2 - R_S r'} + R_S \ln\left(\sqrt{r' - R_S} + \sqrt{r'}\right)\right]_{R_S}^{r} \end{aligned}$$

$$= \sqrt{r^2 - R_S r} + R_S \ln\left(\frac{\sqrt{r - R_S} + \sqrt{r}}{\sqrt{R_S}}\right)$$

$$= r\sqrt{1 - \frac{R_S}{r}} + \frac{R_S}{2}\ln\left(\sqrt{r/R_S - 1} + \sqrt{r/R_S}\right)^2 \tag{S17.1}$$

$$= r\sqrt{1 - \frac{R_S}{r_f}} + \frac{R_S}{2}\ln\left(\frac{1 + \sqrt{1 - R_S/r}}{1 - \sqrt{1 - R_S/r}}\right).$$

(b) See Fig. S17.2.

(c) By inspection of Eq. (S17.1), as $r/R_S \to \infty$,

$$\Delta\mathcal{L} \to r + \frac{R_S}{2}\ln\left(\frac{4r}{R_S}\right).$$

For large values of r, the first term on the right dominates the second term and $\Delta\mathcal{L} \simeq r$. So for large r, the radial coordinate can be interpreted as the proper distance to the event horizon.

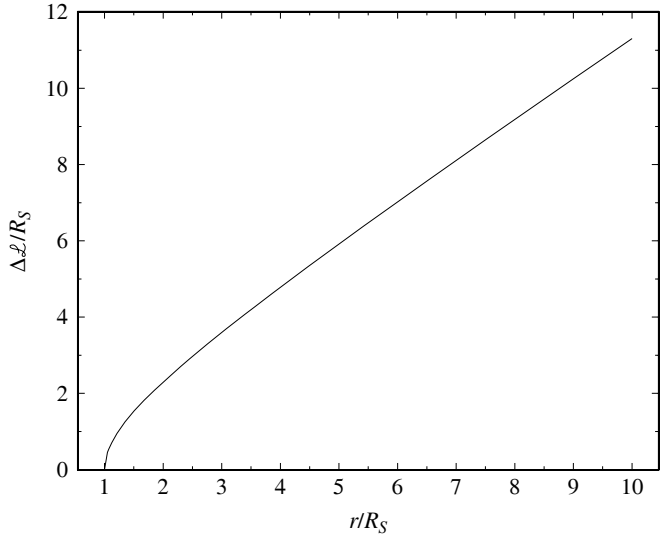

Figure S17.2: Results for Problem 17.13.

17.14 From the Schwarzschild metric (Eq. 17.22) with $dr = 0$ for a spherical surface, we see that the differential element of area is

$$dA = (r\,d\theta)(r\sin\theta\,d\phi) = r^2\sin\theta\,d\theta\,d\phi.$$

Setting $r = R_S$ and integrating this over the usual limits of $\theta = 0$ to π and $\phi = 0$ to 2π gives the area of the event horizon,

$$A_{\text{horizon}} = R_S^2\int_{\phi=0}^{2\pi}\int_{\theta=0}^{\pi}\sin\theta\,d\theta\,d\phi = 4\pi R_S^2.$$

17.15 (a) Equation (17.26) gives the coordinate speed of a particle orbiting a nonrotating black hole, $v = \sqrt{GM/r}$. Evaluating this at $r = 3R_S = 6GM/c^2$ (Eq. 17.27) shows that $v = c/\sqrt{6}$.

(b) The coordinate speed is $v = r\,d\phi/dt$, so the orbital period at $r = 3R_S$ is

$$P = \int_0^{2\pi} \frac{r}{v}\,d\phi = \int_0^{2\pi} \frac{3R_S}{c/\sqrt{6}}\,d\phi = \frac{6\sqrt{6}\pi R_S}{c}.$$

Using $R_S = 2GM/c^2 = 29.5$ km for a 10 $M_\odot$ black hole, we find $P = 4.55 \times 10^{-3}$ s.

17.16 (a) The coordinate speed of light in the ϕ-direction can be found from the Schwarzschild metric (Eq. 17.22) using $ds = 0$ for light. Setting $dr = d\theta = 0$ and $\theta = 90°$ results in

$$0 = \left(c\,dt\sqrt{1 - 2GM/rc^2}\right)^2 - (r\,d\phi)^2.$$

The coordinate speed of light in the ϕ-direction is thus

$$r\,\frac{d\phi}{dt} = c\sqrt{1 - 2GM/rc^2}.$$

(b) Equation (17.26) for the speed of a particle orbiting a nonrotating black hole, $v = \sqrt{GM/r}$, does not contain the particle's mass. Setting this equal to the coordinate speed of light in the ϕ-direction,

$$\sqrt{\frac{GM}{r}} = c\sqrt{1 - \frac{2GM}{rc^2}},$$

and solving for r gives the radius of a photon's circular orbit around a black hole,

$$r_{\text{photon}} = \frac{3GM}{c^2} = 1.5R_S,$$

where Eq. (17.27) for the Schwarzschild radius was used.

(c) At $r = 1.5R_S = 3GM/c^2$, the coordinate speed of light in the ϕ-direction is

$$r\,\frac{d\phi}{dt} = c\sqrt{1 - 2GM/rc^2} = c/\sqrt{3}.$$

The orbital period at $r = 1.5R_S$ is

$$P = \int_0^P dt = \int_0^{2\pi} \frac{r}{c/\sqrt{3}}\,d\phi = \frac{3\pi\sqrt{3}R_S}{c}.$$

Using $R_S = 2GM/c^2 = 29.5$ km for a 10 $M_\odot$ black hole, we find $P = 1.61 \times 10^{-3}$ s.

(d) If a flashlight were beamed in the ϕ-direction at $r = 1.5R_S$, the photons would orbit the black hole.

17.17 Assuming that the maximum angular momentum of a rotating rigid sphere occurs when the surface of the sphere is the speed of light,

$$\omega_{\max} = \frac{c}{R}.$$

Taking the moment of inertia to be $I = 2MR^2/5$, the maximum angular momentum is given by

$$L_{\max} = I\omega_{\max} = \frac{2}{5}MRc.$$

For a black hole, the radius is the Schwarzschild radius, $R = R_S = 2GM/c^2$. Substituting gives

$$L_{\max} = \frac{4}{5}\frac{GM^2}{c}.$$

This crude estimate is 80% of the general relativistic value given by Eq. 17.29.

17.18 From Eq. (17.29), the maximum angular momentum of a 1.4 $M_\odot$ black hole is

$$L_{\max} = \frac{GM^2}{c} = 1.73 \times 10^{42} \text{ kg m}^2 \text{ s}^{-1}.$$

The angular momentum of the fastest known pulsar ($P = 0.00139$ s) may be estimated (assuming a 1.4 $M_\odot$ uniform sphere of radius 10 km) as

$$L = I\omega = \frac{2}{5}MR^2\left(\frac{2\pi}{P}\right) = 5.04 \times 10^{41} \text{ kg m}^2 \text{ s}^{-1}.$$

17.19 For an electron,

$$\left(\frac{GM}{c}\right)^2 = \left(\frac{Gm_e}{c}\right)^2$$
$$= 4.11 \times 10^{-98} \text{ m}^4 \text{ s}^{-2}$$
$$G\left(\frac{Q}{c}\right)^2 = G\left(\frac{-e}{c}\right)^2$$
$$= 1.71 \times 10^{-55} \text{ m}^4 \text{ s}^{-2}$$
$$\left(\frac{L}{M}\right)^2 = \left(\frac{\hbar/2}{m_e}\right)^2$$
$$= 3.35 \times 10^{-3} \text{ m}^4 \text{ s}^{-2}.$$

For an electron,

$$\left(\frac{GM}{c}\right)^2 \ll G\left(\frac{Q}{c}\right)^2 + \left(\frac{L}{M}\right)^2,$$

so an electron is not a black hole.

17.20 (a) Assume that Ω is given by an expression of the form

$$\Omega = \text{constant} \times G^\alpha L^\beta r^\gamma c^\delta,$$

where the values of the exponents α, β, γ, and δ are to be determined. Let $[x]$ designate the units of the variable x, so

$$[\Omega] = \text{s}^{-1}$$
$$[G] = \text{m}^3 \text{ kg}^{-1} \text{ s}^{-2}$$
$$[L] = \text{kg m}^2 \text{ s}^{-1}$$
$$[r] = \text{m}$$
$$[c] = \text{m s}^{-1}.$$

The units involved in the expression for Ω are therefore

$$\text{s}^{-1} = (\text{m}^3 \text{ kg}^{-1} \text{ s}^{-2})^\alpha (\text{kg m}^2 \text{ s}^{-1})^\beta (\text{m})^\gamma (\text{m s}^{-1})^\delta,$$

which leads to

$$\begin{aligned} 3\alpha + 2\beta + \gamma + \delta &= 0 \\ -\alpha + \beta &= 0 \\ -2\alpha - \beta - \delta &= -1. \end{aligned}$$

Four equations with three unknowns cannot be solved. However, if we assume that $\Omega \propto L$ so $\beta = 1$, we can solve for the remaining exponents to find $\alpha = 1$, $\gamma = -3$, and $\delta = -2$. Therefore,

$$\Omega = \text{constant} \times \frac{GL}{r^3 c^2}.$$

(b) The angular momentum of Earth may be estimated as

$$L_\oplus = I_\oplus \omega_\oplus = \frac{2}{5} M_\oplus R_\oplus^2 \left(\frac{2\pi}{P_\oplus} \right) = 7.09 \times 10^{33} \text{ kg m}^2 \text{ s}^{-1},$$

where $r = R_\oplus$ and $P_\oplus$ is Earth's sidereal day, $P = 23^{\text{h}}56^{\text{m}}04^{\text{s}} = 8.62 \times 10^4$ s. Then, setting the leading constant equal to one,

$$\Omega_\oplus = \frac{GL_\oplus}{R_\oplus^3 c^2} = 2.03 \times 10^{-14} \text{ s}^{-1} = 1.33 \times 10^{-16} \text{ }'' \text{ yr}^{-1}.$$

The time for a pendulum at the north pole to rotate once relative the distant stars because of frame dragging would be

$$t = \frac{2\pi}{\Omega_\oplus} = 3.10 \times 10^{14} \text{ s},$$

about 9.8 million years.

(c) From Problem 17.18, the angular momentum of the fastest known pulsar ($P = 0.00139$ s) may be estimated (assuming a 1.4 $M_\odot$ uniform sphere of radius 10 km) is

$$L = I\omega = \frac{2}{5} MR^2 \left(\frac{2\pi}{P} \right) = 5.04 \times 10^{41} \text{ kg m}^2 \text{ s}^{-1}.$$

At the surface of this pulsar,

$$\Omega = \frac{GL}{R^3 c^2} = 374 \text{ s}^{-1} = 59.4 \text{ rev s}^{-1}.$$

17.21 (a) Assume that the mass of the least massive primordial black hole, m_P, is given by a expression of the form

$$m_P = \hbar^\alpha c^\beta G^\gamma,$$

where the values of the exponents α, β, and γ are to be determined. Let $[x]$ designate the units of the variable x, so

$$\begin{aligned} [m_P] &= \text{kg} \\ [\hbar] &= \text{kg m}^2 \text{ s}^{-1} \\ [c] &= \text{m s}^{-1} \\ [G] &= \text{m}^3 \text{ kg}^{-1} \text{ s}^{-2}. \end{aligned}$$

The units involved in the expression for m_P are therefore

$$m_P = (\text{kg m}^2\ \text{s}^{-1})^{\alpha}(\text{m s}^{-1})^{\beta}(\text{m}^3\ \text{kg}^{-1}\ \text{s}^{-2})^{\gamma},$$

which leads to

$$\begin{aligned} \alpha - \gamma &= 1 \\ 2\alpha + \beta + 3\gamma &= 0 \\ -\alpha - \beta - 2\gamma &= 0. \end{aligned}$$

Solving these shows that $\alpha = 1/2$, $\beta = 1/2$, and $\gamma = -1/2$. Therefore,

$$m_P = \sqrt{\frac{\hbar c}{G}} = 2.18 \times 10^{-8}\ \text{kg}.$$

(b) From Eq. (17.27), the Schwarzschild radius for a black hole of mass m_P would be

$$r_P = \frac{2Gm_P}{c^2} = 3.24 \times 10^{-35}\ \text{m}.$$

(c) $t = r_P/c = 1.08 \times 10^{-43}$ s.

(d) $t_{\text{evap}} \approx \left(\dfrac{m_P}{M_\odot}\right)^3 \times 10^{66}\ \text{yr} = 1.3 \times 10^{-48}\ \text{yr} = 4.2 \times 10^{-41}\ \text{s}.$

17.22 (a) On the left-hand side

$$[kT] = \text{J} = \text{kg m}^2\ \text{s}^{-2}.$$

On the right-hand side

$$\left[\frac{\hbar c}{4\pi R_S}\right] = \frac{\left(\text{kg m}^2\ \text{s}^{-1}\right)\left(\text{m s}^{-1}\right)}{\text{m}} = \text{kg m}^2\ \text{s}^{-2} = \text{J}.$$

(b) $kT = 1 \times 10^{-11}$ J $= 62$ MeV. This implies that $T = 7.2 \times 10^{11}$ kg.

(c) From Wien's law, this corresponds to $\lambda_{\text{max}} = 4 \times 10^{-15}$ m. This is in the gamma-ray portion of the spectrum.

(d) 344 m.

(e) 6.2×10^{-9} K.

17.23 (a) Beginning with the Stefan–Boltzmann law, and substituting we have

$$\begin{aligned} L &= 4\pi R_S^2 \sigma T^4 \\ &= 4\pi \left(\frac{2GM}{c^2}\right)^2 \left(\frac{2\pi^5 k^4}{15c^2h^3}\right)\left(\frac{\hbar}{8\pi kGM}\right)^4. \end{aligned}$$

After some tedious rearranging we arrive at the desired result.

(b) The time to evaporate is given by

$$t = \int_0^M \frac{c^2 dM}{L}.$$

Integration gives Eq. (17.30).

17.24 (a) From Eq. (7.7), the mass function is the right-hand side of

$$\frac{m_c^3}{(m_s + m_c)^2} \sin^3 i = \frac{P}{2\pi G} v_{sr}^3.$$

Using $P = 0.3226\,\text{d} = 2.79 \times 10^4$ s and $v_{sr} = 4.57 \times 10^5$ m s^{-1},

$$\frac{m_c^3}{(m_s + m_c)^2} \sin^3 i = 6.35 \times 10^{30}\ \text{kg}.$$

Because the left-hand side must be less than m_c, the mass of the compact object must be greater than 6.35×10^{30} kg $= 3.19\,\text{M}_\odot$.

(b) The ratio of the masses is, from Eq. (7.5),

$$\frac{m_s}{m_c} = \frac{v_{cr}}{v_{sr}} = 0.0941.$$

Combining this with the result for part (a) and assuming that $i = 90°$ gives

$$m_c = 3.19\,\text{M}_\odot (m_s/m_c + 1)^2 = 3.82\,\text{M}_\odot.$$

Because $\sin^3 i \leq 1$, $m_c \geq 3.19\,\text{M}_\odot$.

(c) If the angle of inclination were $i = 45°$, then the mass obtained for the compact object would be larger by a factor of $1/\sin^3 45° = 2.83$. That is, m_c would be $10.8\,\text{M}_\odot$.

17.25 The K0 IV companion has a measured periodic radial velocity of 211 ± 4 km s^{-1} and an orbital period of 6.473 ± 0.001 d. The approximate mass of the companion is $0.9\,\text{M}_\odot$. Assuming an inclination of $i = 90°$, Eq. (7.7) implies

$$\frac{m_2^3}{(m_1 + m_2)^2} = \frac{P}{2\pi G} v_{1r}^3 = 1.25 \times 10^{31}\ \text{kg} = 6.3\,\text{M}_\odot.$$

Let

$$k \equiv \frac{m_2^3}{(m_1 + m_2)^2} = 6.3\,\text{M}_\odot.$$

Expanding the expression leads to the cubic expression

$$m_2^3 - k m_2^2 - 2k m_1 m_2 - k m_1^2 = 0.$$

This can be solved to give $m_2 = 7.9\,\text{M}_\odot$.

This result is a lower limit because we simply assumed $i = 90°$. An improved estimate of i will yield a more accurate result, as will a more careful estimate of the mass of the K0 IV companion.

CHAPTER 18

Close Binary Star Systems

18.1 Because equipotential surfaces are level surfaces for binary stars, we expect the density to be constant along a surface of constant Φ. The behavior of the pressure may be deduced from the equation of hydrostatic equilibrium (Eq. 10.6) combined with Eq. (18.8) for the gravitational potential,

$$\frac{dP}{dr} = -\rho g = \rho \frac{d\Phi}{dr}.$$

For constant density, the pressure and gravitational potential vary spatially in the same way, so the pressure should be approximately constant along an equipotential surface. Now consider the ideal gas law (Eq. 10.11),

$$P_g = \frac{\rho k T}{\mu m_H},$$

making the reasonable assumption that the mean molecular weight, μ, is constant. This shows that if the pressure and density are roughly constant along an equipotential surface, then the temperature will also be approximately constant. The proximity of the other star could cause heating of each star on the side that faces the other.

18.2 For the equilateral triangle formed by M_1, M_2, and L_4 (or L_5), we have $s_1 = s_2 = a$ in Fig. 18.1. Then Eqs. (18.4) and (18.7) give

$$\Phi = -G\,\frac{M_1 + M_2}{a} - \frac{1}{2}\omega^2 r^2 = -G\,\frac{M_1 + M_2}{a}\left(1 + \frac{r^2}{2a^2}\right).$$

Equations (18.3) show that

$$r_1 = a\left(\frac{M_2}{M_1 + M_2}\right)$$

$$r_2 = a\left(\frac{M_1}{M_1 + M_2}\right),$$

and so Eqs. (18.6) may be expressed as

$$a^2 = a^2\left(\frac{M_2}{M_1 + M_2}\right)^2 + r^2 + 2a\left(\frac{M_2}{M_1 + M_2}\right) r\cos\theta$$

$$a^2 = a^2\left(\frac{M_1}{M_1 + M_2}\right)^2 + r^2 - 2a\left(\frac{M_1}{M_1 + M_2}\right) r\cos\theta.$$

Solving these for r yields

$$r = a\sqrt{1 - \frac{M_1 M_2}{(M_1 + M_2)^2}}$$

and so the gravitational potential at L_4 (or L_5) is

$$\Phi = -G\,\frac{M_1 + M_2}{2a}\left[3 - \frac{M_1 M_2}{(M_1 + M_2)^2}\right].$$

In units of $G(M_1 + M_2)/a$, this is

$$\Phi = -\frac{1}{2}\left[3 - \frac{M_1 M_2}{(M_1 + M_2)^2}\right] = -1.431.$$

This agrees with the value given in Fig. 18.3.

18.3 (a) As the gas passes perpendicularly across the area A with velocity v, in time dt it will travel a distance $v\,dt$ and sweep out a volume $vA\,dt$. For gas density ρ, the mass of gas within this volume is $dM = \rho v A\,dt$. The rate at which mass crosses the area is therefore $\dot{M} \equiv dM/dt = \rho v A$, which is Eq. (18.11).

(b) Referring to Fig. 18.5, start with

$$R^2 = \left(R - \frac{d}{2}\right)^2 + x^2$$

or

$$x^2 = Rd - \frac{d^2}{4}.$$

When $d \ll R$, we recover Eq. (18.12), $x = \sqrt{Rd}$.

18.4 Let $x = R/r$, so Eq. (18.19) for the disk temperature is

$$T = T_{\text{disk}} x^{3/4}(1 - \sqrt{x})^{1/4}.$$

T will be a maximum when $dT/dx = 0$, or when

$$\frac{3}{4}x^{-1/4}(1 - \sqrt{x})^{1/4} - \frac{1}{4}(1 - \sqrt{x})^{-3/4}\frac{1}{2\sqrt{x}} = 0.$$

Thus T is a maximum when $x = 36/49$, or when $r = (49/36)R$. Evaluating T at this point results in $T_{\text{max}} = 0.488 T_{\text{disk}}$.

18.5 Integrating Eq. (18.15) for the ring luminosity, and using Eqs. (18.19) and (18.20) for the disk temperature, we have

$$L_{\text{disk}} = \int_R^\infty 4\pi r\sigma \left(\frac{3GM\dot{M}}{8\pi\sigma R^3}\right)\left(\frac{R}{r}\right)^3\left(1 - \sqrt{\frac{R}{r}}\right) dr$$

$$= \frac{3GM\dot{M}}{2R^2}\int_R^\infty \left(\frac{R}{r}\right)^2\left(1 - \sqrt{\frac{R}{r}}\right) dr.$$

Defining $x = R/r$, we find

$$L_{\text{disk}} = \frac{3GM\dot{M}}{2R}\int_0^1 \left(1 - \sqrt{x}\right)\,dx = \frac{GM\dot{M}}{2R},$$

which is Eq. (18.23) for the disk luminosity.

18.6 We will use the mass and radius of the white dwarf of Z Cha given in Example 18.4.1: $M = 0.85\ \mathrm{M}_\odot$ and $R = 0.0095\ \mathrm{R}_\odot$. For a mass-transfer rate of $\dot{M} = 10^{13.5}\ \mathrm{kg\ s^{-1}}$, the disk luminosity is (Eq. 18.23)

$$L_{\mathrm{disk}} = G\,\frac{M\dot{M}}{2R} = 2.70 \times 10^{26}\ \mathrm{W} = 0.705\ \mathrm{L}_\odot.$$

In $t = 10$ days, the total energy released is $E = L_{\mathrm{disk}}t = 2.33 \times 10^{32}$ J. From Eq. (3.8) with $M_{\mathrm{Sun}} = 4.74$, the absolute magnitude of the dwarf nova is

$$M = M_{\mathrm{Sun}} - 2.5 \log_{10}\left(\frac{L}{L_\odot}\right) = 5.12.$$

(This neglects the small amount of light contributed by the primary and secondary stars.)

18.7 During quiescence, the absolute magnitude of the dwarf nova is $M = 7.5$. From Eq. (3.7) with $M_{\mathrm{Sun}} = 4.74$, the luminosity of the system is

$$L_{\mathrm{quiet}} = 100^{(M_{\mathrm{Sun}}-M)/5}\ \mathrm{L}_\odot = 0.08\ \mathrm{L}_\odot = 3.0 \times 10^{25}\ \mathrm{W}.$$

During the outburst, the absolute magnitude of the dwarf nova would be $M = 7.5 - 3 = 4.5$. Again using Eq. (3.7), the luminosity of the system is

$$L_{\mathrm{out}} = 100^{(M_{\mathrm{Sun}}-M)/5}\ \mathrm{L}_\odot = 1.25\ \mathrm{L}_\odot = 4.79 \times 10^{26}\ \mathrm{W}.$$

The disk luminosity during the outburst is then $L_{\mathrm{out}} - L_{\mathrm{quiet}} = 1.179\ \mathrm{L}_\odot$. Using $M = 0.85\ \mathrm{M}_\odot$ and $R = 0.0095\ \mathrm{R}_\odot$ with Eq. (18.23) results in a mass-transfer rate of

$$\dot{M} = \frac{2RL_{\mathrm{disk}}}{GM} = 5.3 \times 10^{13}\ \mathrm{kg\ s^{-1}} = 8.4 \times 10^{-10}\ \mathrm{M}_\odot\ \mathrm{yr^{-1}}.$$

18.8 As shown in Fig. 18.12, the binary system and the accretion disk rotate in the same direction.

18.9 (a) From $\omega = 2\pi/P$, we have

$$\frac{1}{\omega}\frac{d\omega}{dt} = \frac{P}{2\pi}\left(\frac{-2\pi}{P^2}\right)\frac{dP}{dt} = -\frac{1}{P}\frac{dP}{dt}.$$

Substituting this into Eq. (18.29) and then using Eq. (18.28) shows that

$$\frac{1}{P}\frac{dP}{dt} = \frac{3}{2}\frac{1}{a}\frac{da}{dt} = 3\dot{M}_1\frac{M_1 - M_2}{M_1 M_2}.$$

(b) For $M_1 = 2.9\ \mathrm{M}_\odot$, $M_2 = 1.4\ \mathrm{M}_\odot$, $P = 2.49\ \mathrm{d} = 2.15 \times 10^5$ s, and $dP/dt = (20\ \mathrm{s})/(100\ \mathrm{yr}) = 6.3 \times 10^{-9}\ \mathrm{s\ s^{-1}}$, we have

$$\dot{M}_1 = \frac{1}{3P}\frac{dP}{dt}\frac{M_1 M_2}{M_1 - M_2} = 5.3 \times 10^{16}\ \mathrm{kg\ s^{-1}} = 8.4 \times 10^{-7}\ \mathrm{M}_\odot\ \mathrm{yr^{-1}}.$$

Because $dP/dt > 0$ and $M_1 > M_2$, we have $\dot{M}_1 > 0$. Star 1 is gaining mass.

18.10 The subgiant began as the more massive star. It evolved faster and expanded to overflow its Roche lobe while its companion was still on the main sequence. Enough mass was transferred to the companion to make it the more massive B8 main sequence star that is observed today.

18.11 The amount of energy released in the fusion of $m = 10^{-4}\ \mathrm{M}_\odot$ of hydrogen is $E = 0.007mc^2 = 1.25\times10^{41}$ J. For a luminosity equal to the Eddington limit of $L_{\mathrm{Ed}} \approx 10^{31}$ W (Eq. 10.6), the outburst would last for a time of

$$t = \frac{E}{L_{\mathrm{Ed}}} = 1.25 \times 10^{10}\ \mathrm{s} \approx 400\ \mathrm{yr}.$$

Typically, a classical nova's outburst lasts about 100 days, so only a very small fraction of the hydrogen surface layer actually undergoes fusion. The rest is ejected into space by the explosion.

18.12 The gravitational potential energy of $m = 10^{-4}\ \mathrm{M}_\odot$ of hydrogen on the surface of a white dwarf of mass $M = 0.85\ \mathrm{M}_\odot$ and $R = 0.0095\ \mathrm{R}_\odot$ is, from Eq. (2.14),

$$U = -G\frac{Mm}{R} = -3.4 \times 10^{39}\ \mathrm{J}$$

(using values of M and R for Z Cha from Example 18.4.1). With a speed of $v = 10^6\ \mathrm{m\ s^{-1}}$, the kinetic energy of the ejected layer is

$$K = \frac{1}{2}mv^2 = 9.9 \times 10^{37}\ \mathrm{J}.$$

Note that $K/|U| \approx 0.029$. Since the gravitational potential energy is negligibly small when the ejecta is far from the white dwarf, we conclude that the total energy given to the ejecta is just barely enough to allow it to escape from the system.

18.13 (a) In time dt, the amount of mass that passes through a spherical surface of radius r, centered on the nova, is $dM = \dot{M}_{\mathrm{eject}}\,dt$. In time dt, the material at r travels a distance $dr = v\,dt$ as it sweeps through a spherical shell of volume $dV = 4\pi r^2\,dr = 4\pi r^2 v\,dt$. The density of the material at r is therefore

$$\rho = \frac{dM}{dV} = \frac{\dot{M}_{\mathrm{eject}}}{4\pi r^2 v}.$$

(b) From Eq. (9.17), the optical depth of the photosphere at time $t = 0$ is

$$\tau = \int_{R_0}^{R} \overline{\kappa}\rho\,dr = \frac{2}{3} = \int_{R_0}^{R} \overline{\kappa}\left(\frac{\dot{M}_{\mathrm{eject}}}{4\pi r^2 v}\right) dr,$$

where R is the outer radius of the shell and R_0 is the radius of the photosphere at $t = 0$. Solving this for R gives

$$\frac{1}{R} = \frac{1}{R_0} - \frac{8\pi v}{3\overline{\kappa}\dot{M}_{\mathrm{eject}}} = \frac{1}{R_0} - \frac{1}{R_\infty},$$

which defines R_∞.

(c) At a later time t, the outer radius of the shell is $R + vt$ and the radius of the photosphere is $R(t)$. [$R(t = 0) = R_0$.] The optical depth of the photosphere at time t is given by

$$\tau = \int_{R(t)}^{R+vt} \overline{\kappa}\rho\,dr = \frac{2}{3} = \int_{R(t)}^{R+vt} \overline{\kappa}\left(\frac{\dot{M}_{\mathrm{eject}}}{4\pi r^2 v}\right) dr.$$

As in part (b), this leads to

$$\frac{1}{R + vt} = \frac{1}{R(t)} - \frac{1}{R_\infty}.$$

(d) From the answer to part (b),

$$R = \frac{R_0 R_\infty}{R_\infty - R_0}.$$

Substituting this for R in the answer to part (c) and simplifying results in

$$R(t) = R_0 + \frac{vt(1 - R_0/R_\infty)^2}{1 + (vt/R_\infty)(1 - R_0/R_\infty)}.$$

(e) If R_0 is comparable to the radius of the white dwarf (i.e., $R_{\rm wd} = 0.0095\ {\rm R}_\odot$ for Z Cha from Example 18.4.1) and if $v = 10^6\ {\rm m\ s^{-1}}$, then $vt < R_0$ for approximately 7 s. So except for the first seconds of the outburst, the first term on the right can be neglected. Also, neglecting terms involving R_0/R_∞ results in

$$R(t) \simeq \frac{vt}{1 + vt/R_\infty}.$$

(f) At early times when $R_0 \ll vt \ll R_\infty$, $R(t) \simeq vt$, so initially the photosphere expands linearly with time. When $vt \gg R_\infty$, the second term in the denominator dominates the first, and t approaches the limiting value of R_∞.

(g) Using $\overline{\kappa} = 0.04\ {\rm m^2\ kg^{-1}}$, $\dot{M}_{\rm ejecta} = 10^{19}\ {\rm kg\ s^{-1}}$ and $v = 10^6\ {\rm m\ s^{-1}}$, the value of R_∞ is

$$R_\infty = \frac{3\overline{\kappa}\dot{M}_{\rm eject}}{8\pi v} = 4.8 \times 10^{10}\ {\rm m}.$$

As seen in Fig. S18.1, the end of the linear expansion period — the "knee" in the graph — occurs roughly at $t \sim 1$ day. This is comparable to the duration of the optically thick fireball phase, which lasts for a few days.

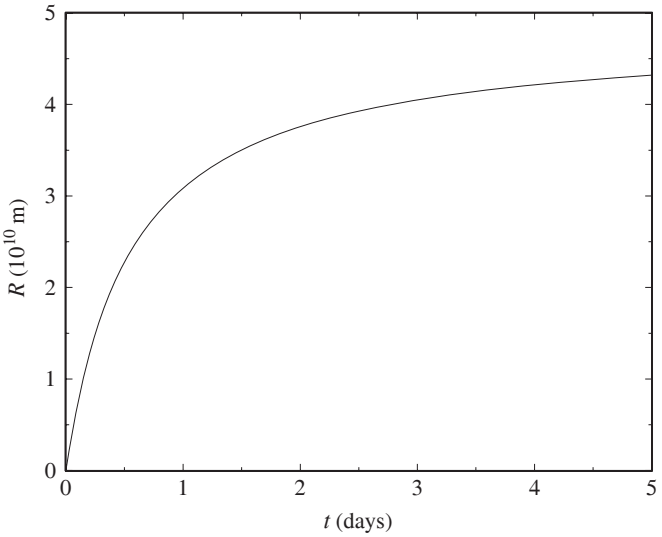

Figure S18.1: Results for Problem 18.13.

18.14 Equation (18.31) shows that the temperature of the nova's photosphere approaches

$$T_\infty = \left(\frac{L}{4\pi\sigma}\right)^{1/4} \left(\frac{8\pi v}{3\overline{\kappa}\dot{M}_{\rm eject}}\right)^{1/2}.$$

Adopting $L_{\rm Ed} \approx 10^{31}$ W for the Eddington limit, together with $\overline{\kappa} = 0.04$ m^2 kg^{-1}, $\dot{M}_{\rm ejecta} = 10^{19}$ kg s^{-1} and $v = 10^6$ m s^{-1}, results in $T_\infty = 8900$ K.

18.15 If a mass of $M = 10^{-4}$ M$_\odot$ is ejected at a constant rate over a time of $t = 100$ days, then

$$\dot{M}_{\rm eject} = \frac{M}{t} = 2.3 \times 10^{19} \text{ kg s}^{-1} = 3.7 \times 10^{-4} \text{ M}_\odot \text{ yr}^{-1}.$$

18.16 The gravitational potential energy of a realistic model white dwarf is $U = -5.1 \times 10^{43}$ J. For a nuclear energy production of $E/m = 7.3 \times 10^{13}$ J kg^{-1}, the amount of iron that would have to be produced to cause the star to become gravitationally unbound is

$$m_U = \frac{|U|}{E/m} = 7.0 \times 10^{29} \text{ kg} = 0.35 \text{ M}_\odot.$$

The fusion of this mass of white-dwarf material would supply the ejecta (the entire mass of the star, $M_{\rm wd} = 1.38$ M$_\odot$) with just enough energy to escape the star's gravitational pull. However, if the speed of the ejecta far from the star is $v = 5000$ km s^{-1}, then the ejecta must be supplied with its kinetic energy,

$$K = \frac{1}{2} M_{\rm wd} v^2 = 3.4 \times 10^{43} \text{ J}.$$

The additional iron that would have to be produced is

$$m_K = \frac{K}{E/m} = 4.7 \times 10^{29} \text{ kg} = 0.24 \text{ M}_\odot.$$

The total amount of iron produced is $m_U + m_K = 0.59$ M$_\odot$, a bit less than one-half of the white dwarf's mass.

18.17 After star 1 explodes, the total energy, E_f, of the binary system is given by Eq. (18.34). For an unbound system, $E_f \geq 0$, so

$$\frac{1}{2} M_R v_1^2 + \frac{1}{2} M_2 v_2^2 - G \frac{M_R M_2}{a} \geq 0.$$

Using $v_2/v_1 = M_1/M_2$ (Eq. 7.4) to substitute for v_2, we obtain

$$\frac{1}{2} \left(M_R + \frac{M_1^2}{M_2} \right) v_1^2 - G \frac{M_R M_2}{a} \geq 0. \tag{S18.1}$$

Before star 1 explodes, the total energy, E_i, of the binary system is given by Eq. (18.33),

$$\frac{1}{2} M_1 v_1^2 + \frac{1}{2} M_2 v_2^2 - G \frac{M_R M_2}{a} = -G \frac{M_R M_2}{2a}.$$

Again using $v_2/v_1 = M_1/M_2$ to substitute for v_2, we obtain an expression for v_1^2,

$$v_1^2 = G \frac{M_2^2}{a(M_1 + M_2)}.$$

Substituting this into Eq. (S18.1), we find that for an unbound system,

$$\frac{M_R}{M_1 + M_2} \leq \frac{1}{(2 + M_2/M_1)(1 + M_2/M_1)} < \frac{1}{2},$$

which is Eq. (18.35).

18.18 (a) The Alfvén radius, r_A, is where the kinetic and magnetic energy densities are equal,

$$\frac{1}{2}\rho v^2 = \frac{B^2}{2\mu_0}$$

(Eq. 18.36). We now use Eq. (18.37) [derived in part (a) of Problem 18.13],

$$\rho = \frac{\dot{M}}{4\pi r^2 v},$$

the free-fall velocity $v = \sqrt{2GM/r}$, and the radial dependence of a magnetic dipole (Eq. 18.38),

$$B(r) = B_s \left(\frac{R}{r}\right)^3,$$

to evaluate this. At $r = R_A$,

$$\frac{1}{2}\left(\frac{\dot{M}}{4\pi r_A^2}\right)\sqrt{\frac{2GM}{r_A}} = \frac{1}{2\mu_0}\left[B_s\left(\frac{R}{r_A}\right)^3\right]^2,$$

which, when simplified, produces Eq. (18.39),

$$r_A = \left(\frac{8\pi^2 B_s^4 R^{12}}{\mu_0^2 GM\dot{M}^2}\right)^{1/7}.$$

(b) Taking a time derivative of $L = I\omega$ for a rotating neutron star gives

$$\frac{dL}{dt} = I\frac{d\omega}{dt} = I\frac{d}{dt}\left(\frac{2\pi}{P}\right) = -2\pi I\frac{\dot{P}}{P^2},$$

where I is the moment of inertia of the neutron star and P its rotation period. Near the disruption radius, r_d, angular momentum is transferred to the neutron star. The angular momentum per unit mass of gas parcels orbiting with velocity $v = \sqrt{GM/r_d}$ at the disruption radius is $vr_d = \sqrt{GMr_d}$. If $\dot{M}$ is the rate at which mass arrives at the disruption radius, then the time derivative of the star's angular momentum is

$$\frac{dL}{dt} = \dot{M}vr_d = \dot{M}\sqrt{GMr_d} = -2\pi I\frac{\dot{P}}{P^2}.$$

Solving for $\dot{P}/P$ gives

$$\frac{\dot{P}}{P} = -\frac{P\dot{M}}{2\pi I}\sqrt{GMr_d}.$$

Finally, substituting $r_d = \alpha r_A$ (Eq. 18.40), with the Alfvén radius given by Eq. (18.39), leads to

$$\frac{\dot{P}}{P} = -\frac{P\dot{M}}{2\pi I}\sqrt{GM\alpha}\left(\frac{8\pi^2 B_s^4 R^{12}}{\mu_0^2 GM\dot{M}^2}\right)^{1/14}.$$

When this is simplified, Eq. (18.41) emerges.

18.19 If the Alfvén radius, r_A, is equal to the star's radius, R, then from Eq. (18.39),

$$r_A = R = \left(\frac{8\pi^2 B_s^4 R^{12}}{\mu_0^2 GM\dot{M}^2}\right)^{1/7}.$$

Solving for the surface value of the magnetic field, we find

$$B_s = \left(\frac{\mu_0^2 G M \dot{M}^2}{8\pi^2 R^5} \right)^{1/4}.$$

For the white dwarf in Example 18.2.1, $M = 0.85\ \mathrm{M}_\odot$, $R = 0.0095\ \mathrm{R}_\odot$, and $\dot{M} = 10^{13}\ \mathrm{kg\ s^{-1}}$, so $B_s = 0.366$ T. For the neutron star in that example, $M = 1.4\ \mathrm{M}_\odot$, $R = 10$ km, and $\dot{M} = 10^{14}\ \mathrm{kg\ s^{-1}}$, so $B_s = 4390$ T.

18.20 Using the value of the neutron star's mass-transfer rate in Example 18.2.1 of $\dot{M} = 10^{14}\ \mathrm{kg\ s^{-1}}$, the time to transfer $M = 1\ \mathrm{M}_\odot$ is roughly $t = M/\dot{M} = 2.0 \times 10^{16}\ \mathrm{s} = 6.3 \times 10^8\ \mathrm{yr}$.

18.21 From Eq. (18.24) with an accretion luminosity in X-rays of $L_x = 3.8 \times 10^{29}$ W,

$$\dot{M}_{\mathrm{ns}} = \frac{R L_X}{GM} = 2.0 \times 10^{13}\ \mathrm{kg\ s^{-1}}$$

for a $1.4\ \mathrm{M}_\odot$ neutron star with a radius of 10 km. If its surface magnetic field is 10^8 T, then Eq. (18.41) shows that the neutron star's rotation period of $P = 3.61$ s is decreasing as

$$\left(\frac{\dot{P}}{P} \right)_{\mathrm{ns}} = -\frac{P\sqrt{\alpha}}{2\pi I} \left(\frac{2\sqrt{2}\pi B_s^2 R^6 G^3 M^3 \dot{M}^6}{\mu_0} \right)^{1/7} = -7.0 \times 10^{-5}\ \mathrm{yr^{-1}},$$

using $I = 1.11 \times 10^{38}\ \mathrm{kg\ m^2}$ (Example 18.6.3) and $\alpha = 0.5$ (Eq. 18.40). We now repeat these calculations for a $0.85\ \mathrm{M}_\odot$ white dwarf with a radius of 6.6×10^6 m and a surface magnetic field of 1000 T. For a uniform sphere, $I = 2MR^2/5 = 2.95 \times 10^{43}\ \mathrm{kg\ m^2}$. With $\alpha = 0.5$, we find

$$\dot{M}_{\mathrm{wd}} = \frac{R L_X}{GM} = 2.2 \times 10^{16}\ \mathrm{kg\ s^{-1}}$$

and

$$\left(\frac{\dot{P}}{P} \right)_{\mathrm{wd}} = -\frac{P\sqrt{\alpha}}{2\pi I} \left(\frac{2\sqrt{2}\pi B_s^2 R^6 G^3 M^3 \dot{M}^6}{\mu_0} \right)^{1/7} = -8.3 \times 10^{-7}\ \mathrm{yr^{-1}}.$$

The neutron star model is in better agreement with the observed value of $\dot{P}/P = -3.2 \times 10^{-5}\ \mathrm{yr^{-1}}$.

18.22 (a) Using Eq. (18.24) for the accretion luminosity to replace $\dot{M}$ in Eq. (18.41) gives

$$\frac{\dot{P}}{P} = -\frac{P\sqrt{\alpha}}{2\pi I} \left(\frac{2\sqrt{2}\pi B_s^2 R^{12} L_{\mathrm{acc}}^6}{\mu_0 G^3 M^3} \right)^{1/7}$$

or

$$\log_{10}\left(-\frac{\dot{P}}{P} \right) = \log_{10}\left(P L_{\mathrm{acc}}^{6/7} \right) + \log_{10}\left[\frac{\sqrt{\alpha}}{2\pi I} \left(\frac{2\sqrt{2}\pi B_s^2 R^{12}}{\mu_0 G^3 M^3} \right)^{1/7} \right].$$

(b) We can evaluate the second term on the right using $\alpha = 0.5$ (Eq. 18.40) and values from Example 18.6.3 and the solution to Problem 18.22. For a $1.4\ \mathrm{M}_\odot$ neutron star with a radius of 10 km, moment of inertia $I = 1.11 \times 10^{38}\ \mathrm{kg\ m^2}$, and a surface magnetic field of 10^8 T, it is -43.56. For a $0.85\ \mathrm{M}_\odot$ white dwarf with a radius of 6.6×10^6 m, moment of inertia $I = 2.95 \times 10^{43}\ \mathrm{kg\ m^2}$, and a surface magnetic field of 1000 T, it is -45.49. See Fig. S18.2.

(c) See Fig. S18.2.

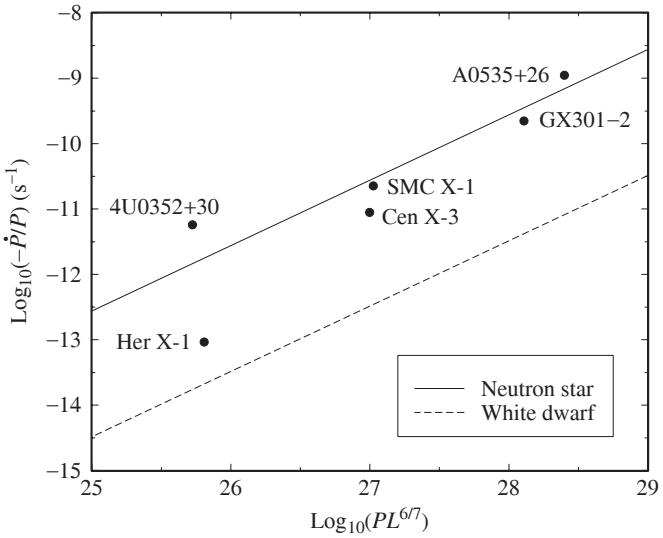

Figure S18.2: Results for Problem 18.23 (b) and (c).

(d) Except for Her X-1, the points in Fig. S18.2 lie along the line for the neutron-star model of a binary X-ray pulsar. According to Rappaport and Joss (1977), for Her X-1 "the value of $\dot{P}/P$ fluctuates and its sign even reverses. These sporadic intervals of spin-down, together with the small average value of $|\dot{P}/P|$, are indicative of a near balance between spinup and spindown for this source. Hence, external torques are probably important for this system."

18.23 (a) The average luminosity of the burster is $L = (10^{32}\ \mathrm{J})/(5\ \mathrm{s}) = 2 \times 10^{31}$ W. Using a blackbody temperature of $T = 2 \times 10^7$ K, the Stefan–Boltzmann equation (Eq. 3.17) yields the radius of the neutron star,

$$R = \frac{1}{T^2}\sqrt{\frac{L}{4\pi\sigma}} = 13.2\ \mathrm{km}.$$

(b) The value of R in part (a) corresponds to R_∞ in Eq. (17.33),

$$R_\infty = \frac{R}{\sqrt{1 - 2GM/Rc^2}},$$

as calculated by an observer on Earth at a great distance from the neutron star. A more accurate value (obtained at the surface of the neutron star) is the value of R found by numerically solving the cubic equation obtained from the preceding expression for R_∞,

$$\left(\frac{R}{R_\infty}\right)^3 - \frac{R}{R_\infty} + \frac{2GM}{R_\infty c^2} = 0.$$

Assuming a 1.4 $\mathrm{M}_\odot$ neutron star, this has the solution $R/R_\infty = 0.772$, or $R = 10.2$ km. [The other positive root of this cubic equation, $R/R_\infty = 0.358$, is too small for a neutron star, and the third root, $R/R_\infty = -1.13$, is unphysical and does not satisfy Eq. (17.33).]

18.24 The SMC X-1 binary pulsar system consists of a neutron star of mass $M_1 = 1.4\ \mathrm{M}_\odot$ and a secondary star that has a mass of $M_2 = 17\ \mathrm{M}_\odot$ and a radius of $R_2 = 16.5\ \mathrm{R}_\odot$. The two stars are separated by $a = 0.107\ \mathrm{AU} = 23.0\ \mathrm{R}_\odot$. From Eq. (7.1),

$$\frac{M_2}{M_1} = \frac{r_1}{r_2} = \frac{a - r_2}{r_2},$$

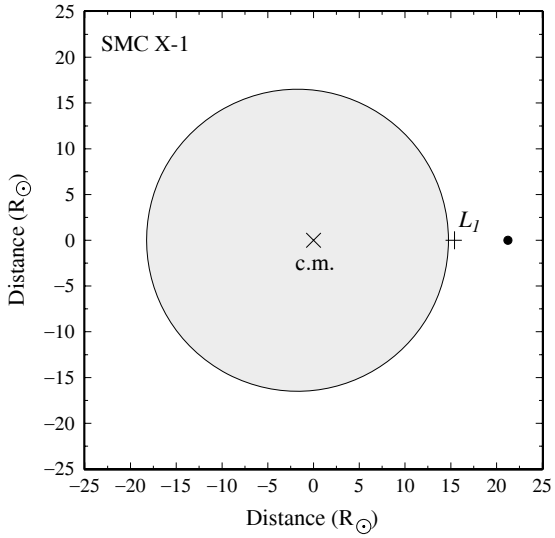

Figure S18.3: Results for Problem 18.25. This scale drawing of the binary pulsar system SMC X-1 shows the center of mass ("×") at the origin and the inner Lagrangian point, L_1 ("+"). The size of the neutron star (right) is greatly exaggerated.

so the distance from the center of the secondary to the center of mass is

$$r_2 = \frac{aM_1}{M_1 + M_2} = 0.0761a = 1.75\ \mathrm{R}_\odot.$$

Equation (18.10) shows that the distance from the center of the secondary to the inner Lagrangian point, L_1, is

$$\ell_2 = a\left[0.500 + 0.227 \log_{10}\left(\frac{M_2}{M_1}\right)\right] = 0.746a = 17.2\ \mathrm{R}_\odot.$$

Figure S18.3 shows a scale drawing of the SMC X-1 system.

18.25 Equation (4.32) for the relativistic Doppler shift with $\theta = 90°$ for motion perpendicular to the line of sight is

$$\frac{\nu_{\mathrm{obs}}}{\nu_{\mathrm{rest}}} = \sqrt{1 - u^2/c^2}.$$

For SS 433, $u/c = 0.26$ and so the $\nu_{\mathrm{obs}}/\nu_{\mathrm{rest}} = 0.9656$ for this transverse Doppler shift. If this is wrongly interpreted as a Doppler shift due to motion along the line of sight, then the radial velocity attributed to the source would be, from Eq. (4.33),

$$\frac{v_r}{c} = \frac{1 - (\nu_{\mathrm{obs}}/\nu_{\mathrm{rest}})^2}{1 + (\nu_{\mathrm{obs}}/\nu_{\mathrm{rest}})^2} = 0.03498.$$

This corresponds to $v_r = 10{,}490$ km s^{-1}, in agreement with the value obtained from the crossing of the radial-velocity curves of SS 433.

18.26 SS 433 is $r = 5.5$ kpc from Earth, and the X-ray emitting regions extend as much as $\theta = 44' = 0.0128$ rad from SS 433. This corresponds to a separation of $s = r\theta = 2.17 \times 10^{18}$ m. With a jet velocity of $v = 0.26c$, it would take the jets $t = s/v = 2.79 \times 10^{10}$ s $= 883$ yr to travel to the edge of the X-ray emitting regions. The jets must have slowed as they penetrated the gases of the supernova remnant W50, so this may be taken as a lower limit for the amount of time the jets have been active.

18.27 Using

$$t = \frac{P}{2\dot{P}}$$

from Problem 16.22 with $P = 6.133$ ms and $\dot{P} = 3\times10^{-20}$, the age of PSR 1953+29 is $t = 1.02\times10^{17}$ s $= 3.24\times10^{9}$ yr. Adopting 1.4 $M_\odot$ and 10 km for the mass and radius of the neutron star, its moment of inertia is $I = 2MR^2/5 = 1.11\times10^{38}$ kg m^2. The magnetic field at the pole of the neutron star comes from Eq. (16.33) with $\theta = 90°$,

$$B = \frac{1}{2\pi R^3 \sin\theta}\sqrt{\frac{3\mu_0 c^3 I P \dot{P}}{2\pi}} = 9.16\times10^{4}\ \text{T}.$$

Such a small magnetic field (compared with $\sim 10^8$ T for longer-period pulsars) distinguishes the millisecond pulsars.

18.28 Equation (18.41) may be written as

$$\frac{\dot{P}}{P^2} = -K,$$

where

$$K = \frac{\sqrt{\alpha}}{2\pi I}\left(\frac{2\sqrt{2}\pi B_s^2 R^6 G^3 M^3 \dot{M}^6}{\mu_0}\right)^{1/7}.$$

Adopting $M = 1.4\,M_\odot$, $R = 10^6$ km, $I = 2MR^2/5 = 1.11\times10^{38}$ kg m^2, $\dot{M} = 10^{14}$ kg s^{-1}, $B_s = 10^4$ T, and $\alpha = 0.5$ (Eq. 18.40) results in $K = 1.75\times10^{-13}$ s^{-2}. We now integrate from an initial period, P_i, at $t = 0$ to a final period, P_f, at some final time t:

$$\int_{P_i}^{P_f}\frac{dP}{P^2} = -\int_0^t K\,dt',$$

so the spin-up time is

$$t = \frac{1}{K}\left(\frac{1}{P_f} - \frac{1}{P_i}\right).$$

For $P_i = 100\,s$ and $P_f = 1$ ms, $t = 5.72\times10^{15}$ s $= 1.81\times10^{8}$ yr. Assuming a constant value of $\dot{M}$, the total mass transferred is $M = \dot{M}t = 5.72\times10^{29}$ kg $= 0.288\,M_\odot$.

18.29 The semimajor axes and orbital periods of the planets orbiting the pulsar PSR 1257+12 are $a_1 = 0.19$ AU, $P_1 = 25.34$ d; $a_2 = 0.36$ AU, $P_2 = 66.54$ d; and $a_3 = 0.47$ AU, $P_3 = 98.22$ d. According to Kepler's third law, Eq. (2.37), $P^2/a^3 =$ constant. In the units given,

$$P_1^2/a_1^3 = 9.36\times10^{4}\ \text{d}^2\ \text{AU}^{-3}$$

$$P_2^2/a_2^3 = 9.49\times10^{4}\ \text{d}^2\ \text{AU}^{-3}$$

$$P_3^2/a_3^3 = 9.29\times10^{4}\ \text{d}^2\ \text{AU}^{-3}$$

To the precision of the values of a and P, these three planets obey Kepler's third law.

18.30 (a) The masses of the two neutron stars in the binary Hulse–Taylor pulsar PSR 1913+16 are $M_1 = 1.4414\,M_\odot$ and $M_2 = 1.3867\,M_\odot$. For an orbital period of $P = 27907$ s, Kepler's third law (Eq. 2.37) gives the semimajor axis of the orbit as

$$a = \left[\frac{G(M_1 + M_2)P^2}{4\pi^2}\right]^{1/3} = 1.949\times10^{9}\ \text{m}.$$

(b) Taking a time derivative of Kepler's third law in the form of $P^2 = Ka^3$, where K is a constant, results in

$$2P\frac{dP}{dt} = 3Ka^2\frac{da}{dt}.$$

Dividing by the third law and using $\dot{P} = -2.4056 \times 10^{-12}$ for the time derivative of the orbital period produces

$$\frac{da}{dt} = \frac{2a\dot{P}}{3P} = -1.120 \times 10^{-7}\ \text{m s}^{-1}.$$

During one orbit, the semimajor axis changes by

$$\Delta a = P\frac{da}{dt} = -3.12\ \text{mm}.$$

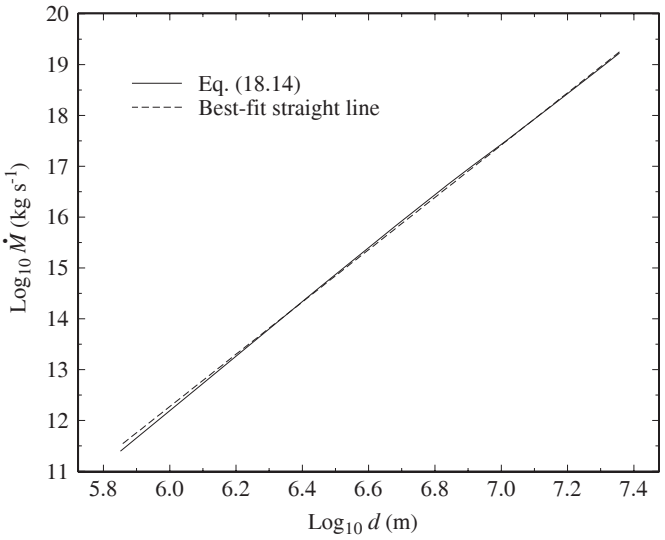

Figure S18.4: Results for Problem 18.32.

18.31 (a) See Fig. S18.4. The slope of the best-fitting straight line is 5.14, so $\dot{M} \propto d^{5.14}$ for this simple model.

(b) The ideal gas law (Eq. 10.11) states that $\rho \propto P/T$. Combining this with Eq. (18.14) for the mass-transfer rate,

$$\dot{M} \approx \pi R d\rho\sqrt{\frac{3kT}{m_H}},$$

shows that $\dot{M} \propto Pd/\sqrt{T}$. From Eq. (L.1), the pressure near the surface of a star depends on the temperature as $P \propto T^{4.25}$, so $\dot{M} \propto T^{3.75}d$. Finally, according to Eq. (L.2), the temperature near the surface is

$$T = GM\left(\frac{\mu m_H}{4.25k}\right)\left(\frac{1}{r} - \frac{1}{R}\right) = GM\left(\frac{\mu m_H}{4.25k}\right)\left(\frac{R-r}{rR}\right),$$

where M is the star's mass and R is its radius. If the overlap distance is $d \equiv R - r$, with $d \ll R$, we have $(R-r)/rR \simeq d/R^2$, and so $T \propto d$ near the surface. The result is that $\dot{M} \propto d^{4.75}$.

18.32 The Schwarzschild radius of a black hole of mass 3.82 $M_\odot$ black hole is (Eq. 17.27) $R_S = 2GM/c^2 =$ 11.3 km. The inner edge of the disk is at $r/R_S = 3$. To find the outer edge of the disk, we first use Kepler's

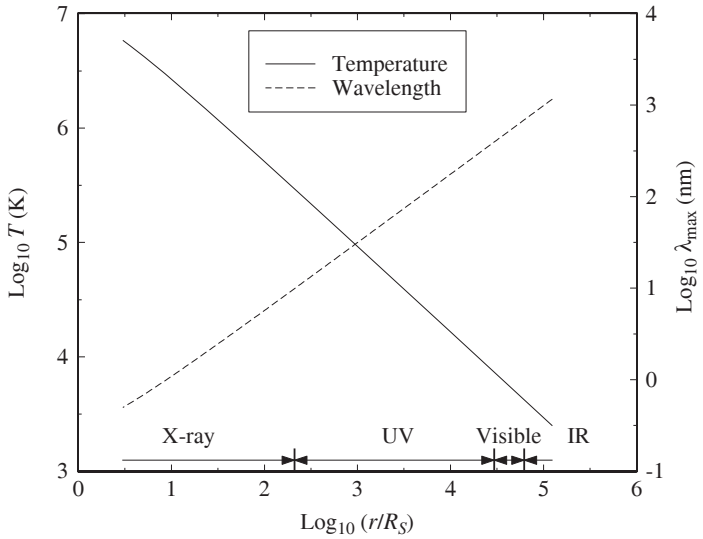

Figure S18.5: Results for Problem 18.33.

third law (Eq. 2.37) to determine the semimajor axis,

$$a = \left[\frac{G(M_1 + M_2)P^2}{4\pi^2}\right]^{1/3} = 2.22 \times 10^9 \text{ m},$$

where $P = 0.3226$ d, $M_1 = 3.82\ M_\odot$, and $M_2 = 0.36\ M_\odot$. Equations (18.25) and (18.26) then locate the outer edge of the disk at

$$R_{\text{disk}} \approx 2a\left[0.500 - 0.227 \log_{10}\left(\frac{M_2}{M_1}\right)\right]^4 \left(1 + \frac{M_2}{M_1}\right)$$
$$= 1.40 \times 10^9 \text{ m} = 1.24 \times 10^5 R_S.$$

The disk temperature, $T(r)$, comes from Eq. (18.19) in the form

$$T(r) = \left(\frac{3GM_1\dot{M}}{8\pi\sigma R_S^3}\right)^{1/4} \left(\frac{R_S}{r}\right)^{3/4} \left(1 - \sqrt{R_S/r}\right)^{1/4},$$

where $\dot{M} = 10^{14}$ kg s^{-1} and r varies from $3R_S$ to R_{disk}. The peak wavelength, $\lambda_{\text{max}}(r)$, is obtained from Wien's law, Eq. (3.15). Figure S18.5 shows the resulting graphs of $\log_{10} T$ and $\log_{10} \lambda_{\text{max}}$ (λ_{max} in nm). The regions of the disk that emit X-rays, ultraviolet, visible, and infrared radiation are indicated.

CHAPTER 19

Physical Processes in the Solar System

19.1 (a) The masses are (in terms of the mass of Mercury):

$$M_{\text{Moon}} = 0.223\,M_{\text{Mercury}}$$
$$M_{\text{Io}} = 0.270\,M_{\text{Mercury}}$$
$$M_{\text{Europa}} = 0.148\,M_{\text{Mercury}}$$
$$M_{\text{Ganymede}} = 0.452\,M_{\text{Mercury}}$$
$$M_{\text{Callisto}} = 0.327\,M_{\text{Mercury}}$$
$$M_{\text{Titan}} = 0.409\,M_{\text{Mercury}}$$
$$M_{\text{Triton}} = 0.065\,M_{\text{Mercury}}$$
$$M_{\text{Pluto}} = 0.040\,M_{\text{Mercury}}$$

(b) The radii are (in terms of the radius of Mercury):

$$R_{\text{Moon}} = 0.712\,R_{\text{Mercury}}$$
$$R_{\text{Io}} = 0.744\,R_{\text{Mercury}}$$
$$R_{\text{Europa}} = 0.643\,R_{\text{Mercury}}$$
$$R_{\text{Ganymede}} = 1.078\,R_{\text{Mercury}}$$
$$R_{\text{Callisto}} = 0.984\,R_{\text{Mercury}}$$
$$R_{\text{Titan}} = 1.055\,R_{\text{Mercury}}$$
$$R_{\text{Triton}} = 0.555\,R_{\text{Mercury}}$$
$$R_{\text{Pluto}} = 0.460\,R_{\text{Mercury}}$$

19.2 (a) See Fig. S19.1.

(b) See Fig. S19.1. Using a least-squares fit to the data, $\log_{10} A = 0.2333068$ (or $A = 1.71$) and $\log_{10} r_0 = -0.670528$ (or $r_0 = 0.214$).

(c) See Table S19.1.

19.3 (a) See Fig. S19.2.

(b) See Fig. S19.2. Using a least-squares fit to the data, $\log_{10} A = 0.21506$ (or $A = 1.6408$) and $\log_{10} r_0 = 0.5476$ (or $r_0 = 3.5286$).

(c) See Table S19.2.

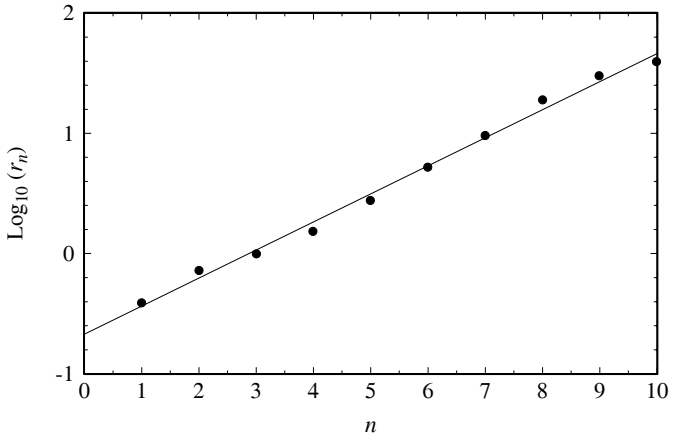

Figure S19.1: The least-squares fit to data for Problem 19.2.

Table S19.1: The results of Problem 19.2(c).

Object	n	r_n (AU)	$\log_{10} r_n$	$\Delta r/r$ (%)
Mercury	1	0.39	−0.412	−5.579
Venus	2	0.72	−0.141	−13.514
Earth	3	1.00	0.000	7.002
Mars	4	1.52	0.183	20.147
Ceres	5	2.77	0.442	13.117
Jupiter	6	5.20	0.716	3.053
Saturn	7	9.54	0.980	−3.914
Uranus	8	19.19	1.283	−18.182
Neptune	9	30.06	1.478	−10.619
Pluto	10	39.53	1.597	16.309

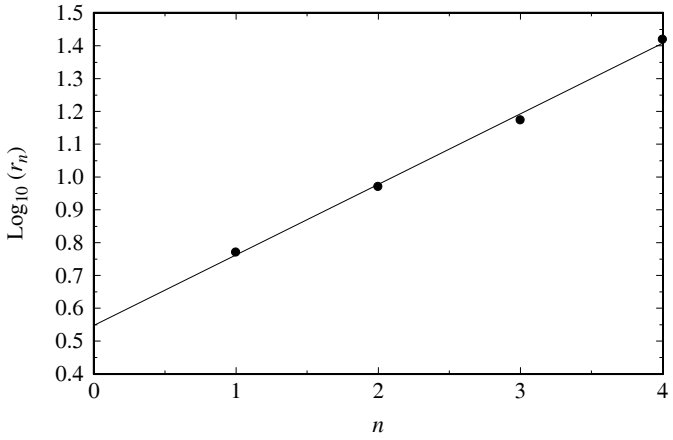

Figure S19.2: The least-squares fit to data for Problem 19.3.

Table S19.2: The results of Problem 19.3(c).

Moon	n	$r_n\ (R_J)$	$\log_{10} r_n$	$\Delta r/r\ (\%)$
Io	1	5.91	0.772	−1.985
Europa	2	9.40	0.973	1.063
Ganymede	3	14.99	1.176	3.973
Callisto	4	26.34	1.421	2.906

19.4 Using the small-angle relations $\cos\phi \simeq 1$ and $\sin\phi \simeq R\sin\theta/r$, and substituting into Eq. (19.2), produces the x and y components of the differential force as

$$\begin{aligned}\Delta F_x &\simeq \frac{GMm}{r^2}\left[\frac{2R}{r}\cos\theta\right]\\ \Delta F_y &\simeq -\frac{GMm}{r^2}\left[1+\frac{2R}{r}\cos\theta\right]\left(\frac{R\sin\theta}{r}\right)\\ &\simeq -\frac{GMmR}{r^3}\sin\theta\end{aligned}$$

where the last approximation is because $R \ll r$.

19.5 (a) Angular momentum is given by $L_{\rm rot} = I\omega_{\rm rot}$. Assuming constant I,

$$\frac{dL_{\rm rot}}{dt} = I\frac{d\omega_{\rm rot}}{dt} = I\frac{d(2\pi/P_{\rm rot})}{dt} = -\frac{2\pi I}{P_{\rm rot}^2}\dot{P}_{\rm rot}.$$

For Earth (assuming constant density),

$$\begin{aligned}I &= \frac{2}{5}M_\oplus R_\oplus^2 = 9.7\times10^{37}\ \text{kg m}^2\\ P_{\rm rot} &= 86{,}164\ \text{s}\\ \dot{P}_{\rm rot} &= 0.0016\ \text{s century}^{-1} = 5.070\times10^{-13}\ \text{s s}^{-1}.\end{aligned}$$

Note that $\dot{P}_{\rm rot} > 0$ (the period is lengthening). Combining

$$\frac{dL_{\rm rot}}{dt} = -4.16\times10^{16}\ \text{kg m}^2\ \text{s}^{-2} < 0.$$

(b) Treating the Moon as an orbiting point mass, and assuming a circular orbit, $L_{\rm orbit} = M_m v r = 2\pi M_m r^2/P_{\rm orbit}$. Assuming constant M_m, this leads to

$$\begin{aligned}\frac{dL_{\rm orbit}}{dt} &= \frac{d\left(2\pi M_m r^2/P_{\rm orbit}\right)}{dt}\\ &= \frac{4\pi M_m r}{P_{\rm orbit}}\frac{dr}{dt} - \frac{2\pi M_m r^2}{P_{\rm orbit}^2}\frac{dP_{\rm orbit}}{dt}.\end{aligned}$$

From Kepler's third law, $P_{\rm orbit}^2 = 4\pi^2 r^3/G\,(M_\oplus + M_m)$, where $r = a$,

$$\frac{dP_{\rm orbit}}{dt} = \frac{6\pi^2 r^2}{G\,(M_\oplus + M_m)\,P_{\rm orbit}}\frac{dr}{dt}.$$

From the text, $dr/dt \sim 3.5$ cm yr^{-1} $= 1.1 \times 10^{-9}$ m s^{-1}. Substituting, $dP_{\rm orbit}/dt = 1.0 \times 10^{-11}$ s s^{-1}, and

$$\frac{dL_{\rm orbit}}{dt} = 1.6 \times 10^{17}\ {\rm kg\ m^2\ s^{-2}} - 4.0 \times 10^{16}\ {\rm kg\ m^2\ s^{-2}} = 1.2 \times 10^{17}\ {\rm kg\ m^2\ s^{-2}} > 0.$$

(c) The crude estimates of the change in angular momentum of Earth and the Moon are roghly consistent with a total change of zero for the system.

19.6 (a) Earth's spin is decreasing at a rate of 0.0016 s century^{-1} $= 1.92 \times 10^{-10}$ d yr^{-1}. If this rate were to remain constant, then the length of the day would reach 47 days when

$$47\ {\rm d} = 1\ {\rm d} + \left(1.92 \times 10^{-10}\ {\rm d\ yr^{-1}}\right) \Delta t.$$

Solving for the time interval gives $\Delta t = 2.4 \times 10^{11}$ yr.

(b) Since the entire main-sequence lifetime of the Sun is on the order of 10^{10} yr, Earth will likely not become fully synchronized before the Sun becomes a red giant star.

19.7 (a) Substituting $P = 47$ d and $M_\oplus + M_{\rm Moon} = 6.05 \times 10^{24}$ kg into Kepler's third law (Eq. 2.37) results in $a = 5.5 \times 10^8$ m.

(b) The radius of the Moon is $R_{\rm Moon} = 1.74 \times 10^6$ m. Thus, its angular diameter would be $\theta = 2R_{\rm Moon}/a = 0.0063$ rad $= 0.36°$.

(c) For comparison, the Sun's angular diameter is $\theta_\odot = 2R_\odot/1$ AU $= 0.53°$. Since the angular diameter of the Moon would only by 68% of this value, the Moon would not completely cover the solar disk, and a total eclipse would not be possible.

19.8 (a) Let r_{EM} and r_{ES} be the distances from Earth to the Moon and the Sun, respectively. Then, considering the x-component of the tidal force given in Eq. (19.3) for a given value of θ, the ratio of the tidal forces is

$$\frac{\Delta F_M}{F_\odot} = \frac{M_M/R_{EM}^3}{M_\odot/R_{ES}^3} = \left(\frac{M_M}{M_\odot}\right)\left(\frac{r_{ES}}{r_{EM}}\right)^3 = 2.2.$$

(b) Since, for spring tides, the Sun and the Moon are both along nearly the same line relative to Earth's center (either aligned or anti-aligned), the tidal force contributions are additive. At neap tide, The Sun, Earth's center, and the Moon form a right angle and the differential force vectors are perpendicular, so that each body partially negates the effect of the other.

19.9 Near the poles $\theta = \pm 90°$, the differential tidal force goes to zero in the direction parallel to the Earth-Moon axis (e.g., Eq. 19.3). The component of the tidal force perpendicular to the axis is directed toward the center of the planet.

19.10 Using $\overline{\rho}_p = 3933$ kg m^{-3}, $\overline{\rho}_m = 2000$ kg m^{-3}, $R_p = 0.533\ {\rm R}_\oplus = 3.4 \times 10^6$ m, and $f_R = 2.456$, Eq. (19.4) gives $r < 1.05 \times 10^7$ m.

Phobos is currently orbiting at essentially the Roche limit for the Mars–Phobos system. As Phobos continues to spiral in toward Mars it will likely become disrupted in the future.

19.11 An artificial satellite has a significant amount of structural integrity beyond internal gravitational effects.

19.12 Rotation implies an additional term that self-gravity must overcome. Therefore, for disruption to occur,

$$\frac{2GM_pR_m}{r^3} + \omega^2 R_m > \frac{GM_m{}^2}{R_m}.$$

If the moon is in synchronous rotation, its rotation period is equal to its orbital period, or from Kepler's law (Eq. 2.37),

$$P^2 = \frac{4\pi^2}{G\left(M_p + M_m\right)} r^3.$$

Since $\omega = 2\pi/P$,

$$\omega^2 = \frac{G\left(M_p + M_m\right)}{r^3}.$$

Substituting,

$$\frac{2GM_p R_m}{r^3} + \frac{G\left(M_p + M_m\right) R_m}{r^3} > \frac{GM_m}{R_m^2}$$

$$\frac{GM_p R_m}{r^3}\left[2 + \left(1 + \frac{M_m}{M_p}\right)\right] > \frac{GM_m}{R_m^2}$$

Solving for r^3,

$$r^3 < \frac{M_p/R_p^3}{M_m/R_m^3}\left[3 + \frac{M_m}{M_p}\right] R_p^3.$$

Since for a spherical body,

$$\overline{\rho} = \frac{M}{\frac{4\pi}{3} R^3},$$

we find that

$$r < \left(\frac{\overline{\rho}_p}{\overline{\rho}_m}\right)^{1/3}\left[3 + \frac{M_m}{M_p}\right]^{1/3} R_p,$$

or

$$r < f_R\left(\frac{\overline{\rho}_p}{\overline{\rho}_m}\right)^{1/3} R_p$$

where

$$f_R \equiv \left[3 + \frac{M_m}{M_p}\right]^{1/3}.$$

If $M_m/M_p \ll 1$, then $f_R \simeq 3^{1/3} = 1.44$.

19.13 (a) According to the Stefan–Boltzmann law (Eq. 3.17), the luminosity of the Sun is $L_\odot = 4\pi R_\odot^2 \sigma T_\odot^4$. At the radius of the planet's orbit, the amount of solar energy received per second is

$$P_{\text{in}} = L_\odot(1 - a)\left(\frac{\pi R_p^2}{4\pi D^2}\right),$$

where a is the planet's albedo, πR_p^2 is its cross-sectional area as seen by the Sun, and $4\pi D^2$ is the surface area of a sphere of radius D centered on the Sun. Assuming that the planet radiates as a spherical blackbody, its luminosity is given by

$$P_{\text{out}} = 4\pi R_p^2 \sigma T_p^4.$$

If the planet is in thermodynamic equilibrium, then $P_{\text{in}} = P_{\text{out}}$. Solving for T_p leads to Eq. (19.5).

(b) The energy radiated into space from the top of the greenhouse gas layer is $P_{\text{out}} = 4\pi R_\oplus^2 \sigma T_\oplus^4$. However, if the temperature of the layer is to remain constant, the energy per second radiated into the layer from Earth's surface minus the energy per second radiated out of the layer toward Earth must give P_{out}, or

$$4\pi R_\oplus^2 \sigma T_\oplus^4 = 4\pi R_\oplus^2 \sigma T_{\text{surf}}^4 - 4\pi R_\oplus^2 \sigma T_\oplus^4.$$

Solving, $T_{\text{surf}} = 2^{1/4} T_\oplus$. From the result of Example 19.3.1, $T_\oplus = 255$ K, which gives $T_{\text{surf}} = 303$ K $= 30°$C. This temperature is just slightly higher than the average temperature of Earth's surface; good agreement given the crude nature of the calculation.

19.14 Using $M_p = M_\oplus$, $R_p = R_\oplus$, and $m = m_H$, $T_{\text{esc}} > 140$ K. Thus, the surface temperature of Earth is well above the value needed for atomic hydrogen to escape.

19.15 (a) For Jupiter, $a = 0.343$ and $D = 5.2$ AU. Thus, according to Eq. (19.5), $T_J \simeq 110$ K.

(b) Given $M_J = 317.83\ M_\oplus$ and $R_J = 11.21\ R_\oplus$ for Jupiter, and $m = 2m_H$ for molecular hydrogen, $T_{\text{esc}} > 7950$ K.

(c) Since $T_{\text{esc}} \gg T_J$, molecular hydrogen has not had time to escape the atmosphere of Jupiter. Furthermore, since the primary constituent of the solar nebula was molecular hydrogen, Jupiter should be composed primarily of hydrogen.

19.16 Eq. (19.8) is

$$\dot{N} = \frac{n\pi R^2}{4}\left(\frac{m}{2\pi kT}\right)^{3/2} \int_{v_{\text{esc}}}^{\infty} 4\pi v^3 e^{-mv^2/2kT}\, dv.$$

The formula for integration by parts is

$$\int u\, dw = uw - \int w\, du.$$

Letting $u \equiv v^2$ and $dw = ve^{-mv^2/2kT}\, dv$, imply that $du = 2v\, dv$ and

$$w = \int v\, e^{-mv^2/2kT}\, dv$$

$$= -\frac{kT}{m} e^{-mv^2/2kT}.$$

Substituting into the integration-by-parts formula,

$$\dot{N} = \frac{n\pi R^2}{4}\left(\frac{m}{2\pi kT}\right)^{3/2} 4\pi \left[-\frac{kTv^2}{m} e^{-mv^2/2kT}\Big|_{v_{\text{esc}}}^{\infty} + \frac{2kT}{m}\int_{v_{\text{esc}}}^{\infty} v\, e^{-mv^2/2kT}\, dv\right]$$

$$= \frac{n\pi R^2}{4}\left(\frac{m}{2\pi kT}\right)^{3/2} 4\pi \left[\frac{kTv_{\text{esc}}^2}{m} e^{-mv_{\text{esc}}^2/2kT} + \frac{2k^2T^2}{m^2} e^{-mv_{\text{esc}}^2/2kT}\right]$$

$$= n\pi^2 R^2 \left(\frac{m}{2\pi kT}\right)^{3/2} \left(\frac{kT}{m}\right)\left(v_{\text{esc}}^2 + \frac{2kT}{m}\right) e^{-mv_{\text{esc}}^2/2kT}$$

$$= \frac{n\pi}{2}\left(\frac{m}{2\pi kT}\right)^{1/2} R^2 \left(v_{\text{esc}}^2 + \frac{2kT}{m}\right) e^{-mv_{\text{esc}}^2/2kT}$$

$$= 4\pi R^2 \nu n(z),$$

where

$$\nu \equiv \frac{1}{8}\left(\frac{m}{2\pi kT}\right)^{1/2} \left(v_{\text{esc}}^2 + \frac{2kT}{m}\right) e^{-mv_{\text{esc}}^2/2kT}.$$

19.17 Approximately 78% of Earth's atmosphere is N_2 and 21% is O_2. Assuming for simplicity that the remainder (roughly 1%) is water,

$$\rho_{\text{air}} = 0.78 n_t m_{N_2} + 0.21 n_t m_{O_2} + 0.01 n_t m_{H_2O},$$

where n_t is the total number density of all air molecules. Taking $\rho_{\text{air}} = 1.3$ kg m, $m_{N_2} \simeq 28$ u, $m_{O_2} \simeq 32$ u, and $m_{H_2O} \simeq 18$ u, we find $n_t = 2.7 \times 10^{25}$ m^{-3}. Thus, $n_{N_2} = 0.78 n_t = 2.1 \times 10^{25}$ m^{-3}.

19.18 According to Eq. (9.12), $\ell = 1/n\sigma$. Assuming that the separation between atoms in a diatomic molecule is roughly $d = 0.2$ nm, the cross section of a diatomic molecule is (very roughly) $\sigma = \pi(d/2)^2 = 3\times10^{-20}$ m^2. Taking $\ell = 500$ km, we find $n = 1/\ell\sigma \sim 6 \times 10^{13}$ m^{-3}. This is slightly more than two orders of magnitude greater than the value quoted for N_2 in Example 19.3.3. Note that in our estimate here we only calculated collisions of particles without distinguishing between species. The difference can be explained in part by gravitational separation.

19.19 (a) Using $v_{\text{esc}} = 11.7$ km s^{-1}, $m_H = 1.67 \times 10^{-27}$ kg, and $T = 1000$ K, Eq. (19.9) gives $\nu = 1.24$ m s^{-1}.

(b) From Problem 19.18, $n \sim 6 \times 10^{13}$ m^{-3}.

(c) From Eq. (19.8), $\dot{N} = 4\pi R_\odot^2 \nu n = 4 \times 10^{28}$ s^{-1}.

(d) Taking $N_0 = 9 \times 10^{43}$ (see Example 19.3.3), $t \sim N_0/\dot{N} = 2 \times 10^{15}$ s $= 7 \times 10^7$ yr. Since the age of Earth is 4.6×10^9 yr, the hydrogen atmosphere would have leaked off by now.

19.20 Taking the logarithm of Eq. (19.9),

$$\log_{10} \nu = -\log_{10} 8 + \frac{1}{2}\log_{10}\left(\frac{m}{2\pi kT}\right) + \log_{10}\left(v_{\text{esc}}^2 + \frac{2kT}{m}\right) - \frac{m v_{\text{esc}}^2}{2kT}\log_{10} e.$$

For Jupiter, Eq. (2.17) gives $v_{\text{esc}} = \sqrt{2GM_J/R_J} = 59.7$ km s^{-1}. Furthermore, using $m = m_H$ and $T = 1000$ K gives $\log_{10}\nu = -10.9$. Thus $\nu = 10^{-10.9}$ m s^{-1} $= 1.3 \times 10^{-11}$ m s^{-1}.

19.21 (a) The initial eastward velocity of a projectile launched straight south from the North Pole is zero. Thus it gets "left behind" as observers at lower latitudes move with the planet's rotation. This makes the motion of the projectile appear to drift to the right as viewed from the launch point (i.e., westward drift).

(b) As a particle "falls" into a low pressure region, it's motion deflects to the right if it is moving either northward or southward. This sets up a counterclockwise rotation about the center of the low pressure region in the Northern Hemisphere (a consequence of the Coriolis effect).

(c) clockwise

19.22 (a) At some latitutde L, $\boldsymbol{\omega} = \omega\left(\cos L\hat{\mathbf{j}} + \sin L\hat{\mathbf{k}}\right)$. The Coriolis force is then

$$\begin{aligned}
\mathbf{F}_c &= -2m\boldsymbol{\omega} \times \boldsymbol{v} \\
&= -2m\omega\left[\left(\cos L\hat{\mathbf{j}} + \sin L\hat{\mathbf{k}}\right) \times \left(v_x\hat{\mathbf{i}} + v_y\hat{\mathbf{j}} + v_z\hat{\mathbf{k}}\right)\right] \\
&= -2m\omega\left[\left(v_z\cos L - v_y \sin L\right)\hat{\mathbf{i}} + v_x \sin L\hat{\mathbf{j}} - v_x\cos L\hat{\mathbf{k}}\right].
\end{aligned}$$

(b) $\omega_\oplus = 2\pi/P_\oplus = 7.29 \times 10^{-5}$ rad s^{-1}.

(c) If $\mathbf{v} = v_x\hat{\mathbf{i}}$ at a latitude of $L = 40°$, where $v_x = 30$ m s^{-1}, then

$$\begin{aligned}
\mathbf{a} = \mathbf{F}_c/m &= -2\omega\left[v_x \sin L\hat{\mathbf{j}} - v_x\cos L\hat{\mathbf{k}}\right] \\
&= -\left(2.8 \text{ mm s}^{-2}\right)\hat{\mathbf{j}} + \left(3.3 \text{ mm s}^{-2}\right)\hat{\mathbf{k}}.
\end{aligned}$$

The ball is deflected southward and upward (neglecting gravity of course!).

(d) If $\mathbf{v} = v_y\hat{\mathbf{j}}$, where $v_y = 30$ m s^{-1},

$$\mathbf{a} = 2\omega v_y \sin L\hat{\mathbf{i}} = \left(2.8 \text{ mm s}^{-2}\right)\hat{\mathbf{i}}$$

The ball is deflected eastward.

(e) If $\mathbf{v} = v_z\hat{\mathbf{k}}$, where $v_z = 30$ m s^{-1},

$$\mathbf{a} = -2\omega v_z \cos L\hat{\mathbf{i}} = -\left(3.3 \text{ mm s}^{-2}\right)\hat{\mathbf{i}}.$$

The ball is deflected westward. This is because during the time the ball is in the air, Earth has rotated under it.

CHAPTER 20

The Terrestrial Planets

20.1 To find the velocities of the approaching and receding limbs of the planets, we need their rotation periods and radii: $P_{\text{Mercury}} = 58.65\ \text{d} = 5.067 \times 10^6\ \text{s}$, $P_{\text{Venus}} = 243.02\ \text{d} = 2.100 \times 10^7\ \text{s}$, $R_{\text{Mercury}} = 0.383\ \text{R}_\oplus = 2.440 \times 10^6\ \text{m}$, and $R_{\text{Venus}} = 6.052 \times 10^6\ \text{m}$. These values imply that $v_{\text{Mercury}} = 2\pi R/P = 3.026\ \text{m s}^{-1}$ and $v_{\text{Venus}} = 1.811\ \text{m s}^{-1}$. Thus, given the opposite signs for the velocities of the receding and approaching limbs,

$$\left(\frac{\Delta v}{c}\right)_{\text{Mercury}} = \frac{2v}{c} = 1.9 \times 10^{-8}$$

$$\left(\frac{\Delta v}{c}\right)_{\text{Venus}} = \frac{2v}{c} = 1.2 \times 10^{-8}.$$

20.2 The component of the differential force per unit mass lying along the line connecting the centers of mass of the Sun and the planet is (see Eq. 19.3)

$$\left|\frac{\Delta F}{m}\right| = \frac{2GM_\odot R}{r^3}.$$

From Eq. (2.5) and the data in Appendix C, $r_{p,\text{Mercury}} = a(1-e) = 4.60 \times 10^{10}\ \text{m}$ and $r_{p,\text{Earth}} = 1.47 \times 10^{11}\ \text{m}$. These values, combined with the planets' radii give

$$\frac{[\Delta F/m]_{\text{Mercury}}}{[\Delta F/m]_{\text{Earth}}} = 12.5.$$

The significantly greater tidal force per unit mass on Mercury relative to Earth has resulted in Mercury's current 3-to-2 spin-orbit coupling.

20.3 (a) The amount of solar energy absorbed per second by a surface of area A at a point on the planet at the latitude θ is

$$L_{\text{in}} = \left(\frac{L_\odot}{4\pi D^2}\right)(A\cos\theta)\,(1-a)\,.$$

At equilibrium, this value must equal the amount of energy radiated per second by that surface, $L_{\text{out}} = A\sigma T^4$. Equating and solving for the temperature gives the desired result.

(b) See Fig. S20.1. (Note that there was an error in the first printing of the text, the albedo should be 0.119, as in Appendix C.)

(c) $T(\theta = 0) = 614\ \text{K}$.

(d) $\theta = 87.8°$.

(e) The effect of sublimation should diminish the amount of ice found on the surface.

20.4 (a) From Eq. (6.6), the Rayleigh criterion is

$$\theta_{\text{radar}} = 1.22\frac{\lambda}{D} = 6.1 \times 10^{-4}\ \text{rad}.$$

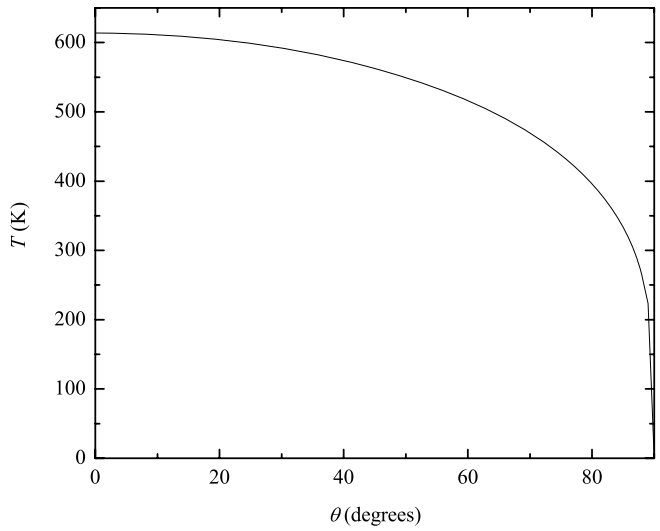

Figure S20.1: Results of Problem 20.3 for the approximate temperature on Mercury's surface as a function of latitude.

(b) The angular size of Mercury is

$$\theta_{\text{Mercury}} = \frac{2R_{\text{Mercury}}}{1\text{ AU} - a_{\text{Mercury}}} = 5.3 \times 10^{-5}\text{ rad.}$$

(c) The fraction of the original signal striking the surface of Mercury was about

$$f = \frac{\theta^2_{\text{Mercury}}}{\theta^2_{\text{radar}}} = 0.0076.$$

This implies a total amount of power received by Mercury of $P_{\text{Mercury}} = fP_{\text{radar}} = (0.0076)(500\,\text{kW}) = 3.8$ kW.

(d) Assuming that Mercury acted like a point source radiating energy back into the hemisphere facing Earth, the flux received at Earth is $F = fP_{\text{radar}}/2\pi(1\text{ AU} - 0.3871\text{ AU})^2$. This gives $F = 4.4 \times 10^{-20}$ W m^{-2}.

20.5 (a) It is estimated that the impactor had a mass approximately one-fifth of Mercury's present mass and a velocity of about 20 km s^{-1}. Using these values $K = \frac{1}{2}mv^2 = 6.6 \times 10^{31}$ J.

(b) Assume that the extra mass was initially a uniform-density shell sitting on the present-day Mercury, and that the density of the shell was ρ. The gravitational potential energy of that shell would have been

$$U_s = -\int_{R_M}^{R_s} \frac{GM_M\rho}{r} dV = -2\pi GM_M\rho\left(R_s^2 - R_M^2\right),$$

where R_s is the outer radius of the shell, R_M is the present-day radius of Mercury, and M_M is the mass of the present-day Mercury. R_s is determined from

$$M_s = \frac{4\pi}{3}\rho\left(R_s^3 - R_M^3\right) = \frac{M_M}{5}.$$

If $\rho = 3350$ kg m^{-3}, the density of Earth's Moon, then $R_s = 2.7 \times 10^6$ m $= 0.42\,R_\oplus$. This implies that

$$U_s = -5.7 \times 10^{29}\text{ J.}$$

If we assume that the entire mass of the impactor was also ejected from the surface of the present-day Mercury, its potential energy at the time of impact would have been

$$U_i = -G\frac{M_M M_i}{R_M} = -6.0 \times 10^{29} \text{ J}.$$

Thus the energy required to eject the shell and the impactor would have been $E = -(U_s + U_i) = 1.2 \times 10^{30}$ J.

(c) There would have been plenty of energy available from the kinetic energy of the impactor to eject both the impactor and the extra shell of material.

20.6 The surface pressure on Venus is 90 atm $= 9 \times 10^6$ N m^{-2}. From the ideal gas law (Eq. 10.10) with $T = 740$ K, $n = P/kT = 8.8 \times 10^{26}$ m^{-3}. This value is roughly 44 times the value quoted in Example 19.3.3 for Earth's surface.

20.7 (a) Image that the atmosphere is composed of τ layers (assumed to be an integer for simplicity), each of optical depth unity. Further assume that each layer has a different constant temperature. Let $T_1 = T_{bb}$ be the blackbody temperature at the top of the atmosphere (i.e., in the top-most layer). Since the layer has two surfaces, top and bottom (each of essentially the same area), the energy per second radiated out of that first layer is $2A\sigma T_{bb}^4$ while the energy radiated into it from the second layer is $A\sigma T_2^4$. Equating the two rates gives $T_2^4 = 2T_{bb}^4$. Similarly, the next layer down (layer 2) loses energy at the rate $2\sigma A T_2^4$ but gains energy from its neighbors, or

$$2\sigma A T_2^4 = \sigma A T_1^4 + \sigma A T_3^4.$$

This implies that

$$T_3^4 = \left(2T_2^4 - T_1^4\right) = 4T_{bb}^4 - T_{bb}^4 = 3T_{bb}^4.$$

Continuing down through the atmosphere, we find that in general for layer n, $T_n^4 = nT_{bb}^4$. Now, at the surface,

$$2\sigma A T_\tau^4 = A\sigma T_{\text{surf}}^4 + A\sigma T_{\tau-1}^4,$$

or

$$T_{\text{surf}}^4 = \left(2T_\tau^4 - T_{\tau-1}^4\right) = \left[2\left(\tau T_{bb}^4\right) - (\tau - 1)\, T_{bb}^4\right] = (\tau + 1)\, T_{bb}^4.$$

Thus

$$T_{\text{surf}} = (1 + \tau)^{1/4}\, T_{bb}. \tag{S20.1}$$

(b) From Eq. (19.5), $T_{bb} = 226$ K for Venus. According to Eq. (S20.1), this value for T_{bb}, combined with $\tau = 70$ implies that $T_{\text{surf}} = 658$ K. Given the crude nature of the approximation, this result is in reasonable agreement with the observed value of 740 K.

20.8 Taking $\Delta v \simeq 0.03$ m yr^{-1}, $t = d/v = 1.6 \times 10^8$ yr.

20.9 Following the approach taken in Example 10.1.1, $P_c \sim GM_\oplus \overline{\rho}/R_\oplus = 3.4 \times 10^{11}$ N m^{-2} $= 3.6 \times 10^6$ atm, remarkably close to the detailed computer simulation.

20.10 (a) From Eq. (16.30), $dK/dt = -4\pi^2 I \dot{P}/P^3$. Making the approximation that the moment of inertia of Earth is $I = 2M_\oplus R_\oplus^2/5 = 9.7 \times 10^{37}$ kg m^2, and using the values of $\dot{P} = 0.0016$ s century^{-1} and $P \simeq 24$ hr $= 8.64 \times 10^4$ s, the rate of decrease of rotational kinetic energy is $|dK/dt| = 3.0 \times 10^{12}$ W.

(b) The value obtained in part (a) is approximately 7.5% of the observed rate of energy outflow from the interior (4×10^{13} W).

20.11 The converging B-field lines produce a force that acts to retard the motion of the particles, ultimately changing their directions. For most particles, the change in direction occurs before they strike the atmosphere.

20.12 (a) Using a weighted average for the average density of the "two-zone" model,

$$\begin{aligned}\overline{\rho} &= \frac{\overline{\rho}_c V_c + \overline{\rho}_m V_m}{V_c + V_m} \\ &= \frac{\frac{4}{3}\pi R_c^3 \overline{\rho}_c + \left(\frac{4}{3}\pi R_\oplus^3 - \frac{4}{3}\pi R_c^3\right)\overline{\rho}_m}{\frac{4}{3}\pi R_\oplus^3} \\ &= \left(\frac{R_c}{R_\oplus}\right)^3 \overline{\rho}_c + \left[1 - \left(\frac{R_c}{R_\oplus}\right)^3\right]\overline{\rho}_m.\end{aligned}$$

Solving for the radius of the core,

$$\frac{R_c}{R_\oplus} = \left(\frac{\overline{\rho} - \overline{\rho}_m}{\overline{\rho}_c - \overline{\rho}_m}\right)^{1/3} = 0.54.$$

(b) For the two-zone model,

$$\begin{aligned}I_{2\text{ zone}} &= I_c + I_m \\ &= \frac{8\pi}{15}\left[\overline{\rho}_c R_c^5 + \overline{\rho}_m\left(R_\oplus^5 - R_c^5\right)\right] \\ &= 8.48 \times 10^{37}\ \text{kg m}^2.\end{aligned}$$

This implies that $I/MR^2 = 0.349$.

(c) For a constant-density sphere, $I/MR^2 = 2/5 = 0.4$. The lower value found in part (b) reflects the centrally condensed nature of Earth's interior.

20.13 (a) Since the moment-of-inertia ratio is very close to the constant-density value of 0.4 for a sphere, the Moon must be only very slightly centrally condensed.

(b) The result is consistent with the lack of a detectable magnetic field. A strong magnetic dynamo requires a fluid, conducting (presumably molten iron-nickel) core of significant size. If such a core existed it would imply a much higher core density relative to the mantle. This would then imply a smaller value for the moment-of-inertia ratio than is observed.

20.14 (a) See Fig. S20.2.

(b) The slope of the best-fit straight line is $m = e^{\lambda t} - 1 = 0.023698$. Given the value of $\tau_{1/2} = 106.0$ Gyr for the half-life of ${}^{147}_{62}\text{Sm}$ (see Table 20.1), $\lambda = \ln 2/\tau_{1/2} = 6.539 \times 10^{-3}\ \text{Gyr}^{-1}$. Thus, $t = 3.582$ Gyr. This is much younger than the lunar highlands sample of 4.39 Gyr.

20.15 Equating the centripetal force to the gravitational force,

$$\frac{M_m v^2}{R_\oplus} = \frac{GM_\oplus M_m}{R_\oplus^2},$$

and substituting the velocity of Earth's surface at the equator in terms of its rotation period, $v = 2\pi R_\oplus/P$, leads to

$$P = \frac{2\pi R_\oplus^{3/2}}{(GM_\oplus)^{1/2}} = 5060\ \text{s} = 1.4\ \text{hr}.$$

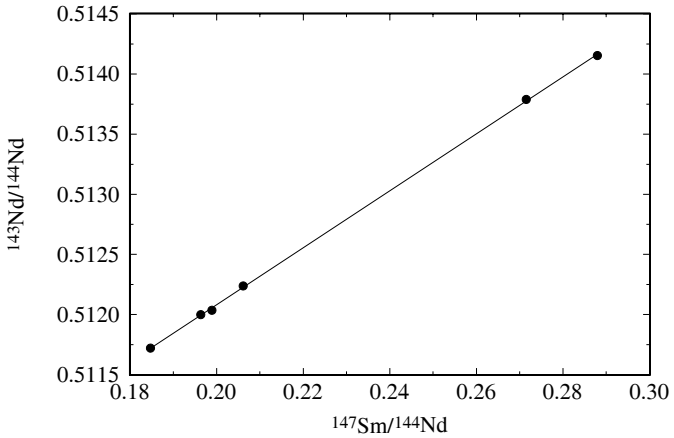

Figure S20.2: The results of Problem 20.14(a).

20.16 Using $\overline{\rho}_\oplus = 5520$ kg m^{-3} and $\overline{\rho}_{\rm Moon} = 3340$ kg m^{-3}, the Roche limit is (Eq. 19.4)

$$r = 2.456 \left(\frac{\overline{\rho}_\oplus}{\overline{\rho}_{\rm Moon}} \right)^{1/3} R_\oplus = 1.85 \times 10^7 \text{ m} = 0.048 a_{\rm Moon},$$

where $a_{\rm Moon}$ is the semimajor axis of the Moon's orbit. The Moon is not in danger of being tidally disrupted.

20.17 (a) $\dfrac{T_p}{T_a} = \sqrt{\dfrac{r_a}{r_p}} = \sqrt{\dfrac{1+e}{1-e}} = 1.098.$

(b) The southern hemisphere's polar ice cap varies more dramatically.

20.18 $P_{\rm Phobos} = 7^{\rm h}\ 30^{\rm m} = 2.75 \times 10^4$ s and $P_{\rm Deimos} = 30^{\rm h}\ 17^{\rm m} = 1.09 \times 10^5$ s. Then, from Kepler's third law (Eq. 2.37),

$$a_{\rm Phobos} = 9.36 \times 10^6 \text{ m} = 2.75\ R_{\rm Mars}$$

$$a_{\rm Deimos} = 2.34 \times 10^7 \text{ m} = 6.89\ R_{\rm Mars}.$$

20.19 Since $P_{\rm Phobos} = 7^{\rm h}\ 30^{\rm m}$, $P_{\rm Deimos} = 30^{\rm h}\ 17^{\rm m}$, and $P_{\rm Mars} = 24^{\rm h}\ 37^{\rm m}$, Phobos will appear to move eastward and Deimos will appear to move westward.

CHAPTER 21

The Realms of the Giant Planets

21.1 Following the procedure given in Example 10.1.1, $P_c \sim GM\overline{\rho}/R_p$, and using the data found in Appendix C, $P_{c,\text{Jupiter}} \sim 2.4 \times 10^{12}$ N m^{-2} and $P_{c,\text{Saturn}} \sim 4.5 \times 10^{11}$ N m^{-2}. For comparison, the central pressure in the Sun is 2.5×10^{17} N m^{-2} (see Table 11.1). The central pressures of Jupiter and Saturn are significantly less.

21.2 (a) Beginning with Eq. (10.6) for hydrostatic equilibrium,

$$\frac{dP}{dr} = -G\frac{M_r \rho}{r^2},$$

and substituting the polytropic relation, $P(r) = K\rho^2(r)$, leads to

$$\frac{d\rho}{dr} = -\frac{G}{2K}\frac{M_r}{r^2}. \tag{S21.1}$$

Differentiating again,

$$\frac{d^2\rho}{dr^2} = -\frac{G}{2K}\left(\frac{1}{r^2}\frac{dM_r}{dr} - \frac{2M_r}{r^3}\right). \tag{S21.2}$$

Using the mass conservation equation (Eq. 10.7),

$$\frac{dM_r}{dr} = 4\pi r^2 \rho,$$

rewriting Eq. (S21.1),

$$\frac{M_r}{r^2} = -\frac{2K}{G}\frac{d\rho}{dr},$$

and substituting into Eq. (S21.2) leads to the desired result,

$$\frac{d^2\rho}{dr^2} + \frac{2}{r}\frac{d\rho}{dr} + \left(\frac{2\pi G}{K}\right)\rho = 0. \tag{S21.3}$$

(b) Starting from

$$\rho(r) = \rho_c\left(\frac{\sin kr}{kr}\right), \tag{S21.4}$$

and differentiating,

$$\frac{d\rho}{dr} = \rho_c\left(\frac{\cos kr}{r} - \frac{\sin kr}{kr^2}\right). \tag{S21.5}$$

The second derivative is

$$\frac{d^2\rho}{dr^2} = \rho_c\left(\frac{2\sin kr}{kr^3} - \frac{2\cos kr}{r^2} - \frac{k\sin kr}{r}\right). \tag{S21.6}$$

Substituting Eqs. (S21.4), (S21.5), and (S21.6) into Eq. (S21.3) verifies that the equation is satisfied.

(c) $k = \pi/R_\text{J} = 4.50 \times 10^{-8}$ m^{-1} and $K = 2\pi G/k^2 = 2GR_\text{J}^2/\pi = 2.07 \times 10^5$ N m^4 kg^{-2}.

(d) Integrating Eq. (10.7),

$$\begin{aligned} M_{\rm J} &= \int_0^r 4\pi r^2 \rho \, dr \\ &= \frac{4\pi\rho_c}{k} \int_0^r r(\sin kr)\, dr \\ &= \frac{4\pi\rho_c}{k^3} [\sin kr - (kr)\cos kr] \end{aligned}$$

(e) Substituting $r = R_{\rm J}$ and recalling that $kR_{\rm J} = \pi$ leads to

$$\rho_c = \frac{\pi}{4} \frac{M_{\rm J}}{R_{\rm J}^3} = 4100 \text{ kg m}^{-3}.$$

(f) See Figs. S21.1 and S21.2.

(g) $P_c = K\rho_c^2 = 3.6 \times 10^{12}$ N m^{-2}.

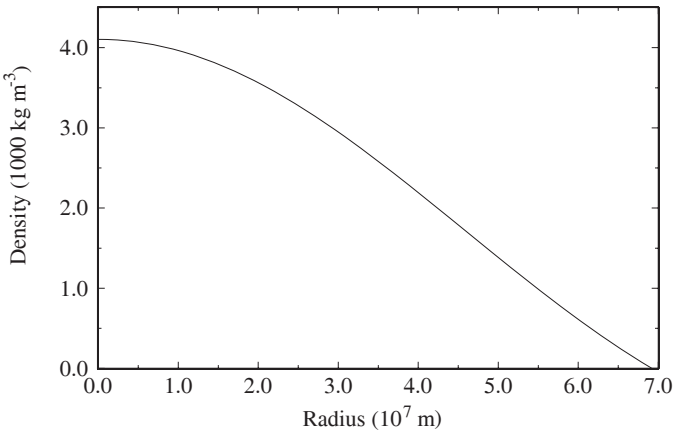

Figure S21.1: A polytropic model of the variation of density with radius for Jupiter's interior according to Problem 21.2(f).

21.3 (a) Consider a ring of mass dm and radius a centered on the rotation axis, with the edge of the ring a distance r from the center of the planet. Then, for an angle θ measured from the rotation axis, $a = r\sin\theta$. Furthermore, for a density distribution of $\rho(r)$, the mass of the ring is given by $dm = \rho\, dV = \rho(2\pi a\, r\, d\theta\, dr)$. Substituting into the expression for the moment of inertia,

$$\begin{aligned} I &= \int_{\rm vol} a^2\, dm \\ &= \int_{\rm vol} (r\sin\theta)^2 \left[2\pi r^2 \sin\theta\rho(r)\right] dr\, d\theta. \end{aligned}$$

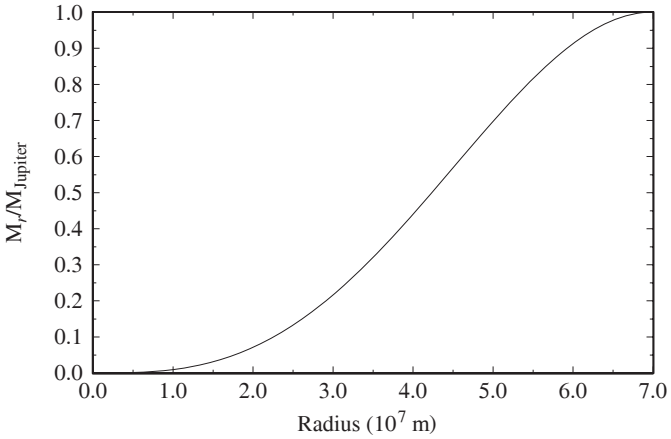

Figure S21.2: A polytropic model of the variation of interior mass with radius for Jupiter's interior according to Problem 21.2(f).

Introducing the polytropic result,

$$\rho(r) = \rho_c \left(\frac{\sin k r}{k r} \right),$$

the moment of inertia becomes

$$I = \int_{\theta=0}^{\pi} \int_{r=0}^{R_J} 2\pi r^4 \sin^3\theta \rho_c \left(\frac{\sin k r}{k r} \right) dr\, d\theta$$

$$= \frac{2\pi\rho_c}{k} \int_0^{\pi} \sin^3\theta\, d\theta \int_0^{R_J} r^3 \sin k r\, dr.$$

Recalling from Problem 21.2 that $k R_J = \pi$, the expression for the moment of inertia reduces to

$$I = \frac{8\rho_c}{3\pi} \left(1 - \frac{6}{\pi^2} \right) R_J^5.$$

(b) Using the estimate from Problem 21.2(e) that $\rho_c = 4100$ kg m^{-3} and the data in Appendix C, the moment-of-inertia ratio of this polytropic model of Jupiter is

$$\frac{I}{M_J R_J^2} = 0.134.$$

(c) The polytropic model overestimates the central mass concentration.

21.4 (a) First consider the case of a uniform density, ρ_{env} (in other words, let $f = 0$ initially). Then

$$I = 4\pi\rho_{env} \int_0^{R_p} \int_0^{R_e\sqrt{1-(z/R_P)^2}} a^3\, da\, dz$$

$$= \pi R_e^4 \rho_{env} \int_0^{R_p} \left[1 - \left(\frac{z}{R_P} \right)^2 \right]^2 dz$$

$$= \frac{8\pi}{15} R_p R_e^4 \rho_{env}$$

The core can be included by subtracting the moment of inertia of a constant-density spherical core of density $\rho_{\rm env}$ and radius fR_e, and replacing it with the moment of inertia of the constant-density spherical core of density $\rho_{\rm core}$ having the same radius. Thus,

$$I = \frac{8\pi}{15} R_p R_e^4 \rho_{\rm env} + \frac{2}{5}(\rho_{\rm core} - \rho_{\rm env}) \left(\frac{4\pi}{3}\right) f^5 R_e^5.$$

Simplifying results in Eq. (21.5).

(b) If the planet is spherical, $b = 0$. Furthermore, if the planet has a constant density, $\rho_{\rm core}$ throughout, then $f = 1$. Also, in this case

$$\rho_{\rm core} = \frac{M}{4\pi R_e^3/3}.$$

Substituting these values gives the usual result, $I = 2MR_e^2/5$.

21.5 (a) $M_{\rm core} = \rho_{\rm core} V_{\rm core} = 4\pi f^3 R_e^3 \rho_{\rm core}/3$.

(b) $fR_e = 9.8 \times 10^6$ m, implying that $f = 0.138$.

(c) The mass of the planet as a two-component model can be expressed as

$$M = 4\pi \int_0^{R_p} \int_0^{R_e\sqrt{1-(z/R_P)^2}} \rho(a,z)\, a\, da\, dz.$$

Using a procedure similar to finding the moment of inertia in Problem 21.4, we find

$$M_{\rm total} = \frac{4\pi}{3}\left[R_e^2 R_p \rho_{\rm env} + f^3 R_e^3 (\rho_{\rm core} - \rho_{\rm env})\right].$$

$$= \frac{4\pi}{3} R_e^3 \left[(1-b)\rho_{\rm env} + f^3 (\rho_{\rm core} - \rho_{\rm env})\right].$$

Solving for $\rho_{\rm env}$,

$$\rho_{\rm env} = \frac{M_{\rm total}/(4\pi R_e^3/3) - f^3 \rho_{\rm core}}{1 - b - f^3}.$$

Applying the result from part (a), we find

$$\rho_{\rm env} = \left(\frac{M_{\rm total}/M_{\rm core} - 1}{1 - b - f^3}\right) f^3 \rho_{\rm core}.$$

For Jupiter, $M_{\rm total} = 317.83\ M_\oplus$ and $b = 0.064874$ (see Appendix C). The density of the two-zone envelope is then $\rho_{\rm env} = 1300$ kg m^{-3}.

(d) From Eq. (21.5), $I/MR_e^2 = 0.393$.

(e) The measured moment of inertia ratio for Jupiter is only 0.258. This points out that the envelope structure must be must more centrally condensed than the constant value assumed here.

21.6 The diameter of Jupiter's magnetosphere is $D_{\rm mag} = 3 \times 10^{10}$ m. At opposition Jupiter is at a distance of $d = 5.2$ AU $- 1.0$ AU $= 4.2$ AU $= 6.3 \times 10^{11}$ m. Thus, the angular diameter of the magnetosphere is $\theta_{\rm mag} = D_{\rm mag}/d = 0.048$ rad $= 2.7°$. Since the angular diameter of the Moon is about $\theta_{\rm Moon} \simeq 0.5°$, we find $\theta_{\rm mag} \simeq 5.5\theta_{\rm Moon}$.

21.7 Assuming a spherical fragment of diameter $d = 700$ m and a constant density of $\rho = 200$ kg m^{-3}, the mass of the fragment was $m_{\rm G} = 4\pi(d/2)^3\rho/3 = 3.6 \times 10^{11}$ kg. The escape velocity of Jupiter is (see Eq. 2.17) $v_{\rm esc} = \sqrt{2GM_{\rm J}/R_{\rm J}} = 60$ km s^{-1}. These values imply a kinetic energy of $E = \frac{1}{2} m_{\rm G} v_{\rm esc}^2 = 6.4 \times 10^{19}$ J $=$ 15,000 MTons.

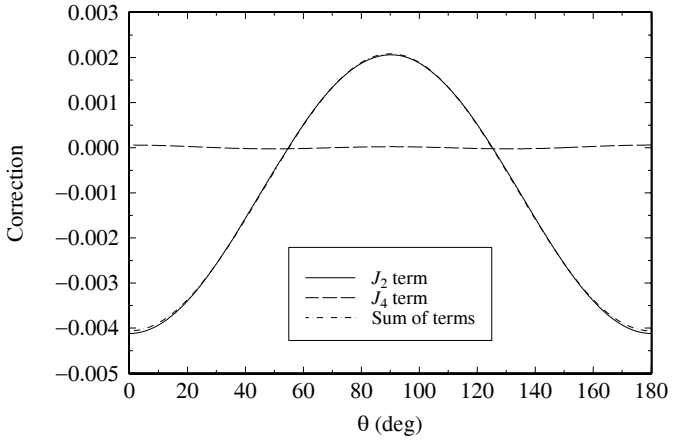

Figure S21.3: The results for Problems 21.8(a) and (b) for the gravitational potential of Saturn.

21.8 (a) See Fig. S21.3.

(b) The gravitational potential is largest at $\theta = 90°$ and smallest at $\theta = 0°$ and 180°. At 0° and 180° the deviation is approximately 0.4%; at 90° the deviation is approximately 0.2%.

21.9 (a) From Eq. (10.23) and following Example 10.3.1,

$$\Delta E = \frac{3}{10}\frac{GM_{\rm J}^2}{R_{\rm J}} = 1.0 \times 10^{36}\ \text{J}.$$

(b) The average rate of gravitational energy output from Jupiter over the age of the solar system is

$$\left\langle \frac{dE}{dt} \right\rangle = \frac{\Delta E}{4.55 \times 10^9\ \text{yr}} = 7.0 \times 10^{18}\ \text{W}.$$

(c) The current intrinsic power output of Jupiter is 3.3×10^{17} W. This value is roughly one-twentieth of the average output over the planet's lifetime, implying that the output must have been much greater in the past. The larger rate for the energy output in the past would have contributed to early heating of the Jupiter subnebula, helping to deplete volatiles near Io and Europa.

21.10 The rate at which solar energy is absorbed by Neptune is

$$\left(\frac{dE}{dt}\right)_{\text{absorbed}} = \left(\pi R_{\rm N}^2\right)\left(\frac{L_\odot}{4\pi r_{\rm N}^2}\right)(1-a) = 2 \times 10^{15}\ \text{W},$$

where $R_{\rm N}$ is Neptune's equatorial radius, $r_{\rm N}$ is its orbital radius, and a is its albedo (see Appendix C). Since roughly an equal amount of energy is emitted by internal sources, the total energy per second given off by Neptune is

$$\left(\frac{dE}{dt}\right)_{\text{emitted}} \simeq 2\left(\frac{dE}{dt}\right)_{\text{absorbed}} = 4 \times 10^{15}\ \text{W}.$$

Assuming that the energy is emitted as blackbody radiation,

$$\left(\frac{dE}{dt}\right)_{\text{emitted}} = 4\pi R_{\rm N}^2 \sigma T_{\rm N}^4.$$

Solving for the temperature, $T_{\rm N} = 55$ K. This crude estimate is about 7% less than the observed value of 59.3 K.

21.11 Consider the upper value given in the text of $dN/dt = 10^{29}$ ions s^{-1} leaving Io. Assuming that all of the ions are sulfur, the mass of each ion is $m_{\rm ion} \simeq 32$ u $= 5.3 \times 10^{-26}$ kg and the rate of mass loss is $dm/dt = 5300$ kg s^{-1}. Over 4.55 billion years, the amount of mass lost is $\Delta m = 7.5 \times 10^{20}$ kg. This value is roughly 0.85% of Io's present mass. Hence, Io is in no danger of vanishing any time soon.

21.12 (a) The approximate volume of the disk is

$$V_{\rm rings} = (30 \text{ m}) \left(\pi R_{\rm out}^2 - \pi R_{\rm in}^2 \right) = 2.3 \times 10^{18} \text{ m}^3.$$

From Eq. (9.12), the number density of ice spheres in the rings is

$$n = \frac{1}{\ell \sigma} = \frac{1}{\ell \left[\pi \, (1 \text{ cm})^2 \right]} = 110 \text{ m}^{-3}.$$

Given that the mass of an individual ice sphere of radius $r_{\rm ice} = 1$ cm is

$$m_{\rm ice} = \frac{4}{3} \pi r_{\rm ice}^3 \rho_{\rm ice} = 0.0042 \text{ kg},$$

the mass of ice in the rings is

$$m_{\rm rings} = \rho_{\rm rings} V_{\rm rings} = n m_{\rm ice} V_{\rm rings} = 1 \times 10^{18} \text{ kg}.$$

(b) 62 km.

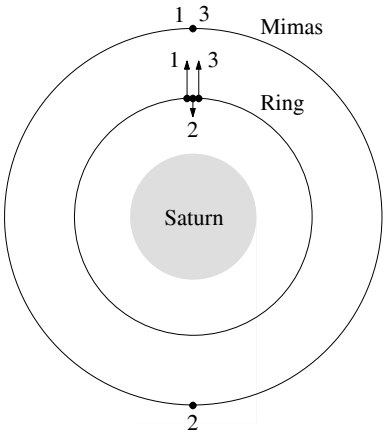

Figure S21.4: The sketch for Problem 21.13.

21.13 The sketch is shown in Fig. S21.4. Mimas and a characteristic ring particle are depicted at three points in their orbits, labeled 1, 2, and 3, respectively. For each one-half orbit that Mimas completes, the ring particle completes one full orbit. Also drawn are force vectors (not shown to correct relative lengths) between Mimas and the particle at each of the three locations. Given that the force vectors are longer at positions 1 and 3 than at 2, Mimas systematically elongates the orbit, resulting in an ellipse.

21.14 Saturn's rotation period is 0.444 d $= 3.84 \times 10^4$ s. From Kepler's third law (Eq. 2.37), this corresponds to an orbital radius of $a = 1.1 \times 10^8$ m $= 1.9$ R_S. According to Table 21.4, a portion of the B ring, as well as the A, F, G, and E rings exist beyond this radius.

21.15 (a) The energy absorbed by the grain per unit time is

$$\left(\frac{dE}{dt}\right)_{\text{absorbed}} = \sigma_g \left(\frac{L_\odot}{4\pi r_\odot^2}\right),$$

where $r_\odot$ is the grain's distance from the Sun.

(b) The angular momentum of the dust grain is $\mathcal{L} = mvr$, where r is the distance of the grain from the object that it is orbiting. Therefore, the rate at which the angular momentum decreases is given by

$$\frac{d\mathcal{L}}{dt} \simeq \left(\frac{dm}{dt}\right) vr,$$

where we have assumed that v and r are essentially constant. Considering the energy radiated away by a photon as being associated with an effective mass, the angular momentum loss rate is

$$\frac{d\mathcal{L}}{dt} \simeq \frac{vr}{c^2}\frac{dE_\gamma}{dt}.$$

At equilibrium, $dE_\gamma/dt = -(dE/dt)_{\text{absorbed}}$. Substitution leads to the desired result for the case where the particle is orbiting the Sun, or $r = r_\odot$.

21.16 (a) Beginning with Eq. (21.6), setting $r = r_\odot$ (assumed essentially constant), and integrating gives

$$\ln\left(\frac{\mathcal{L}_f}{\mathcal{L}_0}\right) = -\frac{\sigma_g}{4\pi r_\odot^2}\frac{L_\odot}{mc^2} t_{\text{Saturn}}, \tag{S21.7}$$

where $\mathcal{L}_0$ and $\mathcal{L}_f$ are the initial and final angular momenta of the particle, respectively, and t_{Saturn} is the elapsed time. The initial and final angular momenta can be found from $\mathcal{L}(r) = mvr$, where

$$m = \rho\left(\frac{4}{3}\pi R^3\right),$$

and R is the radius of the grain. Furthermore, $v = 2\pi r/P$, and from Kepler's third law (Eq. 2.37),

$$P = \frac{2\pi}{(GM_{\text{S}})^{1/2}} r^{3/2},$$

so that

$$v = (GM_{\text{S}})^{1/2}\, r^{-1/2}.$$

Combining, the angular momentum is

$$\mathcal{L}(r) = \frac{4}{3}\pi\rho R^3\, (GM_{\text{S}})^{1/2}\, r^{1/2}.$$

Setting $\mathcal{L}_0 = \mathcal{L}(R_0)$, $\mathcal{L}_f = \mathcal{L}(R_{\text{S}})$, and $\sigma_g = \pi R^2$, and substituting into Eq. (S21.7) gives the desired result.

(b) $t_{\text{Saturn}} = 2 \times 10^{13}$ s $= 6 \times 10^5$ yr.

(c) The estimate is much less than the age of the Solar System. Hence, the E ring cannot be a permanent feature unless the particles are replenished.

21.17 (a) From Eq. (2.17), $v_{\text{esc}} = 0.213$ km s^{-1}.

(b) $v = \sqrt{2GM_{\text{U}}/r_{\text{M}}} = 9.4$ km s^{-1}.

(c) $|U_g| = 3GM_{\text{M}}^2/5R_{\text{M}} = 1.09 \times 10^{24}$ J.

(d) Beginning with

$$K = |U_g| = \frac{1}{2}mv^2 = \frac{1}{2}\left(\frac{4}{3}\pi\rho R^3\right)^3 v^2,$$

and solving for the radius gives $R = 14.3$ km.

CHAPTER 22

Minor Bodies of the Solar System

22.1 (a) From Eq. (3.13),

$$F_{\rm rad} = \frac{\langle S \rangle A}{c} \cos\theta = \frac{L_\odot \left(\pi R^2\right)}{4\pi r^2 c} = 1.4 \times 10^{-19}\ {\rm N},$$

where $R = 100$ nm and $r = 1$ AU. Given a density of $\rho_g = 3000$ kg m^{-3}, the mass of the grain is $m_g = \rho_g \left(\frac{4}{3}\pi R^3\right) = 1.3 \times 10^{-17}$ kg. Thus, the acceleration is $a = F_{\rm rad}/m_g = 0.011$ m s^{-2}.

(b) $g = GM_\odot/r^2 = 0.0059$ m s^{-2}.

22.2 (a) Beginning with Eq. (21.6),

$$\frac{d\mathcal{L}}{dt} = -\frac{\sigma_g}{4\pi r^2}\frac{L_\odot}{mc^2}\mathcal{L},$$

where r is the orbital radius of the grain. After substituting $\sigma_g = \pi R^2$ (where R is the grain radius), $\mathcal{L} = mvr$, and $m = \frac{4}{3}\pi R^3 \rho$, and simplifying,

$$\frac{d(vr)}{dt} = -\frac{R^2}{4r^2}\frac{L_\odot}{mc^2}(vr).$$

Using Kepler's third law (Eq. 2.37), $P^2 = 4\pi^2 r^3/GM_\odot$, and substituting $P = 2\pi r/v$ for a circular orbit, the velocity can be written as $v = \sqrt{GM_\odot/r}$. Placing the result into the differential equation, simplifying, and integrating from the initial orbital radius to the solar radius we find

$$\int_r^{R_\odot} r\, dr = -\int_0^{t_{\rm Sun}} \frac{R^2 L_\odot}{2mc^2}\, dt.$$

Evaluating,

$$\frac{1}{2}\left(R_\odot^2 - r^2\right) = -\frac{R^2 L_\odot}{2mc^2} t_{\rm Sun}.$$

Making use of the approximation $r \gg R_\odot$, and writing the mass in terms of the density of the spherically symmetric grain, $m = \frac{4}{3}\pi R^3 \rho$, leads to the desired expression for the time required for the dust grain to spiral into the Sun.

(b) 0.92 m.

22.3 Combining the rates of mass loss for dust and gas, $dm/dt = 2.5 \times 10^4$ kg s^{-1}. In one year (the active portion of one trip around the Sun), $\Delta m/{\rm trip} = (dm/dt)\,\Delta t = 8 \times 10^{11}$ kg. Taking the mass of the nucleus to be $m \sim 10^{14}$ kg, we find $N = m/(\Delta m/{\rm trip}) = 125$ trips.

22.4 The mass-loss rate, dm/dt, combined with the gas velocity, $\mathbf{v}_g$ implies a rate of change of momentum (i.e., a force):

$$F = m_{\rm nucleus} a_{\rm nucleus} = v_g \frac{dm}{dt} = \frac{d\left(mv_g\right)}{dt} = \frac{dp}{dt}.$$

Measurement of the acceleration of the nucleus gives an estimate of the mass.

22.5 (a) From Kepler's third law [Eq. (2.37) written in the form $P^2 = a^3$, where P and a are in years and AU, respectively], $a = 64$ AU.

(b) From Eq. (2.5), $r_p = a(1-e) = 0.0055$ AU, and from Eq. (2.6), $r_a = a(1+e) = 128$ AU.

(c) The Kuiper belt.

22.6 The orbital period of Jupiter is $P_\text{J} = 11.8622$ yr (see Appendix C). Thus, an object with a 2:1 orbital resonance with Jupiter has a period of $P_{21} = P_\text{J}/2 = 5.931$ yr. This corresponds to a semimajor axis of 3.28 AU [Eq. (2.37) written in the form $P^2 = a^3$, where P and a are in years and AU, respectively]. Similarly, for a 3:1 resonance, $P = P_\text{J}/3 = 3.954$ yr and $a = 2.5$ AU. These values agree with Fig. 22.13.

22.7 (a) From Eq. (19.5),

$$\begin{aligned} T_V &= T_\odot (1-a)^{1/4} \sqrt{\frac{R_\odot}{2D}} \\ &= (5777 \text{ K})(1-0.38)^{1/4} \left[\frac{6.96 \times 10^8 \text{ m}}{2(2.362 \text{ AU})}\right]^{1/2} \\ &= 161 \text{ K}. \end{aligned}$$

(b) $\dfrac{dE}{dt} = L_V = 4\pi R_V^2 \sigma T_V^4 = 2 \times 10^{13}$ W.

22.8 (a) The total volume occupied by the asteroids is

$$V_\text{asteroids} = N\left(\frac{4\pi}{3}R^3\right) = 1.3 \times 10^{21} \text{ m}^3.$$

(b) The volume of the belt in this crude estimate is

$$V_\text{belt} = h\pi\left(R_2^2 - R_1^2\right) = 4.9 \times 10^{32} \text{ m}^3.$$

(c) 2.6×10^{-12}

(d) This is unrealistic, at least in our Solar System! You would have to go out of your way to hit an asteroid.

22.9 (a) $m_V = \frac{4}{3}\pi R_V^3 \rho_V = 1.9 \times 10^{20}$ kg.

(b) $N_\text{Si} = m_V/m_\text{Si} = 4.1 \times 10^{45}$.

(c) $\Delta E = (\Delta m)c^2 = (25.986892 \text{ u} - 25.982594 \text{ u})c^2 = 6.4 \times 10^{-13}$ J.

(d) $N_{^{26}_{13}\text{Al}} = \left(5 \times 10^{-5}\right)\left(\dfrac{8680}{10^6}\right) N_\text{Si} = 1.8 \times 10^{39}$.

(e) The amount of energy released per second is

$$\frac{dE}{dt} = \Delta E \, \frac{dN}{dt}.$$

However, from Eq. (15.9), $dN/dt = -\lambda N$, and from Eq. (15.10), $N(t) = N_0 e^{-\lambda t}$. Substituting,

$$\frac{dE}{dt} = -\lambda(\Delta E) N_0 e^{-\lambda t}.$$

For a half-life of $\tau_{1/2} = 716{,}000$ yr, the decay constant is

$$\lambda = \frac{\ln 2}{\tau_{1/2}} = 9.7 \times 10^{-7} \text{ yr}^{-1}.$$

Furthermore, $\lambda(\Delta E)N_0 = 3.5 \times 10^{13}$ J. Thus

$$\left|\frac{dE}{dt}\right| = \left(3.5 \times 10^{13}\ \mathrm{W}\right) e^{-(9.7\times10^{-7}\ \mathrm{yr}^{-1})t}.$$

The plot is given in Fig. S22.1.

(f) 5.6×10^5 yr.

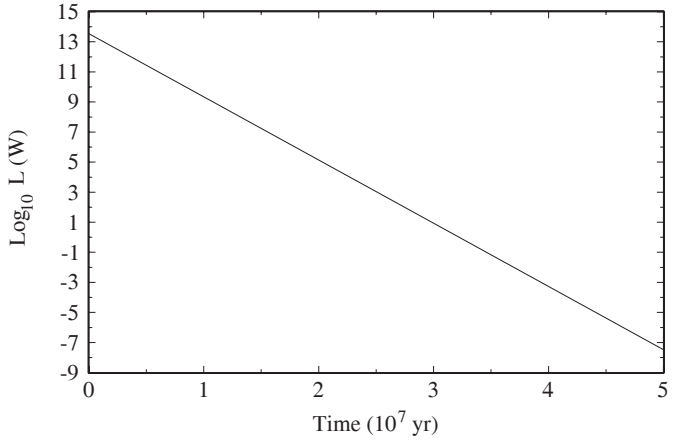

Figure S22.1: An estimate of the energy output from Vesta as a function of time [see Problem 22.9(e)].

22.10 Earth spins on its axis in the same direction that it orbits the Sun. Hence, on the side of Earth away from the Sun, the rotation and velocity vectors add, implying a larger value for the net relative velocity between a meteoroid and Earth. Also, the sky is dark on the side of Earth away from the Sun.

22.11 The energy released in the Tunguska event was roughly $E = K = mv^2/2 = 10^{15}$ J. If the impact velocity was Earth's escape velocity of 11.2 km s^{-1} (see Eq. 2.17), the mass was 2×10^7 kg. Assuming a density of 2000 kg m^{-3} and spherical symmetry, the radius of the impactor was 12 m.

CHAPTER 23

Formation of Planetary Systems

23.1 (a) Both HD 80606 and HD 80607 are G5V stars, implying that their masses are each just slightly less than 1 $M_\odot$. If we adopt 1 $M_\odot$ for the mass of each star in this example, and we use Kepler's third law in the form $(M_1 + M_2)P^2 = a^3$, where the masses are in solar units, P is in years, and a is in astronomical units, we find $P = 63{,}000$ yr.

(b) If $a = 0.44$ AU, then the orbital period of HD 80606b about HD 80606 (neglecting any influences from the companion star) is $P = 0.29$ yr. This would imply roughly 220,000 orbits of the planet for each orbit of the two stars about their common center of mass.

(c) The ratio of the two forces is roughly

$$F_{80607}/F_{80606} = \left(\frac{.44}{2000}\right)^2 = 5 \times 10^{-8}.$$

23.2 Comparing densities:

Object	density (10^3 kg m^{-3})	class
Pluto	2.1	planet
Ida	2.2–2.9	asteroid
Vesta	2.9	asteroid
Halley	< 1	comet
Triton	2.1	moon of Neptune

(Note that the data on Vesta is given in Problem 22.9.)

Comparing radii:

Object	radius (km)	class
Pluto	1135	planet
Ceres	500	asteroid
Vesta	250	asteroid
Ida	55	asteroid (long axis)
Halley	15	comet
Triton	1353	moon of Neptune

(Note that the data for Ceres was found in Section 19.1.)

Pluto is very similar to Triton, in terms of density, radius, and composition. Comets are icier and smaller than Pluto, while asteroids tend to be rockier and smaller. Pluto is consistent with being formed farther out from the Sun than were the hotter asteroids. Pluto grew larger than cometary nuclei.

23.3 (a) According to Fig. 23.8, $L_{\rm tot}/M_{\rm tot} = 10^{17.2}$. Taking $M_{\rm tot} \simeq M_\odot$ gives $L_{\rm tot} = 3.2 \times 10^{43}$ kg m^2 s^{-1}. From the definition of the moment-of-inertia ratio given in Problem 20.12, the Sun's moment of inertia is $I_\odot = 0.073 M_\odot R_\odot^2 = 7 \times 10^{46}$ kg m^2. Furthermore, since $L_{\rm tot} = I_\odot \omega = 2\pi I_\odot / P$, where ω and P are the angular velocity and rotation period, respectively, solving for the rotation period gives $P = 1.4 \times 10^4$ s $= 0.16$ d.

(b) $v_e = 2\pi R_\odot / P = 3.2 \times 10^5$ m s^{-1}.

(c) Setting the centripetal acceleration equal to the gravitational acceleration,

$$\frac{v_{e,\max}^2}{R_\odot} = \frac{GM_\odot}{R_\odot^2},$$

and solving for the maximum velocity gives

$$v_{e,\max} = \sqrt{\frac{GM_\odot}{R_\odot}} = 4.4 \times 10^5 \text{ m s}^{-1}.$$

This corresponds to a rotation period of $P = 2\pi R_\odot / v_{e,\max} = 1 \times 10^4$ s $= 0.12$ d.

23.4 If we simply add up all of the mass of planets, comets, asteroids, and moons, we get (very roughly) $M = 2.6 \times 10^{27}$ kg for the planets, 6.3×10^{23} kg for the largest moons in Appendix C, 6×10^{26} kg $= 100\ M_\oplus$ for the Oort cloud, perhaps 1000 $M_{\text{Pluto}} = 10^{25}$ kg in the Kuiper belt (wild guess), and $5 \times 10^{-4}\ M_\oplus = 3 \times 10^{21}$ kg for the asteroid belt. Combining gives a very crude estimate of $M_{\text{MMSN}} = 4 \times 10^{27}$ kg.

23.5 $R_H = 0.5$ AU $= 1000\ R_J$.

23.6 (a) The mass of a K4V star is roughly $0.7\ M_\odot$. Using Kepler's third law with an orbital period of $P = 2.81782$ d implies $a = 0.035$ AU $= 5.2 \times 10^9$m.

(b) If the planet produces a radial reflex velocity of 64.3 m s^{-1} on the star, and the planet's orbital speed is $v_p = 2\pi a / P = 134$ km s^{-1}, the mass of the planet is about

$$m_p = \frac{v_{\text{star}}}{v_p} M_{\text{star}} = 6.7 \times 10^{26} \text{ kg} = 0.35\ M_J.$$

(c) The orbital radius of the star about the center of mass is $r = v_{\text{star}} P / 2\pi = 2.5 \times 10^6$ m. This implies a maximum wobble of

$$\theta = \frac{2r}{d} = \frac{5 \times 10^6 \text{ m}}{35.8 \text{ pc}} = 4.5 \times 10^{-12} \text{ rad} = 9.7 \times 10^{-7} \text{ arcsec} = 0.97\ \mu\text{as}.$$

23.7 (a) The mass of a K0V star is approximately $0.79\ M_\odot$. Therefore, $a = (P^2/M)^{1/3} = 3.1$ AU.

(b) $r_a = (1 + e)a = 4.2$ AU.

(c) From Eq. (2.33), $v_p = 2.1 \times 10^4$ m s^{-1} $= 21$ km s^{-1}.

23.8 High metallicity implies that the formation of dust grains will be more effective. The merger of grains will lead to the build-up of planetesimals.

23.9 If Jupiter and Saturn were originally at 5.7 AU and 8.6 AU, their orbital periods would have been 13.6 yr and 25.2 yr, respectively, corresponding to a period ratio of $(P_S/P_J)_0 = 1.85$. Today's period ratio is $P_S/P_J = 29.46$ yr$/11.86$ yr $= 2.48$. At some point during their migrations they would have passed through a period ratio of 2.

CHAPTER 24

The Milky Way Galaxy

24.1 Using $R_0 = 8$ kpc and $\Theta_0 = 220$ km s^{-1}, $P = 2\pi R_0/\Theta_0 = 220$ Myr. Taking the age of the Sun to be 4.56 Gyr, the Sun has made approximately 20 trips around the Galactic center.

24.2 (a) See Table S24.1.

(b) $L_{\rm bol,\ tot} = 3.6 \times 10^{10}\ {\rm L}_\odot$.

Table S24.1: Results for Problem 24.2(a).

component	$L_B(10^{10}\ {\rm L}_\odot)$	%
gas	0	0
thin disk	1.8	81
thick disk	0.02	0.9
bulge	0.3	13.5
stellar halo	0.1	4.5
dark matter halo	0	0
Total L_B [1]	2.22	100

[1] Note that the value in the text is $L_B = 2.3 \pm 0.6 \times 10^{10}\ {\rm L}_\odot$.

24.3 (a) Beginning with Eq. (24.1) and solving for a_V,

$$a_V = V - M_V + 5 - 5\log_{10} d = 2.38.$$

(b) $a_V/9.0\ {\rm kpc} = 0.26\ {\rm mag\ kpc}^{-1}$.

24.4 From the discussion leading up to Eq. (3.5),

$$F = F_{10}\, 100^{-(m-M)/5}$$

is the flux received from a star of apparent magnitude m relative to a star of absolute magnitude M located 10 pc from Earth.

Next, from Eq. (24.4), the number of stars with absolute magnitudes between M and $M + dM$ found within a solid angle Ω and having apparent magnitudes between m and $m + dm$ is given by

$$d\overline{N}_M = A_M\, dm.$$

Thus, the total flux due to all stars with apparent magnitudes between m and $m + dm$ is

$$dF_m = F_{10} 100^{-(m-M)/5}\, A_M\, dm.$$

Substituting the expression for A_M given by Eq. (24.5), and adding up the contributions from all stars between the observer ($m \to -\infty$) and some distance d corresponding to an apparent magnitude m,

$$F_m = \int_{-\infty}^{m} \left[F_{10} 10^{-2(m-M)/5} \right] \left[\frac{\ln 10}{5} \Omega n_M 10^{3(m-M+5)/5} \right] dm$$

$$= C \int_{-\infty}^{m} 10^{m/5}\, dm,$$

where C is a constant. After integrating,

$$F_m = \frac{5C}{\ln 10}\, 10^{m/5}.$$

As $d \to \infty$, $m \to \infty$, and $F_m \to \infty$.

24.5 (a) From Eq. (24.5),

$$\log_{10} A_M = \frac{3}{5}(m - M + 5) + \log_{10}\left(\frac{\ln 10}{5}\right) + \log_{10} \Omega + \log_{10} n_M(M, S).$$

(b) $\Delta \log_{10} A_M(m) = 0.6$.

(c) The distribution of stars is not constant, but decreases with increasing distance.

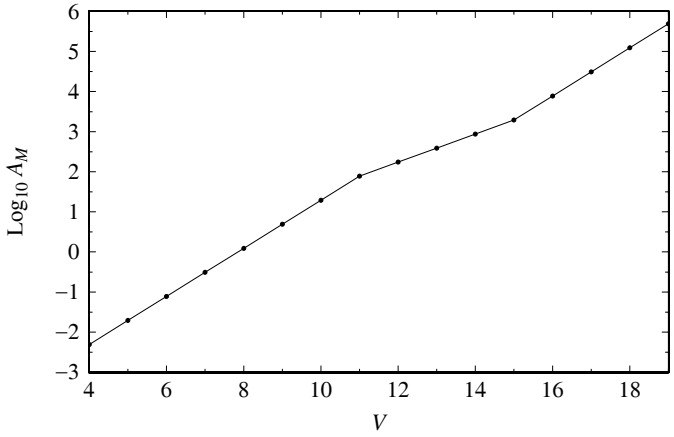

Figure S24.1: Results for Problem 24.6(a).

24.6 (a) See Fig. S24.1.

(b) The slope of the curve over the range $4 < V < 11$ is 0.6. This implies that no interstellar extinction is present, or $a_V = 0$.

(c) From Eq. (24.1) with $a = 0$, $d = 631$ pc.

(d) From Table 24.2, $V = 11$ corresponds to $\log_{10} A_M = 1.89$. Employing the result of Problem 24.5(a), we find $n_M(M, S) = 2.9 \times 10^{-3}$ pc^{-3}.

(e) A monotonic decrease in the stellar number density with increasing V or interstellar extinction.

24.7 (a) Returning to the derivation of Eq. (24.5), if interstellar extinction is included

$$A_M = \frac{\ln 10}{5} \Omega n_M 10^{3(m-M-a+5)/5}$$

or

$$\log_{10} A_M = \frac{3}{5}(m - M - a + 5) + \log_{10}\left[\frac{\ln 10}{5}\Omega n_M\right].$$

If we consider the values at $V = 15$ and $V = 11$, and noting that $a = 0$ for $V < 11$ (i.e., in front of the cloud), we find the difference

$$\log_{10} A_M(15) - \log_{10} A_M(11) = \frac{3}{5}(15 - a) - \frac{3}{5}(11) = 3.29 - 1.89 = 1.4 = 7/5.$$

Solving, we find $a = 5/3$.

(b) If $da/d\ell = 10$ mag kpc^{-1}, $\Delta\ell = 40$ pc.

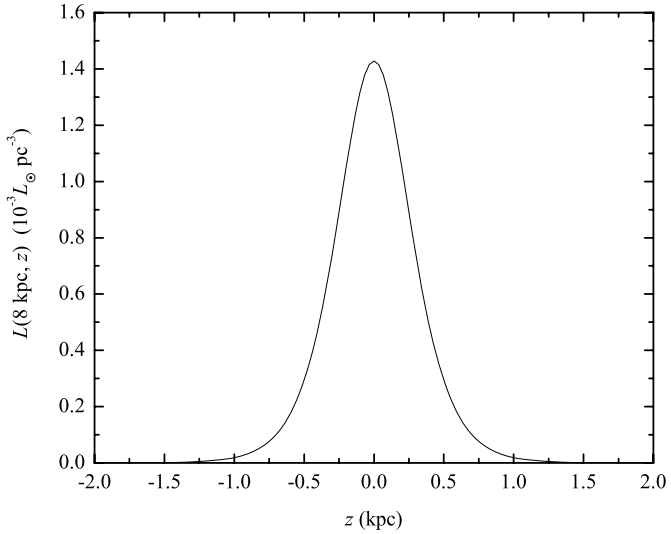

Figure S24.2: Results of Problem 24.8(a).

24.8 (a) See Fig. S24.2.

(b) Beginning with the expression for sech (z/z_0) found immediately after Eq. (24.10),

$$\text{sech}^2\,(z/z_0) = \frac{4}{e^{2z/z_0} + e^{-2z/z_0} + 2}.$$

In the case where $z \gg z_0$, sech$^2\,(z/z_0) \simeq 4e^{-2z/z_0}$. Substituting into Eq. (24.10) gives the expected result.

24.9 (a) The number of hydrogen atoms is given by $N = M_{\rm gas}/m_{\rm H} \simeq 6 \times 10^{66}$ atoms. Assuming that each atom has a thermal energy given by $E = \frac{3}{2}kT$, the total thermal energy content of hydrogen gas in the Galaxy is $E_{\rm thermal} = 1.86 \times 10^{45}$ J. Dividing by the volume of the of the disk $V \simeq \pi R^2 h$ gives $u_{\rm thermal} = 2 \times 10^{-15}$ J m^{-3}.

(b) Using $B \simeq 0.4$ nT, Eq. (11.9) gives $u_m \simeq 6 \times 10^{-14}$ J m^{-3}. In this rough estimate, $u_m \simeq 30u_{\rm thermal}$, implying that magnetic field effects should play a significant role in the structure of the Milky Way.

24.10 $\ell = 0.944°$, $b = -0.0461°$.

24.11 (a) For the NCP: $\ell = 123.932°$, $b = 27.128°$.

(b) For the vernal equinox: $\ell = 97.337°$, $b = -60.185°$.

(c) For Deneb: $\ell = 85.285°$, $b = 1.9976$.

24.12 (a) For M13, $z = d \sin b = 4.6$ kpc and for the Orion Nebula, $z = d \sin b = -149$ pc.

(b) M13 belongs to the Galactic stellar halo and the Orion Nebula is a member of the thin disk. These conclusions are supported by their heights above the Galactic midplane and by their classifications as a globular cluster and a young star-forming region (a nebula), respectively.

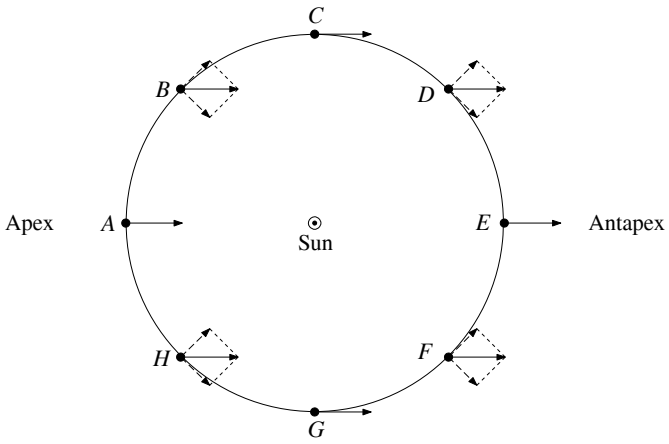

Figure S24.3: The results for Problem 24.13. (a) The solid-line arrows represent the apparent motions of the stars, while (b) the dashed-line arrows represent the radial and transverse velocity components.

24.13 (a) See Fig. S24.3.

(b) See Fig. S24.3.

(c) Stars near the apex (approaching) have the largest negative radial velocities and stars near the antapex (receding) have the largest positive radial velocities.

(d) Stars located at the apex have no measurable proper motions due to the solar motion with respect to the LSR. As we consider stars farther from the apex, the proper motions increase, and appear to move directly away from the apex. Stars 90° from the apex have the largest proper motions due to the solar motion relative to the LSR, and stars near the antapex appear to be converging at the antapex.

24.14 12 km s^{-1}

24.15 (a) From Eq. (2.17), $v_{\rm esc} = \sqrt{2GM/R_0}$. Using $v_{\rm esc} = 300$ km s^{-1} and $R_0 = 8.0$ kpc gives $M = 8.3 \times 10^{10}$ M$_\odot$. This result agrees well with the value of 8.8×10^{10} M$_\odot$ found in Example 24.3.1.

(b) Using a value of $v_{\rm esc} = 500$ km s^{-1} leads to a mass of $M = 2.3 \times 10^{11}$ M$_\odot$. The dark matter halo could account for the extra mass.

(c) Since much of the mass in the Galaxy is located at $r > R_0$ and appears to be approximately spherically distributed, dynamic motions in the solar neighborhood do not reflect the existence of that matter.

24.16 Begin with Eqs. (24.37) and (24.38), respectively:

$$v_r = (\Omega - \Omega_0) R_0 \sin \ell$$

$$v_t = (\Omega - \Omega_0) R_0 \cos \ell - \Omega d.$$

Substituting the first-order Taylor expansion,

$$\Omega - \Omega_0 \simeq \left.\frac{d\Omega}{dR}\right|_{R_0} (R - R_0)$$

and using the approximation

$$\Omega \simeq \Omega_0.$$

gives

$$v_r = \left.\frac{d\Omega}{dR}\right|_{R_0} (R - R_0)\, R_0 \sin\ell$$

$$v_t = \left.\frac{d\Omega}{dR}\right|_{R_0} (R - R_0)\, R_0 \cos\ell - \Omega_0 d.$$

But $\Omega = \Theta/R$. Differentiating,

$$\left.\frac{d\Omega}{dR}\right|_{R_0} = \frac{1}{R_0} \left.\frac{d\Theta}{dR}\right|_{R_0} - \frac{\Theta_0}{R_0^2}.$$

Substituting leads to

$$v_t = \left[\left.\frac{d\Theta}{dR}\right|_{R_0} - \frac{\Theta_0}{R_0}\right](R - R_0)\sin\ell$$

$$v_r = \left[\left.\frac{d\Theta}{dR}\right|_{R_0} - \frac{\Theta_0}{R_0}\right](R - R_0)\cos\ell - \Omega_0 d.$$

Using the geometry of Fig. 24.22, $R_0 = d\cos\ell + R\cos\beta \simeq d\cos\ell + R$ implies that $R - R_0 = -d\cos\ell$. We now have

$$v_r = -\left[\left.\frac{d\Theta}{dR}\right|_{R_0} - \frac{\Theta_0}{R_0}\right] d\sin\ell\,\cos\ell$$

$$v_t = -\left[\left.\frac{d\Theta}{dR}\right|_{R_0} - \frac{\Theta_0}{R_0}\right] d\cos^2\ell\,\Theta_0 d.$$

Employing the trigonometric relation, $\sin\ell\,\cos\ell = \frac{1}{2}\sin 2\ell$, leads us to Eq. (24.41),

$$v_r = Ad\sin 2\ell,$$

where

$$A \equiv -\frac{1}{2}\left[\left.\frac{d\Theta}{dR}\right|_{R_0} - \frac{\Theta_0}{R_0}\right]$$

is Eq. (24.39).

Invoking another trigonometric relation, $\cos^2\ell = \frac{1}{2}(1 + \cos 2\ell)$, substituting the definition of A, and using $\Omega_0 = \Theta_0/R_0$, gives

$$v_t = Ad\,(1 + \cos 2\ell) - \frac{\Theta_0}{R_0} d$$

$$= Ad\cos 2\ell + \left(A - \frac{\Theta_0}{R_0}\right) d.$$

But

$$A - \frac{\Theta_0}{R_0} = -\frac{1}{2}\left[\left.\frac{d\Theta}{dR}\right|_{R_0} - \frac{\Theta_0}{R_0}\right] - \frac{\Theta_0}{R_0}$$

$$= -\frac{1}{2}\left[\left.\frac{d\Theta}{dR}\right|_{R_0} + \frac{\Theta_0}{R_0}\right]$$

$$\equiv B,$$

which is Eq. (24.40). Substituting, we finally arrive at Eq. (24.42),

$$v_t = Ad\cos 2\ell + Bd.$$

24.17 Since from Earth we measure Δv_t, the maximum values occur at $\ell = 0°$ and 180°, and minima occur at 90° and 270°.

24.18 (a) From Kepler's third law (Eq. 2.37),

$$P = \frac{2\pi}{[G\,(m_1 + m_2)]^{1/2}} R^{3/2}.$$

However, $P = 2\pi R/\Theta$. Substituting and rearranging,

$$\Theta = \left[\frac{G\,(m_1 + m_2)}{R}\right]^{1/2}.$$

(b) Differentiating our expression for Θ gives

$$\frac{d\Theta}{dR} = -\frac{1}{2}\frac{[G\,(m_1 + m_2)]^{1/2}}{R^{3/2}} = -\frac{1}{2}\frac{\Theta}{R}.$$

Substituting into Eqs. (24.39) and (24.40) leads to

$$A = \frac{3}{4}\frac{\Theta_0}{R_0}$$

$$B = -\frac{1}{4}\frac{\Theta_0}{R_0}.$$

(c) Using the Keplerian expressions, we find $A = 20.6\ \text{km s}^{-1}\ \text{kpc}^{-1}$ and $B = -6.88\ \text{km s}^{-1}\ \text{kpc}^{-1}$.

(d) The values do not agree because they assume that all of the Galaxy's mass resides interior to R_0.

24.19 (a) Combining Eqs. (24.39) and (24.40),

$$\left.\frac{d\Theta}{dR}\right|_{R_0} = -(A + B) = -2.4\ \text{km s}^{-1}\ \text{kpc}^{-1}.$$

The orbital velocity is decreasing with increasing R.

(b) If $A = -B = 13\ \text{km s}^{-1}\ \text{kpc}^{-1}$, then

$$\left.\frac{d\Theta}{dR}\right|_{R_0} = 0.$$

This implies that at, least within the solar neighborhood, the rotation curve is flat.

24.20 (a) Equating the expression for centripetal acceleration with the gravitational acceleration,

$$\frac{\Theta^2}{R} = \frac{GM_r}{R^2},$$

or

$$\Theta = \sqrt{\frac{GM_r}{R}}.$$

Assuming a constant mass density, $M_r = \frac{4}{3}\pi\rho R^3$ and

$$\Theta = \sqrt{4\pi G\rho}R \propto R,$$

which is rigid-body rotation.

(b) The model for the distribution of dark matter described in the text is given by Eq. (24.51),

$$\rho(r) = \frac{\rho_0}{1 + (r/a)^2}.$$

When $r \ll a$, the density distribution approaches $\rho(r) \simeq \rho_0 =$ constant. As was shown in part (a), a constant density distribution implies rigid-body rotation.

24.21 In the solar neighborhood, $r = R_0$ and $V = \Theta_0$. Thus

$$\begin{aligned}\rho\,(R_0) &= \frac{\Theta_0^2}{4\pi G R_0^2} \\ &= 9.5 \times 10^{-22}\ \text{kg m}^{-3} \\ &= 0.014\ \text{M}_\odot\ \text{pc}^{-3} \\ &= 1.6 \times 10^{-18}\ \text{M}_\odot\ \text{AU}^{-3}.\end{aligned}$$

The stellar mass density is approximately $0.05\ \text{M}_\odot\ \text{pc}^{-3}$ in the solar neighborhood.

24.22 (a) The amount of mass located between $r = 0$ and r is given by integrating Eq. (10.7), or

$$M_r = \int_0^r 4\pi r^2 \rho(r)\, dr.$$

Substituting the mass density of dark matter (Eq. 24.51),

$$M_r = 4\pi\rho_0\, a^2 \int_0^r \frac{r^2}{1 + (r/a)^2}\, dr = 4\pi\rho_0\, a^2 \left[r - a\tan^{-1}\left(\frac{r}{a}\right)\right].$$

(b) Using $a = 2.8$ kpc, $M_r = 5.5 \times 10^{11}\ \text{M}_\odot$, and $r = 100$ kpc, gives $\rho_0 = 5.9 \times 10^7\ \text{M}_\odot\ \text{kpc}^{-3}$. If $M_r = 1.3 \times 10^{12}\ \text{M}_\odot$ within $r = 230$ kpc, then we also find that $\rho_0 = 5.9 \times 10^7\ \text{M}_\odot\ \text{kpc}^{-3}$.

(c) Using the value of ρ_0 found in part (b), $M_r = 2.6 \times 10^{11}\ \text{M}_\odot$. From Table 24.1, the mass of the stellar halo is $3 \times 10^9\ \text{M}_\odot$. Apparently the mass of dark matter far exceeds the mass of the stars in the Galaxy.

24.23 (a) If $r \ll a$, then $1 + r/a \simeq 1$ and $\rho_{\text{NFW}} \propto r^{-1}$. If $r \gg a$, then $1 + r/a \simeq r/a$ and $\rho_{\text{NFW}} \propto r^{-3}$.

(b) For the spherically-symmetric distribution

$$M = \int_0^\infty \rho(r)\, 4\pi r^2\, dr = 4\pi\rho_0\, a^3 \int_0^\infty \frac{r^2}{r\,(a + r)^2}\, dr.$$

For $r \gg a$, the integral looks like $\int_0^\infty r^{-1}\, dr$, which is $\ln r|_0^\infty$. Since $\ln r$ is unbounded, the mass is infinitely large.

24.24 Referring to Table 24.1, the mass of the dark-matter halo interior to 50 kpc is about 5.4×10^{11} $M_\odot$, while it is estimated to be 1.9×10^{12} $M_\odot$ interior to about 230 kpc. These values imply

$$\rho(50) = 1.0 \times 10^6 \text{ M}_\odot \text{ kpc}^{-3}$$

$$\rho(230) = 3.7 \times 10^4 \text{ M}_\odot \text{ kpc}^{-3}.$$

Using Eq. (24.52) and taking the ratio of the results gives

$$27.7 = \frac{(230/a)(1 + 230/a)^2}{(50/a)(1 + 50/a)^2} = \left(\frac{230}{50}\right)\left[\frac{(a + 230)^2}{(a + 50)^2}\right].$$

This gives

$$2.45 = \frac{a + 230}{a + 50},$$

or $a = 73.9$ kpc. Solving for the density immediately gives $\rho_0 = 1.9 \times 10^6$ $M_\odot$ kpc^{-3}.

24.25 (a) We need to put together all of the pieces to the structure of the Galaxy from Table 24.1, as well as include the contribution of dark matter to the total mass of the Galaxy. To include the later, we can integrate the NFW distribution (Eq. 24.52) from $r = 0$ to some $r = r_0$:

$$\begin{aligned} M_{\text{NFW}}(r_0) &= \int_0^{r_0} \rho_{\text{NFW}}(r)\, 4\pi r^2\, dr \\ &= 4\pi\rho_0 \int_0^{r_0} \frac{r^2}{(r/a)(1 + r/a)^2}\, dr \\ &= 4\pi\rho_0 a^3 \int_0^{r_0} \frac{r\, dr}{(a + r)^2} \\ &= 4\pi\rho_0 a^3 \left[\ln(a + r) + \frac{a}{a + r}\right]_0^{r_0} \\ &= 4\pi\rho_0 a^3 \left[\ln(1 + r_0/a) - \frac{r_0/a}{1 + r_0/a}\right]. \end{aligned}$$

This expression can be evaluated for various values of r_0 using the results obtained from Problem 24.24; $a = 73.9$ kpc and $\rho_0 = 1.9 \times 10^6$ $M_\odot$ kpc^{-3}. For $r_0 = 25$ kpc, $M_{\text{NFW}} = 3.7 \times 10^{11}$ $M_\odot$.

The mass of the visible components of the Galaxy interior to 25 kpc is (from Table 24.1) is 7.9×10^{10} $M_\odot$ (the stellar halo was neglected for $r < 25$ kpc but represents only a small component to the total mass).

The B-band luminosity for those components totals $L_B = 2.1 \times 10^{10}$ $L_\odot$. Thus, the mass-to-light ratio interior to $r_0 = 25$ kpc is approximately $M/L_B = 21.4$ $M_\odot/L_\odot$

(b) For $r_0 = 100$ kpc, $M_{\text{NFW}} = 2.7 \times 10^{12}$ $M_\odot$. This implies that the total mass interior to 100 kpc (including the stellar halo) is approximately 2.78×10^{12} $M_\odot$. The B-band luminosity is (again including the stellar halo) $L_B = 2.2 \times 10^{10}$ $M_\odot$, implying a mass-to-light ratio of 126 $M_\odot/L_\odot$.

The presence of dark matter increases the mass-to-light ratio significantly throughout the universe.

24.26 Integrating the gravitational "Gauss's law" gives

$$4\pi r^2 g = -4\pi G M_{\text{in}}.$$

Solving for g then gives $g = -GM_{\text{in}}/r^2$; the expected result.

24.27 (a) Consider a cylinder centered on the midplane with its ends oriented parallel to the midplane. Each end has an area A and is located a distance z from the midplane. Then, integrating Eq. (24.56) gives

$$2Ag = -4\pi GM_{\rm in} = -4\pi G\rho A(2z).$$

Solving for the gravitational acceleration gives

$$g = -4\pi G\rho z. \tag{S24.1}$$

(b) The gravitational acceleration is just $g = d^2z/dt^2$. Substituting the expression for g given in Eq. (S24.1) and rewriting gives

$$\frac{d^2z}{dt^2} + kz = 0,$$

where $k \equiv 4\pi G\rho$.

(c) The solutions for position and velocity are of the form

$$z(t) = z_0 \cos(\omega t + \delta)$$

$$w = \dot{z} = -\omega z_0 \sin(\omega t + \delta),$$

where $\omega = \sqrt{k} = \sqrt{4\pi G\rho}$, and δ is a phase constant.

(d) $P_{\rm osc} = \dfrac{2\pi}{\omega} = 6.8 \times 10^7$ yr.

(e) Let $t = 0$ when the Sun passes through the midplane, heading north. Then $\delta = -\pi/2$, and at the present time, $z_\odot = z_0 \sin\omega t$ and $w_\odot = \omega z_0 \cos\omega t$, where $z_\odot = 30$ pc (see Section 24.2) and $w_\odot = 7.2$ km s^{-1} (Eq. 24.35). Combining the equations leads to

$$\omega t = \tan^{-1}\left(\omega \frac{z_\odot}{w_\odot}\right) = 0.36 \text{ rad}.$$

Therefore, $z_0 = z_\odot/\sin\omega t = 85$ pc. This rough estimate compares well with the scale height of the thin disk (350 pc) quoted in Table 24.1.

(f) Since the Sun's orbital period is $P_{\rm orbit} = 2.2 \times 10^8$ yr, the number of oscillations per orbital period is $P_{\rm orbit}/P_{\rm osc} = 3.2$.

24.28 Carrying out the unit conversions:

$$d = \frac{\langle v_r \left(\text{km s}^{-1}\right)\rangle \tan\phi \left(\frac{10^3 \text{ m}}{1 \text{ km}}\right)\left(\frac{1 \text{ pc}}{3.08\times10^{16} \text{ m}}\right)}{\langle \mu'' \rangle \left(\frac{1'}{60''}\right)\left(\frac{1^\circ}{60'}\right)\left(\frac{2\pi^{\rm rad}}{360^\circ}\right)\left(\frac{1 \text{ yr}}{3.16\times10^7 \text{ s}}\right)}$$

$$= \frac{\langle v_r \rangle \tan\phi}{4.74\langle \mu'' \rangle}.$$

24.29 For Altair, $d = 5.14$ pc, $\mu'' = 0.66092''$ yr^{-1} and $v_r = -26.3$ km s^{-1}.

(a) $\phi = \tan^{-1}\left(\dfrac{4.74 d \langle \mu'' \rangle}{\langle v_r \rangle}\right) = -31.5^\circ$.

(b) $v_t = v_r \tan\phi = 16.1$ km s^{-1} and $v = \sqrt{v_r^2 + v_t^2} = 30.8$ km s^{-1}.

24.30 Using Newtonian gravity for a black hole of mass $M_{\rm bh} = 3.7 \times 10^6\ {\rm M}_\odot$ and Schwarzschild radius $R_S = 16\ {\rm R}_\odot$ (see Eq. 17.27),

$$\Delta U = -GM_{\rm bh}m\left(\frac{1}{r_f} - \frac{1}{R_S}\right) = 9 \times 10^{53}\ {\rm J}.$$

(This crude estimate is approximately two orders of magnitude larger than the value quoted in Section 24.2.) The typical kinetic energy of a Type II supernova is 10^{44} J, far below the estimate obtained here.

24.31 $\Delta M = \dot{M}\ \Delta t = 5 \times 10^6\ {\rm M}_\odot$, which is consistent with the estimate of a supermassive black hole.

24.32 (a) Assuming a maximum possible radius of Sgr A* equal to the closest approach of S2 (1.8×10^{13} m, the density would be $3 \times 10^{-4}\ {\rm kg\ m^{-3}}$.

(b) Assuming a maximum possible radius of 1 AU, the density would need to be $530\ {\rm kg\,m^{-3}}$, $8.8 \times 10^5\ {\rm M_\odot\ AU^{-3}}$, or $1 \times 10^{-10}\ {\rm M_\odot\ pc^{-3}}$.

24.33 From Eq. (2.33) for Newtonian mechanics, $v_p = 7.1 \times 10^6\ {\rm m\ s^{-1}} = 0.024c$.

24.34 According to Eq. (17.27), the Schwarzschild radius of a $M_{\rm bh} = 3.7 \times 10^6\ {\rm M}_\odot$ black hole is $R_S = 2GM_{\rm bh}/c^2 = 16\ {\rm R}_\odot$, implying that the average density of this supermassive black hole is

$$\rho_{\rm bh} = \frac{3.7 \times 10^6\ {\rm M}_\odot}{\frac{4}{3}\pi\ (16\ {\rm R}_\odot)^3} = 1.35 \times 10^6\ {\rm kg\ m^{-3}}.$$

The average density of the Sun is

$$\rho_{\rm Sun} = \frac{1\ {\rm M}_\odot}{\frac{4}{3}\pi\ (1\ {\rm R}_\odot)^3} = 1400\ {\rm kg\ m^{-3}}.$$

Thus, from Eq. (19.4) the Roche limit is,

$$r = 2.456\left(\frac{\rho_{\rm bh}}{\rho_{\rm Sun}}\right)^{1/3} R_S = 24.2\ R_S = 380\ {\rm R}_\odot.$$

24.35 Assuming $\kappa = 0.02\ {\rm m^2\ kg^{-1}}$, the Eddington luminosity (Eq. 10.114) gives $9 \times 10^{37}\ {\rm W} = 2 \times 10^{11}\ {\rm L}_\odot$. However, observations put an upper limit on the luminosity of $3 \times 10^4\ {\rm L}_\odot$. The Eddington luminosity exceeds the upper limit by 8,000,000 times.

24.36 (a) The isothermal component has a density of $\rho_i(r) = C'/r^2$, where C' is a constant. The interior mass due to that component is

$$M_{r,i} = \int_0^r 4\pi r^2 \rho_i(r)\, dr = 4\pi C' r.$$

Adding a single point mass (M_0) at the center gives

$$M_r = k\,r + M_0,$$

where $k \equiv 4\pi C'$.

(b) For Newtonian gravity and perfectly circular motion,

$$\frac{mv^2}{r} = \frac{GM_r m}{r^2},$$

or,

$$v = \left[\frac{GM_r}{r}\right]^{1/2} = \left[G\left(k + \frac{M_0}{r}\right)\right]^{1/2}.$$

(c) $k = v^2/G - M_0/r = 5.2 \times 10^{19}$ kg m^{-1}.

(d) See Fig. S24.4.

(e) See Fig. S24.5. The central black hole begins to become important at approximately $\log_{10} r = 0.5$, or $r = 3$ pc.

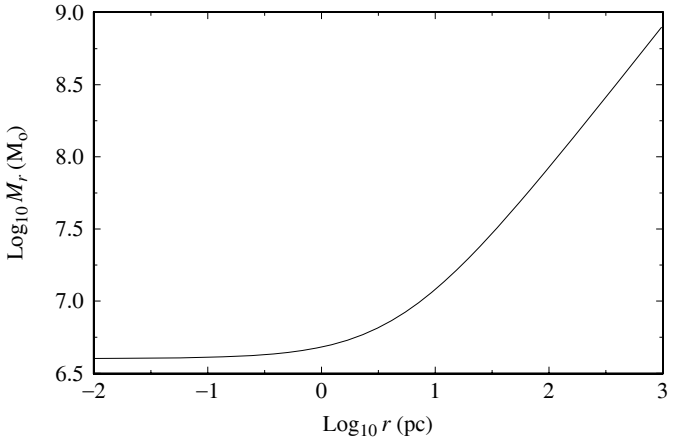

Figure S24.4: The solution for Problem 24.36(d).

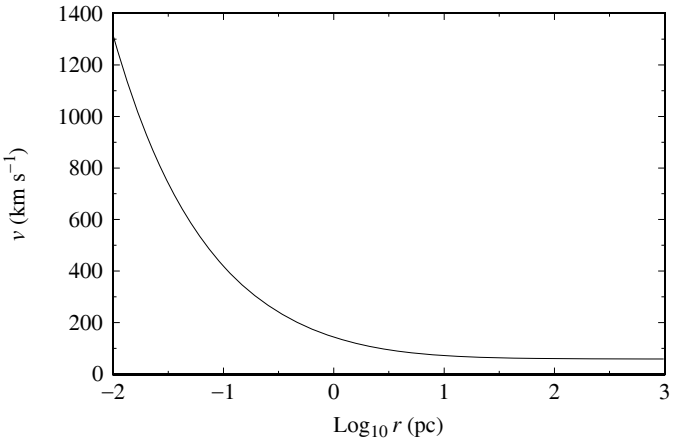

Figure S24.5: The solution for Problem 24.36(e).

CHAPTER 25

The Nature of Galaxies

25.1 Taking $d = 100$ kpc, or $r = 50$ kpc, and $\mu = 0.02'' \text{ yr}^{-1}$ implies $v = \mu r = 4730 \text{ km s}^{-1}$. For the Milky Way, $v_{\max} = 250 \text{ km s}^{-1}$.

25.2 (a) $R_{25} = 22.7$ kpc.

(b) $V_{\max} \simeq 181 \text{ km s}^{-1}$ for an Sc galaxy with $M_B = -21.51$.

(c) $\Omega = v/R = 2.6 \times 10^{-16} \text{ rad s}^{-1} = 0.00168'' \text{ yr}^{-1}$.

(d) It would have taken 600 yr to rotate through $1''$. Since maximum resolutions observable from the ground today are roughly $0.5''$, it is unlikely that van Maanen could have detected the rate of rotation.

25.3 (a) For the Sun, $L_B = 2.3 \times 10^{10} \text{ L}_\odot$. Since $M_{V,\text{Sun}} = 4.82$ and $B - V = 0.65$, we find $M_{B,\text{Sun}} = 5.47$. Thus, from Eq. (3.8), $M_B = M_{B,\text{Sun}} - 2.5 \log_{10}(L_B/L_\odot) = -20.4$.

(b) Using the relation for an Sb galaxy, $V_{\max} = 184 \text{ km s}^{-1}$. Observationally, $V_{\max} = 250 \text{ km s}^{-1}$.

25.4 Surface brightness is given by the amount of light contained in a cone of solid angle $\Omega = A/4\pi d^2$, where A is the surface area of the galaxy contained within the cone. For a given value of Ω, A increases as d^2, implying that the light-producing area increases as d^2. Therefore, the amount of light produced by area A, divided by A, is a constant.

25.5 Begin with Eq. (24.13),

$$\log_{10}\left(\frac{I}{I_e}\right) = -3.3307\left[\left(\frac{r}{r_e}\right)^{1/4} - 1\right].$$

Since the intensity is the luminosity per unit surface area of the galaxy,

$$I = \frac{\Delta L}{\Delta A},$$

or

$$\log_{10}\left(\frac{I}{I_e}\right) = \log_{10}\left(\frac{\Delta L/\Delta A}{\Delta L_e/\Delta A_e}\right) = \log_{10}\left(\frac{\Delta L}{\Delta L_e}\right) - \log_{10}\left(\frac{\Delta A}{\Delta A_e}\right).$$

Assuming for simplicity, that $\Delta A = \Delta A_e$ (the same unit surface area is being considered in each case), then

$$\log_{10}\left(\frac{I}{I_e}\right) = \log_{10}\left(\frac{\Delta L}{\Delta L_e}\right).$$

From $M = M_{\text{Sun}} - 2.5 \log_{10}(L/L_\odot)$ (Eq. 3.8),

$$\log_{10}\left(\frac{\Delta L}{\Delta L_e}\right) = \frac{\Delta M_e - \Delta M}{2.5},$$

where ΔM and ΔM_e are the absolute magnitudes of the small regions of the galaxy associated with ΔA and ΔA_e, respectively. Making the appropriate substitutions,

$$\frac{\Delta M_e - \Delta M}{2.5} = \frac{\mu_e - \mu}{2.5} = -3.3307\left[\left(\frac{r}{r_e}\right)^{1/4} - 1\right],$$

where we have replaced ΔM by μ and ΔM_e by μ_e since (1) we have assumed the same associated surface area, and (2) the solid angle is proportional to the surface area (assuming the same distance to any appropriate sample). Rearrangement leads immediately to Eq. (25.2).

25.6 According to Eq. (24.10),

$$L(R, z) = L_0 e^{-R/h_R} \operatorname{sech}^2(z/z_0).$$

Considering the case where $z = 0$,

$$\log_{10}\left[\frac{L(R)}{L_0}\right] = -\left(\frac{R}{h_R}\right)\log_{10} e = -0.434\left(\frac{R}{h_R}\right).$$

Following the procedure outlined in the solution to Problem 25.5 leads directly to Eq. (25.3).

25.7 (a) Eq. (24.13) leads immediately to

$$I(r) = I_e 10^{-3.3307[(r/r_e)^{1/4}-1]} = I_e e^{-b[(r/r_e)^{1/4}-1]}$$

where $b = 3.3308 \ln 10 = 7.67$.

(b)

$$L_{\text{tot}} = \int_0^\infty 2\pi r I(r)\, dr = 2\pi I_e e^b \int_0^\infty r e^{-b(r/r_e)^{1/4}} dr.$$

Letting $x \equiv b(r/r_e)^{1/4}$ implies $r = r_e(x/b)^4$ and $dr = 4r_e x^3/b^4\, dx$. Substituting,

$$L_{\text{tot}} = 8\pi I_e e^b r_e^2/b^8 \int_0^\infty x^7 e^{-x}\, dx = 8!\frac{e^b}{b^8}\pi r_e^2 I_e = 7.22\pi r_e^2 I_e.$$

(c) If the integration is carried out from $r = 0$ to $r = r_e$, then the limits of integration of the last integral of part (b) become $x = 0$ to $x = b$. Evaluating,

$$\int_0^b x^7 e^{-x}\, dx = 7!\left[e^{-x}\sum_{i=0}^{7}(-1)^i \frac{x^{7-i}}{(7-i)!(-1)^{i+1}}\right]_0^b = (0.5)\,7! = \frac{1}{2}\int_0^\infty x^7 e^{-x}\, dx.$$

Therefore $L(r_e) = \frac{1}{2}L_{\text{tot}}$.

25.8 (a) From Eqs. (25.4), $M_B = -21.8$.

(b) According to Eq. (3.6), $B - M_B = 5\log_{10}(d/10\text{ pc})$, or $d = 6.45$ Mpc.

(c) From Eq. (25.11), $R_{25} = 26.8$ kpc.

(d) $M_{25} = 6.5 \times 10^{11}\ \text{M}_\odot$ from Eq. (25.10).

(e) From Problem 25.3, $M_{B,\text{Sun}} = 5.47$. Then, according to Eq. (3.8), $L_B = 8.1 \times 10^{10}\ \text{L}_\odot$.

(f) $M_{25}/L_B = 8.0$.

25.9 For Sa, $\langle B - V\rangle = 0.75$, corresponding to spectral class G8; for Sb, $\langle B - V\rangle = 0.64$, which corresponds to spectral class G2; and for Sc, $\langle B - V\rangle = 0.52$, corresponding to F8.

25.10 The rotational velocity at $1''$ (3.7 pc) is about 50 km s^{-1}. From

$$\frac{v^2}{r} = \frac{GM}{r^2}$$

we find $M = 2.2 \times 10^6\ \text{M}_\odot$, well within the uncertainty range.

25.11 (a) The rotational velocity at 1″ (3.7 pc) is roughly 200 km s^{-1}. This implies a mass of $M = 3.5\times10^7\,\mathrm{M}_\odot$. This value is roughly four times smaller than the value quoted in the text.

(b) The peak of the velocity dispersion is almost 400 km s^{-1}. Again using $R = 3.7$ pc we find a virial mass of $M_{\rm virial} = 6.9\times10^8\,\mathrm{M}_\odot$.

(c) Recall that M31 has a complex, multi-component core.

25.12 Beginning with the Cartesian representation, $\mathbf{r} = x\hat{\mathbf{i}} + y\hat{\mathbf{j}} + z\hat{\mathbf{k}}$, and substituting $x = R\cos\phi$ and $y = R\sin\phi$ gives

$$\mathbf{r} = R\left(\cos\phi\hat{\mathbf{i}} + \sin\phi\hat{\mathbf{j}}\right) + z\hat{\mathbf{k}}.$$

Identifying $\hat{\mathbf{e}}_R = \hat{\mathbf{i}}\cos\phi + \hat{\mathbf{j}}\sin\phi$ and $\hat{\mathbf{e}}_z = \hat{\mathbf{k}}$ lead to Eq. (25.16).

25.13 Starting with Eq. (25.16),

$$\mathbf{r} = R\hat{\mathbf{e}}_R + z\hat{\mathbf{e}}_z,$$

and differentiating gives

$$\dot{\mathbf{r}} = \dot{R}\hat{\mathbf{e}}_R + R\dot{\hat{\mathbf{e}}}_R + \dot{z}\hat{\mathbf{e}}_z + z\dot{\hat{\mathbf{e}}}_z.$$

However, since the unit vector in the z direction always points in the same direction (i.e., it is *not* time dependent), $\dot{\hat{\mathbf{e}}}_z = 0$. Thus, differentiating again

$$\ddot{\mathbf{r}} = \ddot{R}\hat{\mathbf{e}}_R + 2\dot{R}\dot{\hat{\mathbf{e}}}_R + R\ddot{\hat{\mathbf{e}}}_R + \ddot{z}\hat{\mathbf{e}}_z. \tag{S25.1}$$

Now, differentiating the unit vector $\hat{\mathbf{e}}_R = \hat{\mathbf{i}}\cos\phi + \hat{\mathbf{j}}\sin\phi$, realizing that $\hat{\mathbf{i}}$ and $\hat{\mathbf{j}}$ are constants, and noting that $\hat{\mathbf{e}}_\phi = -\hat{\mathbf{i}}\sin\phi + \hat{\mathbf{j}}\cos\phi$, gives

$$\dot{\hat{\mathbf{e}}}_R = -\hat{\mathbf{i}}\sin\phi\,\dot{\phi} + \hat{\mathbf{j}}\cos\phi\,\dot{\phi} = \hat{\mathbf{e}}_\phi\dot{\phi}.$$

Taking the second time derivative,

$$\ddot{\hat{\mathbf{e}}}_R = \dot{\hat{\mathbf{e}}}_\phi\dot{\phi} + \hat{\mathbf{e}}_\phi\ddot{\phi}.$$

However, $\dot{\hat{\mathbf{e}}}_\phi = -\hat{\mathbf{e}}_R\dot{\phi}$, so

$$\ddot{\hat{\mathbf{e}}}_R = -\hat{\mathbf{e}}_R\dot{\phi}^2 + \hat{\mathbf{e}}_\phi\ddot{\phi}. \tag{S25.2}$$

Substituting Eq. (S25.2) into Eq. (S25.1) and rearranging leads to Eq. (25.18).

25.14 According to Eq. (25.34) for the Sun, $\rho(t) = A_R\sin\kappa_0 r$, so $\dot{\rho}(t) = \kappa_0 A_R\cos\kappa_0 t$. From Example 25.3.1, $\kappa_0 = 35.6$ km s^{-1} kpc^{-1}, and from Eq. (24.33), $\dot{\rho} = u_\odot = -9$ km s^{-1}. Assuming that the Sun is currently passing through equilibrium in its radial (epicycle) oscillation, $A_R = \dot{\rho}/\kappa_0 = 250$ pc.

25.15 (a) Beginning with Eq. (25.22), $\Phi_{\rm eff} = \Phi + J_z^2/2R^2$, where J_z is the *constant* angular momentum per unit mass. Differentiating,

$$\frac{\partial^2\Phi_{\rm eff}}{\partial R^2} = \frac{\partial}{\partial R}\left(\frac{\partial\Phi}{\partial R}\right) + \frac{3J_z^2}{R^4}. \tag{S25.3}$$

But $\partial\Phi/\partial R = \Theta^2/R$, so that

$$\frac{\partial}{\partial R}\left(\frac{\partial\Phi}{\partial R}\right) = \frac{2\Theta}{R}\frac{\partial\Theta}{\partial R} - \frac{\Theta^2}{R^2}.$$

Furthermore, $J_z = R\Theta$. Making the appropriate substitutions into Eq. (S25.3) and simplifying gives

$$\kappa^2 \equiv \frac{\partial^2\Phi_{\rm eff}}{\partial R^2} = 2\frac{\Theta_0}{R_0}\left[\frac{\Theta_0}{R_0} + \left.\frac{\partial\Theta_0}{\partial R}\right|_{R_0}\right],$$

which is Eq. (25.37).

(b) By combining Eqs. (24.39) and (24.40),

$$\left.\frac{\partial\Theta}{\partial R}\right|_{R_0} = -(A+B)$$

$$\frac{\Theta_0}{R_0} = A - B.$$

Substituting into Eq. (25.37), we arrive at Eq. (25.38):

$$\kappa_0^2 = 2(A-B)\left[(A-B)-(A+B)\right] = -4B(A-B).$$

25.16 For a Keplerian orbit, $\Theta^2/R = GM/R^2$,

$$\Theta = \left(\frac{GM}{R}\right)^{1/2}.$$

Differentiating,

$$\frac{\partial\Theta}{\partial R} = -\frac{1}{2}\frac{(GM)^{1/2}}{R^{3/2}}.$$

Substituting into Eq. (25.37) leads to

$$\kappa_0 = \frac{(GM)^{1/2}}{R_0^{3/2}}.$$

However, we also have that $\Omega_0 = \Theta_0/R_0 = (GM)^{1/2}/R_0^{3/2}$. Thus, $\chi_{\max}/\rho_{\max} = 2\Theta_0/\kappa_0 = 2$.

25.17 According to Eq. (24.13),

$$\log_{10}\left[\frac{I(r)}{I_e}\right] = -3.3307\left[\left(\frac{r}{r_e}\right)^{1/4} - 1\right],$$

implying

$$I(r) = I_e 10^{-3.3307\left[(r/r_e)^{1/4}-1\right]}.$$

This can be rewritten in terms of a power of e by realizing that if $10^x = e^y$, then $y = \ln 10^x = x\ln 10 = 2.3026x$. Therefore,

$$I(r) = I_e e^{-\alpha\left[(r/r_e)^{1/4}-1\right]},$$

where $\alpha = (2.3026)(3.3307) = 7.6692$.

Now, the integral average of the intensity is given by

$$\langle I\rangle = \frac{1}{\pi r_e^2}\int_0^{r_e} I_e e^{-\alpha\left[(r/r_e)^{1/4}-1\right]}\,2\pi r\,dr.$$

The integral can be evaluated by recalling that integrating the intensity over the surface area between $r = 0$ and $r = r_e$ (the effective radius) yields one-half of the entire luminosity of the galaxy, or

$$L_e = \int_0^{r_e} I(r)\,2\pi r\,dr = \frac{1}{2}\int_0^{\infty} I(r)\,2\pi r\,dr.$$

Substituting into our expression for the average intensity,

$$\langle I\rangle = \frac{I_e}{2\pi r_e^2}\int_0^{\infty} e^{-\alpha\left[(r/r_e)^{1/4}-1\right]}\,2\pi r\,dr = \frac{I_e e^{\alpha}}{r_e^2}\int_0^{\infty} e^{-\alpha(r/r_e)^{1/4}} r\,dr.$$

Making the substitution, $u \equiv \alpha\,(r/r_e)^{1/4}$ within the integral implies that $r/r_e = u^4/\alpha^4$ and $r\,dr = 4r_e^2 u^7 \alpha^{-8}\,du$. Therefore

$$\langle I \rangle = \frac{4I_e e^\alpha}{\alpha^8}\int_0^\infty u^7 e^{-u}\,du = \frac{4I_e e^\alpha}{\alpha^8}\,\Gamma(8) = \left[\frac{(4)(7!)e^\alpha}{\alpha^8}\right] I_e = 3.607 I_e.$$

25.18 Equation (25.2) states that

$$\mu(r) = \mu_e + 0.3268\left[\left(\frac{r}{r_e}\right)^{1/4} - 1\right].$$

Setting $\mu\,(r_H) = \mu_H = 26.5$ B-mag arcsec^{-2}, and solving for r_H gives

$$\begin{aligned} r_H &= r_e\left(\frac{\mu_H - \mu_e}{8.3268} + 1\right)^4 \\ &= r_e\left(\frac{26.5}{8.3268} - \frac{\mu_e}{8.3268} + 1\right)^4 \\ &= r_e\,(4.18 - 0.12\mu_e)^4\,. \end{aligned}$$

25.19 (a) From Problem 25.17, $\langle I \rangle = 3.607 I_e$, implying that $\log_{10}\langle I \rangle = \log_{10} 3.607 + \log_{10} I_e$. Following the procedure described in Problems 25.5 and 25.6, we arrive at $\langle \mu \rangle = \mu_e - 2.5\log_{10} 3.607 = \mu_e - 1.393$.

(b) $\mu_e = \langle \mu \rangle + 1.393 = 21.52 + 1.393 = 22.913$ B-mag arcsec^{-2}.

(c) $r_H = r_e\,(4.18 - 0.12\mu_e)^4 = 42.1$ kpc.

25.20 The virial theorem implies that $\sigma_r^4 \propto M^2/R^2$ [the square of Eq. (25.13)]. If the mass-to-light ratio is roughly the same for all elliptical galaxies, then $M/L = K_{ML}$ is a constant. Thus, $\sigma_r^4 \propto K_{ML}^2 L^2/R^2$. But, assuming that the average surface brightness is also essentially constant for all elliptical galaxies, then $L/R^2 \propto I$ is constant. Therefore, $\sigma_r^4 \propto L$.

25.21 (a) $m = -0.115$.

(b) The slope of Eq. (25.41) is $m = -0.1$. The slope of Fig. 25.33 is close to, but not exactly the same as the slope of Eq. (25.41). The difference is due in part to systematic variations in surface brightness.

25.22 (a) From Eq. (25.15), $S_N = N_t 10^{0.4(M_V+15)} = (350)\,10^{0.4(-21.7+15)} = 0.73$.

(b) $S_N = 18.6$.

(c) The relative abundance of globular clusters per luminosity interval in CDs far exceeds the values found in spirals. If CDs are produced via mergers with spirals then apparently globular clusters must be formed in the process.

25.23 (a) Assuming that all terms beyond first-order are zero, Eq. (25.44) becomes

$$a(\theta) = a_0 + a_2\cos(2\theta).$$

But, from Eq. (25.1), $\beta/\alpha = 1 - \epsilon$, where $\alpha = a\,(0°) = a_0 + a_2$ and $\beta = a\,(90°) = a_0 - a_2$. Substituting,

$$a_0 - a_2 = (a_0 + a_2)(1 - \epsilon).$$

Solving for a_2 gives

$$a_2 = \left(\frac{\epsilon}{2 - \epsilon}\right) a_0.$$

(b) For an E4 galaxy with $a_0 = 30$ kpcs and $\epsilon = 0.4$, $a_2 = 7.5$ kpc. The polar-coordinate plot is shown in Fig. S25.1.

(c) See Fig. S25.1.

(d) See Fig. S25.1.

(e) $a_4 = +0.1a_0$ looks more like a lenticular galaxy than does $a_4 = -0.1a_0$.

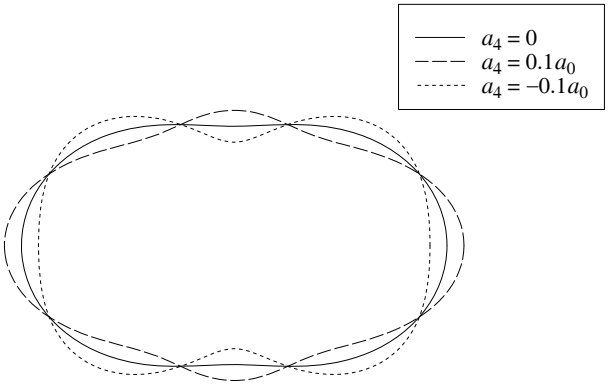

Figure S25.1: The results of Problem 25.23.

25.24 See Fig. S25.2. The results look qualitatively similar to Eq. (25.46).

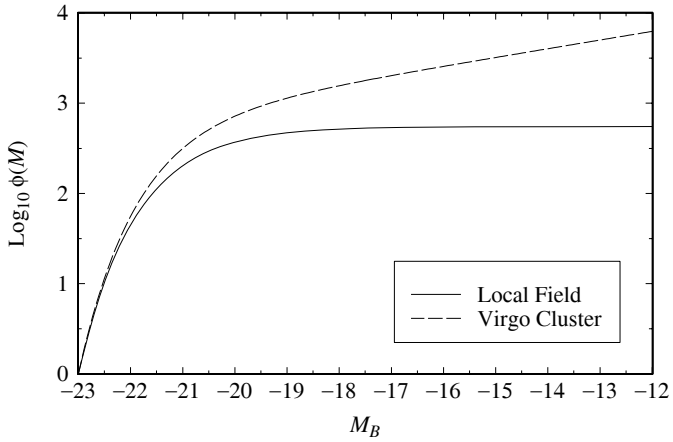

Figure S25.2: The results of Problem 25.24.

CHAPTER 26

Galactic Evolution

26.1 (a) From Appendix G, the mass and radius of a main-sequence M0 star are $M = 0.51\ M_\odot$ and $R = 0.63\ R_\odot$, respectively. If the mass density of stars near the Sun is $\rho = 0.05\ M_\odot\ \text{pc}^{-3}$, then the number density of stars may be estimated as $n = \rho/M = 0.098\ \text{pc}^{-3}$. The average volume of Galactic space per star is $V_{\text{space}} = 1/n$, and the volume of a single M0 star is

$$V_{\text{star}} = \frac{4}{3}\pi R^3 = 3.5 \times 10^{26}\ \text{m}^3 = 1.2 \times 10^{-23}\ \text{pc}^3.$$

The fraction of Galactic space occupied by stars is

$$f = \frac{V_{\text{star}}}{V_{\text{space}}} = nV_{\text{star}} = 1.2 \times 10^{-24}.$$

(b) If an intruder M0 star travels through the Galactic stars, the mean free path between collisions is given by Eq. (9.12), $\ell = 1/n\sigma$, where the collision cross section is

$$\sigma = \pi(2R)^2 = 2.4 \times 10^{18}\ \text{m}^2 = 2.5 \times 10^{-15}\ \text{pc}^2.$$

The mean free path is therefore $\ell = 1/n\sigma = 4.0 \times 10^{15}$ pc. If the thickness of the Galactic disk is about $z \approx 1$ kpc, then the probability of a stellar collision with the intruder star during its perpendicular passage through the disk is only $z/\ell \approx 2.5 \times 10^{-13}$.

26.2 Assume that the force of dynamical friction is given by a expression of the form

$$f_d \simeq C(GM)^\alpha (v_M)^\beta \rho^\gamma,$$

where C is dimensionless and the values of the exponents α, β, and γ are to be determined. Let $[x]$ designate the units of the variable x, so

$$[f_d] = \text{kg m s}^{-2}$$
$$[GM] = \text{m}^3\ \text{s}^{-2}$$
$$[v_M] = \text{m s}^{-1}$$
$$[\rho] = \text{kg m}^{-3}.$$

The units involved in the expression for f_d are therefore

$$\text{kg m s}^{-2} = (\text{m}^3\ \text{s}^{-2})^\alpha (\text{m s}^{-1})^\beta (\text{kg cm}^{-3})^\gamma.$$

which leads to

$$\gamma = 1$$
$$3\alpha + \beta - 3\gamma = 1$$
$$-2\alpha - \beta = -2.$$

Solving for the exponents, we find $\alpha = 2$, $\beta = -2$, and $\gamma = 1$. Therefore,

$$f_d \simeq C\,\frac{G^2 M^2 \rho}{v_M^2},$$

which is Eq. (26.1).

26.3 From Eq. (26.3), the greatest distance from which a globular cluster could have spiraled into the Galactic nucleus is

$$r_{\max} = \sqrt{\frac{t_{\max} C G M}{2\pi v_M}}.$$

Using $C = 76$ for globular clusters, with $t_{\max} = 13$ Gyr for the oldest globular clusters, $M = 5 \times 10^6\ \mathrm{M}_\odot$ for the cluster's mass, and $v_M = 220\ \mathrm{km\ s^{-1}}$ for the orbital speed of the local standard of rest (Eq. 24.36), we obtain $r_{\max} = 1.2 \times 10^{20}\ \mathrm{m} = 4$ kpc. This is similar to the size of the Milky Way's central bulge (Table 24.1).

26.4 (a) The time for the LMC to spiral into the Milky Way may be estimated from Eq. (26.2),

$$t_c = \frac{2\pi v_M r_i^2}{CGM}.$$

With $v_M = 220\ \mathrm{km\ s^{-1}}$, $r_i = 51$ kpc, $C = 23$, and $M = 2 \times 10^{10}\ \mathrm{M}_\odot$, this is $t_c = 5.4 \times 10^{16}\ \mathrm{s} = 1.7$ Gyr.

(b) The time quoted in the text, some 14 billion years, is about eight times longer than our estimate here.

26.5 Treating the Milky Way and the LMC as a binary system with a separation of $d_{\mathrm{LMC}} = 51$ kpc, we can use Eq. (18.10) to estimate the tidal radius of the LMC due to the Milky Way. From Table 24.1, we take $M_1 = 5.4 \times 10^{11}\ \mathrm{M}_\odot$ for the Milky Way within 50 kpc of the center (including its dark matter halo) and $M_2 = 2 \times 10^{10}\ \mathrm{M}_\odot$ for the LMC to find

$$\ell_2 = d_{\mathrm{LMC}}\left[0.500 + 0.227 \log_{10}\left(\frac{M_2}{M_1}\right)\right] = 8.9\ \mathrm{kpc}.$$

If the angular diameter of the LMC is $\theta = 460' = 0.134$ rad, then its linear radius is $r_{\mathrm{LMC}} = d_{\mathrm{LMC}}\theta/2 = 3.3$ kpc. Since $r_{\mathrm{LMC}} < \ell_2$, the LMC lies within its tidal radius.

26.6 In this problem, we treat the LMC and the SMC as a binary system.

(a) Applying the law of cosines to the triangle formed by the LMC, the SMC, and Earth, the present distance between the LMC and the SMC is found to be

$$\begin{aligned} a_0 &= \left[(51\ \mathrm{kpc})^2 + (60\ \mathrm{kpc})^2 - 2(51\ \mathrm{kpc})(60\ \mathrm{kpc})\cos 21^\circ\right]^{1/2} \\ &= 22.3\ \mathrm{kpc}. \end{aligned}$$

(b) The present tidal radii of the LMC and the SMC due to the other may be estimated from Eqs. (18.9) and (18.10). We find

$$\ell_{\circ,\mathrm{LMC}} = a_0\left[0.500 - 0.227 \log_{10}\left(\frac{M_{\mathrm{SMC}}}{M_{\mathrm{LMC}}}\right)\right] = 16.2\ \mathrm{kpc}$$

$$\ell_{\circ,\mathrm{SMC}} = a_0\left[0.500 + 0.227 \log_{10}\left(\frac{M_{\mathrm{SMC}}}{M_{\mathrm{LMC}}}\right)\right] = 6.1\ \mathrm{kpc},$$

using $M_{\mathrm{SMC}}/M_{\mathrm{LMC}} = 0.1$.

(c) The distance between the LMC and the SMC varies with time as $a(t) = a_0 + vt$, where $v = 110\,\text{km s}^{-1}$. The tidal radius of the LMC as a function of time may therefore be estimated as

$$\ell_{\text{LMC}}(t) = (a_0 + vt)\left[0.500 - 0.227\log_{10}\left(\frac{M_{\text{SMC}}}{M_{\text{LMC}}}\right)\right].$$

Setting $\ell_{\text{LMC}}(t) = r_{\text{LMC}} = 3.3$ kpc (from Problem 26.5) shows that the LMC last extended beyond its tidal radius when

$$t = \frac{r_{\text{LMC}} - \ell_{0,\text{LMC}}}{v\,[0.500 - 0.227\log_{10}(M_{\text{SMC}}/M_{\text{LMC}})]} = -5.0 \times 10^{15}\text{ s} = -1.6 \times 10^{8}\text{ yr}.$$

At a distance of $d_{\text{SMC}} = 60$ kpc, the angular diameter of the SMC is $\theta = 150' = 0.0436$ rad, so its linear radius is $r_{\text{SMC}} = d_{\text{SMC}}\theta/2 = 1.3$ kpc. The tidal radius of the SMC as a function of time may be estimated as

$$\ell_{\text{SMC}}(t) = (a_0 + vt)\left[0.500 + 0.227\log_{10}\left(\frac{M_{\text{SMC}}}{M_{\text{LMC}}}\right)\right].$$

Setting $\ell_{\text{SMC}}(t) = r_{\text{SMC}} = 1.3$ kpc, we find that the SMC last extended beyond its tidal radius when

$$t = \frac{r_{\text{SMC}} - \ell_{0,\text{SMC}}}{v\,[0.500 + 0.227\log_{10}(M_{\text{SMC}}/M_{\text{LMC}})]} = -4.9 \times 10^{16}\text{ s} = -1.6 \times 10^{8}\text{ yr}.$$

According to these results, the Magellanic Stream was formed before about 160 million years ago by the LMC and the SMC.

26.7 (a) The semimajor axis of the gaseous ring orbiting the central galaxies of the M96 group is $a = 101$ kpc. The motion of a parcel of gas obeys Kepler's third law (Eq. 2.37). With $P = 4.1\times10^9$ yr, $m_1 = M_{\text{galaxies}}$ and $m_2 = m_{\text{gas}} \ll M_{\text{galaxies}}$, the combined mass of the central galaxies M105 and NGC 3394 is

$$M_{\text{galaxies}} \simeq \frac{4\pi^2 a^3}{P^2 G} = 1.07 \times 10^{42}\text{ kg} = 5.38 \times 10^{11}\,\text{M}_\odot.$$

(b) $M_{\text{galaxies}}/L = 23$.

26.8 Making the assumption that $r \gg a$, Eq. (24.51) becomes

$$\rho(r) \simeq \frac{C_0}{r^2}.$$

For a spherically symmetric mass distribution, only M_r (the mass interior to r) will affect a test particle's motion, where

$$M_r = \int_0^r \rho(r)\,4\pi r^2\,dr = 4\pi C_0 r.$$

Thus, the radial equation of motion becomes

$$\frac{d^2r}{dt^2} = -\frac{GM_r}{r^2} = -\frac{4\pi G C_0}{r}.$$

Multiplying through by $v = dr/dt$, and integrating,

$$\int_0^t v\,\frac{dv}{dt}\,dt = -\int_{r_0}^r \frac{4\pi G C_0}{r}\,dr,$$

which gives

$$v^2 = 8\pi G C_0 \ln\left(\frac{r_0}{r}\right).$$

Taking the square root and choosing the minus sign since the nebula is collapsing,

$$\frac{dr}{dt} = -\left(8\pi G C_0\right)^{1/2}\left[\ln\left(\frac{r_0}{r}\right)\right]^{1/2}.$$

Integrating again,

$$\int_{r_0}^{0} \frac{dr}{\left[\ln\left(\frac{r_0}{r}\right)\right]^{1/2}} = -\int_0^{t_{\rm ff}} \left(8\pi G C_0\right)^{1/2}\, dt.$$

Setting $u \equiv r/r_0$, and solving for $t_{\rm ff}$ gives

$$t_{\rm ff} = \frac{1}{\left(8\pi G C_0\right)^{1/2}} \int_0^1 \frac{r_0\, du}{\left[\ln\left(\frac{1}{u}\right)\right]^{1/2}} = \frac{r_0}{\left(8 G C_0\right)^{1/2}}.$$

The free-fall time is proportional to r_0.

26.9 There was an error in the first printing of *An Introduction to Modern Astrophysics*. The value of x should have been $x = 1.8$.

(a) Integrating Eq. (26.5),

$$N_{\Delta M} = \int_{M_1}^{M_2} C M^{-(1+x)}\, dM = \frac{C}{x}\left(M_1^{-x} - M_2^{-x}\right).$$

Thus, the ratio of the number of stars formed with masses between 2–3 $M_\odot$ and 10–11 $M_\odot$ is

$$\frac{N_{\Delta M}|_{2-3}}{N_{\Delta M}|_{10-11}} = \frac{2^{-1.8} - 3^{-1.8}}{10^{-1.8} - 11^{-1.8}} = 59.5.$$

(b) Writing Eq. (24.12) in solar units, $L = M^\alpha$. Solving for M and differentiating,

$$\frac{dM}{dL} = \frac{1}{\alpha} L^{(1-\alpha)/\alpha}.$$

Applying the chain rule,

$$\frac{dN}{dL} = \frac{dN}{dM}\,\frac{dM}{dL} = \left[C M^{-(1+x)}\right]\left[\frac{1}{\alpha} L^{(1-\alpha)/\alpha}\right].$$

Replacing M using the mass–luminosity relation leads to

$$\frac{dN}{dL} = \frac{C}{\alpha} L^{-(x+\alpha)/\alpha}.$$

(c) Following a procedure similar to part (a),

$$N_{\Delta L} = -\frac{C}{x}\left(L_2^{-x/\alpha} - L_1^{-x/\alpha}\right).$$

Therefore,

$$\frac{N_{\Delta L}|_{2-3}}{N_{\Delta L}|_{10-11}} = \frac{2^{-1.8/4} - 3^{-1.8/4}}{10^{-1.8/4} - 11^{-1.8/4}} = 8.20.$$

(d) More massive stars are much brighter.

26.10 The star formation rate is roughly 5.0 $M_\odot$ pc^{-2} Gyr^{-1}. Assuming that most of the dust and gas within the thin disk is located inside the solar circle, the total mass of stars formed in one year would be

$$M = \left(5\ M_\odot\ \text{pc}^{-2}\ \text{Gyr}^{-1}\right)(\pi)\,(8000\ \text{pc})^2\left(10^{-9}\ \text{Gyr}\right) = 1\ M_\odot.$$

Assuming that the average mass of each star formed is approximately 0.5 $M_\odot$, then roughly two stars are formed per year in the Milky Way Galaxy.

26.11 (a) From the data in Example 26.2.2, $T_{\text{virial}} = 6 \times 10^5$ K, $\mu = 0.6$, and $n = 5 \times 10^4$ m^{-3}, implying $\rho = \mu m_H n = 5 \times 10^{-23}$ kg m^{-3}. Then from Eq. (12.14),

$$M_J \simeq \left(\frac{5kT}{G\mu m_H}\right)^{3/2}\left(\frac{3}{4\pi\rho_0}\right)^{1/2} = 5.3 \times 10^{11}\ M_\odot.$$

(b) Assuming that $T_{\text{virial}} \simeq 10^4$ K and all other values are as given in part (a), then $M_J = 1.1 \times 10^9\ M_\odot$.

(c) Using $T \simeq 6 \times 10^5$ K, Eq. (12.16) gives

$$R_J = \left(\frac{15kT}{4\pi G\mu m_H \rho_0}\right)^{1/2} = 55\ \text{kpc}.$$

This value is comparable to the radius of the stellar halo ($R = 50$ kpc).

26.12 (a) The cooling time scale is given by Eq. (26.8),

$$t_{\text{cool}} = \frac{3}{2}\frac{kT_{\text{virial}}}{n\Lambda},$$

and the free-fall time scale is given by Eq. (12.26),

$$t_{\text{ff}} = \left(\frac{3\pi}{32}\frac{1}{G\rho_0}\right)^{1/2}.$$

Equating the two time scales, replacing T_{virial} with the expression for the virial temperature given by Eq. (26.7),

$$T_{\text{virial}} = \frac{\mu m_H \sigma^2}{3k},$$

where (see Eq. 26.6)

$$\sigma = \left(\frac{3}{5}\frac{GM}{R}\right)^{1/2},$$

and noting that $\rho_0 = 4M/3\pi R^3$ (assuming spherical symmetry) and $n = \rho/\mu m_H$, leads to the desired result.

(b) Assuming $\mu = 0.6$ gives $M = 7 \times 10^{12}\ M_\odot$.

26.13 (a) Taking $M = 3 \times 10^{13}\ M_\odot$ and $R = 300$ kpc, Kepler's third law (Eq. 2.37) implies an orbital period of

$$P = \frac{4\pi R^{3/2}}{G^{1/2}M^{1/2}} = 1.8 \times 10^{17}\ \text{s} = 5.6\ \text{Gyr}.$$

This is roughly one-third the age of the Milky Way Galaxy.

(b) M87 is not in virial equilibrium. Objects near the outer edges of the galaxy take too long to orbit relative to the age of the universe.

26.14 (a) $v = 2\pi R/P = 2\pi(300 \text{ kpc})/5.6 \text{ Gyr} = 330 \text{ km s}^{-1}$.

(b) If $v \simeq \sigma$, then from Eq. (26.7),

$$T_{\text{virial}} = \frac{\mu m_H \sigma^2}{3k} = 2.6 \times 10^6 \text{ K},$$

where $\mu = 0.6$ has been assumed.

(c) The number density of particles is roughly

$$n = \frac{\rho}{\mu m_H} = \frac{M}{\mu m_H \left(\frac{4}{3}\pi R^3\right)} = 1.8 \times 10^4 \text{ m}^{-3}.$$

Substituting this value into the expression for the cooling time scale (Eq. 26.8) gives

$$t_{\text{cool}} = \frac{3}{2}\frac{kT_{\text{virial}}}{n\Lambda} = 9.5 \times 10^8 \text{ yr}.$$

(d) Using $\rho_0 = \mu m_H n = 1.8 \times 10^{-23} \text{ kg m}^{-3}$, the free-fall time scale is (see Eq. 12.26)

$$t_{\text{ff}} = \left(\frac{3\pi}{32}\frac{1}{G\rho_0}\right)^{1/2} = 5 \times 10^8 \text{ yr}.$$

This is approximately one-half of the cooling time scale.

26.15 Using $T \simeq 10^4$ K, $m \simeq m_H$, and $\rho_0 \simeq 0.15 \text{ M}_\odot \text{ pc}^{-3}$ gives $h(T) = 0.22$ kpc. This corresponds to the neutral gas component of the Milky Way (see Table 24.1).

26.16 The current rate of star formation is SFR $= 5 \text{ M}_\odot \text{ pc}^{-2} \text{ Gyr}^{-1}$, and the mass of neutral gas in the Galaxy is $5 \times 10^9 \text{ M}_\odot$ (see Table 24.1). If we assume uniform star formation within the Galactic disk interior to the solar circle ($R_0 = 8$ kpc), then the time remaining for star formation is

$$t \simeq \frac{M_{\text{gas}}}{(\text{SFR})\left(\pi R_0^2\right)} = 5 \text{ Gyr}.$$

This would be prolonged by capturing other small galaxies, as well as adding new material to the ISM via stellar mass loss.

26.17 (a) Choosing the upper limits for dwarf elliptical galaxies listed in Table 25.4, $M \sim 10^9 \text{ M}_\odot$ and $R \sim 5$ kpc. Then Eq. (2.17) gives $v_{\text{esc}} \sim 42 \text{ km s}^{-1}$.

(b) From the information given in Section 15.3, $v_{\text{SN}} \simeq 0.1c = 3 \times 10^4 \text{ km s}^{-1}$. Thus, $v_{\text{SN}} \gg v_{\text{esc}}$.

(c) The thermal velocity is $v_{\text{thermal}} = \sqrt{3kT/m_H} = 160 \text{ km s}^{-1}$, and so $v_{\text{thermal}} > v_{\text{esc}}$.

(d) These galaxies lost their gas early in their histories and have ceased forming new stars. Hence they are now primarily composed of ancient stars.

26.18 (a) At about 210 million years (step 175), a spiral structure begins to develop, becoming clear by 240 million years (step 200). The appearance of the target and intruder galaxies begins to resemble the Whirlpool galaxy and its companion as an apparent bridge of stars connecting the two galaxies develops sometime around 270 million years (step 225). It reaches a "best match" between approximately 300 million years (step 250) and 330 million years (step 275). The apparent bridge begins to fade around 360 million years (step 300), becomes disrupted by about 420 million years (step 350), and is nearly gone after about 450 million years (step 375).

(b) Near the end of the 648 million-year time period, the spiral arms begin to dissipate, and many of the stars have apparently escaped from the central nucleus of the target galaxy.

(c) In this case, the intruder galaxy passes by in a direction opposite to the orbital motion of the stars in the target galaxy. Small, relatively tight spiral arms begin to develop around 240 million years (step 200), but they tend to wind back up again and are gone by 330 million years (step 275). The final result is a galaxy with a disrupted disk. No stars escape from the central nucleus of the target galaxy.

26.19 (a) The initial speed of the intruder galaxy matches the orbital speed of the nearby stars in the outer ring. Stars behind the intruder gain energy as they are pulled forward and up out of the plane of the disk. They form the "bridge" of stars that appears to link the target galaxy with the intruder. Stars behind the intruder are pulled backward; they lose energy and drop into lower orbits with larger angular velocities. As a result, these stars overtake the stars in higher orbits to form a loop of stars. These loops comprise the spiral arm that develops opposite the "bridge."

(b) In this case, the intruder galaxy passes by in a direction opposite to the orbital motion of the stars in the target galaxy. The intruder spends a relatively brief time near any single star, and succeeds only in pulling a "spike" of stars up out of the plane of the target galaxy. Orbital motion carries the spike away from the intruder galaxy, and differential rotation causes the development and then the winding up of a tight spiral feature. Less energy is transferred to the stars in their short encounter with the intruder, and no stars escape from the gravity of the target nucleus.

26.20 (a) The intruder galaxy pulls rings of stars up and away from the nucleus of the target galaxy. At first these stellar rings contract, and then expand. Such a process could produce a ring galaxy such as the Cartwheel.

(b) As the intruder galaxy pulls inward on a star in the ring, the force of gravity does positive work on the star and increases its energy as the star approaches the target nucleus. The star's orbit becomes more energetic, with a larger semimajor axis (c.f., Eq. 2.35), and it also becomes elongated ($e \neq 0$). After reaching perigalacticon, the star's new orbit carries it away from the nucleus, and the ring expands. If the star gains enough energy, it may no longer be bound to the target nucleus. [To see these effects, rerun the program with just two rings containing one star each, changing v_z from -1 to -2. Follow the motion for at least 720 million years (600 steps).]

(c) A nearly head-on collision is usually required to produce a ring galaxy, with values of the initial x-coordinate ranging from 0 to 2. Although values of 3 or greater typically result in a significant disruption of the target galaxy, an elliptical ring may be produced by larger values, such as 7.5.

CHAPTER 27

The Structure of the Universe

27.1 The periods of classical Cepheids range from 1 – 50 days (Table 14.1). Setting Eqs. (14.1) and (27.1) for $M_{\langle V\rangle}$ equal to each other,

$$-2.81\log_{10} P_d - 1.43 = -3.53\log_{10} P_d - 2.13 + 2.13(B-V),$$

and solving for $(B-V)$ gives the estimates

$$\begin{aligned} B-V &= 0.338\log_{10} P_d + 0.329 \\ &= 0.329 \quad \text{for } P_d = 1 \text{ d} \\ &= 0.903 \quad \text{for } P_d = 50 \text{ d}. \end{aligned}$$

27.2 (a) On Fig. 15.14, the major axis of the ring of SN 1987A measures $a = 19$ mm, and the minor axis measures $b = 14$ mm. Thus if θ is the angle between the plane of the ring and the plane of the sky, $\cos\theta = b/a = 0.7368$, so $\theta = 42.5°$.

(b) If D is the linear diameter of the ring, then light from the far side must travel an extra distance of $D\sin\theta$ to reach Earth. It took light an extra $\Delta t = 340$ days to make the trip, so $D\sin\theta = c\,\Delta t$, or

$$D = \frac{c\,\Delta t}{\sin\theta} = 1.30\times10^{18} \text{ cm} = 0.422 \text{ pc}.$$

(c) Since the long axis of the light ring has a length D and subtends an angle $\alpha = 1.66'' = 8.05\times10^{-6}$ rad, the distance to SN 1987A is $d = D/\alpha = 52.4$ kpc.

27.3 The average visual absolute magnitude of a galaxy's three brightest red stars is $M_V = -8.0$. We can use Eq. (12.1) to find the distance to M101,

$$d = 10^{(V-M_V-a+5)/5} = 10^{[20.9-(-8.0)-0.3+5]/5} \text{ pc} = 5.2 \text{ Mpc}.$$

This is about 30% below the value of 7.5 Mpc obtained using classical Cepheids.

27.4 The distance modulus (Eq. 3.6) is

$$m - M = 5\log_{10}(d) - 5.$$

Let $\Delta(m-M)$ represent an error in the distance modulus. Then

$$\Delta(m-M) = 5\log_{10} e\left(\frac{\Delta d}{d}\right) = 2.17\,\frac{\Delta d}{d}.$$

Solving for the fractional error in d we find

$$\frac{\Delta d}{d} = \frac{\Delta(m-M)}{2.17}.$$

An error in $m-M$ of 0.4 results in an error in the distance estimate of 18.4%. To produce a 5% uncertainty in the distance, the error in $m-M$ would be 0.11. For an uncertainty of 50%, $\Delta(m-M) = 1.1$.

27.5 From Eq. (27.5) with $C_{\text{Fornax}} = -1.264$, $C_{\text{Virgo}} = -1.237$, $C_{\text{Coma}} = -1.967$, we find

$$\frac{d_{\text{Virgo}}}{d_{\text{Fornax}}} = 10^{C_{\text{Fornax}} - C_{\text{Virgo}}} = 0.940$$

and

$$\frac{d_{\text{Coma}}}{d_{\text{Fornax}}} = 10^{C_{\text{Fornax}} - C_{\text{Coma}}} = 5.05.$$

27.6 From Hubble's velocity–distance diagram, Fig. 27.7, the solid line extends from the origin and reaches 1000 km s^{-1} at a distance of 1.96 Mpc. The slope of the line is $H_0 = 510$ km s^{-1} Mpc^{-1}. This is much larger than today's WMAP value of $H_0 = 71$ km s^{-1} Mpc^{-1}. In 1929, when Hubble published his first velocity–distance diagram, Trumpler's demonstration of interstellar extinction was still a year in the future, and Baade's distinction between classical Cepheids and W Virginis stars would not be made until 1952. Hubble calculated that his galaxies were closer than their actual distances, so his diagram showed that velocity increases more rapidly with distance than it actually does.

27.7 Use Eq. (27.16),

$$v^2 - \frac{2GM}{r} + \left(\frac{2\pi GM}{P}\right)^{2/3} = 0,$$

with $r = 770$ kpc, $v = 119$ km s^{-1}, and $P = t_H + t_c = t_H + r/v$. For $h = 0.5$, the Hubble time is $t_H = 6.18 \times 10^{17}$ s (Eq. 27.14). Numerically solving this cubic equation for M, we find that $M = 6.62 \times 10^{42}$ kg $= 3.33 \times 10^{12}$ M$_\odot$. Using the total B-band luminosity for the Milky Way and Andromeda given in the text of about $L = 6.9 \times 10^{10}$ L$_\odot$, we find $M/L_B = 48$ M$_\odot$/L$_\odot$.

27.8 (a) From Kepler's third law, Eq. (2.37),

$$P^2 = \left(\frac{2\pi a}{v}\right)^2 = \frac{4\pi^2}{G(M_{\text{MW}} + M_{\text{gas}})}\, a^3.$$

Using $a = 75$ kpc and $v = 244$ km s^{-1}, we can solve for the mass of the Milky Way, M_{MW} (assuming that the mass of the clump of gas is negligible compared with that of the Milky Way). We obtain

$$M_{\text{MW}} = \frac{v^2 a}{G} = 2.06 \times 10^{42} \text{ kg} = 1.04 \times 10^{12} \text{ M}_\odot.$$

Taking $L_B = 2.3 \times 10^{10}$ L$_\odot$ from Table 24.1, we find $M/L_B = 45$ M$_\odot$/L$_\odot$.

(b) From conservation of energy and Eq. (2.14),

$$\frac{1}{2}m\left(v_r^2 + v_t^2\right)_i - G\frac{Mm}{r_i} = \frac{1}{2}m\left(v_r^2 + v_t^2\right)_f - G\frac{Mm}{r_f},$$

where M and m are the masses of the Milky Way and the clump of gas, respectively, and v_r and v_t are the radial and transverse components of the clump's velocity. The initial radial velocity is zero and the transverse velocity does not change, so

$$M = \frac{v_r^2}{2G(1/r_f - 1/r_i)}.$$

With $r_i = 100$ kpc, $r_f = 50$ kpc, and a final radial velocity of $v_r = -220$ km s^{-1}, the mass of the Milky Way is estimated as $M = 1.1 \times 10^{42}$ kg $= 5.6 \times 10^{11}$ M$_\odot$. Using $L_B = 2.3 \times 10^{10}$ L$_\odot$ for the Milky Way (Table 24.1), we find $M/L_B = 24$ M$_\odot$/L$_\odot$.

27.9 The distance to the Sculptor group is $d = 1.8$ Mpc, and the group subtends an angle of about $\theta = 20° = 0.349$ rad. The distances to the front and back of the group are $d_{\rm front} = d(1 - \theta/2) = 1.49$ Mpc and $d_{\rm back} = d(1 + \theta/2) = 2.11$ Mpc. For two identical stars with the same absolute magnitude, M, located at the front and back of the group, Eq. (3.6) for the distance modulus, $m - M = 5\log_{10}(d) - 5$, shows that

$$m_{\rm back} - m_{\rm front} = 5\log_{10}\left(\frac{d_{\rm back}}{d_{\rm front}}\right) = 0.755.$$

27.10 Start with Eq. (10.6),

$$\frac{dP}{dr} = -G\frac{M_r\rho}{r^2},$$

and use the ideal gas law (Eq. 10.11) to substitute for P. Assuming that μ is a constant, we have

$$\frac{d}{dr}\left(\frac{\rho kT}{\mu m_H}\right) = -G\frac{M_r\rho}{r^2}$$

$$\frac{k}{\mu m_H}\left(T\frac{d\rho}{dr} + \rho\frac{dT}{dr}\right) = -G\frac{M_r\rho}{r^2}$$

$$M_r = -\frac{kTr}{\mu m_H G}\left(\frac{r}{\rho}\frac{d\rho}{dr} + \frac{r}{T}\frac{dT}{dr}\right)$$

$$= -\frac{kTr}{\mu m_H G}\left(\frac{d\ln\rho}{d\ln r} + \frac{d\ln T}{d\ln r}\right).$$

The use of partial derivatives in the text's Eq. (27.17) is unnecessary, except as a reminder that $\mu =$ constant in our derivation.

27.11 For a flat rotation curve, Eq. (24.49) shows that $M_r = C_M r$, where C_M is a constant, and similarly Eq. (24.50) shows that $\rho = C_\rho r^{-2}$, where C_ρ is a constant. (These expressions are assumed to apply to both dark matter and interstellar gas.) Let $T = C_T r^\alpha$, where C_T and α are constants. Equation (27.17) is then

$$C_M r = -\frac{kC_T r^{\alpha+1}}{\mu m_H G}\left[\frac{d\ln(C_\rho r^{-2})}{d\ln r} + \frac{d\ln(C_T r^\alpha)}{d\ln r}\right]$$

$$= -\frac{kC_T r^{\alpha+1}}{\mu m_H G}(-2 + \alpha).$$

Thus we must have $\alpha = 0$, and so $T = C_T r^\alpha = C_T r^0 = C_T$ for an isothermal gas.

27.12 There were errors in the first printing of *An Introduction to Astrophysics* in Eqs. (27.18) and (27.19). The powers of 10 in the coefficients should have been 10^{-52} and 10^{-40}, respectively. The error was also propagated into the equation for n_e in Example 27.3.2, although the result of $n_e = 300$ m^{-3} is correct.

(a) From Eq. (27.20) with $L_x = 1.5 \times 10^{36}$ W and $R = 1.5$ Mpc for the Virgo cluster, the luminosity density is

$$\mathcal{L}_{\rm vol} = \frac{3L_x}{4\pi R^3} = 3.6 \times 10^{-33}\ \text{W m}^{-3}.$$

Then, using Eq. (27.19) for the luminosity density with $T = 7 \times 10^7$ K, the electron number density is found to be

$$n_e = \left(\frac{\mathcal{L}_{\rm vol}}{1.42 \times 10^{-40} T^{1/2}\ \text{W m}^{-3}}\right)^{1/2} = 55\ \text{m}^{-3}.$$

If the Virgo cluster is filled with completely ionized hydrogen, then the mass of the hydrogen is

$$M_{\rm gas} = \frac{4}{3}\pi R^3 m_H n_e = 3.8 \times 10^{43}\ {\rm kg} = 1.9 \times 10^{13}\ {\rm M}_\odot.$$

(b) Using $M/L \simeq 3\ {\rm M}_\odot/{\rm L}_\odot$ for the Milky Way's luminous matter (Table 24.1) and $L_V = 1.2\times10^{12}\ {\rm L}_\odot$ for the Virgo cluster's visual luminosity, the amount of luminous matter in the Virgo cluster is approximately $M_{\rm lum} = (M/L)L_V = 3.6 \times 10^{12}\ {\rm M}_\odot$, roughly 20% of the mass of the intracluster gas.

(c) Equation (10.17) states that the average kinetic energy per particle is $3kT/2$, so the energy density, u, of the intracluster gas (including both protons and electrons) is approximately

$$u = 2n_e\left(\frac{3}{2}kT\right) = 1.6 \times 10^{-13}\ {\rm J\ m^{-3}}.$$

The gas will lose its energy by emitting x-rays in a time of roughly

$$t = \frac{u}{\mathcal{L}_{\rm vol}} = 4.4 \times 10^{19}\ {\rm s} = 1.4 \times 10^{12}\ {\rm yr},$$

which exceeds the Hubble time of $t_H = 1.38 \times 10^{10}$ yr by two orders of magnitude.

27.13 The diameter of the Coma cluster is $D = 6$ Mpc. Setting the speed of a galaxy equal to the cluster's radial velocity dispersion, so $v = 977\ {\rm km\ s^{-1}}$, shows that the galaxy would travel across the cluster in a time of $t = D/v = 1.9 \times 10^{17}\ {\rm s} = 6.0 \times 10^9$ yr. This is about one-half of the Hubble time ($t_H = 13.8$ Gyr). The Coma cluster must be gravitationally bound, because otherwise there has been sufficient time for its member galaxies to have escaped.

27.14 The radius of the Virgo cluster is $R = 1.5$ Mpc and its radial velocity dispersion is $\sigma_r = 666\ {\rm km\ s^{-1}}$. The virial mass (Eq. 25.13) of the Virgo cluster is therefore

$$M_{\rm virial} \approx \frac{5R\sigma_r^2}{G} = 1.5 \times 10^{45}\ {\rm kg} = 7.7 \times 10^{14}\ {\rm M}_\odot.$$

27.15 In Section 25.2, we used Eq. (2.44),

$$\frac{1}{2}\left\langle\frac{d^2I}{dt^2}\right\rangle - 2\langle K\rangle = \langle U\rangle,$$

with $\left\langle d^2I/dt^2\right\rangle = 0$ to derive the virial mass,

$$M_{\rm virial} = \frac{5R\sigma_r^2}{G}. \tag{S27.1}$$

To see the effect of a non-zero $\left\langle d^2I/dt^2\right\rangle$, repeat the derivation of the virial mass, keeping this term to arrive at

$$M = \frac{5R\sigma_r^2}{G} - \frac{5R}{6GM}\left\langle\frac{d^2I}{dt^2}\right\rangle.$$

Multiplying by M results in a quadratic equation that has the solution

$$M = \frac{1}{2}\left\{\frac{5R\sigma_r^2}{G} + \left[\left(\frac{5R\sigma_r^2}{G}\right)^2 - \frac{10R}{3G}\left\langle\frac{d^2I}{dt^2}\right\rangle\right]^{1/2}\right\}.$$

If $\left\langle d^2I/dt^2\right\rangle = 0$, we recover $M_{\rm virial}$. However, if $\left\langle d^2I/dt^2\right\rangle > 0$, then $M < M_{\rm virial}$, and the virial mass would be an overestimate. Similarly, if $\left\langle d^2I/dt^2\right\rangle < 0$, then $M > M_{\rm virial}$, and the virial mass would be an

underestimate.

Assume that the Coma cluster is in virial equilibrium before the motion of its galaxies is miraculously redirected radially outward, so $-2\langle K\rangle = \langle U\rangle$ and $\left\langle d^2I/dt^2\right\rangle = 0$. Immediately after the redirection there would be no change in the cluster's kinetic or potential energy; $\left\langle d^2I/dt^2\right\rangle$ is still zero and $M = M_{\rm virial}$. However, this situation does not last, as seen by writing Eq. (2.44) as

$$\frac{1}{2}\left\langle\frac{d^2I}{dt^2}\right\rangle = \langle K\rangle + \langle E\rangle\,.$$

Here, $\langle E\rangle = \langle K\rangle + \langle U\rangle < 0$ is the total mechanical energy and remains constant. This shows that as time passes and $\langle K\rangle$ decreases due to the cluster's gravitational attraction, $\left\langle d^2I/dt^2\right\rangle$ becomes negative. Observations made at this later time to calculate $M_{\rm virial}$ via Eq. (S27.1) would therefore underestimate the cluster's mass. On the other hand, if the motion of each of the Coma cluster's galaxies was redirected radially inward, again there would be no initial change in the cluster's kinetic or potential energy and so $M_{\rm virial}$ would be valid. However, in this case as time passes and $\langle K\rangle$ increases due to the cluster's gravitational attraction, $\left\langle d^2I/dt^2\right\rangle$ becomes positive. Calculations of $M_{\rm virial}$ made at this later time would therefore overestimate the cluster's mass.

27.16 The Tully–Fisher relation, Eq. (27.5), with $2v_r/\sin i = 218$ km s^{-1} for NGC 5535, shows that the galaxy's absolute H-magnitude is

$$M_H = -10.0\log_{10}\left(\frac{2v_r}{\sin i}\right) + 3.61 = -19.77.$$

Then the distance to NGC 5535 is, from Eq. (3.5) with $H = 9.55$,

$$d = 10^{(H-M_H+5)/5} = 7.31 \text{ Mpc}.$$

27.17 The average absolute visual magnitude for the brightest galaxy in a cluster is $M_V = -22.83 \pm 0.61$. Using $V = 10.99$ and Eq. (3.5) with $M_V = -22.83$,

$$d = 10^{(V-M_V+5)/5} = 58.1 \text{ Mpc}.$$

If $M_V = -22.83 + 0.61 = -22.22$, then

$$d = 10^{(V-M_V+5)/5} = 43.9 \text{ Mpc}.$$

If $M_V = -22.83 - 0.61 = -23.44$, then

$$d = 10^{(V-M_V+5)/5} = 76.9 \text{ Mpc}.$$

27.18 Use Eqs. (24.12) to convert $\ell = 309°$, $b = 18°$ into equatorial coordinates. We find $\alpha = 200° = 13^{\rm h}20^{\rm m}$ and $\delta = -44°$. This is in the constellation of Centaurus.

27.19 (a) For the minimum Δ, $d_{\rm ave} = 15.8$ Mpc; see Fig. S27.1.

(b) The weighted mean value of the distance to the Virgo cluster is $d_w = 15.8$ Mpc. This is the same as was found in part (a).

(c) The minimum value of Δ will occur when

$$\frac{d\Delta}{d(d_{\rm ave})} = \frac{d}{d(d_{\rm ave})}\left[\sum_i\left(\frac{d_i - d_{\rm ave}}{\delta_i}\right)^2\right] = 0,$$

or when

$$-2\sum_i\left(\frac{d_i - d_{\rm ave}}{\delta_i^2}\right) = 0.$$

This can be solved for the value of d_{ave} that minimizes Δ,

$$(d_{\text{ave}})_{\text{min}} = \frac{\sum_i (d_i/\delta_i^2)}{\sum_i (1/\delta_i^2)} = d_w.$$

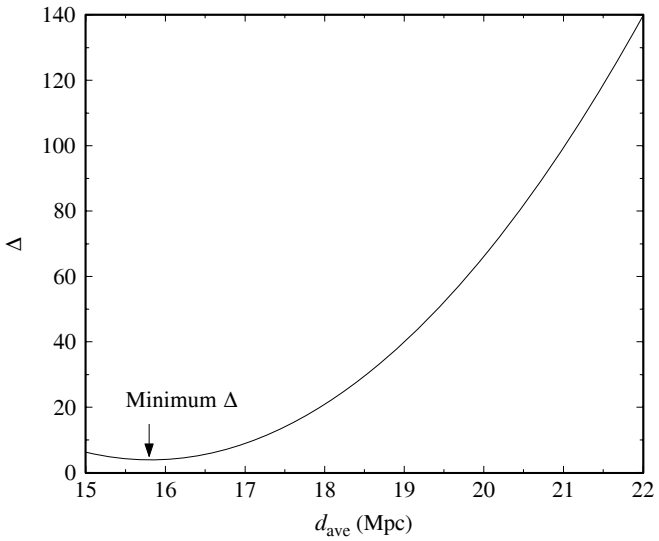

Figure S27.1: Results for Problem 27.19. The minimum value of Δ occurs for $d_{\text{ave}} = 15.8$ Mpc.

CHAPTER 28

Active Galaxies

28.1 Using $z = 0.00157$ for Centaurus A, the distance to Cen A is, from Eq. (27.8), $d = cz/H_0 = 6.6$ Mpc. Following the procedure of Example 28.1.1, integrating from $\nu_1 = 10^7$ Hz to $\nu_2 = 3 \times 10^9$ Hz,

$$L_{\rm radio} = 4\pi d^2 (9.12 \times 10^{-24}\ {\rm W\ m^{-2}\ Hz^{-1}}) \int_{\nu_1}^{\nu_2} \left(\frac{\nu}{1400\ {\rm MHz}}\right)^{-0.6} d\nu$$

$$= 1.0 \times 10^{34} h^{-2}\ {\rm W} = 2 \times 10^{34}\ {\rm W} \quad \text{for } h = 0.71.$$

28.2 A frequency of $\nu = 1400$ MHz corresponds to $\log_{10} \nu = 9.15$. Referring to Fig. 28.14 for the spectrum of 3C 273, the slope of the curve at this frequency is approximately

$$\frac{\Delta(\log_{10} \nu F_\nu)}{\Delta(\log_{10} \nu)} = 0.85.$$

From Eq. (28.1), if $F_\nu \propto \nu^{-\alpha}$, then

$$\frac{d \log_{10} \nu F_\nu}{d \log_{10} \nu} = 1 - \alpha = 0.85,$$

so the spectral index is $\alpha = 0.15$, somewhat smaller than the value of $\alpha \simeq 0.24$ given in Example 28.1.2.

28.3 See Fig. S28.1, which shows a spectrum that is much more sharply peaked than the very broad spectrum of the quasar 3C 273 seen in Fig. 28.14.

28.4 (a) Choose two points from the left-hand side of Fig. 28.16: $L_1 \approx 2{\times}10^{39}$ W at $z_1 = 2.2$ and $L_2 \approx 10^{38}$ W at $z_2 = 0.3$. So

$$L_1 = L_0(1 + z_1)^\alpha \quad \text{and} \quad L_2 = L_0(1 + z_2)^\alpha.$$

Solving for α, we estimate that

$$\alpha = \frac{\ln(L_1/L_2)}{\ln[(1 + z_1)/(1 + z_2)]} = 3.3.$$

(b)

$$\frac{L(z = 2)}{L(z = 0)} = \frac{L_0(1 + 2)^{3.3}}{L_0(1 + 0)^{3.3}} = 38.$$

28.5 The Schwarzschild radius of an $M = 10^8\ {\rm M}_\odot$ black hole is $R_S = 2GM/c^2 = 2.95 \times 10^{11}$ m (Eq. 17.27). The average density is

$$\rho = \frac{M}{\frac{4}{3}\pi R_S^3} = 1.85\ {\rm g\ cm^{-3}},$$

slightly greater than the Sun's average density of 1410 kg m^{-3} given in Example 8.2.1. The "surface gravity" of the black hole is (Eq. 2.12)

$$g = G\frac{M}{R_S^2} = 1.52 \times 10^5\ {\rm m\ s^{-1}},$$

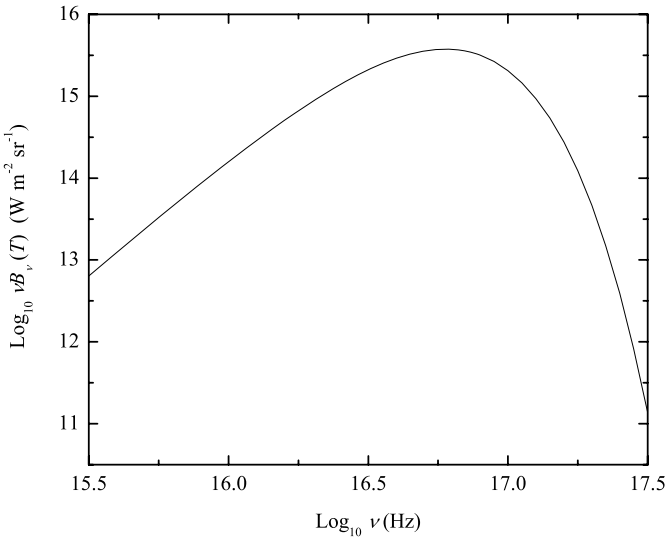

Figure S28.1: Results for Problem 28.3, $\log_{10} \nu B_\nu(T)$ for $T = 7.3 \times 10^5$ K.

which is about 550 times greater than the Sun's value of

$$g_\odot = G\frac{M_\odot}{R_\odot^2} = 274 \text{ m s}^{-1}.$$

28.6 Using Eqs. (17.27) and (18.23), the efficiency of the accretion luminosity is, from Eq. (28.6),

$$\eta = \frac{L_{\text{disk}}}{\dot{M}c^2} = \frac{GM\dot{M}/2R}{\dot{M}c^2} = \frac{R_S}{4R}.$$

For the inner edge of a nonrotating black hole, $R = 3R_S$ and we estimate $\eta = 0.0833$, while for the inner edge of a maximally rotating black hole, $R = 0.5R_S$ and $\eta = 0.5$.

28.7 (a) Setting

$$L_{\max} = I\omega_{\max} = MR_S^2\omega_{\max} = \frac{GM^2}{c},$$

and using Eq (17.27) for the Schwarzschild radius, for an $M = 10^8$ $M_\odot$ black hole we find

$$\omega_{\max} = \frac{c^3}{4GM} = 5.1 \times 10^{-4} \text{ s}^{-1}.$$

(b) The Schwarzschild radius (Eq. 17.27) is $R_S = 2GM/c^2 = 2.95 \times 10^{11}$ m.
Divide the wire into elements of length dr. The motional emf between the ends of the wire element located at a distance r from the axis of rotation is $d\mathcal{E} = Bv\,dr = B\omega r\,dr$ for the wire rotating perpendicular to the magnetic field. Integrating from $r = 0$ to $r = R_S$, we find that the induced voltage is

$$\mathcal{E} = \int_0^{R_S} B\omega_{\max} r\,dr = \frac{1}{2}B\omega_{\max}R_S^2 = 2.2 \times 10^{19} \text{ V}$$

for $B = 1$ T.

(c) $P = \mathcal{E}^2/(30\ \Omega) = 1.6 \times 10^{37}$ watts.

This is about 6% of the power generated by the Blandford–Znajek mechanism.

28.8 Define n_e and n_H as the electron and proton number densities in a cloud of ionized hydrogen gas, and let $\alpha_{\rm qm} n_e n_H$ be the number of recombinations per unit volume per second in those clouds. If the clouds of ionized hydrogen fill only a fraction, ϵ, of the total volume of the narrow-line region, then $\alpha_{\rm qm}\epsilon n_e n_H$ is the number of recombinations per unit volume per second for the entire volume. We now model the narrow-line region as a sphere of radius $r_{\rm NLR}$ and assume that the clouds are pure hydrogen, so $n_e = n_H$. Assuming equilibrium, the number of ionizing photons produced per second by the central source, N, is equal to the number of recombinations per second. We then have

$$\alpha_{\rm qm}\epsilon n_e^2 \left(\frac{4}{3}\pi r_{\rm NLR}^3\right) = N,$$

which yields Eq. (28.13) when solved for $r_{\rm NLR}$.

28.9 In Example 28.2.2, the number of photons emitted per second in the continuum and capable of ionizing hydrogen was found to be

$$N = \int_{\nu_H}^{\nu_2} \frac{0.029L}{h\nu^2}\, d\nu = \frac{0.029L}{h\nu_H},$$

where $\nu_H = 3.29 \times 10^{15}$ Hz and $\nu_2 = 10^{25}$ Hz. In the same manner, the total number of photons emitted per second in the continuum is

$$N_t = \int_{\nu_1}^{\nu_2} \frac{0.029L}{h\nu^2}\, d\nu = \frac{0.029L}{h\nu_1},$$

where $\nu_1 = 10^{10}$ Hz. So $N/N_t = \nu_1/\nu_H = 3.04 \times 10^{-6}$.

28.10 Defining $\beta = v/c$ and $\beta_{\rm app} = v_{\rm app}/c$, Eq. (28.15) shows that $\beta < 1$ when

$$\beta_{\rm app} < \sin\phi + \beta_{\rm app}\cos\phi$$

$$\beta_{\rm app} < \sqrt{1-\cos^2\phi} + \beta_{\rm app}\cos\phi$$

$$\beta_{\rm app}^2(1-\cos\phi)^2 < 1 - \cos^2\phi.$$

Divide by $(1-\cos\phi)$ (we are requiring that $\cos\phi < 1$) to get

$$\beta_{\rm app}^2(1-\cos\phi) < 1 + \cos\phi$$

$$\frac{\beta_{\rm app}^2 - 1}{\beta_{\rm app}^2 + 1} < \cos\phi < 1,$$

which is Eq. (28.16). To find the value of ϕ for the minimum β, use Eq. (28.15) to set $\partial\beta/\partial\phi = 0$ (holding $\beta_{\rm app}$ constant) to obtain

$$\frac{\partial}{\partial\phi}\left(\frac{\beta_{\rm app}}{\sin\phi + \beta_{\rm app}\cos\phi}\right) = 0$$

$$\frac{-\beta_{\rm app}(\cos\phi_{\rm min} - \beta_{\rm app}\sin\phi_{\rm min})}{(\sin\phi_{\rm min} + \beta_{\rm app}\cos\phi_{\rm min})^2} = 0.$$

This reduces to $\cot\phi_{\min} = \beta_{\text{app}}$, which is Eq. (28.18). Note, from $\sin^2\phi_{\min} + \cos^2\phi_{\min} = 1$, that

$$\sin\phi_{\min} = \sqrt{\frac{1}{1+\cot^2\phi_{\min}}} = \sqrt{\frac{1}{1+\beta_{\text{app}}^2}}$$

and

$$\cos\phi_{\min} = \sqrt{\frac{\cot^2\phi_{\min}}{1+\cot^2\phi_{\min}}} = \sqrt{\frac{\beta_{\text{app}}^2}{1+\beta_{\text{app}}^2}}.$$

Inserting these into Eq. (28.15) shows that the minimum value of β for the source is

$$\beta_{\min} = \frac{\beta_{\text{app}}}{\sqrt{\frac{1}{1+\beta_{\text{app}}^2}} + \beta_{\text{app}}\sqrt{\frac{\beta_{\text{app}}^2}{1+\beta_{\text{app}}^2}}},$$

which quickly reduces to

$$\beta_{\min} = \sqrt{\frac{\beta_{\text{app}}^2}{1+\beta_{\text{app}}^2}},$$

which is Eq. (28.17). The minimum Lorentz factor is, from Eq. (4.20),

$$\gamma_{\min} = \frac{1}{\sqrt{1-\beta_{\min}^2}} = \frac{1}{\sqrt{1-\frac{\beta_{\text{app}}^2}{1+\beta_{\text{app}}^2}}} = \sqrt{1+\beta_{\text{app}}^2} = \frac{1}{\sin\phi_{\min}},$$

which is Eq. (28.19).

28.11 (a) Start by dividing each side of the relativistic velocity transformation, Eq. (4.40), by c to get

$$\frac{v_x'}{c} = \frac{v_x/c - u/c}{1 - uv_x/c^2}.$$

Referring to Fig. 4.2, let Earth be at the origin of frame S and the QSO be at the origin of frame S' moving with speed $u/c = v_Q/c = \beta_Q$ relative to Earth. The ejecta has speed $v_x/c = v_{\text{ej}}/c = \beta_{\text{ej}}$ relative to Earth, and speed $v_x'/c = v_{\text{ej}}'/c = \beta_{\text{ej}}'$ relative to the QSO. (Note that $v_x' < 0$ if the material is ejected by the QSO in the direction of Earth.) The velocity transformation is therefore

$$\beta_{\text{ej}}' = \frac{\beta_{\text{ej}} - \beta_Q}{1 - \beta_{\text{ej}}\beta_Q}.$$

From Eq.(4.36) for the redshift parameter,

$$z_Q + 1 = \sqrt{\frac{1+\beta_Q}{1-\beta_Q}} \quad \text{and} \quad z_{\text{ej}} + 1 = \sqrt{\frac{1+\beta_{\text{ej}}}{1-\beta_{\text{ej}}}},$$

or

$$\beta_Q = \frac{(z_Q+1)^2 - 1}{(z_Q+1)^2 + 1} \quad \text{and} \quad \beta_{\text{ej}} = \frac{(z_{\text{ej}}+1)^2 - 1}{(z_{\text{ej}}+1)^2 + 1}.$$

Inserting these into the velocity transformation results in

$$\beta_{\text{ej}}' = \frac{\frac{(z_{\text{ej}}+1)^2-1}{(z_{\text{ej}}+1)^2+1} - \frac{(z_Q+1)^2-1}{(z_Q+1)^2+1}}{1 - \left[\frac{(z_{\text{ej}}+1)^2-1}{(z_{\text{ej}}+1)^2+1}\right]\left[\frac{(z_Q+1)^2-1}{(z_Q+1)^2+1}\right]}$$

or $\beta_{\rm ej}{}' =$

$$\frac{[(z_{\rm ej}+1)^2-1][(z_Q+1)^2+1]-[(z_{\rm ej}+1)^2+1][(z_Q+1)^2-1]}{[(z_{\rm ej}+1)^2+1][(z_Q+1)^2+1]-[(z_{\rm ej}+1)^2-1][(z_Q+1)^2-1]}$$

or

$$-\beta_{\rm ej}{}' = \frac{(z_Q+1)^2-(z_{\rm ej}+1)^2}{(z_Q+1)^2+(z_{\rm ej}+1)^2}.$$

On left-hand side we have $\beta_{\rm ej}{}' = v_x{}'/c$, the x'-component of the ejecta velocity relative to the quasar. Because $v_x{}' < 0$, the *speed* of the ejecta relative to the QSO, is $-\beta_{\rm ej}{}' = -v_x{}'/c$, which is the desired result.

(b) We use $z_Q + 1 = 1.158$ for the quasar 3C 273 and, with $\beta_{\rm ej} = -0.9842$ for the *approaching* knot,

$$z_{\rm ej}+1 = \sqrt{\frac{1+\beta_{\rm ej}}{1-\beta_{\rm ej}}} = 0.08924$$

for the ejecta. The speed of the knot relative to the quasar is therefore

$$\frac{v}{c} = \frac{(z_Q+1)^2-(z_{\rm ej}+1)^2}{(z_Q+1)^2+(z_{\rm ej}+1)^2} = 0.9882,$$

which corresponds to a Lorentz factor of $\gamma = 1\Big/\sqrt{1-v^2/c^2} = 6.53$ (Eq. 4.20).

28.12 Using Eq. (4.31) with $\theta = 180^\circ$ and Eq.(4.20) for the Lorentz factor, we have

$$\Delta t_{\rm obs} = \frac{\Delta t_{\rm rest}(1-u/c)}{\sqrt{1-u^2/c^2}} = \gamma \Delta t_{\rm rest}\left(1-\frac{u}{c}\right).$$

But

$$1-\frac{u}{c} = \frac{1-u^2/c^2}{1+u/c} = \frac{1}{(1+u/c)\gamma^2} \to \frac{1}{2\gamma^2}$$

as $u/c \to 1$. Therefore, when $\gamma \gg 1$,

$$\Delta t_{\rm obs} \approx \frac{\Delta t_{\rm rest}}{2\gamma}.$$

28.13 With $M = 10^{14}\ {\rm M}_\odot$ and $r = 10^4$ pc,

$$n = \left(1-\frac{2GM}{rc^2}\right)^{-1} = 1.000958.$$

28.14 From Eq. (28.20) with $M = 1\ {\rm M}_\odot$ and $r_0 = 1\ {\rm R}_\odot$,

$$\phi = \frac{4GM}{r_\circ c^2} = 8.49\times 10^{-6}\ {\rm rad} = 1.75''.$$

28.15 Referring to Fig. 28.35, let P be the point at the apex of angle ϕ, directly above L. Since $\overline{SO} = d_S$ and $\overline{SP} = d_S - d_L$ for the small angles involved, applying the law of sines to the triangle SPO gives

$$\frac{\sin(\theta-\beta)}{d_S-d_L} = \frac{\sin(\pi-\phi)}{d_S} = \frac{\sin\phi}{d_S}.$$

Using Eq. (28.20), $r_\circ = \theta d_L$, and $\sin x \simeq x$ for small x,

$$\frac{\theta - \beta}{d_S - d_L} = \frac{\phi}{d_S} = \frac{4GM}{r_\circ c^2 d_S} = \frac{4GM}{\theta d_L c^2 d_S},$$

or

$$\theta^2 - \beta\theta - \frac{4GM}{c^2}\left(\frac{d_S - d_L}{d_S d_L}\right) = 0,$$

which is Eq. (28.21). Consider two solutions, θ_1 and θ_2. They satisfy

$$\theta_1^2 - \beta\theta_1 - \frac{4GM}{c^2}\left(\frac{d_S - d_L}{d_S d_L}\right) = 0$$

$$\theta_2^2 - \beta\theta_2 - \frac{4GM}{c^2}\left(\frac{d_S - d_L}{d_S d_L}\right) = 0,$$

so subtracting leads to

$$\theta_1^2 - \theta_2^2 - \beta(\theta_1 - \theta_2) = 0,$$

or $\theta_1 + \theta_2 = \beta$, which is Eq. (28.22). Substituting for β in the preceding quadratic equation for θ_1, we find

$$\theta_1^2 - (\theta_1 + \theta_2)\theta_1 - \frac{4GM}{c^2}\left(\frac{d_S - d_L}{d_S d_L}\right) = 0,$$

which yields Eq. (28.23) when solved for M.

28.16 The images are located at $\theta_1 = -0.8'' = -3.88 \times 10^{-6}$ rad and $\theta_2 = (2.22 - 0.8)'' = 6.88 \times 10^{-6}$ rad. (Which angle assumes the minus sign is arbitrary.) The distance to the source (Q0142−100 with $z_S = 2.727$) is, from Eq. (27.7),

$$d_S \simeq \frac{c}{H_0}\frac{(z_S + 1)^2 - 1}{(z_S + 1)^2 + 1} = 2600h^{-1}\ \text{Mpc},$$

and similarly, the distance to the lensing galaxy ($z_L = 0.493$) is $d_L \simeq 1140h^{-1}$ Mpc. Equation (28.23) then gives the mass of the lensing galaxy as approximately

$$M = -\frac{\theta_1\theta_2 c^2}{4G}\left(\frac{d_S d_L}{d_S - d_L}\right) = 5.6 \times 10^{41}h^{-1}\ \text{kg} = 2.8 \times 10^{11}h^{-1}\ \text{M}_\odot.$$

28.17 The distance to the source ($z_S = 1.74$) is, from Eq. (27.7),

$$d_S \simeq \frac{c}{H_0}\frac{(z_S + 1)^2 - 1}{(z_S + 1)^2 + 1} = 2290h^{-1}\ \text{Mpc},$$

and similarly, the distance to the lensing galaxy ($z_L = 0.25$) is $d_L \simeq 660h^{-1}$ Mpc. From Eq. (28.24) with $\theta_E = 2.1''/2 = 5.1 \times 10^{-6}$ rad, the mass of the lensing galaxy is about

$$M = \frac{\theta_E^2 c^2}{4G}\left(\frac{d_S d_L}{d_S - d_L}\right) = 2.5 \times 10^{41}h^{-1}\ \text{kg} = 1.3 \times 10^{11}h^{-1}\ \text{M}_\odot.$$

28.18 The mass of the MACHO is assumed to be, from Appendix C, $M = 1.90 \times 10^{28}$ kg (ten Jupiter masses). The distance to the source star in the LMC is $d_S = 52$ kpc, and the distance to the lensing MACHO is assumed to be $d_L = 25$ kpc. Then, from Eq. (28.24),

$$\theta_E = \sqrt{\frac{4GM}{c^2}\left(\frac{d_S - d_L}{d_S d_L}\right)} = 1.91 \times 10^{-10}\ \text{rad}.$$

Moving with a speed of $v = 220$ km s^{-1}, the MACHO will travel a distance of $2\theta_E d_L$ in a time of $t = 2\theta_E d_L/v = 1.34 \times 10^6$ s $= 15.5$ d. Comparing this time with the time shown in Fig. 24.15, we see that the temporary brightening of a lensed star in the LMC lasted for roughly 20 days, in good agreement with our crude estimate.

28.19 (a) If we set $r_R = R_S$, $\overline{\rho}_{\rm BH} = M_{\rm BH}/(4\pi R_S^3/3)$, and $R_S = 2GM_{\rm BH}/c^2$ (the expression for the Schwarzschild radius), the mass of the black hole is found to be

$$M_{\rm BH} = \left[\frac{2.4^3 c^6}{(32\pi/3)G^3\overline{\rho}_\star}\right]^{1/2} = 1.6 \times 10^{10}\overline{\rho}_\star^{-1/2}\ {\rm M}_\odot.$$

(b) If the Sun falls in, $\overline{\rho}_\star = 1410$ kg m^{-3}. This implies a mass required for the black hole of $M_{\rm BH} = 4.2 \times 10^8\ {\rm M}_\odot$.

(c) For a more massive black hole, the star would not be disrupted prior to falling through the event horizon. As a result, the liberation of the gravitational potential energy would be very inefficient, meaning that there would be little gravitational energy available to power an AGN.

28.20 (a) See Fig. S28.2. From Eq. (28.1), using the two points on either side of $\log_{10}\nu = 8.0$ in Table 28.2,

$$\alpha = -\frac{\log_{10} F_2 - \log_{10} F_1}{\log_{10}\nu_2 - \log_{10}\nu_1} = 0.7$$

at $\log_{10}\nu = 8.0$.

(b) The distance to Cygnus A is $d = 170h^{-1}$ Mpc. As in Example 28.1.1, we integrate over radio frequencies from $\nu_1 = 10^7$ Hz ($\log_{10}\nu_1 = 7$, $\log_{10} F_\nu = -18.88$) to $\nu_2 = 3 \times 10^9$ Hz ($\log_{10}\nu_2 = 9.5$, $\log_{10} F_\nu = -20.17$, obtained by interpolating the data in Table 28.2). A numerical integration results in

$$L_{\rm radio} = 4\pi d^2 \int_{\nu_1}^{\nu_2} F_\nu\, d\nu = 4\pi d^2 (9.0 \times 10^{-11}\ {\rm erg\ s^{-1}\ cm^{-2}})$$
$$= 3.1 \times 10^{37} h^{-2}\ {\rm W}.$$

This is in reasonable agreement with the estimate for Cyg A obtained in Example 28.1.1, $2.4 \times 10^{37} h^{-2}$ W.

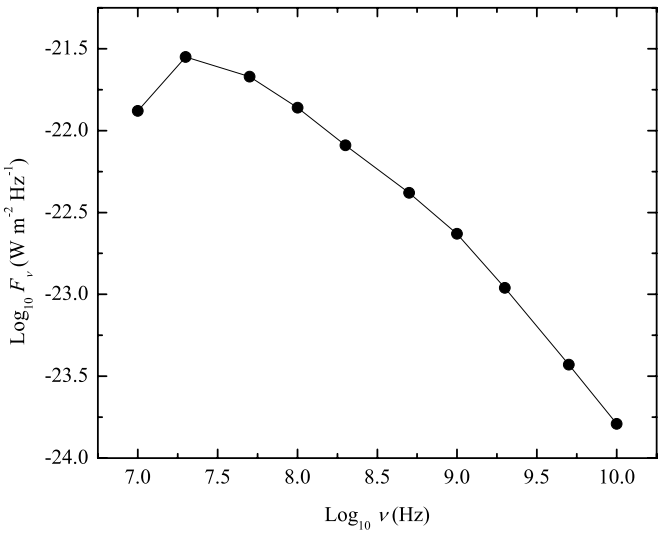

Figure S28.2: Results for Problem 28.20 for Cygnus A.

CHAPTER 29

Cosmology

29.1 The total number of stars in a thin spherical shell of radius r_1 and thickness Δr that contains n stars per unit volume is $N_1 = 4\pi r_1^2 n \Delta r$. Assuming stars of luminosity L, the radiant flux received from a single star is, from the inverse square law (Eq. 3.2),

$$F_1 = \frac{L}{4\pi r_1^2}.$$

Therefore, the total flux received from this shell is $F_t = N_1 F_1 = Ln\Delta r$. This is independent of r, so the same result would be found for a shell of radius r_2.

29.2 Assume a WMAP density of baryonic matter of $\rho_{b,0} = 4.17 \times 10^{-28}$ kg m^{-3}. Setting the corresponding rest energy density (Eq. 4.47) equal to the blackbody energy density (Eq. 9.7), we have $\rho_{b,0}c^2 = aT^4$. Solving this for T to find that the temperature of the universe gives

$$T = \left(\frac{\rho_{b,0}c^2}{a}\right)^{1/4} = 14.9 \text{ K}.$$

According to Wien's law, Eq. (3.15), the blackbody radiation would have a peak wavelength of $\lambda_{\text{max}} = (0.00290 \text{ m K})/T = 0.19$ mm, in the infrared part of the electromagnetic spectrum (Table 3.1). Even if all of the matter in the universe were converted into the energy of blackbody radiation, there is too little matter to cause the sky to glow. There would not be visually detectable amounts of blackbody radiation at visible wavelengths.

29.3 We want to show that Eqs. (29.32) and (29.34),

$$R = \frac{4\pi G\rho_0}{3kc^2}\,[1 - \cos(x)]$$

$$t = \frac{4\pi G\rho_0}{3k^{3/2}c^3}\,[x - \sin(x)]\,.$$

are solutions to Eq. (29.11),

$$\left(\frac{dR}{dt}\right)^2 - \frac{8\pi G\rho_0}{3R} = -kc^2,$$

for a closed universe. For the first term on the left, we use

$$\frac{dR}{dt} = \frac{dR/dx}{dt/dx}$$

with

$$\frac{dR}{dx} = \frac{4\pi G\rho_0}{3kc^2}\,\sin(x)$$

$$\frac{dt}{dx} = \frac{4\pi G\rho_0}{3k^{3/2}c^3}\,[1 - \cos(x)]\,.$$

This results in

$$\left(\frac{dR}{dt}\right)^2 = kc^2\left\{\frac{\sin^2(x)}{[1-\cos(x)]^2}\right\}.$$

The second term on the left in Eq. (29.11) is

$$\frac{8\pi G\rho_0}{3R} = \frac{2kc^2}{1-\cos(x)}.$$

Inserting these results on the left-hand side of Eq. (29.11) and simplifying leads to $-kc^2$, the term on the right.

29.4 We want to show that Eqs. (29.36) and (29.38),

$$R = \frac{4\pi G\rho_0}{3|k|c^2}\,[\cosh(x)-1]$$

$$t = \frac{4\pi G\rho_0}{3|k|^{3/2}c^3}\,[\sinh(x)-x].$$

are solutions to Eq. (29.11),

$$\left(\frac{dR}{dt}\right)^2 - \frac{8\pi G\rho_0}{3R} = -kc^2,$$

for an open universe. For the first term on the left, use

$$\frac{dR}{dt} = \frac{dR/dx}{dt/dx}$$

with

$$\frac{dR}{dx} = \frac{4\pi G\rho_0}{3|k|c^2}\,\sinh(x)$$

$$\frac{dt}{dx} = \frac{4\pi G\rho_0}{3|k|^{3/2}c^3}\,[\cosh(x)-1].$$

This results in

$$\left(\frac{dR}{dt}\right)^2 = |k|c^2\left\{\frac{\sinh^2(x)}{[\cosh(x)-1]^2}\right\}.$$

The second term on the left in Eq. (29.11) is

$$\frac{8\pi G\rho_0}{3R} = \frac{2|k|c^2}{\cosh(x)-1}.$$

Inserting these results on the left-hand side of Eq. (29.11), simplifying and noting that $|k| = -k$ since $k < 0$, leads to $-kc^2$, the term on the right.

29.5 To go from Eq. (29.32) to Eq. (29.33), we must show that the coefficients of $[1-\cos(x)]$ are equal. Use Eqs. (29.15), (29.19), and (29.25),

$$\rho_{c,0} = \frac{3H_0^2}{8\pi G}$$

$$\Omega_0 = \frac{\rho_0}{\rho_{c,0}}$$

$$H_0^2(\Omega_0 - 1) = kc^2,$$

respectively, to find

$$\frac{4\pi G\rho_0}{3kc^2} = \frac{4\pi G(\rho_0/\rho_{c,0})}{3H_0^2(\Omega_0-1)/\rho_{c,0}} = \frac{4\pi G\Omega_0}{8\pi G(\Omega_0-1)}$$

so

$$\frac{4\pi G\rho_0}{3kc^2} = \frac{1}{2}\,\frac{\Omega_0}{\Omega_0-1}.$$

Similarly, to go from Eq. (29.34) to Eq. (29.35), we must show that the coefficients of $[x-\sin(x)]$ are equal:

$$\frac{4\pi G\rho_0}{3k^{3/2}c^3} = \frac{4\pi G(\rho_0/\rho_{c,0})}{3[H_0^2(\Omega_0-1)]^{3/2}/\rho_{c,0}} = \frac{4\pi G\Omega_0}{8\pi GH_0(\Omega_0-1)^{3/2}}$$

so

$$\frac{4\pi G\rho_0}{3k^{3/2}c^3} = \frac{1}{2H_0}\,\frac{\Omega_0}{(\Omega_0-1)^{3/2}}.$$

29.6 The procedure to go from Eq. (29.36) to Eq. (29.37), and to go from Eq. (29.38) to Eq. (29.39), is nearly identical to the one followed for Problem 29.5. The only difference is that because $k < 0$ for an open universe, we replace $|k|$ with $-k$ in Eqs. (29.36) and (29.38). This causes $(\Omega_0 - 1)$ in Eqs. (29.33) and (29.35) to be replaced $(1-\Omega_0)$ in Eqs. (29.37) and (29.39).

29.7 (a) When the scale height R is a maximum for a closed universe, it is necessary that $dR/dt = 0$. Substituting into Eq. (29.11) implies that

$$R_{\max} = \frac{8\pi G\rho_0}{3kc^2}.$$

This result is in agreement with Eq. (29.33); $R(x)$ is a maximum when $x = \pi$ and $\cos(x) = -1$.

(b) Setting $R = 0$ in Eq. (29.33) and solving for x, we find that the lifetime of a closed universe corresponds to $\cos(x) = 1$, or $x = 2\pi$. Inserting this into Eq. (29.35) and using $t_H = 1/H_0$ for the Hubble time (Eq. 27.14), the lifetime is

$$t_{\rm life} = \frac{1}{2H_0}\,\frac{\Omega_0}{(\Omega_0-1)^{3/2}}\,[x-\sin(x)] = \frac{\pi\Omega_0}{(\Omega_0-1)^{3/2}}\,t_H.$$

29.8 For a flat universe, the scale factor is given by Eq. (29.31). Inserting $1+z = 1/R$ from Eq. (29.4), we have

$$R = \left(\frac{3}{2}\right)^{2/3}\left(\frac{t}{t_H}\right)^{2/3} = \frac{1}{1+z},$$

or

$$\frac{t(z)}{t_H} = \frac{2}{3}\left(\frac{1}{1+z}\right)^{3/2},$$

which is Eq. (29.40) for $k = 0$.

For a closed universe, the time is parameterized by Eq. (29.35) [with $t_H = 1/H_0$, Eq. (27.14)],

$$\frac{t}{t_H} = \frac{1}{2}\,\frac{\Omega_0}{(\Omega_0-1)^{3/2}}\,[x-\sin(x)]. \tag{S29.1}$$

To find x, use Eq. (29.33) for the scale factor with $1+z = 1/R$,

$$R = \frac{1}{2}\,\frac{\Omega_0}{\Omega_0-1}\,[1-\cos(x)] = \frac{1}{1+z},$$

to get

$$\cos(x) = 1 - \frac{2(\Omega_0-1)}{\Omega_0(1+z)},$$

so

$$x = \cos^{-1}\left(\frac{\Omega_0 z - \Omega_0 + 2}{\Omega_0 z + \Omega_0}\right).$$

To find $\sin(x)$, use $\sin(x) = \sqrt{1 - \cos^2(x)}$ so

$$\sin(x) = \sqrt{1 - \left[1 - \frac{2(\Omega_0 - 1)}{\Omega_0(1+z)}\right]^2} = \frac{2\sqrt{(\Omega_0 - 1)(\Omega_0 z + 1)}}{\Omega_0(1+z)}.$$

Inserting these expressions for x and $\sin(x)$ into Eq. (S29.1) produces Eq. (29.41) for $k > 0$.

For an open universe, the time is parameterized by Eq. (29.39) (again with $t_H = 1/H_0$),

$$\frac{t}{t_H} = \frac{1}{2}\frac{\Omega_0}{(1-\Omega_0)^{3/2}}\left[-x + \sinh(x)\right]. \tag{S29.2}$$

To find x, use Eq. (29.37) for the scale factor with $1 + z = 1/R$,

$$R = \frac{1}{2}\frac{\Omega_0}{1-\Omega_0}\left[\cosh(x) - 1\right] = \frac{1}{1+z}$$

to get

$$\cosh(x) = 1 + \frac{2(1-\Omega_0)}{\Omega_0(1+z)},$$

so

$$x = \cosh^{-1}\left(\frac{\Omega_0 z - \Omega_0 + 2}{\Omega_0 z + \Omega_0}\right).$$

To find $\sinh(x)$, use $\sinh(x) = \sqrt{\cosh^2(x) - 1}$ so

$$\sinh(x) = \sqrt{\left[1 + \frac{2(1-\Omega_0)}{\Omega_0(1+z)}\right]^2 - 1} = \frac{2\sqrt{(1-\Omega_0)(\Omega_0 z + 1)}}{\Omega_0(1+z)}.$$

Inserting these expressions for x and $\sinh(x)$ into Eq. (S29.2) produces Eq. (29.42) for $k < 0$.

29.9 (a) Start with Eq. (29.10),

$$\left[\left(\frac{1}{R}\frac{dR}{dt}\right)^2 - \frac{8}{3}\pi G\rho\right]R^2 = -kc^2.$$

From Eq (29.12) for the critical density and Eq. (29.8) for H,

$$\frac{8}{3}\pi G\rho R^2 = \frac{8}{3}\pi G R^2 \frac{\rho}{\rho_c}\frac{3H^2}{8\pi G} = R^2\Omega\left(\frac{1}{R}\frac{dR}{dt}\right)^2 = \Omega\left(\frac{dR}{dt}\right)^2.$$

So Eq. (29.10) becomes

$$\left(\frac{dR}{dt}\right)^2 - \Omega\left(\frac{dR}{dt}\right)^2 = -kc^2,$$

or

$$\Omega(t) = 1 + \frac{kc^2}{(dR/dt)^2},$$

which is Eq. (29.194). Ω is very close to unity in the early universe.

(b) The right-hand side of Eq. (29.11),

$$\left(\frac{dR}{dt}\right)^2 - \frac{8\pi G\rho_0}{3R} = -kc^2,$$

is a constant. However, $R \to 0$ as $t \to 0$, and so the second term on the left diverges, $8\pi G\rho_0/(3R) \to \infty$. Therefore the first term on the left, $(dR/dt)^2$, must also diverge as $t \to \infty$. Equation (29.194), then shows that $\Omega \to 1$ as $t \to 0$, so at very early times it is difficult to distinguish between a closed, flat, and open universe.

29.10 Eq. (29.23) can be used to eliminate H^2 from Eq. (29.26), giving

$$\left(\frac{(1+z)^3\Omega_0}{\Omega}\right) H_0^2(1-\Omega) = H_0^2(1-\Omega_0)(1+z)^2,$$

which simplifies immediately to

$$\frac{1}{\Omega} - 1 = \left(\frac{1}{\Omega_0} - 1\right)(1+z)^{-1},$$

which is Eq (29.195). This implies that as $z \to \infty$, $\Omega \to 1$.

29.11 Define

$$u \equiv \frac{1}{\Omega_0(1+z)}.$$

In terms of u, Eq. (29.41) is

$$\frac{t}{t_H} = \frac{\Omega_0}{2(\Omega_0-1)^{3/2}}\left\{\cos^{-1}[1-2u(\Omega_0-1)] - 2\sqrt{u(\Omega_0-1)}\,\sqrt{1-u(\Omega_0-1)}\right\}.$$

As $z \to \infty$, $u \to 0$. Use

$$\cos^{-1}(1-x) = \sqrt{2}\,x^{1/2} + \frac{\sqrt{2}}{12}\,x^{3/2} + \cdots$$

and

$$\sqrt{1-x} = 1 - \frac{1}{2}x + \cdots$$

for $x \ll 1$ to find

$$\frac{t}{t_H} = \frac{\Omega_0}{2(\Omega_0-1)^{3/2}}\left\{\sqrt{2}\,[2u(\Omega_0-1)]^{1/2} + \frac{\sqrt{2}}{12}\,[2u(\Omega_0-1)]^{3/2} - 2\sqrt{u(\Omega_0-1)}\left[1 - \frac{1}{2}u(\Omega_0-1)\right]\right\}.$$

The first-order terms, those involving $u^{1/2}$, cancel. The second-order terms, involving $u^{3/2}$, produce

$$\frac{t}{t_H} = \frac{\Omega_0}{2(\Omega_0-1)^{3/2}}\,\frac{4}{3}u^{3/2}(\Omega_0-1)^{3/2} = \frac{2}{3}\,\Omega_0\left[\frac{1}{\Omega_0(1+z)}\right]^{3/2} = \frac{2}{3}\frac{1}{(1+z)^{3/2}\Omega_0^{1/2}},$$

which is Eq. (29.43).

29.12 Beginning with Eq. (29.10) and multiplying through by R gives

$$R\left(\frac{dR}{dt}\right)^2 - \frac{8}{3}\pi G\rho R^3 = -kc^2R.$$

Differentiating with respect to t,

$$\left(\frac{dR}{dt}\right)^3 + 2R\left(\frac{dR}{dt}\right)\left(\frac{d^2R}{dt^2}\right) - \frac{8}{3}\pi G\frac{d\left(\rho R^3\right)}{dt} = -kc^2\frac{dR}{dt}.$$

Using Eqs. (29.50) and (29.10) to replace $d(\rho R^3)/dt$ and $-kc^2$, respectively, gives

$$\left(\frac{dR}{dt}\right)^3 + 2R\left(\frac{dR}{dt}\right)\left(\frac{d^2R}{dt^2}\right) + \frac{8\pi GP}{3c^2}\frac{d\left(R^3\right)}{dt} = \left(\frac{dR}{dt}\right)^3 - \frac{8}{3}\pi GR^2\rho\frac{dR}{dt}.$$

Finally, simplifying gives Eq. (29.51).

29.13 Assume that an expanding shell of mass dm lies immediately above a sphere of mass M, constant density ρ, and radius R. From Newton's second law and Newtonian gravitation,

$$dm\,\frac{d^2R}{dt^2} = -\frac{GM\,dm}{R^2}.$$

But $M = 4\pi\rho R^3/3$. Substituting immediately gives Eq. (29.51) for the special case that $P = 0$.

29.14 From the ideal gas law, $P = \rho kT/\mu m_H$. Furthermore, the thermal energy of an average hydrogen atom is given by $K = 3kT/2 = m_H v_{\text{rms}}^2/2$. Substituting T into the ideal gas law gives (with $\mu = 1$ for pure neutral hydrogen), $\rho = P/(v_{\text{rms}}^2/3) \gg P/c^2$ when $v_{\text{rms}} = 600$ km s^{-1}.

When $\rho = P/c^2$, it is necessary that

$$\frac{P}{\rho c^2} = \frac{kT}{\mu m_H c^2} = 1$$

from the ideal gas law. This corresponds to a temperature of $T = 1.1\times10^{13}$ K. (Of course at this temperature, the assumption that $\mu = 1$ could no longer be valid.) Now, for an adiabatically expanding universe, $RT = T_0$, or

$$R = \frac{T_0}{T} = \frac{2.725\text{ K}}{1.1\times10^{13}\text{ K}} = 2.5\times10^{-13},$$

and

$$z = \frac{1}{R} - 1 = 4\times10^{12}.$$

29.15 Substituting Eq. (29.52) into Eq. (29.50) gives

$$\frac{d\left(R^3\rho\right)}{dt} = -w\rho\frac{d\left(R^3\right)}{dt}.$$

This immediately gives

$$\rho\frac{d\left(R^3\right)}{dt} + R^3\frac{d\rho}{dt} = -w\rho\frac{d\left(R^3\right)}{dt}.$$

Rearranging

$$(1+w)\frac{1}{R^3}\frac{d\left(R^3\right)}{dt} = -\frac{1}{\rho}\frac{d\rho}{dt}.$$

This can also be written as

$$(1+w)\frac{d\ln R^3}{dt} = -\frac{d\ln\rho}{dt}.$$

Integrating, we find

$$(1+w)\ln R^3 = -\ln\rho + C,$$

where C is a constant of integration. Rewriting,

$$\ln R^{3(1+w)} + \ln \rho = C,$$

which immediately leads to

$$R^{3(1+w)}\rho = e^C = \text{constant} = \rho_0.$$

29.16 Starting with the definition of the deceleration parameter (Eq. 29.54),

$$q(t) \equiv -\frac{R(t)\left[d^2R(t)/dt^2\right]}{[dR(t)/dt]^2},$$

and using Eqs. (29.51) and (29.10) to replace d^2R/dt^2 and $(dR/dt)^2$, respectively, $q(t)$ becomes

$$q(t) = -\frac{4\pi G\rho R^2/3}{8\pi G\rho R^2/3 - kc^2}.$$

From the definition of the density parameter (Eq. 29.18), we find

$$q(t) = -\frac{\Omega(t)\, H^2(t)\, R^2/2}{\Omega(t)\, H^2(t)\, R^2 - kc^2}.$$

Finally, using Eq. (29.24) to replace $-kc^2$ gives $q(t) = \frac{1}{2}\Omega(t)$.

29.17 (a) The binding energy is

$$E_b = (m_H + m_n - m_D)c^2 = (1.007825 + 1.008665 - 2.014102)uc^2 = 2.224\,\text{MeV},$$

(b) The wavelength of a photon with this energy is, from Eq. (5.3),

$$\lambda = \frac{hc}{E} = 5.57 \times 10^{-13}\ \text{m}.$$

(c) According to Wien's law (Eq. 3.15), this photon corresponds to the peak wavelength for a blackbody temperature of

$$T = \frac{0.00290\ \text{m K}}{\lambda_{\text{max}}} = 5.20 \times 10^9\ \text{K}.$$

29.18 For a redshift of $z = 1.776$, the scale factor is, from (Eq. 29.4), $R = (1+z)^{-1} = 0.3602$. The temperature of the CBR was, from Eq. (29.58), $T = T_0/R = (2.726\ \text{K})/R = 7.57$ K, in good agreement with the temperature of the intergalactic cloud, 7.4 ± 0.8 K.

29.19 Use the Boltzmann equation (Eq. 8.6),

$$\frac{N_b}{N_a} = \frac{g_b}{g_a}\, e^{-(E_b - E_a)/kT}$$

with $g_a = 1$ (one ground state), $g_b = 3$ (three degenerate first excited states), $N_b/N_a = 27/100$, and $E_b - E_a = 4.8 \times 10^{-4}$ eV. Solving for T, we have

$$T = \frac{-(E_b - E_a)}{k \ln[(N_b g_a)/(N_a g_b)]} = 2.3\ \text{K}.$$

29.20 Assuming for simplicity that the television transmitter radiates equally in all directions with a power of $P = 2.5 \times 10^4$ W, the magnitude of the time-averaged Poynting vector, $\langle S \rangle$, at a distance of $r = 70$ km from the transmitter is $\langle S \rangle = P/(4\pi r^2)$. The energy density of channel 6 photons at this distance is then approximately

$$u_{\text{TV}} \simeq \frac{P}{4\pi r^2 c} = 1.35 \times 10^{-15} \text{ J m}^{-3}.$$

From Eq. (9.5) with $T = 2.73$ K, the energy density of CBR photons with wavelengths between $\lambda_1 = 3.41$ m and $\lambda_2 = 3.66$ m is about

$$u_{\text{CBR}} \simeq u_\lambda \Delta\lambda = \frac{8\pi hc/\lambda_{\text{ave}}^5}{e^{hc/\lambda_{\text{ave}}kT} - 1} (\lambda_2 - \lambda_1) = 1.52 \times 10^{-24} \text{ J m}^{-3},$$

where the average of λ_1 and λ_2 was used to evaluate u_λ. Therefore $u_{\text{TV}}/u_{\text{CBR}} \simeq 9 \times 10^8$; the CBR does not interfere with your television viewing.

29.21 Combining Eq. (4.32) for the relativistic Doppler shift with Wien's law, Eq. (29.59), gives

$$\frac{\nu_{\text{obs}}}{\nu_{\text{rest}}} = \frac{T_{\text{obs}}}{T_{\text{rest}}} = \frac{\sqrt{1 - v^2/c^2}}{1 + (v/c)\cos\phi}.$$

Here, ϕ is the angle between the velocity of the source and the line-of-sight of the observer, so the source moving directly away corresponds to $\phi = 0$. But in Eq. (29.61), θ is the angle between the line-of-sight and the *observer's* motion, so moving directly toward the source corresponds to $\theta = 0$. Thus we must replace ϕ with $180° - \theta$ to obtain

$$T_{\text{moving}} = \frac{T_{\text{rest}}\sqrt{1 - v^2/c^2}}{1 - (v/c)\cos\theta},$$

which is Eq. (29.61). For $v/c \ll 1$, we can use

$$\frac{1}{1 - (v/c)\cos\theta} \simeq 1 + \frac{v}{c}\cos\theta$$

and

$$\sqrt{1 - v^2/c^2} \simeq 1 - \frac{1}{2}\frac{v^2}{c^2} \simeq 1,$$

both to first-order in v/c, to obtain Eq. (29.62).

29.22 The Sun's peculiar velocity relative to the Hubble flow is $v_\odot = 370.6$ km s^{-1}. From Eq. (29.62) with $\theta = 0$ and $T_{\text{rest}} = 2.725$ K, the magnitude of the variation in the temperature of the CBR due to the Sun's motion is

$$T_{\text{moving}} - T_{\text{rest}} = T_{\text{rest}}\frac{v}{c} = 3.37 \times 10^{-3} \text{ K}.$$

29.23 (a) The peak wavelength of the CMB is

$$\lambda_{\text{max}} = \frac{0.002897755 \text{ m K}}{2.725 \text{ K}} = 1.06 \times 10^{-3} \text{ m}.$$

Since the Compton shift is just $\lambda_f - \lambda_i = (h/m_e c)(1 - \cos\theta)$, a characteristic shift is just the Compton wavelength of $\Delta\lambda = \lambda_C \equiv h/m_e c^2 = 2.43 \times 10^{-12}$ m. Thus, the relative shift is only

$$\frac{\Delta\lambda}{\lambda_{\text{max}}} = 2.29 \times 10^{-9}.$$

This implies that the shift in the wavelength of the photon in the electron's rest frame can safely be neglected.

Now consider the four situations depicted in Fig. 29.31. When viewed from the right neither cases 1 or 3 result in any shift in wavelength or frequency of the photon, meaning that $\nu_{f,1} = \nu_{f,3} = \nu_0$, where ν_f is the final frequency and ν_0 is the initial frequency. On the other hand, cases 2 and 4 show reflection of the photon from moving electrons. In case 2, the frequency shift is just the Doppler shift from approach and reflection giving

$$\nu_{f,2} = \nu_0 \left(\sqrt{\frac{1+\beta}{1-\beta}} \right)^2 = \nu_0 \left(\frac{1+\beta}{1-\beta} \right),$$

where $\beta \equiv v_e/c$, and v_e is the velocity of the electron. Similarly

$$\nu_{f,4} = \nu_0 \left(\sqrt{\frac{1-\beta}{1+\beta}} \right)^2 = \nu_0 \left(\frac{1-\beta}{1+\beta} \right).$$

The average final frequency of the four cases is then

$$\nu_f = \frac{1}{4} \left(\nu_{f,1} + \nu_{f,2} + \nu_{f,3} + \nu_{f,4} \right) = \frac{\nu_0}{4} \left(1 + \frac{1+\beta}{1-\beta} + 1 + \frac{1-\beta}{1+\beta} \right) = \frac{\nu_0}{2} \left(1 + \frac{1+\beta^2}{1-\beta^2} \right). \tag{S29.3}$$

For electrons with an average thermal energy associated with $T_e = 10^8$ K,

$$\frac{1}{2} m_e v_e^2 = \frac{3}{2} k T_e,$$

and

$$\beta^2 = \frac{v_e^2}{c^2} = \frac{3kT_e}{m_e c^2} = 0.05.$$

Given that $\beta^2 \ll 1$, ν_f from Eq. (S29.3) can be approximated by

$$\nu_f \simeq \frac{\nu_0}{2} \left[1 + \left(1 + \beta^2 \right) \left(1 + \beta^2 \right) \right] \simeq \frac{\nu_0}{2} \left[1 + 1 + 2\beta^2 + \beta^4 \right] = \nu_0 \left[1 + \beta^2 + \frac{1}{2} \beta^4 \right].$$

Keeping terms to second order, we arrive at

$$\frac{\Delta \nu}{\nu_0} = \frac{\nu_f - \nu_0}{\nu_0} \approx \frac{v_e^2}{c^2} = \frac{3kT_e}{m_e c^2}.$$

(b) From the discussion of opacity leading up to Eq. (9.15), the fraction of photons scattered is roughly

$$\tau = 2 n_e \sigma_T R,$$

where R is the radius of the gas cloud, and $\sigma_T = 6.65 \times 10^{-29}$ m^2 is the Thomson scattering cross section (see Eq. 9.20). Therefore, $\tau = 0.12$.

(c) A fractional shift in the temperature of the CMB is roughly given by

$$\frac{\Delta T}{T_0} \sim -\tau \frac{\Delta \nu}{\nu_0} = -\frac{3kT_e}{m_e c^2} \tau.$$

29.24 From the pressure integral (Eq. 10.8)

$$P = \frac{1}{3}\int_0^\infty n_p p v \, dp.$$

If all of the particles in the sample are highly relativistic, then $v \simeq c$ and $p \simeq \gamma mc$. Substituting,

$$P = \frac{1}{3}\int_0^\infty n_p \gamma mc^2 \, dp.$$

Noting that $E = \gamma mc^2$, and n_p is the number density of particles with momenta between p and $p + dp$, the integral reduces to the total energy density of the relativistic particles. Therefore, $P = \frac{1}{3}u = wu$.

29.25 We will assume that the universe is flat in this problem. Since $R^4\rho_{\rm rel} = \rho_{\rm rel,0}$, and $RT = T_0$ (Eq. 29.58), the energy density of relativistic particles (photons) must be proportional to T^4, or $u_{\rm rel} = aT^4$.

From the first law of thermodynamics for an expanding volume,

$$\frac{dU}{dt} = -P\frac{dV}{dt}. \tag{S29.4}$$

However, we can substitute

$$U = uV = aT^4\left(\frac{4}{3}\pi r^3\right)$$

on the left-hand side of Eq. (S29.4),

$$\frac{dV}{dt} = 4\pi r^2\frac{dr}{dt}$$

on the right-hand side, and $P = aT^4/3$ for the radiation pressure (also on the right-hand side). Eliminating common terms we find

$$\frac{d}{dt}\left(T^4 r^3\right) = -T^4 r^2\frac{dr}{dt}.$$

Now substituting $T = T_0/R$, $r = DR$ for some initial size, D, of the sphere, and eliminating common terms we arrive at

$$\frac{d}{dt}\left(\frac{1}{R}\right) = -\frac{1}{R^2}\frac{dR}{dt}.$$

Since the left-hand side is consistent with the right-hand side, the original assumption of conservation of energy within the sphere must be consistent as well.

29.26 (a) This is a straightforward derivative.

(b) Equation (29.8) shows that

$$\tau_{\rm exp}(t) = \left(\frac{1}{R}\,\frac{dR}{dt}\right)^{-1} = 1/H(t).$$

(c) For a flat universe $k = 0$ and Eq. (29.83) becomes

$$\frac{dR}{dt} = \sqrt{\frac{8}{3}\pi G\left(\frac{\rho_{m,0}}{R} + \frac{\rho_{\rm rel,0}}{R^2}\right)}$$

This implies that

$$\tau_{\rm exp}(R) = R\left[\frac{8}{3}\pi G\left(\frac{\rho_{m,0}}{R} + \frac{\rho_{\rm rel,0}}{R^2}\right)\right]^{-1/2} = R^2\left[\frac{8}{3}\pi G\left[R\,\rho_{m,0} + \rho_{\rm rel,0}\right]\right]^{-1/2}. \tag{S29.5}$$

29.27 (a) Consider first the portion of Eq. (29.84) in square brackets. Deep in the radiation era, $R_{r,m} \ll R$, implying that we can approximate the radical to second order using $(1+x)^{1/2} = 1 + \frac{1}{2}x - \frac{1}{8}x^2 + \cdots$ when $x \ll 1$. This implies that

$$\begin{aligned} 2 + \left(\frac{R}{R_{r,m}} - 2\right)\sqrt{\frac{R}{R_{r,m}} + 1} &= 2 + \left(\frac{R}{R_{r,m}} - 2\right)\left[1 + \frac{1}{2}\frac{R}{R_{r,m}} - \frac{1}{8}\left(\frac{R}{R_{r,m}}\right)^2 + \cdots\right] \\ &= 2 + \frac{R}{R_{r,m}} + \frac{1}{2}\left(\frac{R}{R_{r,m}}\right)^2 - \frac{1}{8}\left(\frac{R}{R_{r,m}}\right)^3 \\ &\quad -2 - \frac{R}{R_{r,m}} + \frac{1}{4}\left(\frac{R}{R_{r,m}}\right)^2 + \cdots \\ &\simeq \frac{3}{4}\left(\frac{R}{R_{r,m}}\right)^2. \end{aligned}$$

where only terms through second-order have been retained. Eq. (29.84) now becomes

$$t(R) \simeq \frac{1}{2}\frac{R^2}{H_0\left(\Omega_{m,0}R_{r,m}\right)^{1/2}}.$$

But $R_{r,m} = \Omega_{m,0}/\Omega_{\rm rel,0}$ (note that a "0" subscript was inadvertently dropped in this expression in the first printing of *An Introduction to Modern Astrophysics*). Substituting, and solving for R gives

$$R(t) = 2^{1/2}H_0^{1/2}\Omega_{\rm rel,0}^{1/4}t^{1/2}.$$

From Eq. (29.80) we now have

$$R(t) = 2^{1/2}H_0^{1/2}\left(\frac{4\pi G g_* a T_0^4}{3H_0^2c^2}\right)^{1/4}t^{1/2} = \left(\frac{16\pi G g_* a}{3c^2}\right)^{1/4}T_0\,t^{1/2}.$$

(b) In a flat universe ($k = 0$) with only relativistic particles, the Friedmann equation becomes

$$\left(\frac{dR}{dt}\right)^2 = \frac{8}{3}\pi G\rho_{\rm rel}R^2.$$

From Eq. (29.77) we have

$$\left(\frac{dR}{dt}\right)^2 = \frac{8\pi G g_* a T^4}{6c^2}R^2 = \frac{8\pi G g_* a T_0^4}{6c^2}\frac{1}{R^2}.$$

This implies that

$$R\frac{dR}{dt} = \left(\frac{8\pi G g_* a T_0^4}{6c^2}\right)^{1/2}.$$

Integrating,

$$\frac{1}{2}R^2 = \left(\frac{8\pi G g_* a T_0^4}{6c^2}\right)^{1/2}t,$$

or

$$R(t) = 2^{1/2}\left(\frac{8\pi G g_* a T_0^4}{6c^2}\right)^{1/4}t^{1/2} = \left(\frac{16\pi G g_* a}{3c^2}\right)^{1/4}T_0\,t^{1/2},$$

which is again Eq. (29.86).

29.28 From Eq. (29.78), and equating at a general time t with today, we find

$$H^2\,(1-\Omega_{\rm rel})\,R^2 = H_0^2\,(1-\Omega_{\rm rel,0})\,. \tag{S29.6}$$

From Eq. (29.5),

$$R^3\,\rho_{\rm rel} = \rho_{\rm rel,0}\,,$$

or

$$R^3\,\Omega_{\rm rel}\rho_c = \Omega_{\rm rel,0}\,\rho_{c,0}.$$

Substituting Eq. (29.12),

$$R^3\,\Omega_{\rm rel}\,H^2 = \Omega_{\rm rel,0}\,H_0^2\,,$$

or

$$\Omega_{\rm rel}\,R^2\,H^2 = \frac{\Omega_{\rm rel,0}\,H_0^2}{R} \tag{S29.7}$$

Equation (S29.7) can be substituted into Eq. (S29.6), and after some rearrangement, we obtain

$$H^2\,R^2 = \left[1+\left(\frac{1}{R}-1\right)\Omega_{\rm rel,0}\right]H_0^2. \tag{S29.8}$$

Substituting Eq. (S29.8) back into Eq. (S29.7) we finally have

$$\Omega_{\rm rel} = \frac{\Omega_{\rm rel,0}}{R+(1-R)\Omega_{\rm rel,0}}.$$

In the limit as $z\to\infty$ or, equivalently, $R\to 0$, $\Omega_{\rm rel}\to 1$. Thus, this one-component, relativistic-particle model is flat in the limit $z\to\infty$.

29.29 Using $R^3\rho_b = \rho_{b,0}$ (Eq. 29.5) with $\rho_{b_0} = 4.17\times10^{-28}$ kg m^{-3} (Eq. 29.17), and $T_0 = R\,T(R)$ (Eq. 29.58) with $T_0 = 2.725$ K and $T = 10^{10}$ K, we find

$$\rho_b = \frac{\rho_{b,0}}{R^3} = \rho_{b,0}\left(\frac{T}{T_0}\right)^3 = 20.6\ {\rm kg\ m^{-3}}.$$

29.30 Using Eq. (4.47) for the rest energy of an electron–positron pair, set $kT \simeq 2m_ec^2$ so $T\simeq 1.2\times10^{10}$ K.

29.31 (a) Following the discussion in Example 9.2.1, consider a neutron with a collision cross section of $\sigma = \pi(2r)^2$ that moves with speed v through point protons of number density n_p. In time Δt there will be $n_p\sigma v\Delta t$ collisions.

(b) To evaluate $n_p\sigma v\Delta t$, we must estimate the number density of protons. Because protons greatly outnumbered neutrons at that time, assume that all of the baryonic matter was in the form of protons with $T_0 = 2.725$ K and $T = 10^9$ K to write

$$n_p \simeq \frac{\rho_b}{m_p} = \frac{\rho_{b,0}}{m_p}\left(\frac{T}{T_0}\right)^3 = 1.2\times10^{25}\ {\rm m^{-3}}.$$

The collision cross section is, using $r\simeq 10^{-15}$ m, $\sigma = \pi(2r)^2 \simeq 1.3\times10^{-29}$ m^2. The speed, v, of the neutrons comes from Eq. (8.3),

$$v_{\rm rms} = \sqrt{\frac{3kT}{m_n}} = 5.0\times10^6\ {\rm m\ s^{-1}}.$$

The characteristic time in the radiation era is obtained from Eq. (29.89) by solving for t with $T = 10^9$ K and $g_* = 3.363$, giving $t_{\rm rad} = 179$ s. Using this for Δt, we find $n_p\sigma v\Delta t \simeq 1.4\times10^5$, which is certainly $\gg 1$. Each neutron had numerable opportunities to combine with a proton.

29.32 (a) We need the Thomson scattering cross section ($\sigma_T = 6.65 \times 10^{-29}$ m^2 from Eq. 9.20) and the number density of free electrons to calculate the mean free path of a photon, $\ell = 1/(n_e\sigma)$ (Eq. 9.12). For a composition of pure hydrogen, $n_e = \rho_b/m_H$, where ρ_b is the density of baryonic matter (protons and electrons in this case). Using $R^3\rho_b = \rho_{b,0} = 4.17 \times 10^{-28}$ kg m^{-3} (Eqs. 29.5 and 29.17), we have

$$n_e = \frac{\rho_b}{m_H} = \frac{\rho_{b,0}}{R^3 m_H},$$

so the mean free path is

$$\ell = \frac{1}{n_e\sigma_T} = \frac{R^3 m_H}{\rho_{b,0}\sigma_T}. \tag{S29.9}$$

The time for a photon to travel the distance ℓ is

$$t_\ell = \frac{\ell}{c} = \frac{R^3 m_H}{c\rho_{b,0}\sigma_T}.$$

(b) Setting $t_\ell = \tau_{\rm exp}$ from Eq. (S29.5), we have

$$\frac{R^3 m_H}{c\rho_{b,0}\sigma_T} = R^2\left[\frac{8}{3}\pi G\left[R\,\rho_{m,0} + \rho_{\rm rel,0}\right]\right]^{-1/2}.$$

This can be simplified somewhat to give

$$R^3 + \left(\frac{\rho_{\rm rel,0}}{\rho_{m,0}}\right)R^2 - \frac{K}{\rho_{m,0}} = 0, \tag{S29.10}$$

where the constant K is given by

$$K \equiv \left(\frac{3}{8\pi G}\right)\left(\frac{c\rho_{b,0}\sigma_T}{m_H}\right)^2.$$

The cubic equation Eq. (S29.10) can be solved numerically (using a Newton method for example) to give

$$R = 0.0257 \qquad \text{implying} \qquad z = R^{-1} - 1 = 37.9.$$

An example Fortran 95 code:

```
Program Cubic_Solver
USE Constants, ONLY : c, pi, G, m_H

IMPLICIT NONE
REAL(8),    PARAMETER   ::  rho_m0 = 2.56E-27, rho_b0 = 4.17E-28
REAL(8),    PARAMETER   ::  rho_c0 = 9.47E-27, Omega_rel0 = 8.25E-5, rho_rel0 = rho_c0*Omega_rel0
REAL(8),    PARAMETER   ::  sigma_T = 6.65E-29
REAL(8),    PARAMETER   ::  K = (3/(8*pi*G))*(c*rho_b0*sigma_T/m_H)**2

REAL(8),    PARAMETER   ::  rel_error = 1E-6

REAL(8)                 ::  R, dR, F, dF

R = 1
dR = 1000
DO WHILE (ABS(dR/R) > rel_error)
    F = R**3 + (rho_rel0/rho_m0)*R**2 - K/rho_m0
    dF = 3*R**2 + 2*(rho_rel0/rho_m0)*R

    dR = -F/dF

    R = R + dR
```

```
    WRITE(*,*) "R, dR = ", R, dR
END DO

PAUSE
STOP
END
```

From Eq. (29.84), this implies an age for the universe of $t = 2.4 \times 10^{15}$ s $= 75$ Myr.

29.33 Eq. (29.101) gives

$$\frac{m_H R^3}{f\rho_{b,0}} \left(\frac{2\pi m_e k T_0}{h^2 R}\right)^{3/2} e^{-\chi_I R/kT_0} - \frac{f}{1-f} = 0.$$

This can be solved numerically with a Newton method (for example) with $f = 0.5$ to give $R = 7.24806 \times 10^{-4}$.

```
Program Newton_Solver
USE Constants, ONLY : pi, m_H, m_e, h, k_B, eV

IMPLICIT NONE
REAL(8),     PARAMETER   ::  rho_b0 = 4.17E-28, chi = 13.6*eV, T_0 = 2.725, frac = 0.5

REAL(8),     PARAMETER   ::  rel_error = 1E-6

REAL(8)                  ::  R, dR, F, dF

R = 1E-4
dR = 1000
DO WHILE (ABS(dR/R) > rel_error)
    F = m_H*R**3/(frac*rho_b0)*(2*pi*m_e*k_B*T_0/(h**2*R))**1.5*exp(-chi*R/(k_B*T_0)) - frac/(1 - frac)
    dF = 3*m_H*R**2/(frac*rho_b0)*(2*pi*m_e*k_B*T_0/(h**2*R))**1.5*exp(-chi*R/(k_B*T_0)) &
        & - 1.5*m_H*R**3/(frac*rho_b0)*(2*pi*m_e*k_B*T_0/(h**2))**1.5*R**(-2.5)*exp(-chi*R/(k_B*T_0)) &
        & - chi/(k_B*T_0)*m_H*R**3/(frac*rho_b0)*(2*pi*m_e*k_B*T_0/(h**2*R))**1.5*exp(-chi*R/(k_B*T_0))

    dR = -F/dF

    R = R + dR

    WRITE(*,*) "R, dR = ", R, dR
END DO

PAUSE
STOP
END
```

29.34 If $z = 1089$, then $R = 1/(1+z) = 9.174 \times 10^{-4}$. From Eq. (29.84) with other WMAP values of $R_{r,m} = 3.05 \times 10^{-4}$, $H_0 = 2.30 \times 10^{-18}$ s^{-1}, and $\Omega_{m,0} = 0.27$, we find $t = 1.194 \times 10^{13}$ s $= 378$ kyr. This is in excellent agreement with the WMAP result.

29.35 The program used in Problem 29.33 can also be used to find R when 99% of the hydrogen atoms were ionized ($f = 0.99$) and when 1% of the hydrogen atoms are ionized ($f = 0.01$). The results are $R_{99} = 6.300 \times 10^{-4}$ and $R_1 = 8.766 \times 10^{-4}$, respectively. These values of R correspond to $z_{99} = 1586$ and $z_1 = 1140$, implying

$$\Delta z = 447.$$

The times are again obtained from Eq. (29.84), as was done in the solution for Problem 29.36. The results are $t_{99} = 199$ kyr and $t_1 = 350$ kyr. This implies

$$\Delta t = 151 \text{ kyr}.$$

In both cases the range is somewhat larger than the quoted WMAP results.

29.36 Using $R_\oplus = 6.378136 \times 10^6$ m from Appendix A and the Taylor series $\sin x \simeq x - x^3/3! + \cdots$ for small x, the discrepancy for $D = 100$ m is

$$\begin{aligned} C_{\rm exp} - C_{\rm meas} &= 2\pi D - 2\pi R_\oplus \sin(D/R_\oplus) \\ &\simeq 2\pi D - 2\pi R_\oplus \left[\frac{D}{R_\oplus} - \frac{1}{3!}\left(\frac{D}{R_\oplus}\right)^3 \right] \\ &= \frac{\pi D^3}{3R_\oplus^2} = 2.57 \times 10^{-8} \text{ m} = 25.7 \text{ nm}. \end{aligned}$$

29.37 Equating Eqs. (29.120) and (29.121) we have

$$H^2(1-\Omega)R^2 = H_0^2(1-\Omega_0).$$

This can be solved for Ω to give

$$\Omega = 1 - \frac{H_0^2}{H^2}\frac{1-\Omega_0}{R^2} = 1 - \frac{H_0^2}{H^2}(1-\Omega_0)(1+z)^2.$$

Substituting Eq. (29.122), we arrive at

$$\Omega(z) = 1 - \frac{1-\Omega_0}{\Omega_{m,0}(1+z) + \Omega_{\rm rel,0}(1+z)^2 + \Omega_{\Lambda,0}(1+z)^{-2} + 1 - \Omega_0}. \qquad \text{(S29.11)}$$

We can now verify that our last result reduces to Eq. (29.28) in the appropriate special case of baryonic matter only. Let $\Omega_{\rm rel,0} = 0$ and $\Omega_{\Lambda,0} = 0$, which then requires that $\Omega_{m,0} = \Omega_0$. Substituting into Eq. (S29.11) we have

$$\Omega(z) = 1 - \frac{1-\Omega_0}{\Omega_0(1+z) + 1 - \Omega_0} = 1 + \frac{\Omega_0 - 1}{1 + \Omega_0 z},$$

as expected.

29.38 From the Robertson–Walker metric (Eq. 29.106) with $d\varpi = 0$ for a spherical surface and $dt = 0$, we see that the differential element of area is

$$dA = [R(t)\varpi\, d\theta][R(t)\varpi \sin\theta\, d\phi] = [R(t)\varpi]^2 \sin\theta\, d\theta\, d\phi.$$

Integrating this over the usual limits of $\theta = 0$ to π and $\phi = 0$ to 2π gives the area of the spherical surface,

$$A_{\rm horizon} = [R(t)\varpi]^2 \int_{\phi=0}^{2\pi}\int_{\theta=0}^{\pi} \sin\theta\, d\theta\, d\phi = 4\pi[R(t)\varpi]^2.$$

29.39 (a) If we consider the general acceleration equation (Eq. 29.112) with $\rho_{\rm rel} = 0$ and $P_m = P_{\rm rel} = 0$, we have

$$\frac{1}{R}\frac{d^2R}{dt^2} = -\frac{4}{3}\pi G\rho_m + \frac{1}{3}\Lambda c^2.$$

If the universe is static, this requires that $d^2R/dt^2 = 0$ or

$$\Lambda = \frac{4\pi G\rho_m}{c^2}.$$

(b) If the universe is static, we must also have $dR/dt = 0$. This implies that Eq. (29.114) can be solved for k, giving

$$k = \left[\frac{8}{3}\pi G\left(\rho_m + \rho_\Lambda\right)\right]\left(\frac{R^2}{c^2}\right).$$

Noting that from Eq. (29.113), $\rho_\Lambda \equiv \Lambda c^2/8\pi G = \rho_m/2$, we find

$$k = \frac{4\pi G\rho_m R^2}{c^2} > 0.$$

This static universe is closed.

(c) In solving for Λ we assumed that $d^2R/dt^2 = 0$. However, any slight deviation of ρ_m will result in a non-zero acceleration. As a result, this universe is in an unstable equilibrium.

29.40 The WMAP values we will need are:

$$\begin{aligned}
[H_0]_{\text{WMAP}} &= 2.30 \times 10^{-18}\ \text{s}^{-1} \\
[T_0]_{\text{WMAP}} &= 2.725 \pm 0.002\ \text{K} \\
[\Omega_{m,0}]_{\text{WMAP}} &= 0.27 \pm 0.04 \\
\Omega_{\text{rel},0} &= 8.24 \times 10^{-5} \\
[\Omega_{\Lambda,0}]_{\text{WMAP}} &= 0.73 \pm 0.04 \\
\Lambda_0 &= \frac{3H_0^2\Omega_{\Lambda,0}}{c^2} = 1.29 \times 10^{-52}\ \text{m}^{-2} \\
[\Omega_0]_{\text{WMAP}} &= 1.02 \pm 0.02 \\
\rho_{m,0} &= 2.56 \times 10^{-27}\ \text{kg m}^{-3}
\end{aligned}$$

Using $z = 1089$:

From Eq. (29.122), $H = 4.96 \times 10^{-14}\ \text{s}^{-1}$.

From Eq. (29.58), $T = (1+z)T_0 = 2970$ K.

From Eq. (29.6), $\rho_m = (1+z)^3\rho_{m,0} = 3.32 \times 10^{-18}\ \text{kg m}^{-3}$.

From Eq. (29.18), $\Omega_m = \dfrac{8\pi G\rho_m}{3H^2} = 0.75$.

From Eq. (29.80), $\Omega_{\text{rel}} = \dfrac{4\pi G g_* a T^4}{3H^2c^2} = 0.25$.

From Eq. (29.118), $\Omega_\Lambda = \dfrac{\Lambda c^2}{3H^2} = 1.6 \times 10^{-9}$.

29.41 Beginning with Eq. (29.122) and moving $(1+z)$ inside the radical, we find

$$H = H_0\left[\Omega_{m,0}(1+z)^3 + \Omega_{\text{rel},0}(1+z)^4 + \Omega_{\Lambda,0} + (1-\Omega_0)(1+z)^2\right]^{1/2}.$$

Using the generalized equation of state given by Eq. (29.52), $P = w\rho c^2$, we note that for pressureless dust, $w_m = w_1 = 0$. This implies that the quantity $3(1+w_1) = 3$. Similarly, for radiation and relativistic particles, $w_{\text{rel}} = w_2 = 1/3$, so that $3(1+w_2) = 4$. Finally, for dark energy, Eq. (29.115), $w_\Lambda = w_3 = -1$, so that $3(1+w_3) = 0$.

Combining these results leads to the desired equation.

29.42 We begin with Eq. (29.54) and note that $H = (dR/dt)/R$ (Eq. 29.8). This gives

$$q(t) = -\frac{1}{R}\frac{d^2R/dt^2}{H^2}. \tag{S29.12}$$

Turning next to the acceleration equation (Eq. 29.112), using Eq. (29.113) for the equivalent mass density of dark energy, and rearranging, we have

$$\frac{1}{R}\frac{d^2R}{dt^2} = -\frac{4}{3}\pi G\left[\rho_m + \rho_{\rm rel} - 2\rho_\Lambda + \frac{3\,(P_m + P_{\rm rel})}{c^2}\right].$$

However, $P_m = 0$ for pressureless dust, and $P_{\rm rel} = \frac{1}{3}\rho_{\rm rel}c^2$, which leads to

$$\frac{1}{R}\frac{d^2R}{dt^2} = -\frac{4}{3}\pi G\left[\rho_m + 2\rho_{\rm rel} - 2\rho_\Lambda\right]. \tag{S29.13}$$

Substituting back into Eq. (S29.12), we obtain

$$q(t) = \frac{8\pi G}{3H^2}\left[\frac{1}{2}\rho_m + \rho_{\rm rel} - \rho_\Lambda\right].$$

From the definition of the density parameter (Eq. 29.18) we have

$$q(t) = \frac{1}{2}\Omega_m + \Omega_{\rm rel} - \Omega_\Lambda.$$

We also have (see the solution to the previous problem, for example) $w_m = 0$, $w_{\rm rel} = 1/3$, and $w_\Lambda = -1$. Using these values leads to the expression

$$q(t) = \frac{1}{2}\sum_i (1 + 3w_i)\Omega_i(t).$$

29.43 If the acceleration of the universe changed sign at some point in time, then it is necessary that $d^2R/dt^2 = 0$ at that time. Referring to Eq. (S29.13) from the solution to the last problem, it must have been the case that

$$\rho_m + 2\rho_{\rm rel} - 2\rho_\Lambda = 0$$

when this occurred. Assuming that $\rho_\Lambda = \text{constant} = \rho_{\rm upLambda,0}$ (as stated in Eq. 29.113), then

$$\rho_m + 2\rho_{\rm rel} = 2\rho_{\Lambda,0}.$$

We can now express ρ_m and $\rho_{\rm rel}$ in terms of their present values and R by

$$\rho_m = \rho_{m,0}/R^3$$

and

$$\rho_{\rm rel} = \rho_{\rm rel,0}/R^4.$$

Substituting, we find

$$\rho_{m,0}/R^3 + 2\rho_{\rm rel,0}/R^4 = 2\rho_{\Lambda,0},$$

or

$$2\rho_{\Lambda,0}\,R^4 - \rho_{m,0}\,R - 2\rho_{\rm rel,0} = 0.$$

Dividing through by the present-day critical density $\rho_{c,0}$ and using the definition of the acceleration parameter (Eq. 29.18), this expression becomes

$$2\Omega_{\Lambda,0}R^4 - \Omega_{m,0}R - 2\Omega_{\rm rel,0} = 0.$$

Noting that $\Omega_{\rm rel,0} \ll \Omega_{\Lambda,0}$ and $\Omega_{\rm rel,0} \ll \Omega_{m,0}$ we can safely neglect the last term. Thus, either $R = 0$ (where our analysis is invalid), or

$$R = \left(\frac{\Omega_{m,0}}{2\Omega_{\Lambda,0}}\right)^{1/3}.$$

Evaluating with WMAP values gives $R = 0.57$, and $z = 1/R - 1 = 0.76$.

29.44 (a) The look-back time is given by $t_L = t_0 - t(z)$. But t_0 is obtained by substituting $R = 1$ into Eq. (29.129). If we also replace R by $1/(1+z)$ in the expression for $t(R)$, we quickly obtain.

$$t_L(z) = \frac{2}{3}\frac{1}{H_0\sqrt{\Omega_{\Lambda,0}}}\ln\left[\frac{\sqrt{\frac{\Omega_{\Lambda,0}}{\Omega_{m,0}}} + \sqrt{1+\frac{\Omega_{\Lambda,0}}{\Omega_{m,0}}}}{\frac{1}{(1+z)^{3/2}}\left(\sqrt{\frac{\Omega_{\Lambda,0}}{\Omega_{m,0}}} + \sqrt{1+\frac{\Omega_{\Lambda,0}}{\Omega_{m,0}}}\right)}\right] = \frac{1}{H_0\sqrt{\Omega_{\Lambda,0}}}\ln(1+z).$$

(b) See Fig. S29.1. The space density declines rapidly beyond $t_L/t_H = 1.5$.

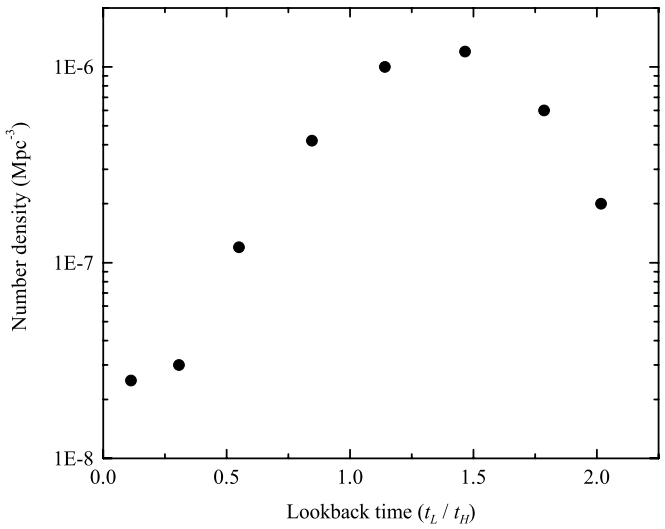

Figure S29.1: The number density of AGNs as a function of lookback time.

29.45 (a) Beginning with Eq. (29.122) and replacing $1+z$ with $1/R$, we find

$$H = H_0\left[\frac{\Omega_{m,0}}{R^3} + \frac{\Omega_{\rm rel,0}}{R^4} + \Omega_{\Lambda,0} + \frac{1-\Omega_0}{R^2}\right]^{1/2}.$$

As R grows well beyond $R = 1$, each term on the right-hand side of the equation approaches zero except the Λ term, which remains constant. Therefore, H approaches a constant, given by

$$H = H_0\sqrt{\Omega_{\Lambda,0}}.$$

(b) Starting with the Friedmann equation in the form of Eq. (29.120), assuming that $\Omega = \Omega_\Lambda = \Lambda c^2/3H^2$, and equating the Friedmann equation with today's values, we find

$$H^2\left(1 - \frac{\Lambda c^2}{3H^2}\right)R^2 = H_0^2(1 - \Omega_{\Lambda,0}).$$

This implies that

$$H^2R^2 - \left(\frac{\Lambda c^2}{3}\right)R^2 = H_0^2(1 - \Omega_{\Lambda,0}).$$

However, $H = (dR/dt)/R$, giving

$$\left(\frac{dR}{dt}\right)^2 = \left(\frac{\Lambda c^2}{3}\right)R^2 + H_0^2(1 - \Omega_{\Lambda,0}).$$

Rewriting and integrating

$$\int_{t_0}^{t} dt' = \int_1^R \frac{dR'}{\sqrt{\left(\frac{\Lambda c^2}{3}\right)R'^2 + H_0^2(1 - \Omega_{\Lambda,0})}}$$

$$t - t_0 = \left(\frac{3}{\Lambda c^2}\right)^{1/2} \int_1^R \frac{dR'}{\sqrt{R'^2 + \left(\frac{3H_0^2}{\Lambda c^2}\right)(1 - \Omega_{\Lambda,0})}}$$

$$= \left(\frac{3}{\Lambda c^2}\right)^{1/2} \ln\left[R' + \sqrt{R'^2 + \left(\frac{3H_0^2}{\Lambda c^2}\right)(1 - \Omega_{\Lambda,0})}\right]\Bigg|_1^R.$$

Define

$$\tau \equiv \left(\frac{3}{\Lambda c^2}\right)^{1/2} = \frac{1}{\sqrt{\Omega_{\Lambda,0}}H_0},$$

where the last expression was obtained from Eq. (29.118). We can now rewrite the result of the integration as

$$\frac{t - t_0}{\tau} = \ln\left[\frac{R + \sqrt{R^2 + \Omega_{\Lambda,0}(1 - \Omega_{\Lambda,0})}}{1 + \sqrt{1 + \Omega_{\Lambda,0}(1 - \Omega_{\Lambda,0})}}\right],$$

which leads to

$$R + \sqrt{R^2 + \Omega_{\Lambda,0}(1 - \Omega_{\Lambda,0})} = Ce^{(t-t_0)/\tau},$$

where

$$C \equiv 1 + \sqrt{1 + \Omega_{\Lambda,0}(1 - \Omega_{\Lambda,0})} = \text{constant}.$$

This expression for R is clearly exponentially increasing with time when $\Lambda > 0$ (implying $\tau > 0$).

(c) Using WMAP values, the characteristic time is $\tau = 16$ Gyr.

29.46 Start with Eq. (29.153). Writing $dt = dR/(dR/dt)$ and using $R = 1/(1 + z)$ (Eq. 29.4) produces

$$d_h(t) = R(t)\int_0^{\frac{1}{1+z}} \frac{c\,dR}{R(dR/dt)}.$$

To evaluate the integral, dR/dt must be expressed in terms of R only. Evaluating Eq. (29.9) at the present epoch with $H = H_0$, $\rho = \rho_0$ and $R = 1$, and equating the left-hand side with the left-hand side of Eq. (29.11) gives

$$\left(\frac{dR}{dt}\right)^2 = \frac{8}{3}\pi G\rho_0\left(\frac{1}{R} - 1\right) + H_0^2.$$

Using Eqs. (29.15) and (29.19), we find

$$\frac{8}{3}\pi G\rho_0 = \Omega_0 H_0^2,$$

and

$$\left(\frac{dR}{dt}\right)^2 = H_0^2\left(\frac{\Omega_0}{R} - \Omega_0 + 1\right).$$

The integral for the horizon distance thus becomes, using $R = 1/(1+z)$ (Eq. 29.4),

$$d_h(z) = \frac{c}{H_0(1+z)}\int_0^{\frac{1}{1+z}} \frac{dR}{\sqrt{\Omega_0 R - (\Omega_0 - 1)R^2}}.$$

The integral has the form

$$\int \frac{dx}{\sqrt{bx - ax^2}} = \frac{1}{\sqrt{a}}\left[\cos^{-1}\left(1 - \frac{2ax}{b}\right) - \frac{\pi}{2}\right]$$

with $a = \Omega_0 - 1$ and $b = \Omega_0$. Evaluating the integral gives the desired result.

29.47 Equation (29.152) for the circumference of a closed universe is, using $R = 1/(1+z)$ (Eq. 29.4),

$$C_{\text{univ}} = \frac{2\pi c}{H_0(1+z)\sqrt{\Omega_0 - 1}}.$$

Using Eq. (29.197) for d_h, the horizon distance in a closed universe, we see that

$$\frac{d_h}{C_{\text{univ}}} = \frac{1}{2\pi}\cos^{-1}\left[1 - \frac{2(\Omega_0 - 1)}{\Omega_0(1+z)}\right].$$

At very early times, as $z \to \infty$, $d_h/C_{\text{univ}} \to 0$. That is, the fractional size of a causally connected region becomes vanishingly small as $t \to 0$. According to Eq. (29.33), the maximum value of R in a closed universe — at the time of maximum expansion — is

$$R_{\max} = \frac{\Omega_0}{\Omega_0 - 1} = \left(\frac{1}{1+z}\right)_{\max}.$$

Then at the time of maximum expansion,

$$\frac{d_h}{C_{\text{univ}}} = \frac{1}{2\pi}\cos^{-1}\left[1 - \frac{2(\Omega_0 - 1)}{\Omega_0}\frac{\Omega_0}{\Omega_0 - 1}\right] = \frac{1}{2\pi}\cos^{-1}(-1) = \frac{1}{2}.$$

29.48 For a flat universe, the proper distance is $d(t) = R(t)\varpi$ (Eq. 29.148). Using Eq. (29.163) for ϖ and Eq. (29.31) for the scale factor shows that the proper distance of the photon is

$$d(t) = \left(\frac{3}{2}\right)^{2/3}\left(\frac{t}{t_H}\right)^{2/3}\left[\varpi_e - \frac{2c}{H_0}\left(\frac{t}{t_0}\right)^{1/3}\right].$$

To evaluate ϖ_e, note that if the photon is just now ($R = 1$) arriving from the present particle horizon, then the present proper distance $d(t) = R(t)\varpi$ to its point of emission at ϖ_e is $d = \varpi_e$. But this is just the present horizon distance, $d_{h,0} = 2c/H_0$ (Eq. 29.159), so $\varpi_e = 2c/H_0$. Inserting this, we find

$$d(t) = \left(\frac{3}{2}\right)^{2/3} \left(\frac{t}{t_H}\right)^{2/3} \frac{2c}{H_0} \left[1 - \left(\frac{t}{t_0}\right)^{1/3}\right].$$

Again using $t_0 = 2t_H/3$ for a flat universe, we arrive at the proper distance of the photon from Earth as a function of time,

$$d(t) = \frac{2c}{H_0} \left[\left(\frac{t}{t_0}\right)^{2/3} - \frac{t}{t_0}\right],$$

which is Eq. (29.165). To find the maximum distance, we solve for the time when

$$\frac{d[d(t)]}{dt} = 0$$

$$\frac{2c}{H_0} \left[\left(\frac{1}{t_0}\right)^{2/3} \frac{2}{3} t^{-1/3} - \frac{1}{t_0}\right] = 0$$

$$\frac{t}{t_0} = \frac{8}{27}.$$

Inserting this into $d(t)$, the maximum proper distance of the photon during its journey is

$$d_{\max} = \frac{8c}{27H_0},$$

or, expressed as a fraction of the present horizon distance $d_{h,0} = 2c/H_0$,

$$\frac{d_{\max}}{d_{h,0}} = \frac{4}{27}.$$

29.49 (a) Beginning with the Robertson–Walker metric (Eq. 29.106), setting $ds = 0$ for a light ray, $d\theta = d\phi = 0$ for the radial expansion of a shell, and $k = 0$ for a flat universe, we find

$$-\frac{c\,dt}{R'(t)} = d\varpi'.$$

From Eq. (29.8), $H(t) = R(t)^{-1} dR(t)/dt$, and $dt = dR/HR$, implying

$$d\varpi' = -\frac{c}{HR'^2} dR.$$

Again changing variables using Eq. (29.4), $R' = (1 + z')^{-1}$ and $dR' = -(1 + z')^{-2}\, dz'$, we have

$$d\varpi' = \frac{c}{H(z')} dz'.$$

Using Eq. (29.27) to write $H(z') = H_0(1 + z')^{3/2}$ with $\Omega_0 = 1$ leads to

$$d\varpi' = \frac{c}{H_0} \frac{1}{(1 + z')^{3/2}}\, dz'.$$

Integrating ϖ' from 0 to ϖ and z' from 0 to z gives

$$\varpi(z) = \frac{2c}{H_0} \left[1 - \frac{1}{\sqrt{1 + z}}\right].$$

(b) The proper distance is given by Eq. (29.144), which implies that

$$d_p(t) = R(t)\varpi.$$

Thus,

$$d_p(z) = R(z)\varpi = \frac{2c}{H_0}\left[(1+z) - \sqrt{1+z}\right].$$

(c) The horizon distance is given by Eq. (29.153),

$$d_h(t) = R(t)\int_0^t \frac{c\,dt'}{R(t')}.$$

Changing variables from t' to z' requires Eq. (29.31) so that

$$t' = \frac{2t_H}{3}R'^{3/2},$$

and

$$dt' = t_H R'^{1/2}\,dR' = -t_H(1+z)^{-5/2}\,dz'.$$

Therefore,

$$d_h(z) = -\frac{ct_H}{1+z}\int_\infty^z \frac{dz'}{(1+z')^{5/2}} = \frac{2ct_H}{3(1+z)}\left[\frac{1}{(1+z')^{3/2}}\right]_\infty^z = \frac{2c}{3H_0(1+z)^{5/2}},$$

where the last expression was obtained from $t_H \equiv 1/H_0$. For the WMAP values of $z = 0$ and $H_0 = 2.30 \times 10^{-18}\ \text{s}^{-1}$ we find $d_h = 8.7 \times 10^{25}$ m $= 2.8$ Gpc. This is roughly a factor of five below the result obtained in Eq. (29.159).

29.50 We begin with the Robertson–Walker metric (Eq. 29.106), setting $ds = 0$ for a light ray, and considering only radial motion ($d\theta = d\phi = 0$). This implies that

$$\int_t^{t_0} \frac{c\,dt'}{R'} = -\int_\varpi^0 \frac{d\varpi'}{\sqrt{1-k\varpi'^2}}. \tag{S29.14}$$

The right-hand side can be integrated directly by

$$-\int_\varpi^0 \frac{d\varpi'}{\sqrt{1-k\varpi'^2}} = -\frac{1}{\sqrt{k}}\int_\varpi^0 \frac{d\varpi'}{\sqrt{\frac{1}{k}-\varpi'^2}}$$

$$= \frac{1}{\sqrt{k}}\sin^{-1}\sqrt{k}\varpi.$$

Note that this solution is general so long as we allow complex values to be used when $k < 0$. This can be seen by noting that

$$\sin\theta = \frac{e^{i\theta} - e^{-i\theta}}{2i},$$

and

$$\sinh\theta = \frac{e^{\theta} - e^{-\theta}}{2}.$$

Comparing gives $\sin i\theta = i\sinh\theta$.

The left-hand side of Eq. (S29.14) is more challenging to integrate. Recalling that

$$H = \frac{1}{R}\frac{dR}{dt},$$

we can change variables to give

$$\int_t^{t_0} \frac{c\,dt'}{R'} = c\int_R^1 \frac{dR'}{H(R')R'^2}.$$

From Eq. (29.27) and $R = 1/(1+z)$, we find

$$\begin{aligned}\int_t^{t_0} \frac{c\,dt'}{R'} &= \frac{c}{H_0}\int_R^1 \frac{dR'}{R'^{1/2}\left[R'(1-\Omega_0)+\Omega_0\right]^{1/2}} \\ &= \frac{c}{H_0\sqrt{1-\Omega_0}}\int_R^1 \frac{dR'}{R'^{1/2}\left[R' - \frac{\Omega_0}{\Omega_0 - 1}\right]^{1/2}} \\ &= \frac{c}{H_0\sqrt{\Omega_0-1}}\int_R^1 \frac{dR'}{R'^{1/2}\left[\frac{\Omega_0}{\Omega_0-1} - R'\right]^{1/2}}.\end{aligned}$$

This can be integrated by making the change of variable $u = R^{1/2}$, giving an integral of the form

$$c\int_t^{t_0}\frac{dt'}{R'} = \frac{2c}{H_0\sqrt{\Omega_0-1}}\int_{R'=R}^{R'=1}\frac{du}{\sqrt{\frac{\Omega_0}{\Omega_0-1}-u^2}}.$$

Again we obtain a solution involving $\sin^{-1}$.

Equating the solutions for the two sides of Eq. (S29.14), and using Eq. (29.25) to write

$$\sqrt{k} = \frac{H_0\sqrt{\Omega_0-1}}{c},$$

eventually leads to the desired result; Mattig's relation.

29.51 Beginning with Eq. (29.168), and setting $\Omega_{\rm rel,0} = 0$, we have

$$I(z) \equiv \int_0^z \frac{dz'}{\sqrt{\Omega_{m,0}(1+z')^3 + \Omega_{\Lambda,0} + (1-\Omega_0)(1+z')^2}}.$$

Now a Taylor's series for a general function $f(z')$ is given by

$$f(z') = f(z'_0) + \left.\frac{\partial f(z')}{\partial z'}\right|_{z'_0}\left(z'-z'_0\right) + \frac{1}{2!}\left.\frac{\partial^2 f(z')}{\partial z'^2}\right|_{z'_0}\left(z'-z'_0\right)^2 + \frac{1}{3!}\left.\frac{\partial^3 f(z')}{\partial z'^3}\right|_{z'_0}\left(z'-z'_0\right)^3 + \cdots. \quad \text{(S29.15)}$$

Setting $f(z')$ equal to the integrand, and expanding around $z' = 0$,

$$\left.\frac{\partial f(z')}{\partial z'}\right|_0 = -\frac{1}{2}f^3(0)\left[3\Omega_{m,0} + 2\left(1-\Omega_0\right)\right], \quad \text{(S29.16)}$$

where

$$f(0) = \frac{1}{\sqrt{\Omega_{m,0}+\Omega_{\Lambda,0}+(1-\Omega_0)}} = 1.$$

The last expression is obtained because $\Omega_{m,0} + \Omega_{\Lambda,0} = \Omega_0$. We can also simplify the rest of Eq. (S29.16) by also noting that $q_0 = \frac{1}{2}\Omega_{m,0} - \Omega_{\Lambda,0}$. This implies that

$$3\Omega_{m,0} + 2(1 - \Omega_0) = \Omega_{m,0} + 2(\Omega_0 - \Omega_{\Lambda,0}) + 2(1 - \Omega_0) = 2q_0 + 2.$$

At this point the first two terms of Eq. (S29.15) are

$$f(z') = 1 - (1 + q_0)z' + \cdots.$$

To obtain the second-order term (the z'^2 term), we proceed similarly. Evaluating the second derivative,

$$\frac{\partial^2 f(z')}{\partial z'^2} = \frac{\partial}{\partial z'}\left\{-\frac{1}{2}f^3(z')\left[3\Omega_{m,0}\left(1 + z'\right)^2 + 2(1 - \Omega_0)\left(1 + z'\right)\right]\right\}$$

$$= \frac{3}{4}f^5(z')\left[3\Omega_{m,0}\left(1 + z'\right)^2 + 2(1 - \Omega_0)\left(1 + z'\right)\right]^2 - \frac{1}{2}f^3(z')\left[6\Omega_{m,0}\left(1 + z'\right) + 2(1 + \Omega_0)\right].$$

Evaluating at $z' = 0$, and noting that $6\Omega_{m,0} + 4(1 - \Omega_0) = 4q_0 + 4$ leads to

$$\left.\frac{\partial^2 f(z')}{\partial z'^2}\right|_0 = 3q_0^2 + 4q_0 - \Omega_0 + 2.$$

Substitution into the second term of Eq. (S29.15), combined with our previous results for the zeroth- and first-order terms gives the desired result.

29.52 (a) The first three terms in a general Taylor series for $R(t)$, expanded about the present time, t_0, are as given in the problem,

$$R(t) = R(t_0) + \left.\frac{dR}{dt}\right|_{t_0}(t - t_0) + \frac{1}{2}\left.\frac{d^2R}{dt^2}\right|_{t_0}(t - t_0)^2 + \cdots.$$

At the present time, the scale factor is $R(t_0) = 1$, and

$$\left.\frac{dR}{dt}\right|_{t_0} = H_0 \quad \text{and} \quad \left.\frac{d^2R}{dt^2}\right|_{t_0} = -H_0^2 q_0,$$

from Eqs. (29.8) and (29.54). Therefore,

$$R(t) = 1 - H_0(t_0 - t) - \frac{1}{2}H_0^2 q_0(t_0 - t)^2 + \cdots.$$

(b) Using $1/(1 - x) = 1 + x + x^2 + \cdots$, we have

$$\frac{1}{R(t)} = \frac{1}{1 - \left[H_0(t_0 - t) + \frac{1}{2}H_0^2 q_0(t_0 - t)^2 + \cdots\right]}$$

$$= 1 + \left[H_0(t_0 - t) + \frac{1}{2}H_0^2 q_0(t_0 - t)^2 + \cdots\right]$$

$$+ \left[H_0(t_0 - t) + \frac{1}{2}H_0^2 q_0(t_0 - t)^2 + \cdots\right]^2 + \cdots$$

$$= 1 + H_0(t_0 - t) + \frac{1}{2}H_0^2 q_0(t_0 - t)^2 + H_0^2(t_0 - t)^2 + \cdots$$

$$= 1 + H_0(t_0 - t) + H_0^2\left(1 + \frac{1}{2}q_0\right)(t_0 - t)^2 + \cdots.$$

to second-order in $H_0(t_0 - t)$. (Long division is actually easier!)

(c) From Eq. (29.4), $1 + z = 1/R(t)$, so

$$1 + z = 1 + H_0(t_0 - t) + H_0^2 \left(1 + \frac{1}{2}q_0\right)(t_0 - t)^2 + \cdots,$$

or

$$t_0 - t = \frac{z}{H_0} - H_0 \left(1 + \frac{1}{2}q_0\right)(t_0 - t)^2 + \cdots.$$

But to first-order, $t_0 - t = z/H_0$, so substituting on the right gives

$$t_0 - t = \frac{z}{H_0} - \left(1 + \frac{1}{2}q_0\right)\frac{z^2}{H_0} + \cdots$$

to second-order in z.

(d) We start with Eq. (29.138),

$$\int_{t_e}^{t_0} \frac{c\,dt}{R(t)} = \int_0^{\varpi_e} \frac{d\varpi}{\sqrt{1 - k\varpi^2}}.$$

Using the first two terms in our expression for $1/R(t)$ in the left-hand integral, and $1/\sqrt{1-x} = 1 + x/2 + \cdots$ with the right-hand integral, we obtain

$$c\int_{t_e}^{t_0} [1 + H_0(t_0 - t) + \cdots]\,dt = \int_0^{\varpi_e} \left[1 + \frac{1}{2}k\varpi^2 + \cdots\right] d\varpi,$$

or

$$c(t_0 - t_e) + cH_0 t_0(t_0 - t_e) - \frac{c}{2}H_0\left(t_0^2 - t_e^2\right) + \cdots = \varpi_e + \frac{1}{6}k\varpi_e^3 + \cdots.$$

The ϖ_e^3-term can be dropped because it is proportional to $(t_0 - t_e)^3$ at least. We also drop the "e" subscripts that identify the time and place of the photon's origin. Solving for ϖ, we obtain an expression for the comoving coordinate of the photon as a function of time,

$$\varpi = c(t_0 - t)\left[1 + \frac{1}{2}H_0(t_0 - t)\right] + \cdots.$$

(e) Using the expression for $(t_0 - t)$ derived in part (c) results in an expression for ϖ in terms of the redshift,

$$\begin{aligned}\varpi &= c\left[\frac{z}{H_0} - \left(1 + \frac{1}{2}q_0\right)\frac{z^2}{H_0} + \cdots\right]\left[1 + \frac{1}{2}H_0\left(\frac{z}{H_0} + \cdots\right)\right] + \cdots \\ &= \frac{cz}{H_0}\left[1 - \frac{1}{2}(1 + q_0)z\right] + \cdots,\end{aligned}$$

to second-order in z.

29.53 A direct comparison of Eq. (29.168) with Eq. (29.122) and Eq. (29.196), combined with substitutions into Eqs. (29.170) – (29.172) lead immediately to the desired result.

29.54 (a) The angular diameter is obtained from Eq. (29.190),

$$\theta = \frac{DH_0(1 + z)}{cS(z)}.$$

For a flat universe, $S(z) = I(z)$ (Eq. 29.173), $\Omega_{\text{rel},0} = \Omega_{\Lambda,0} = 0$, and $\Omega_{m,0} = \Omega_0 = 1$, implying from Eq. (29.168) that

$$S(z) = \int_0^z \frac{dz'}{(1 + z')^{3/2}} = 2\left(1 - \frac{1}{\sqrt{1 + z}}\right).$$

Substitution and some simplification gives

$$\theta = \frac{DH_0}{2c}\frac{(1+z)^{3/2}}{\sqrt{1+z}-1}.$$

(b) For a minimum to occur, it is necessary that $d\theta/dz = 0$, or

$$0 = \frac{DH_0}{2c}\left[\frac{3}{2}\frac{\sqrt{1+z}}{\sqrt{1+z}-1} - \frac{1}{2}\frac{1+z}{\left(\sqrt{1+z}-1\right)^2}\right] = \frac{DH_0}{2c}\left[\frac{(1+z)-\frac{3}{2}\sqrt{1+z}}{\left(\sqrt{1+z}-1\right)^2}\right].$$

Setting the numerator equal to zero leads to the quadratic equation

$$z^2 - \frac{1}{4}z - \frac{5}{4} = \left(z - \frac{5}{4}\right)\left(z+1\right).$$

Therefore either $z = 5/4$ or $z = -1$. Choosing the physical solution, we find that $z = 1.25$ produces a minimum in θ. (Note that $z = -1$ implies that $\theta = 0$.)

(c) Using WMAP values, $\theta_{\min} = 8 \times 10^{-4}$ rad $= 2.7'$.

29.55 The required X-ray flux data were inadvertently omitted in the first printing of *An Introduction to Modern Astrophysics*. The X-ray flux for Abell 697 is $F_X = 5.77 \times 10^{-15}$ W m^{-2}. and the X-ray flux for Abell 2218 is $F_X = 7.16 \times 10^{-15}$ W m^{-2}

(a) Beginning with Eq. (27.19), the X-ray luminosity of the intracluster gas is given by

$$L_X = \mathcal{L}_{\rm vol} V = \left(\frac{4\pi C'}{3}\right) n_e^2 T_e^{1/2} R^3,$$

where $C' = 1.42 \times 10^{-40}$ (note that there was an error in the exponent of the constant in the first printing of *An Introduction to Modern Astrophysics*). From the Sunyaev–Zel'dovich effect (Eq. 29.64)

$$\frac{\Delta T}{T_0} \simeq 2\frac{kT_e}{m_e c^2}\tau = 2\frac{kT_e}{m_e c^2}\sigma_T n_e (2R),$$

where the last expression involving the Thomson cross section (σ_T) and the number density of electrons (n_e) was obtained from the result of Problem 29.23(b). Solving for n_e we have

$$n_e = \frac{(\Delta T/T_0) m_e c^2}{4kT_e \sigma_T R}.$$

Substituting into L_X results in

$$L_X = \frac{\pi}{12} C' \left[\frac{(\Delta T/T_0)^2 m_e^2 c^4}{k^2 \sigma_T^2}\right] R T_e^{-3/2}.$$

This implies that the measured flux at Earth is given by

$$F_X = \frac{L_X}{4\pi d_L^2} = \frac{L_X}{4\pi(1+z)^4 d_A^2} = \frac{L_X H_0^2}{4\pi(1+z)^2 c^2 S^2(z)},$$

where Eqs. (29.191) and (29.192) were used. Substituting L_X and solving for one power of H_0 gives

$$H_0 = \frac{48(1+z)^2 c^2 F_X k^2 T_e^{3/2} \sigma_T^2 S^2(z)}{RC'(\Delta T/T_0)^2 m_e^2 c^4 H_0}.$$

The remaining value of H_0 in the right-hand side can be replaced using Eq. (29.193). Also substituting $D = 2R$ we arrive at

$$H_0 = \left(\frac{96k^2\sigma_T^2}{C'm_e^2c^3}\right)(1+z)^3 S(z)\frac{F_X T_e^{3/2}}{\theta(\Delta T/T_0)^2} = Cf(z)\frac{F_X T_e^{3/2}}{\theta(\Delta T/T_0)^2}.$$

The numerical value of the constant is $C = 2.5\times10^{-26}$, and $f(z) \equiv (1+z)^3 S(z)$.

(b) For the purposes of this problem, comparing Eqs. (29.176) and (29.180) gives

$$S(z) \simeq z - \frac{1}{2}(1+q_0)z^2,$$

where $q_0 \simeq \frac{1}{2}\Omega_{m,0} - \Omega_{\Lambda,0} = -0.595$ for WMAP values.

From the data for Abell 697: $T_e \simeq 9.2\times10^7$ K (the value should *not* be halved, as incorrectly suggested in the first printing of *An Introduction to Modern Astrophysics*), $\theta = 46'' = 2.2\times10^{-4}$ rad, $\Delta T/T_0 = 3.84\times10^{-4}$, $F_X = 5.77\times10^{-15}$ W m^{-2}, $z = 0.282$, and $S(z) = 0.266$. Substituting values gives $H_{0,697} = 2.2\times10^{-18}$ s^{-1}. This would correspond to a value of $h = 0.68$ (differing from the WMAP value by 4.4%).

From the data for Abell 2218: $T_e \simeq 8.4\times10^7$ K (again, the value should not be halved), $\theta = 69'' = 3.3\times10^{-4}$ rad, $\Delta T/T_0 = 2.92\times10^{-4}$, $F_X = 5.77\times10^{-15}$ W m^{-2}, $z = 0.171$, and $S(z) = 0.165$. Substituting values gives $H_{0,2218} = 1.0\times10^{-18}$ s^{-1}. This would correspond to a value of $h = 0.31$ (differing from the WMAP value by 56%).

29.56 Using Eq. (29.166), with the expression for $R(t)$ from Eq. (29.132) substituted on the left-hand side, and the expression for $R(t)$ from Eq. (29.133) substituted on the right-hand side, we have

$$\left(\frac{2}{3\sqrt{\Omega_{m,0}}}\right)^{2/3}\int_{t_e}^{t_0}\left(\frac{t}{t_H}\right)^{-2/3}dt = \left(\frac{4\Omega_{\Lambda,0}}{\Omega_{m,0}}\right)^{1/3}\int_{t_{\rm mva}}^{\infty}e^{-H_0\sqrt{\Omega_{\Lambda,0}}t}\,dt. \qquad \text{(S29.17)}$$

Focusing our attention on the left-hand side initially, we can change variables from t to z by use of Eq. (29.92),

$$\frac{t(z)}{t_H} = \frac{2}{3}\frac{1}{(1+z)^{3/2}\sqrt{\Omega_{m,0}}},$$

which also implies that

$$dt = \frac{2t_H}{3\sqrt{\Omega_{m,0}}}\left(-\frac{3}{2}\right)(1+z)^{-5/2}dz.$$

Making the substitutions, simplifying, and evaluating, the left-hand side of Eq. (S29.17) becomes

$$\left(\frac{2}{3\sqrt{\Omega_{m,0}}}\right)^{2/3}\int_{t_e}^{t_0}\left(\frac{t}{t_H}\right)^{-2/3}dt = \frac{t_H}{\sqrt{\Omega_{m,0}}}\int_0^z\frac{dz'}{(1+z')^{-3/2}} = \frac{2t_H}{\sqrt{\Omega_{m,0}}}\left[1-\frac{1}{\sqrt{1+z}}\right].$$

Eq. (S29.17) now becomes (after evaluating the right-hand side)

$$\frac{2t_H}{\sqrt{\Omega_{m,0}}}\left[1-\frac{1}{\sqrt{1+z}}\right] = \left(\frac{4\Omega_{\Lambda,0}}{\Omega_{m,0}}\right)^{1/3}\left(\frac{1}{-H_0\sqrt{\Omega_{\Lambda,0}}}\right)\left[e^{-\infty} - e^{-H_0\sqrt{\Omega_{\Lambda,0}}t_{\rm mva}}\right].$$

Rearranging, and noting that $t_H H_0 = 1$, we have

$$e^{-H_0\sqrt{\Omega_{\Lambda,0}}t_{\rm mva}} = \frac{2t_H H_0\sqrt{\Omega_{\Lambda,0}}}{\sqrt{\Omega_{m,0}}}\left[\frac{\sqrt{1+z}-1}{\sqrt{1+z}}\right]\left(\frac{\Omega_{m,0}}{4\Omega_{\Lambda,0}}\right)^{1/3}$$

$$= \left(\frac{2\sqrt{\Omega_{\Lambda,0}}}{\sqrt{\Omega_{m,0}}}\right)\left(\frac{\sqrt{\Omega_{m,0}}}{2\sqrt{\Omega_{\Lambda,0}}}\right)^{2/3}\left[\frac{\sqrt{1+z}-1}{\sqrt{1+z}}\right]$$

$$= \left(\frac{2\sqrt{\Omega_{\Lambda,0}}}{\sqrt{\Omega_{m,0}}}\right)^{1/3}\left[\frac{\sqrt{1+z}-1}{\sqrt{1+z}}\right].$$

Taking the natural logarithm of both sides and noting that $-\ln x = \ln x^{-1}$ gives the desired result.

To find the largest value of z for which $t_{\text{mva}} > t_H$ requires that

$$\frac{1}{\sqrt{\Omega_{\Lambda,0}}}\ln\left[\left(\frac{\sqrt{\Omega_{m,0}}}{2\sqrt{\Omega_{\Lambda,0}}}\right)^{1/3}\left(\frac{\sqrt{1+z}}{\sqrt{1+z}-1}\right)\right] < 1.$$

Rewriting,

$$\left(\frac{\sqrt{\Omega_{m,0}}}{2\sqrt{\Omega_{\Lambda,0}}}\right)^{1/3}\left(\frac{\sqrt{1+z}}{\sqrt{1+z}-1}\right) < e^{\sqrt{\Omega_{\Lambda,0}}},$$

or

$$\frac{\sqrt{1+z}}{\sqrt{1+z}-1} - \left(\frac{2\sqrt{\Omega_{\Lambda,0}}}{\sqrt{\Omega_{m,0}}}\right)^{1/3} e^{\sqrt{\Omega_{\Lambda,0}}} < 0.$$

The critical case (when the left-hand side is identically zero) can be solved by a root-finding algorithm, such as a Newton method. An example Fortran 95 code that also returns the specific results for $z = 0.1$, 0.5, 1.0, and 1.5 is given below. The results are:

$$\begin{aligned} z_{\text{largest}} &= 0.9624 \\ t_{\text{mva}}/t_H &= 3.126 \quad \text{for } z = 0.1 \\ &= 1.520 \quad \text{for } z = 0.5 \\ &= 0.973 \quad \text{for } z = 1.0 \\ &= 0.707 \quad \text{for } z = 1.5 \end{aligned}$$

```
Program t_mva_Solver

IMPLICIT NONE
REAL(8),     PARAMETER    ::  H_0 = 2.3E-18 !s^-1
REAL(8),     PARAMETER    ::  t_H = 1/H_0
REAL(8),     PARAMETER    ::  Omega_m0 = 0.27, Omega_Lambda0 = 0.73
REAL(8)                   ::  K

REAL(8),     PARAMETER    ::  rel_error = 1E-6

REAL(8)                   ::  z, dz, F, dF

K = (2*SQRT(Omega_Lambda0)/SQRT(Omega_m0))**(1/3.0)*EXP(SQRT(Omega_Lambda0))

z = 1
dz = 10000
DO WHILE (ABS(dz/z) > rel_error)
    F = SQRT(1+z)/(SQRT(1+z)-1) - K
    dF = 1/(2*SQRT(1+z)*(SQRT(1+z)-1)) - 1/(2*(SQRT(1+z)-1)**2)

    dz = -F/dF

    z = z + dz
```

```
    WRITE(*,*) "z, dz = ", z, dz
END DO

!Find specific values for t_mva
z = 0.1
WRITE(*,*) "For z = ", z, "   t_mva/t_H = ", &
    & 1/SQRT(Omega_Lambda0)*LOG((SQRT(Omega_m0)/(2*SQRT(Omega_Lambda0)))**(1/3.) &
    & *(SQRT(1+z)/(SQRT(1+z) - 1)))

z = 0.5
WRITE(*,*) "For z = ", z, "   t_mva/t_H = ", &
    & 1/SQRT(Omega_Lambda0)*LOG((SQRT(Omega_m0)/(2*SQRT(Omega_Lambda0)))**(1/3.) &
    & *(SQRT(1+z)/(SQRT(1+z) - 1)))

z = 1
WRITE(*,*) "For z = ", z, "   t_mva/t_H = ", &
    & 1/SQRT(Omega_Lambda0)*LOG((SQRT(Omega_m0)/(2*SQRT(Omega_Lambda0)))**(1/3.) &
    & *(SQRT(1+z)/(SQRT(1+z) - 1)))

z = 1.5
WRITE(*,*) "For z = ", z, "   t_mva/t_H = ", &
    & 1/SQRT(Omega_Lambda0)*LOG((SQRT(Omega_m0)/(2*SQRT(Omega_Lambda0)))**(1/3.) &
    & *(SQRT(1+z)/(SQRT(1+z) - 1)))
PAUSE
STOP
END
```

29.57 (a) See Fig. S29.2. The data were generated by the Fortran 95 code given below.

(b) $z = 0.08$.

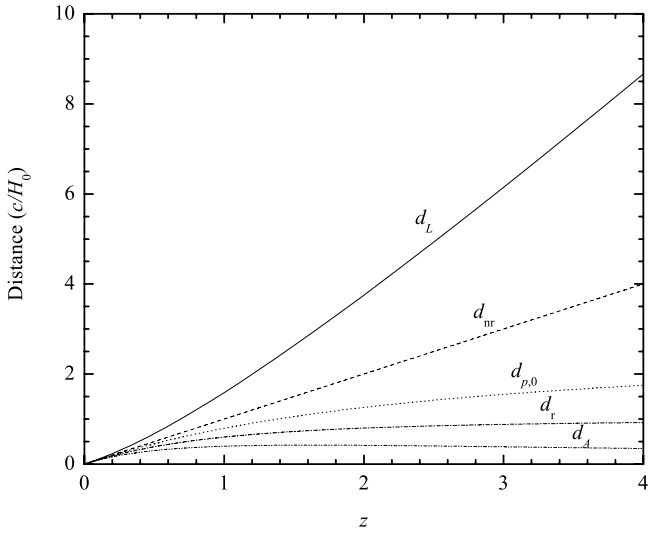

Figure S29.2: Various distances (in units of c/H_0) as a function of z for WMAP values.

```
PROGRAM Problem_29_57
IMPLICIT NONE

REAL(8),     PARAMETER    ::  Omega_m0 = 0.27, Omega_rel0 = 8.24E-5, Omega_L0 = 0.73, Omega_0 = 1.02

REAL(8)                   ::  z_max, z, dz
REAL(8)                   ::  I, g_z, g_zplus, I_1, S
REAL(8)                   ::  d_p0, d_L, d_A, d_nr, d_r
INTEGER                   ::  n = 100000

OPEN(UNIT = 10, FILE = "Prob_29_57.txt")
```

```
z_max = 0
DO WHILE (z_max <= 4.001)
    dz    = z_max/n

    ! integrand of Eq. (29.168)
    z = 0
    g_z = 1/SQRT(Omega_m0*(1 + z)**3 + Omega_rel0*(1 + z)**4 + Omega_L0 + (1 - Omega_0)*(1 + z)**2)

    I = 0
    DO WHILE (z < z_max)
        z = z + dz
        g_zplus = 1/SQRT(Omega_m0*(1 + z)**3 + Omega_rel0*(1 + z)**4 + Omega_L0 + (1 - Omega_0)*(1 + z)**2)

        I = I + (g_z + g_zplus)*dz/2
        g_z = g_zplus
    END DO

    S = SIN(I*SQRT(Omega_0 - 1))/SQRT(Omega_0-1)  !Eq. (29.174) for Omega_0 > 1

    d_L  = S*(1 + z_max)                    !Eq. (29.184) in units of c/H_0
    d_p0 = I                                !Eq. (29.169) in units of c/H_0
    d_A  = d_L/(1 + z_max)**2               !Eq. (29.192) in units of c/H_0
    d_r  = ((z+1)**2 - 1)/((z+1)**2 + 1)    !Eq. (27.7)   in units of c/H_0
    d_nr = z                                !Eq. (27.8)   in units of c/H_0

    WRITE(10,'(7F13.6)') z, d_L, d_p0, d_A, d_r, d_nr, ABS((d_L - d_r)/d_L)

    z_max = z_max + 0.01
END DO

PAUSE
STOP
END
```

29.58 (a) At $z = 4.25$, Eq. (29.4) gives $R = 0.1905$. The age of the universe at that value of z can be obtained by numerically integrating Eq. (29.128). An example Fortran 95 program is given at the end of this problem. The result is $t = 1.4610$ Gyr $= 0.1066 t_0$.

(b) The present proper distance to the radio galaxy 8C 1435+63 comes from Eq. (29.169), so $d_{p,0} = 7570$ Mpc.

(c) The universe was smaller by a factor of $1/(1 + z)$ when the light was emitted, implying that $d_p = 1442$ Mpc.

(d) The luminosity distance is given by Eq. (29.184), $d_L = 3.93 \times 10^4$ Mpc.

(e) The angular diameter distance is given by Eq. (29.191), $d_A = 1427$ Mpc.

(f) With $\theta = 5'' = 2.42 \times 10^{-5}$ rad, the linear diameter of the galaxy is given by Eq. (29.190), or $D = 34.58$ kpc.

(g) Repeating part (f) for $z = 1$ (so the galaxy is *closer*), we have $D = 40.8$ kpc. Even though the galaxy is closer, a *larger* galaxy is needed to produce the same angular size!

```
PROGRAM Problem_29_58

USE Constants, ONLY : c, G, pi, yr, pc, degrees_to_radians

REAL(8),    PARAMETER   ::  rho_c0 = 9.47E-27
REAL(8),    PARAMETER   ::  Omega_m0 = 0.27, Omega_rel0 = 8.24E-5, Omega_L0 = 0.73, Omega_0 = 1.02
REAL(8),    PARAMETER   ::  rho_m0 = rho_c0*Omega_m0, rho_rel0 = rho_c0*Omega_rel0, &
                            & rho_L0 = rho_c0*Omega_L0
REAL(8),    PARAMETER   ::  t_0 = 13.7 !Gyr
REAL(8),    PARAMETER   ::  H_0 = 2.30E-18 !s^-1

REAL(8)                 ::  z_max, z, dz
REAL(8)                 ::  R_max, R, dR
REAL(8)                 ::  t, f_R, f_Rplus
```

```
REAL(8)                 ::  I, g_z, g_zplus, I_1, S
REAL(8)                 ::  d_p0, d_L, d_A, D, theta
INTEGER                 ::  n = 1000000

LOGICAL                 ::  save = .FALSE.

z_max = 4.25
R_max = 1/(1 + z_max)
dR    = R_max/n
dz    = z_max/n

! integrand of Eq. (29.128)
R = 0
f_R = R/SQRT(rho_m0*R + rho_rel0 + rho_L0*R**4)

! integrand of Eq. (29.168)
z = 0
g_z = 1/SQRT(Omega_m0*(1 + z)**3 + Omega_rel0*(1 + z)**4 + Omega_L0 + (1 - Omega_0)*(1 + z)**2)

t = 0
I = 0
DO WHILE (z < z_max)
    R = R + dR
    f_Rplus = R/SQRT(rho_m0*R + rho_rel0 + rho_L0*R**4)

    t = t + (f_R + f_Rplus)*dR/2
    f_R = f_Rplus

    z = z + dz
    g_zplus = 1/SQRT(Omega_m0*(1 + z)**3 + Omega_rel0*(1 + z)**4 + Omega_L0 + (1 - Omega_0)*(1 + z)**2)

    I = I + (g_z + g_zplus)*dz/2
    g_z = g_zplus

    IF (z > 1 .AND. save == .FALSE.) THEN
        I_1 = I
        save = .TRUE.
    END IF
END DO

S = SIN(I*SQRT(Omega_0 - 1))/SQRT(Omega_0-1)  !Eq. (29.174) for Omega_0 > 1

t = t*SQRT(3/(8*pi*G))      !include leading constant in Eq. (29.128)
t = t/(1E9*yr)              !convert to Gyr
WRITE(*,*) "t    = ", t,    "Gyr   t/t0 = ", t/t_0

WRITE(*,*) "I    = ", I
WRITE(*,*) "S    = ", S

d_p0 = c*I/H_0              !Eq. (29.169)
d_p0 = d_p0/(1E6*pc)        !convert to Mpc
WRITE(*,*) "d_p0 = ", d_p0, "Mpc"

WRITE(*,*) "d_p  = ", d_p0/(1 + z_max), "Mpc   (at the time light was emitted)"

d_L  = c*S*(1 + z_max)/H_0     !Eq. (29.184)
WRITE(*,*) "d_L  = ", d_L/(1E6*pc),  "Mpc"

d_A  = d_L/(1 + z_max)**2   !Eq. (29.192)
WRITE(*,*) "d_A  = ", d_A/(1E6*pc),  "Mpc"

theta = 5 !arcsec
theta = (theta/3600)*degrees_to_radians
D    = d_A*theta*1000       !Eq. (29.190)
WRITE(*,*) "D    = ", D/(1E3*pc), "kpc   (when z = 4.25)"

D    = ((c*I_1/H_0)*theta/2)/(1E3*pc)  !Eq. (29.190) for z = 1 with conversion to kpc
WRITE(*,*) "D    = ", D, "kpc   (when z = 1)"

PAUSE
STOP
END
```

CHAPTER 30

The Early Universe

30.1 Using Eqs. (9.7) and (9.65) with $T = 2.725$ K, the present number density of CBR blackbody photons is $n_{\text{photon}} = aT^3/(2.70k) = 4.11 \times 10^8$ m^{-3}. The present number density of baryons in a universe of pure hydrogen is $n_{b,0} = \rho_{b,0}/m_H$. With $\rho_{b,0} = 4.17 \times 10^{-28}$ kg m^{-3} (Eq. 29.17), $n_{b,0} = 0.25$ m^{-3}. The ratio of the two is

$$\frac{n_{b,0}}{n_{\text{photon}}} = 6.08 \times 10^{-10}.$$

There are roughly 1.6 billion photons for every baryon in the universe.

30.2 (a) If most of the dark matter in the Milky Way's dark halo is in the form of ordinary objects such as brown dwarfs and Jupiter-sized objects, this would favor hot dark matter for the nonbaryonic matter in the universe. If the universe were dominated by cold dark matter, it would have also accumulated in the Galactic dark halo and overwhelmed the contribution of ordinary objects.

(b) If less than 20% of the Milky Way's dark halo is in the form of ordinary objects, then no conclusion can be reached. The nonbaryonic matter could be either hot or cold.

30.3 (a) See Fig. S30.1.

(b) By inspection of Fig. S30.1 for $k = +1$ m^{-1}, there is a point of stable equilibrium at $x = 0$.

(c) For $k = -1$ m^{-1}, the points of equilibrium occur where $dV/dx = 0$,

$$\frac{d}{dx}\left(-x^2 + 0.5x^4\right) = 0$$

$$-2x + 2x^3 = 0,$$

which has solutions $x = 0$ (unstable) and $x = \pm 1$ (stable).

(d) For the case of $k = -1$ m^{-1}, when the ball is "at rest" at the origin, it is in a symmetric condition (reflection symmetry about the line $x = 0$). However, Heisenberg's uncertainty principle, $\Delta x\, \Delta p \approx \hbar$ (Eq. 5.19), implies that the ball cannot be perfectly at rest. This law of quantum mechanics requires that the ball move from its symmetric but unstable equilibrium position at $x = 0$ and roll down toward an unsymmetric, stable position of lower potential energy at either $x = +1$ or $x = -1$. In an analogous manner, the universe was initially in a supercooled false vacuum state of unbroken symmetry. Then a quantum fluctuation governed by the uncertainty principle caused a transition to a lower energy state of broken symmetry, the true vacuum.

30.4 The end of the GUTs epoch occurred when the temperature was approximately $T \sim 10^{28}$ K. The energy density of blackbody radiation at that temperature is (Eq. 9.7) $u = aT^4 \sim 8 \times 10^{96}$ J m^{-3}. Comparing this with the energy density of the false vacuum, $u_{\text{fv}} \approx 10^{98}$ J m^{-3} (Eq. 30.9), and considering the crude nature of this estimate, these two energy densities can be described as being of the same order of magnitude.

30.5 The Planck time is $t_p = 5.39 \times 10^{-44}$ s (Eq. 30.3). According to standard Big-Bang cosmology, the scale factor at that time (deep in the radiation era) was, from Eq. (29.87),

$$R_{\text{standard}} = (1.51 \times 10^{-10}\ \text{s}^{-1/2}) g_*^{1/4} t_p^{1/2}.$$

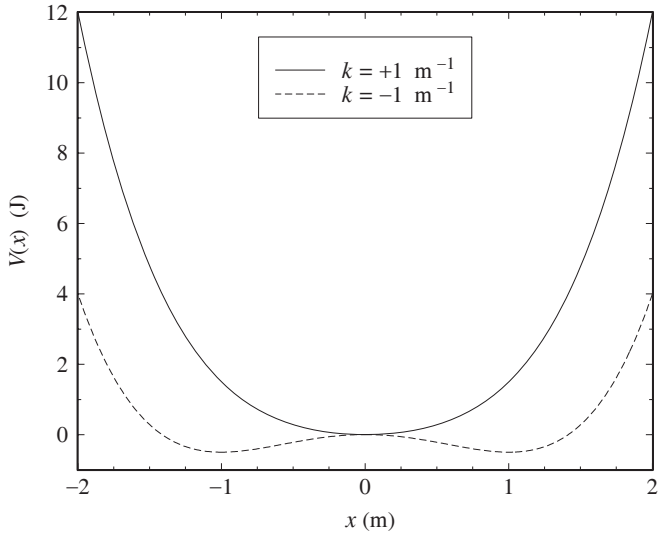

Figure S30.1: Results for Problem 30.3(a).

If we adopt a value of $g_* \simeq 160$ very early in the universe, we find $R_{\text{standard}} = 1.2 \times 10^{-31}$.

Assuming a flat universe, the size of the observable universe (the present horizon distance, Eq. 29.159) is $d_{h,0} = 4.50 \times 10^{26}$ m. At the Planck time, the size of the observable universe was $R_{\text{standard}} d_{h,0} = 5.61 \times 10^{-5}$ m. To take inflation into account, the above value of R at the Planck time must be divided by roughly $e^{t/\tau_i} = e^{100}$ (see Eq. 30.12) to find $R_{\text{inflation}} = 4.46 \times 10^{-75}$. At the Planck time, the size of the observable universe was $R_{\text{inflation}} d_{h,0} = 2.01 \times 10^{-48}$ m.

30.6 Model a cosmic string as a long cylinder filled with false vacuum with an energy density of $u_{\text{fv}} \approx 1.6 \times 10^{98}$ J m^{-3} (Eq. 30.9). If the linear mass density of a cosmic string is $\lambda \sim 10^{21}$ kg m^{-1}, then the energy per unit length is $\lambda c^2 = 9 \times 10^{37}$ J m^{-1} from Eq. (4.47). Assuming that the string has a circular cross section of radius r, then $\lambda c^2 = u_{\text{fv}} \pi r^2$, or

$$r = c\sqrt{\frac{\lambda}{u_{\text{fv}}\pi}} = 4.2 \times 10^{-31} \text{ m}.$$

30.7 (a) In Example 29.4.1 we found that when $T = 10^9$ K, the horizon distance was $d_h = 1.07 \times 10^{11}$ m. The density of baryonic matter at that time comes from combining Eqs. (29.5) and (29.58) with $T_0 = 2.725$ K and $T = 10^9$ K to give

$$\rho_b = \rho_{b,0}\left(\frac{T}{T_0}\right)^3 = 0.0206 \text{ kg m}^{-3}.$$

The mass of baryonic matter contained within a causally connected region of diameter d_h is then

$$m_b = \frac{4}{3}\pi\left(\frac{d_h}{2}\right)^3 \rho_b = 1.32 \times 10^{31} \text{ kg} = 6.6 \text{ M}_\odot.$$

This is about an order of magnitude smaller than the Jeans mass of ≈ 200 M$_\odot$ at $T = 10^9$ K shown in Fig. 30.7.

(b) From Eqs. (29.87) and (29.154), $d_h = 2ct \propto R^2$. Also, $R^3 \rho_b = \rho_{b,0}$ (Eq. 29.5), so $\rho_b \propto R^{-3}$. Thus $m_b \propto d_h^3 \rho_b \propto (R^2)^3 R^{-3} = R^3$. But from $T_0 = RT$ (Eq. 29.58), we have $R \propto T^{-1}$, so $m_b \propto T^{-3}$.

But before recombination, the Jeans mass was also proportional to T^{-3} (Fig. 30.7). This means that the value of m_b remained about an order of magnitude smaller than the Jeans mass throughout the radiation era.

30.8 (*Note:* An oversight occurred in the first printing of *An Introduction to Modern Astrophysics*; the WMAP values should be used rather than $\Omega_0 = 1$ and $h = 1$.)

Eq. (29.84) shows that the transition from the radiation era to the matter era ($R = R_{r,m}$) occurred at about

$$t_{r,m} = 1.74 \times 10^{12} \text{ s} = 5.52 \times 10^4 \text{ yr} \quad \text{(WMAP values)}.$$

At that time the scale factor was $R_{r,m} = 3.05 \times 10^{-4}$ according to WMAP values. According to Eq. (29.154) the horizon distance was $d_h = 2ct = 1.04 \times 10^{21}$ m. Furthermore, the density of baryonic matter was $\rho_b = \rho_{b,0}/R^3 = 1.47 \times 10^{-17}$ kg m^{-3} (using Eq. 29.5 with $\rho_{b,0} = 4.17 \times 10^{-28}$ kg m^{-3} from Eq. 29.17). The mass of baryonic matter contained within a causally connected region of diameter d_h is therefore

$$m_b = \frac{4}{3}\pi \left(\frac{d_h}{2}\right)^3 \rho_b = 6.9 \times 10^{46} \text{ kg} = 3.5 \times 10^{16} \text{ M}_\odot.$$

This is a very large mass, comparable to that of a large cluster of galaxies. Assuming that a typical baryonic density fluctuation was less massive than this, we conclude that most of the baryonic density fluctuations became sub-horizon-sized by the end of the radiation era.

30.9 Equation (30.23) describes the growth of a density fluctuation during the matter era from its initial value at time t_i as,

$$\frac{\delta\rho}{\rho} = \left(\frac{\delta\rho}{\rho}\right)_i \left(\frac{t}{t_i}\right)^{2/3}.$$

From Eq. (29.43), $t \propto (1+z)^{-3/2}$ for a nearly flat universe, so if $\delta\rho/\rho = 1$ today, we have

$$1 = \left(\frac{\delta\rho}{\rho}\right)_i \left(\frac{t}{t_i}\right)^{2/3} = \left(\frac{\delta\rho}{\rho}\right)_i \left[\frac{1}{(1+z)^{-3/2}}\right]^{2/3},$$

or

$$\left(\frac{\delta\rho}{\rho}\right)_i = \frac{1}{1+z}.$$

If a density fluctuation is $(\delta\rho/\rho)_1$ at redshift z_1 and $(\delta\rho/\rho)_2$ at redshift z_2, then

$$\left(\frac{\delta\rho}{\rho}\right)_2 = \left(\frac{\delta\rho}{\rho}\right)_1 \left(\frac{t_2}{t_1}\right)^{2/3} = \left(\frac{\delta\rho}{\rho}\right)_1 \left[\frac{(1+z_2)^{-3/2}}{(1+z_1)^{-3/2}}\right]^{2/3}$$

so

$$\frac{(\delta\rho/\rho)_2}{(\delta\rho/\rho)_1} = \frac{1+z_1}{1+z_2}.$$

30.10 Using $R^3\rho_b = \rho_{b,0}$ (Eq. 29.5) and $T_0 = RT(R)$ (Eq. 29.58), we have $\rho = CT^3$, where C is a constant. Setting $\rho = \rho_0 + \delta\rho$ and $T = T_0 + \delta T$, we have

$$\rho_0 + \delta\rho = C(T_0 + \delta T)^3$$

$$\rho_0\left(1 + \frac{\delta\rho}{\rho_0}\right) = CT_0^3\left(1 + 3\frac{\delta T}{T_0} + \cdots\right)$$

$$\frac{\delta\rho}{\rho_0} = 3\frac{\delta T}{T_0}$$

to first order in the deltas.

30.11 For a flat universe in the matter era, when decoupling occurred at $[z_{\rm dec}]_{\rm WMAP} = 1089 \simeq 1100$, Eq. (29.156) gives the horizon distance as

$$d_h = \frac{2c}{H_0\sqrt{\Omega_{m,0}}}\frac{1}{(1+z)^{3/2}} = \frac{5.02\times 10^{26}\ \text{m}}{(1+z)^{3/2}} = 1.4\times 10^{22}\ \text{m} = 0.45\ \text{Mpc}.$$

This is the linear diameter of the largest causally connected region observed for the CBR. From Eq. (29.193), the angular diameter of this region is

$$\theta = \frac{H_0 d_h}{c}\frac{(1+z)}{S(z)}.$$

$S(z) \equiv I(z)$ for a flat universe, and must be evaluated numerically. This can be done using `PROGRAM Problem_29_58` given in the solution to Problem 29.58. The value of $S(1089) = 3.315$. Using WMAP values we find

$$\theta = 0.035\ \text{rad} = 2.0^\circ.$$

30.12 The characteristic distance associated with Silk damping is given by

$$d_{\rm Silk} = \sqrt{\frac{ct_{\rm dec}}{n\sigma}} = \sqrt{\frac{ct_{\rm dec}m_H}{\rho_{b,0}(1+z)^3\sigma}}.$$

Using WMAP values, $[t_{\rm dec}]_{\rm WMAP} = 379$ kyr, $[z_{\rm dec}]_{\rm WMAP} = 1089$, and $[\rho_{b,0}]_{\rm WMAP} = 4.17\times 10^{-28}$ kg m^{-3}, we find $d_{\rm Silk} = 4\times 10^{20}$ m. Now, from Eq. (29.190) with $D = d_{\rm Silk}$ and $S(z) = 3.315$ (see the solution to Problem 30.11, $\theta = 1.03\times 10^{-3}$ rad $= 0.059^\circ$. This corresponds to a value of $\ell \simeq \pi/\theta = 3100$.

30.13 The first stars ignited at the time of reionization. According to the WMAP CMB polarization results, this corresponded to $z = 10.9$, or $R = 1/(1+z) = 0.084$. From Eq. (29.129), this happened when $t = 1.36\times 10^{16}$ s $= 430$ Myr.